Functional characterisation of *GmSALT3*, a candidate gene for conferring salt tolerance in soybean [*Glycine max* (L.) Merr.]

By

Yue Qu

M.Biotech.

A thesis submitted for the partial fulfilment of the requirements for the degree of Doctor of Philosophy

The University of Adelaide

Faculty of Sciences

School of Agriculture, Food & Wine

Waite Campus

2017

Table of Contents

Abstract

Soybean (*Glycine max* (L.) Merrill) is native to East Asia, which includes China that has a cultivation history stretching back at least 5,000 years. Now soybean is widely cultivated around the world as an important crop. It is an annual plant and its seeds are processed to produce two major products, oil and meal. Many biotic and abiotic stresses threaten soybean production in different areas of the world, such as fungal, bacterial and viral diseases; aluminium, drought, and salinity. In this thesis, the focus is on investigating the salinity stress responses in soybean and how *GmSALT3* (salt tolerance-associated gene on chromosome 3), a dominant gene that is associated with limiting the accumulation of sodium ions in shoots, contributes to soybean's salinity tolerance.

GmSALT3 was identified through fine-mapping; it encodes a protein from the cation/H^+ exchanger (CHX) family that I localized to the endoplasmic reticulum (ER) and which is preferentially expressed in the salt-tolerant parent Tiefeng 8 within root cells associated with phloem and xylem. In the salt-sensitive parent, 85-140, a 3.78-kb copia retrotransposon insertion in exon 3 of *Gmsalt3* was identified that truncates the transcript. In addition, nine haplotypes including two salt-tolerant haplotypes and seven salt-sensitive haplotypes were identified by sequencing 31 soybean landraces and 22 wild soybean (*Glycine soja*) cultivars in China. By analysing the distribution of haplotypes, it was found that haplotype 1 (H1, found in Tiefeng 8) was strongly associated with salt tolerance and is likely to be the ancestral allele. H1, unlike other alleles, has wide geographical range including saline areas, which indicates it is maintained when required but its potent stress tolerance can be lost during natural selection and domestication.

Then, I evaluated the impact of *GmSALT3* on soybean performance under saline or non-saline treatments, with both field and controlled conditions experiments being performed. Three sets of near isogenic lines (NILs), with genetic similarity of 95.6–99.3% between each pair of NIL-T (salt-tolerant) and NIL-S (salt-sensitive), were generated from a cross between 85–140 and Tiefeng 8 by using marker-assisted selection. It was shown that *GmSALT3* does not

contribute to an improvement in seedling emergence rate or early vigor under salt stress. However, when 12-day-old seedlings were exposed to NaCl stress, I found that the NIL-T lines accumulated significantly less leaf Na^+ and Cl^- compared with their corresponding NIL-S, while no significant difference of K^+ concentration was observed between NIL-T and NIL-S. In addition, I found that the NIL-T lines accumulated less Cl^- in the leaf and more in the root prior to any difference in Na^+; in the field, NIL-T accumulated less pod wall Cl^- than the corresponding NIL-S lines. Under non-saline field conditions, no significant differences were observed for yield related traits within each pair of NIL-T and NIL-S lines, indicating there was no observable yield penalty for having the *GmSALT3* gene. In contrast, under saline field conditions the NIL-T lines had significantly greater plant seed weight and 100-seed weight than the corresponding NIL-S lines, meaning *GmSALT3* conferred a yield advantage to soybean plants in salinized fields.

In addition to confirming that Cl^- exclusion occurs prior to Na^+ exclusion using a time course analysis, I found that stem secretion of Na^+ contributes to its exclusion from leaves; NIL-T also accumulated less K^+ in the leaf compared to NIL-S. I observed that Cl^- concentration is significantly higher in both the stem xylem and phloem sap of NIL-T. This likely means that whilst more Cl^- is transported from root-to-shoot more Cl^- is recirculated back to roots, and this contributes to a greater accumulation of Cl^- in NIL-T roots. Na^+ is significantly greater in concentration in NIL-S xylem sap but no differences were detected in phloem sap and roots between NILs, which indicates Na^+ is most likely regulated by exclusion at the root xylem, so in a different way in NIL-T compared to Cl^-. Plants with full-length *GmSALT3* maintain a significantly higher photosynthetic rate than NIL-S plants before and after salt treatment. In heterologous expression systems, GmSALT3 could restore bacterial growth of *E. coli* strain LB2003 (*trkAΔ, kup1Δ, kdpABCDEΔ*) that is defective in K^+ uptake systems; when expressed in *Xenopus laevis* oocytes, GmSALT3 contributes to higher accumulation of Na^+, K^+, and Cl^- and higher net influx of Na^+, K^+, and Cl^- (measured by MIFE, Microelectrode Ion Flux Estimation) compared to water-injected oocytes.

In an attempt to reveal new insights to the potential underlying mechanisms I used RNA-seq analysis of roots from soybean NIL (Near Isogenic Lines); NIL-S (salt-sensitive, *Gmsalt3*) and NIL-T (salt-tolerant, *GmSALT3*). Thirty RNA-seq libraries were constructed and sequenced, including NIL-T and -S roots from three time points of 14 day old plants, 0 hours, 6h, and 3d following salt-treatment (200mM NaCl) and their corresponding non-treatment controls. Gene ontology (GO) analysis showed that unique DEGs under salt treatment in NIL-T are clustered into GO terms such as response to biotic stimulus, oxidation reduction and oxidoredutase activity, while in NIL-S GO terms are more diverse including cell communication, signalling, and biological regulation. Accordingly, reactive oxygen species (ROS) generation and detoxification was measured and differed in NIL consistent with the RNA-seq data. As such, I propose that *GmSALT3* affects the ROS status of roots, which improves the ability of NIL-T to cope with stress.

Overall, the collective findings of this thesis provide new insights into the transport activity of GmSALT3 and how *GmSALT3* contributes to salinity tolerance in soybean.

Declaration

I certify that this work contains no material which has been accepted for the award of any other degree or diploma in my name, in any university or other tertiary institution and, to the best of my knowledge and belief, contains no material previously published or written by another person, except where due reference has been made in the text. In addition, I certify that no part of this work will, in the future, be used in a submission in my name, for any other degree or diploma in any university or other tertiary institution without the prior approval of the University of Adelaide and where applicable, any partner institution responsible for the joint-award of this degree.

I acknowledge that copyright of published works contained within this thesis resides with the copyright holder(s) of those works.

I also give permission for the digital version of my thesis to be made available on the web, via the University's digital research repository, the Library Search and also through web search engines, unless permission has been granted by the University to restrict access for a period of time.

Acknowledgements

Firstly, I would like to thank my principal supervisor and mentor Professor Matthew Gilliham for the continuous support of my Ph.D research, for his patience, motivation, and guidance. Besides my principal supervisor, I also thank my co-supervisor Dr. Stefanie Wege for her critically reading of my work and providing research ideas; my postgraduate coordinator Associate Professor Ken Chalmers for his support; my independent advisor Dr. Tim Sutton for his research ideas and support.

I thank Professor Rongxia Guan, Professor Lijuan Qiu and their soybean research group members from Chinese Academy of Agricultural Sciences in Beijing, for donating soybean seeds and for research support through discussing results and further experiments; Dr. Gwenda Mayo for technical assistance with instruments in Adelaide Microscopy; Dr. Jayakumar Bose for assistance in MIFE experiments; Dr. Rakesh David for assistance in RNA-seq analysis; Dr. Bo Xu, Dr. Jiaen Qiu, Dr. Sam Henderson, Dr. Sunita Ramesh, Dr. Yu Long, Dr. Caitlin Byrt, Dr. Zhengyu Wen, Prof. Stephen Tyerman, Zeyu Xiao, and Siyang Liao for help and advice; Asmini Athman, Wendy Sullivan, Ali Mafakheri, and Dr. Rebecca Vandeleur for technical support.

I also thank Australian Research Centre, Plant Energy Biology Centre of Excellence, School of Agricultural, Food, and Wine, and the University of Adelaide for providing financial support and resources to this project, and the reviewers and Editors of *The Plant Journal*, *Journal of Experimental Botany* and *Frontiers in Plant Science* for their comments that helped to improve the manuscripts within this thesis.

Last but not the least, I would like to thank my family for supporting me throughout my study abroad and my life in general.

List of Abbreviations

APX	Ascorbate peroxidase
AsA	Ascorbic acid
Car	Carotenoid
CAX	Calcium/Proton antiporter
CCC	Cation-chloride cotransporter
CHI	Chalcone isomerase
CHS	Chalcone synthase
CHX	Cation/proton exchanger
Cl^-	Chloride ion
CLC	Chloride channel
CPA	Cation/proton antiporter
CPM	Cytochrome P450 monooxygenase
DAS	Days after sowing
DEG	Differentially expressed genes
DNA	Deoxyribonucleic acid
dS/m	decisiemens per metre
EC	Electrical Conductivity
ER	Endoplasmic Reticulum
FC	Fold change
FDR	False Discovery Rate
FL	First trifoliate leaf
GFP	Green fluorescent protein
GO	Gene ontology
GSH	Glutathione
H^+	Proton
HKT	High affinity K^+ transporter
HS	Higher stem
Hy	Hypocotyl
IRGA	Infrared gas analyzer
K^+	Potassium ion
KEGG	Kyoto Encyclopedia of Genes and Genomes
kg, g, µg, ng	kilograms, grams, micrograms, nanograms
L, mL, µL, nL	Litre, millilitre, microlitre, nanolitre
Li^+	Lithium ion

LS	Lower stem
LTR	Long terminal repeats
mM	Millimolar
mRNA	Messenger RNA
Na^+	Sodium ion
NILs	Near isogenic lines
PCA	Principal Component Analysis
PCR	Polymerase chain reaction
PR	Primary root
qRT-PCR	Quantitative real-time PCR
QTL	Quantitative trait loci
RNA	Ribonucleic acid
ROS	Reactive Oxygen Species
SNP	Single-nucleotide polymorphism
SOD	Superoxide dismutase
SR	Secondary root
SSR	Simple sequence repeats
TEM	Transmission electron microscopy
TMDs	Transmembrane domains
UTR	Untranslated region
v/v	Volume per volume
w/v	Weight per volume
YFP	Yellow fluorescent protein
YL	Youngest trifoliate leaf

Preface

This project was initiated through a collaboration with the laboratories of Professor Rongxia Guan and Professor Lijuan Qiu from the Institute of Crop Sciences at the CAAS (Chinese Academy of Agricultural Science), Beijing, who identified a candidate salt tolerance gene from soybean (*GmSALT3*) via a fine mapping approach; they sought the assistance of my home lab (led by Professor Matthew Gilliham) in characterising the role of this gene in improving soybean salt tolerance. This aim was the focus of my PhD studies – how does GmSALT3 confer improved salt tolerance in soybean. As such an objective of my PhD studies was to contribute to our understanding of possible salt tolerance mechanisms in soybean. As the only fine-mapped gene from a salt tolerance QTL in soybean, this study has promise to improve the salt tolerance of soybean (and related species). Throughout the period of my thesis our collaborators, my supervisors and I have jointly planned experiments and discussed analysis; my principal supervisor and I have visited CAAS on 5 occasions (2014; 2015x2; 2016), and Prof. Guan (the lead CAAS researcher) has visited Adelaide (2017). We have also maintained regular email and videoconference contact throughout. This thesis contains 3 published manuscripts and 2 manuscripts that are intended for publication. It contains a minimal broad introduction to avoid repetition with the introductions of the manuscripts, and a general discussion. Each chapter, in addition to the manuscript includes a brief introduction to orientate the reader and provide some context to the study, and a conclusion with extended discussion to provide a clear link between the manuscripts.

Chapter 1 Literature review

1.1 Background

To meet the food demands of a booming global population – from 3.7 billion in 1970 to a predicted 9.15 billion in 2050 – it has been predicted that world agricultural production in 2050 will need to have increased by 60 percent from the quantities produced in 2005/2007 (Alexandratos and Bruinsma, 2012; Godfray *et al.*, 2010; Taiz, 2013; Tester and Langridge, 2010). Among all the agricultural products, cereal production is currently projected to rise by only 46% from 2068 Mt in 2005/2007 to 3009 Mt in 2050 (Alexandratos and Bruinsma, 2012). In reality, the rate of annual crop yield gains has slowed down considerably from ~2.5% in 1985 to ~1.2% in 2007, as Alexandratos and Bruinsma (2012) reported, so meeting the crop production targets is going to require step changes in how crops are produced. This is a crucial global challenge – especially when it comes coupled with rapid economic growth –, which has associated environmental costs and constraints including climate change, freshwater shortage, and arable land loss (Gilliham *et al.*, 2017). Suitable land and water resources are essential for sustainable agricultural growth, but the incidence and severity of stress events are on the increase (Munns and Gilliham, 2015).

Salinity has become one of the most widespread soil constraints in arid and semi-arid regions on the Earth, such as Australia, Central Asia, the Middle East, and Northern Africa (FAO, 2008). A soil is defined as saline when a range of soluble salts, particularly NaCl, in the soil water (soil solution) has reached an excessive level; soils are generally classified as saline when the salt component of the soil has an ECe (electric conductivity of the saturated paste extract) of ≥ 4 dS/m, which equates to approximately 40 mM NaCl (USDA-ARS, 2008). Sodic soils contain sodium salts but limited amounts of other cations such as calcium, magnesium, and iron (Rengasamy, 2006). The total global area of saline and sodic soils currently stands at 831 million hectares (i.e. 6% of soils worldwide) (Rengasamy, 2006), a figure that can be expected to rise in the near future in regions that are predicted to get hotter and drier to due climate change. Within Australia, about 30% of the land area is affected by different types of

salinization (Rengasamy, 2006); groundwater-associated salinity and irrigation salinity affects about 16% of the agricultural area, and 67% of the agricultural land has a potential for transient salinity (Rengasamy, 2006). Therefore, it is both important and urgent to combat the problem of soil salinization through funding research focused on decreasing soil salinity, decreasing its impact on crops, or improving the salinity tolerance of crops that are grown. The growth of conventional crops on highly saline soils is likely only to be achievable in the distant future; the majority of salinity research is currently concentrating on making incremental increases in salinity tolerance of crops to improve the yield stability of crops encountering transient salinity during a growing season.

Although it is an oversimplification, it can be instructive to classify the effects of salt on plants by breaking them down into two broad categories (Munns and Tester, 2008). When plants first come into contact with high concentrations of salt in the soil solution, sodium and Cl ions (Na^+, Cl^-) impart an osmotic stress, where high concentrations of these solutes in the soil make it harder for roots to extract water; the second is the toxicity (ionic stress) that occurs when high concentration of Na^+ and Cl^- build up within the plant tissue (Munns and Tester, 2008). Fortunately, some relatively tolerant plant species possess mechanisms to adapt to these stresses. As NaCl is the most abundant 'salt' in the soil, and plants have evolved mechanisms to regulate its accumulation (Flowers and Colmer, 2008; Munns and Gilliham, 2015), the term salinity tolerance in this review is adopted to refer to tolerance of NaCl. For most plant species, Na^+ appears to reach concentrations that are toxic to the plant before Cl^- (Munns and Tester, 2008). However, for some salt-sensitive varieties of woody perennials such as citrus, grapevine, and soybean, Cl^- is considered to be the more toxic ion as it accumulates to very high concentrations in leaves, much more than Na^+ (Läuchli, 1984; Storey and Walker, 1998; Teakle and Tyerman, 2010; Wege *et al.*, 2017).

There are large differences in crop plants' tolerance of salinity, as reflected in a wide phenotypic variation across and within species when encountering salt stress (Flowers and Colmer, 2008; Munns and Tester, 2008; Teakle and Tyerman, 2010). For instance, a halophytic

relative of wheat, Tall wheatgrass (T*hinopyrum ponticum, syn. Agropyron elongatum*), is one of the most tolerant monocotyledonous species, and can retain 40% of its shoot growth in 300 mM NaCl contained soil compared to growth in non-salt conditions (Colmer *et al.*, 2005). This contrasts with durum wheat that is unable to complete its life cycle when soil NaCl concentration reaches 200 mM (Munns and Tester, 2008). Salinity tolerance varies in dicotyledonous species even more widely than in monocotyledonous species (Munns and Tester, 2008). Some legumes are very sensitive i.e. less than 100 mM NaCl in the soil is lethal. The most susceptible cultivars of chickpea (*Cicer arietinum* L.) die in just 25 mM NaCl (Flowers *et al.*, 2010). The model plant *Arabidopsis thaliana* is a salt-sensitive species (with 100 mM NaCl being lethal) (Cramer, 2002); however, alfalfa or lucerne (*Medicago sativa*) are very tolerant (surviving in 400 mM NaCl), and halophytes such as saltbush (*Atriplex* spp.) are able to grow well at soil salinities greater than that of seawater (i.e. >600 mM NaCl) (Munns and Tester, 2008). In this review, aspects of salt tolerance for soybean (*Glycine max*) will be discussed.

1.2 Effects of salt stress on soybean

Soybean, due to its high protein and oil content (Schmutz *et al.*, 2010) and relatively good agronomic traits, is one of the most important crop plants globally for animal feed, the human diet, and biodiesel production. Figure 1.1 shows the area harvested in hectare (ha) and production (tonnes) of 10 the most important crops globally in 2014. The area harvested of soybeans was fourth among crops globally in 2014. During the same period of time, the production tonnage of soybeans was just less than that of maize, rice, wheat, and potatoes. Salinity stress is one of the abiotic stresses that significantly reduces soybean production (Hamwieh *et al.*, 2011). Salinity tolerance varies among soybean varieties, and the degree of salt tolerance of soybean germplasm is different across different developmental stages (Phang *et al.*, 2008). These differences are summarised below.

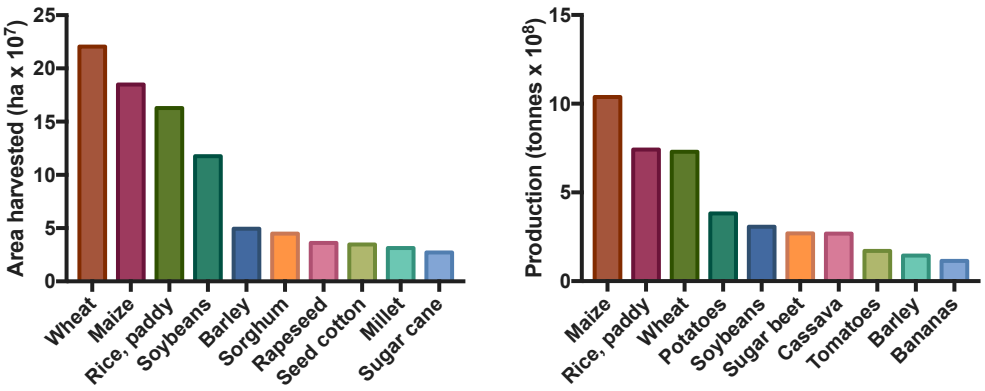

Figure 1.1 Area harvested (ha) and production (tonnes) of 10 crops in the world (2014). Data was obtained from FAO database (http://faostat.fao.org/), and replotted (FAO, 2014).

1.2.1 Growth and nodulation

High soil salinity negatively affects soybean development during its whole life cycle. At the germination stage, low salt conditions (8.6 mM and 17.1 mM NaCl) have been shown to result in delayed germination (Phang *et al.*, 2008). Higher salt conditions (42.8 mM) lead to an absolute decrease in the percentage of germination (15% of control germinated in nonsalinized cultures) (Abel and MacKenzie, 1964). Soybean is considered to be more sensitive to salt stress at the seedling stage compared to the germination stage (Hosseini *et al.*, 2002). Forty percent of soybean seeds could still germinate even when the Na^+ concentration reached a high level in the tissue (9.3 mg/g fresh weight in the embryonic axis), whereas the growth of seedlings was completely inhibited when the Na^+ concentration attained 6.1 mg/g fresh weight (Hosseini *et al.*, 2002).

As a legume, soybean can form root nodules to fix atmospheric nitrogen (N_2); nitrogen being an essential building block of biomolecules. Therefore, root nodules have a key role in determining the nutritional status of the whole plant, and the quantity and quality of seed produced. Salinity stress affects the nodulation capacity of soybean, decreasing the number and biomass of root nodules, and results in reduced nitrogen fixation efficiency (Elsheikh, 1998).

This is because salt stress inhibits nitrogen fixation and also hampers the initiation of symbiosis (Delgado *et al.*, 1994; Duzan *et al.*, 2004). Reduced nitrogen fixation efficiency can significantly decrease crop yield unless there is additional application of N fertilizers (Hirel *et al.*, 2011). The salt tolerance capacity of different strains of symbiotic *Bradyrhizobia Rhizobia* is not associated with their ecological origin, but determined by external factors which include pH, temperature, carbon sources, and osmoprotectant solutes in the soil substratum (Elsheikh, 1998; Elsheikh and Wood, 1989). Furthermore, the salt tolerance capacity of the soybean host is also important for nodulation (Phang *et al.*, 2008). In conclusion, salinity stress is harmful to soybean's growth at both germination and seedling stages, and negatively affects soybean root nodulation.

1.2.2 Agronomic traits and seed quality

The agronomic traits of soybean, including biomass, height, leaf size, number of branches, number of internodes, number of pods, 100 seed weight, and weight per plant, can be significantly reduced under high salinity stress (Chang *et al.*, 1994; Pathan *et al.*, 2007; Phang *et al.*, 2008). Soybean seed, the primary agricultural product of the soybean plant, has its quality affected by salinity stress, reducing the protein content (Chang *et al.*, 1994). The seed protein of soybean cultivar Williams decreased about 2.5% under saline conditions (EC=9 dS/m), 75 days after flowering (Ghassemi-Golezani *et al.*, 2010). However, whether salt stress reduces the oil content in soybean seeds is still under debate since variation exists amongst experimental findings from different field sites using various cultivars treated with different salinity levels (Chang *et al.*, 1994; Wan *et al.*, 2002).

1.3 Mechanisms of salt tolerance in crops, with a focus on soybean

Different soybean germplasm exhibits differences in its ability to tolerate salinity. This differential capability is determined by the efficiency in operating and coordinating the 'salt

tolerance systems' of soybean. The mechanisms of salt tolerance in soybean can be classified into four major categories: adjustment in response to osmotic stress, restoration of oxidative balance, other metabolic and structural adaptations, and maintenance of ion homeostasis (Table 1.1) (Phang *et al.*, 2008). Maintenance of ion homeostasis and restoration of oxidative balance in soybean plants will be discussed in detail.

Table 1.1 Mechanisms of salt tolerance in soybean (Data collected from Phang *et al.*, 2008)

Mechanisms	Components	Examples
Adjustment in response to osmotic stress	Accumulation of osmoprotectants and late embryogenesis abundant (LEA) proteins	Trigonelline (TRG, osmoprotectant) (Malenčić *et al.*, 2003) GmDHN1 (group 2 LEA) (Soulages *et al.*, 2003)
Restoration of oxidative balance	Elevation of the contents and activities of various antioxidative components	Superoxide dismutase (SOD) (Ruzhen, 1997) GmPAP1 (purple acid phosphatases) (Li *et al.*, 2008)
Maintenance of ion homeostasis	Regulation of ion transport by membrane bound ion transporters and associated signalling	GmNHX1 (Li *et al.*, 2006a) GmSCA1 (Ca^{2+} - ATPase) (Chung *et al.*, 2000)
Other metabolic and structural adaptations	Development of salt gland-like structures, modification of cell wall and cell membrane structures	ball-shaped cell (Lu *et al.*, 1998) SbPRP3 (Soybean Proline-rich Protein) (He *et al.*, 2002)

1.3.1 Maintenance of ion homeostasis

As mentioned before, Cl^- has been documented to be more toxic than Na^+ in cultivated soybean; this is in contrast to most annual crop species. This difference may come from the ability of soybean to hold Na^+ in woody roots and stems to prevent much from reaching the leaves, which leads to a low Na^+/K^+ ratio in leaves (Luo *et al.*, 2005). At the same time, Cl^- continues to pass into the aerial parts of the plant, resulting in a high shoot Cl^- accumulation, with high concentrations of Cl^- being toxic to plant cellular metabolism (Xu *et al.*, 2000). However, other reports suggest that different soybean species have little correlation between

leaf chlorosis and leaf Cl^- content (Phang *et al.*, 2008). Salt-tolerant soybean germplasm also accumulated less Na^+ in leaves than salt-sensitive varieties (Li *et al.*, 2006b). In addition, several recent studies support the proposition that Na^+ is the toxic ion in soybean (Ikeda, 2005; Lenis *et al.*, 2011; Luo *et al.*, 2005).

HKT1;5-like cation transporters have been shown to be responsible for leaf Na^+ exclusion in many crops (Byrt *et al.*, 2007; Byrt *et al.*, 2014; James *et al.*, 2011; Mian *et al.*, 2011; Platten *et al.*, 2013). In wheat, it has been discovered that *HKT1;5* encodes a Na^+-selective transporter located on the plasma membrane of root cells surrounding xylem vessels, which retrieves Na^+ from the xylem and reduces transport of Na^+ to leaves (Byrt *et al.*, 2007; Munns *et al.*, 2012). Soybean may possibly have a gene which encodes a protein that fulfils a similar function to *HKT1;5* and this may explain the greater Cl^- accumulation in leaves of soybean; *HKT* genes have frequently been found underlying sodium exclusion QTL in a number of plants (Davenport *et al.*, 2007; Horie *et al.*, 2009; Huang *et al.*, 2008; Ren *et al.*, 2005).

As reviewed by Phang *et al.* (2008), both inter- and intra- cellular compartmentalization is involved in the regulation of Na^+ homeostasis of soybean, and this is likely to be multigenic due to the identification of several genes linked to Na^+ homeostasis and salt tolerance (Table 1.2). Abel (1969) found that leaf Cl^- accumulation was controlled by a single and dominant gene *Ncl* in salt-tolerant soybean varieties, but the genetic information about this gene has not been fully revealed.

Table 1.2 Characterized genes associated with salt tolerance

Gene		Localization	Putative function
GmNHX1	(Li *et al.*, 2006a)	Tonoplast	Vacuolar Na^+/H^+ antiporter
GmSOS1	(Phang, 2008)	Plasma membrane	Na^+/H^+ antiporter
GmCAX1	*(Luo et al., 2005)*	Plasma membrane	Cation/proton exchanger
GmCLC1	(Tsai, 2003)	Tonoplast	Vacuolar CLC chloride channel
GmAKT1	(Tsai, 2003)	N/A	Inward-rectifying K^+ channel
GmCNGC	(Phang, 2008)	Plasma membrane	Cyclic nucleotide-gated cation channel
GmCAX1	(Luo *et al.*, 2005)	Plasma membrane	Cation/proton exchanger
GmNKCC	(Phang, 2008)	N/A	$Na^+/K^+/Cl^-$ co-transporter
GmERF3	(Zhang *et al.*, 2009)	Nucleus	Transcription factor
GmUBC2	(Zhou *et al.*, 2010)	Cytosol and nucleus	Ubiquitin-conjugating enzyme
GmbZIP1	(Gao *et al.*, 2011)	Nucleus	Transcription factor

Whether Na^+ or Cl^- has the most detrimental effect in soybean is still controversial; regardless, homeostasis of both ions is likely to be linked (due to the necessity for charge balance when accumulating salts) and the exclusion of both from the shoot is likely to be significant for improving salt tolerance in soybean.

1.3.2 Restoration of oxidative balance

In plants, Reactive Oxygen Species (ROS) are produced as by-products of various metabolic pathways in different cell types (Foyer and Harbinson, 1994). Under physiologically favourable conditions, ROS work as signalling molecules at low concentrations, and excessive ROS are scavenged by different antioxidative components (Foyer and Noctor, 2005). Salt and osmotic stress are thought to break the equilibrium between evolution and scavenging of ROS through impairing the scavenging process (Phang *et al.*, 2008). ROS at high concentrations can cause lipid peroxidation, DNA damage, protein denaturation, carbohydrate oxidation, and enzymatic activity impairment leading to significant damage to cellular functions and even cell death of plant cells (Foyer and Noctor, 2005; Gill and Tuteja, 2010; Mittler *et al.*, 2004; Noctor and Foyer, 1998).

One possible salt-tolerance mechanism in soybean is to restore the cellular oxidative balance and minimize the secondary oxidative damage, through increasing the activity and contents of antioxidative components (Phang *et al.*, 2008). In one study, the production rate of O_2^- (a class of ROS) in both shoots and roots of the salt-tolerant soybean cultivar "BB52" decreased under increasing NaCl concentration; in contrast, an increased production rate was observed in salt-sensitive cultivar "N23232"; the O_2^- was reduced by enhanced activities of enzymatic ROS scavengers, including superoxide dismutase (SOD) and ascorbate peroxidase (APX), and increased contents of non-enzymatic ROS scavengers, including ascorbic acid (AsA), carotenoid (Car) and glutathione (GSH) (Yu and Liu, 2002).

1.4 Analysis of a candidate salt tolerance gene (*GmSALT3*) in soybean

1.4.1 Gene mapping and QTL analysis

In soybean, Abel (1969) first found that leaf chloride exclusion was controlled by a single and dominant locus *GmNCl* in salt-tolerant soybean varieties, based on the F_2 plants segregated in ratios of 3 chloride excluders to 1 includer, and the progenies of BC_1F_1 (backcross of F_1 plants) being segregated in an excluder : include ratio of 1:1. By using different soybean cultivated populations and even between wild and cultivated soybeans, a major quantitative trait loci (QTL) for salinity tolerance was consistently mapped to chromosome 3 (Linkage group N) (Ha *et al.*, 2013; Hamwieh *et al.*, 2011; Hamwieh and Xu, 2008; Lee *et al.*, 2004).

Since I initiated my PhD in 2014, a few papers have been published focusing on the same gene associated with this soybean salt tolerance QTL. In each of these publications the gene was given a different name: *GmCHX1*, identified through a whole-genome sequencing approach from in wild soybean (*Glycine soja*, W05) (Zhou *et al.*, 2014); *GmNcl*, identified in a Brazilian soybean cultivar FT-Abyara through a map-based cloning strategy (Do *et al.*, 2016), and *GmSALT3*, identified in a commercial soybean cultivar Tiefeng 8 through fine mapping and positional cloning (Guan *et al.*, 2014). All the three identified genes share the same sequence with *Glyma03g32900* in William 82, and based on genetic markers information, this

gene is the most likely candidate for the dominant gene in the major salinity tolerance QTL, and also in the *Ncl* locus reported by Abel (1969). In this thesis, I refer to this dominant gene as *GmSALT3*.

1.5 Summary

Salinity has become one of the most detrimental threats to maintaining and/or improving crop production worldwide. Its impacts are increasing because of the effects of global climate change, drought, and agricultural water deficiency. Soybean is an important crop around the world, but its salt resistance mechanisms are still poorly characterised.

The exploration of salt tolerance mechanisms in soybean and the genes involved is significant as it is likely to enable further applications, including: field trials to examine whether the presence of GmSALT3 improves grain yield of salt-sensitive soybean near-isogenic lines; the generation of locally-adapted soybean lines for salinity-affected areas in the world by marker-assisted breeding or via transgenics; a better understanding of salt tolerance mechanisms in plants and the interaction with other defined mechanisms encoded by genes such as *SOS1*(Shi *et al.*, 2000), *HKT1* (Genet *et al.*, 1995), *NHX* (Yokoi *et al.*, 2002), *CDPKs* (calcium-dependent protein kinases) (Hrabak *et al.*, 2003), and *CBLs* (calcineurin B-like proteins)-*CIPKs* (CBL-interacting protein kinases) network (Luan, 2009).

1.6 Experimental aims

The primary aim of my project was to provide a better understanding of *GmSALT3*-associated salt tolerance mechanisms in soybean and therefore assist in developing salt-tolerant commercial soybean cultivars. To address this aim, five publications (three published, two in manuscript format) will be introduced in the following sections. In brief, the first publication included the fine-mapping of *GmSALT3*, and its cellular and sub-cellular localisations; the second publication investigated the ion accumulation profile in soybean near isogenic lines (NILs) of *GmSALT3* and how *GmSALT3* may contribute to improved soybean yield under saline

stress; the third publication functionally characterised *GmSALT3 in planta* and in heterologous expression systems; and the final publication aimed to investigate how *GmSALT3* transcriptionally confers salinity tolerance in soybean roots by RNA-sequencing, using NIL-T (*GmSALT3*) and NIL-S (*Gmsalt3*) roots. There is also an additional publication in an industry journal included in the appendix that summarizes the discovery of *GmSALT3* and its potential implications for the soybean industry. A number of additional appendices are also included which feature additional work performed during my candidature relevant to *GmSALT3* but were excluded from the manuscripts. The thesis concludes with a final discussion, which examines the future implications of my PhD study.

1.7 Literature cited

Abel, G. H. (1969). Inheritance of the capacity for chloride inclusion and chloride exclusion by soybeans. *Crop Science* **9**, 697.

Abel, G. H. and MacKenzie, A. J. (1964). Salt tolerance of soybean varieties (*Glycine max L. Merrill*) during germination and later growth. *Crop Science* **4**, 157.

Alexandratos, N. and Bruinsma, J. (2012). World agriculture towards 2030/2050: the 2012 revision: ESA Working paper No.12-03. Rome, FAO.

Byrt, C. S., Platten, J. D., Spielmeyer, W., James, R. A., Lagudah, E. S., Dennis, E. S., Tester, M. and Munns, R. (2007). HKT1; 5-like cation transporters linked to Na^+ exclusion loci in wheat, *Nax2* and *Kna1*. *Plant Physiology* **143**, 1918-1928.

Byrt, C. S., Xu, B., Krishnan, M., Lightfoot, D. J., Athman, A., Jacobs, A. K., Watson-Haigh, N. S., Plett, D., Munns, R. and Tester, M. (2014). The Na^+ transporter, TaHKT1; 5-D, limits shoot Na^+ accumulation in bread wheat. *The Plant Journal* **80**, 516-526.

Chang, R. Z., Chen, Y. W., Shao, G. H. and Wan, C. W. (1994). Effect of salt stress on agronomic characters and chemical quality of seeds in soybean. *Soybean Science* **13**, 101-105.

Chung, W. S., Lee, S. H., Kim, J. C., Do Heo, W., Kim, M. C., Park, C. Y., Park, H. C., Lim, C. O., Kim, W. B. and Harper, J. F. (2000). Identification of a calmodulin-regulated soybean Ca^{2+}-ATPase (SCA1) that is located in the plasma membrane. *The Plant Cell* **12**, 1393-1407.

Colmer, T. D., Munns, R. and Flowers, T. J. (2005). Improving salt tolerance of wheat and barley: future prospects. A*ustralian Journal of Experimental Agriculture* **45**, 1425-1443.

Cramer, G. R. (2002). Response of abscisic acid mutants of *Arabidopsis* to salinity. *Functional plant biology* **29**, 561-567.

Davenport, R. J., Munoz-Mayor, A., Jha, D., Essah, P. A., Rus, A. N. A. and Tester, M. (2007). The Na^+ transporter AtHKT1;1 controls retrieval of Na^+ from the xylem in *Arabidopsis*. *Plant, Cell & Environment* **30**, 497-507.

Delgado, M. J., Ligero, F. and Lluch, C. (1994). Effects of salt stress on growth and nitrogen fixation by pea, faba-bean, common bean and soybean plants. *Soil Biology Biochemistry* **26**, 371-376.

Do, T. D., Chen, H., Hien, V. T. T., Hamwieh, A., Yamada, T., Sato, T., Yan, Y., Cong, H., Shono, M. and Suenaga, K. (2016). Ncl synchronously regulates Na^+, K^+, and Cl^- in soybean and greatly increases the grain yield in saline field conditions. *Scientific Reports* **6**.

Duzan, H. M., Zhou, X., Souleimanov, A. and Smith, D. L. (2004). Perception of *Bradyrhizobium japonicum* Nod factor by soybean [*Glycine max (L.) Merr.*] root hairs under abiotic stress conditions. *Journal of Experimental Botany* **55**, 2641-2646.

Elsheikh, E. A. E. (1998). Effects of salt on rhizobia and bradyrhizobia: a review. *Annals of Applied Biology* **132**, 507-524.

Elsheikh, E. A. E. and Wood, M. (1989). Response of chickpea and soybean rhizobia to salt: Influence of carbon source, temperature and pH. *Soil Biology Biochemistry* **21**, 883-887.

FAO. (2008). Land and plant nutrition management service, vol. 2013. http://www.fao.org/ ag/agl/agll/spush

FAO. (2014). FAOSTAT database. Accessed at 12/07/2017. http://www.fao.org/faostat/en/#data/QC.

Flowers, T. J. and Colmer, T. D. (2008). Salinity tolerance in halophytes. *New Phytologist* **179**, 945-963.

Flowers, T. J., Gaur, P. M., Gowda, C. L., Krishnamurthy, L., Samineni, S., Siddique, K. H., Turner, N. C., Vadez, V., Varshney, R. K. and Colmer, T. D. (2010). Salt sensitivity in chickpea. *Plant, Cell & Environment* **33**, 490-509.

Foyer, C. H. and Harbinson, J. (1994). Oxygen metabolism and the regulation of photosynthetic electron transport. *Causes of photooxidative stress and amelioration of defense systems in plants*, Boca Raton, FL: CRC Press.

Foyer, C. H. and Noctor, G. (2005). Redox homeostasis and antioxidant signaling: a metabolic interface between stress perception and physiological responses. *The Plant cell* **17**, 1866-1875.

Gao, S. Q., Chen, M., Xu, Z. S., Zhao, C. P., Li, L., Xu, H. J., Tang, Y. M., Zhao, X. and Ma, Y. Z. (2011). The soybean GmbZIP1 transcription factor enhances multiple abiotic stress tolerances in transgenic plants. *Plant Molecular Biology*, ***75*** (6), 537-553.

Genet, F., Lowman, H., Wells, J. and Lowman, H. (1995). Sodium-driven potassium uptake by the plant potassium transporter HKT1 and mutations conferring salt tolerance. *science* **270**, 8.

Ghassemi-Golezani, K., Taifeh-Noori, M., Oustan, S., Moghaddam, M. and Seyyed-Rahmani, S. (2010). Oil and protein accumulation in soybean grains under salinity stress. *Notulae Scientia Biologicae* **2**, 64-67.

Gill, S. S. and Tuteja, N. (2010). Reactive oxygen species and antioxidant machinery in abiotic stress tolerance in crop plants. *Plant Physiology and Biochemistry* **48**, 909-930.

Gilliham, M., Able, J. A. and Roy, S. J. (2017). Translating knowledge about abiotic stress tolerance to breeding programmes. *The Plant Journal* **90**, 898-917.

Godfray, H. C. J., Beddington, J. R., Crute, I. R., Haddad, L., Lawrence, D., Muir, J. F., Pretty, J., Robinson, S., Thomas, S. M. and Toulmin, C. (2010). Food security: the challenge of feeding 9 billion people. *Science* **327**, 812-818.

Guan, R., Qu, Y., Guo, Y., Yu, L., Liu, Y., Jiang, J., Chen, J., Ren, Y., Liu, G. and Tian, L. (2014). Salinity tolerance in soybean is modulated by natural variation in *GmSALT3*. *The Plant Journal* **80**, 937-950.

Ha, B.-K., Vuong, T. D., Velusamy, V., Nguyen, H. T., Shannon, J. G. and Lee, J.-D. (2013). Genetic mapping of quantitative trait loci conditioning salt tolerance in wild soybean (*Glycine soja*) PI 483463. *Euphytica* **193**, 79-88.

Hamwieh, A., Tuyen, D. D., Cong, H., Benitez, E. R., Takahashi, R. and Xu, D. H. (2011). Identification and validation of a major QTL for salt tolerance in soybean. *Euphytica* **179**, 451-459.

Hamwieh, A. and Xu, D. (2008). Conserved salt tolerance quantitative trait locus (QTL) in wild and cultivated soybeans. *Breeding Science* **58**, 355-359.

He, C.-Y., Zhang, J.-S. and Chen, S.-Y. (2002). A soybean gene encoding a proline-rich protein is regulated by salicylic acid, an endogenous circadian rhythm and by various stresses. *Theoretical and Applied Genetics* **104**, 1125-1131.

Hirel, B., Tétu, T., Lea, P. J. and Dubois, F. (2011). Improving nitrogen use efficiency in crops for sustainable agriculture. *Sustainability* **3**, 1452-1485.

Horie, T., Hauser, F. and Schroeder, J. I. (2009). HKT transporter-mediated salinity resistance mechanisms in *Arabidopsis* and monocot crop plants. *Trends in Plant Science* **14**, 660-668.

Hosseini, M. K., Alison, A. P. and Ian, J. B. (2002). Comparison of the seed germination and early seedling growth of soybean in saline conditions. *Seed Science Research* **12**, 165-172.

Hrabak, E. M., Chan, C. W., Gribskov, M., Harper, J. F., Choi, J. H., Halford, N., Kudla, J., Luan, S., Nimmo, H. G. and Sussman, M. R. (2003). The Arabidopsis CDPK-SnRK superfamily of protein kinases. *Plant Physiology* **132**, 666-680.

Huang, S., Spielmeyer, W., Lagudah, E. S. and Munns, R. (2008). Comparative mapping of HKT genes in wheat, barley, and rice, key determinants of Na^+ transport, and salt tolerance. *Journal of Experimental Botany* **59**, 927-937.

Ikeda, M. (2005). Distribution of K^+, Na^+ and Cl^- in root and leaf cells of soybean and cucumber plants grown under salinity conditions. *Soil Science and Plant Nutrition* **51**, 1053-1057.

James, R. A., Blake, C., Byrt, C. S. and Munns, R. (2011). Major genes for Na^+ exclusion, *Nax1* and *Nax2* (wheat *HKT1; 4* and *HKT1; 5*), decrease Na^+ accumulation in bread wheat leaves under saline and waterlogged conditions. *Journal of Experimental Botany* **62**, 2939-2947.

Läuchli, A. (1984). Salt exclusion: An adaptation of legumes for crops and pastures under saline conditions. In *Salinity Tolerance in Plants: Strageiges for Crop Improvement*, eds. R. C. Staples and G. H. Toenniessen, pp. 171-187. New York: Wiley.

Lee, G. J., Carter, J. T. E., Villagarcia, M. R., Li, Z., Zhou, X., Gibbs, M. O. and Boerma, H. R. (2004). A major QTL conditioning salt tolerance in S-100 soybean and descendent cultivars. *Theoretical and Applied Genetics* **109**, 1610-1619.

Lenis, J., Ellersieck, M., Blevins, D., Sleper, D., Nguyen, H., Dunn, D., Lee, J. and Shannon, J. (2011). Differences in ion accumulation and salt tolerance among *Glycine* accessions. *Journal of Agronomy and Crop Science* **197**, 302-310.

Li, W. Y., Wong, F. L., Tsai, S. N., Phang, T. H., Shao, G. and Lam, H. M. (2006a). Tonoplast-located *GmCLC1* and *GmNHX1* from soybean enhance NaCl tolerance in transgenic bright yellow (BY)-2 cells. *Plant Cell & Environment* **29**, 1122-37.

Li, W. Y. F., Shao, G. and Lam, H. M. (2008). Ectopic expression of *GmPAP3* alleviates oxidative damage caused by salinity and osmotic stresses. *New Phytologist* **178**, 80-91.

Li, X. J., An, P., Inanaga, S., Eneji, A. E. and Tanabe, K. (2006b). Salinity and defoliation effects on soybean growth. *Journal of Plant Nutrition* **29**, 1499-1508.

Lu, J., Liu, Y., Hu, B. and Zhuang, B. (1998). The discovery of salt gland-like structure in Glycine soja. *Chinese Science Bulletin* **43**, 2074-2078.

Luan, S. (2009). The CBL–CIPK network in plant calcium signaling. *Trends in plant science* **14**, 37-42.

Luo, Q., Yu, B. and Liu, Y. (2005). Differential sensitivity to chloride and sodium ions in seedlings of *Glycine max* and *G. soja* under NaCl stress. *Journal of Plant Physiology* **162**, 1003-1012.

Malenčić, D., Popović, M. and Miladinović, J. (2003). Stress tolerance parameters in different genotypes of soybean. *Biologia Plantarum* **46**, 141-143.

Mian, A., Oomen, R. J., Isayenkov, S., Sentenac, H., Maathuis, F. J. and Véry, A. A. (2011). Over-expression of an Na^+-and K^+-permeable HKT transporter in barley improves salt tolerance. *The Plant Journal* **68**, 468-479.

Mittler, R., Vanderauwera, S., Gollery, M. and Van Breusegem, F. (2004). Reactive oxygen gene network of plants. *Trends in Plant Science* **9**, 490-498.

Munns, R. and Gilliham, M. (2015). Salinity tolerance of crops–what is the cost? *New Phytologist* **208**, 668-673.

Munns, R., James, R. A., Xu, B., Athman, A., Conn, S. J., Jordans, C., Byrt, C. S., Hare, R. A., Tyerman, S. D., Tester, M. *et al.* (2012). Wheat grain yield on saline soils is improved by an ancestral Na^+ transporter gene. *Nature biotechnology* **30**, 360-4.

Munns, R. and Tester, M. (2008). Mechanisms of salinity tolerance. *Annual Review of Plant Biology* **59**, 651-81.

Noctor, G. and Foyer, C. H. (1998). Ascorbate and glutathione: keeping active oxygen under control. *Annual Review of Plant Biology* **49**, 249-279.

Pathan, M. S., Lee, J.-D., Shannon, J. G. and Nguyen, H. T. (2007). Recent advances in breeding for drought and salt stress tolerance in soybean. In *Advances in Molecular Breeding Toward Drought And Salt Tolerant Crops*, pp. 739-773: Springer.

Phang, T. H. (2008). High external Phosphate (Pi) increases sodium ion uptake and reduces salt tolerance of "Pi tolerant" soybean, vol. Ph.D.: The Chinese University of Hong Kong.

Phang, T. H., Shao, G. and Lam, H. M. (2008). Salt tolerance in soybean. *the Journal of integrative plant biology* **50**, 1196-212.

Platten, J. D., Egdane, J. A. and Ismail, A. M. (2013). Salinity tolerance, Na^+ exclusion and allele mining of *HKT1; 5* in *Oryza sativa* and *O. glaberrima*: many sources, many genes, one mechanism? *BMC Plant Biology* **13**, 32.

Ren, Z.H., Lin, H.X., Gao, J.P., Li, L.G., Cai, X.L., Huang, W., Chao, D.Y., Zhu, M.Z., Wang, Z.Y. and Luan, S. (2005). A rice quantitative trait locus for salt tolerance encodes a sodium transporter. *Nature Genetics* **37**, 1141-1146.

Rengasamy, P. (2006). World salinization with emphasis on Australia. *Journal of Experimental Botany* **57**, 1017-23.

Ruzhen, C. Yiwu, C., Guihua, S. (1997). The effect of salt stress on superoxide dismutase in various organelles from cotyledon of soybean seedling [j]. *Acta Agronomica Sinica* **2**, 014.

Schmutz, J., Cannon, S. B., Schlueter, J., Ma, J., Mitros, T., Nelson, W., Hyten, D. L., Song, Q., Thelen, J. J. and Cheng, J. (2010). Genome sequence of the palaeopolyploid soybean. *Nature* **463**, 178-183.

Shi, H., Ishitani, M., Kim, C. and Zhu, J.-K. (2000). The *Arabidopsis thaliana* salt tolerance gene *SOS1* encodes a putative Na^+/H^+ antiporter. *Proceedings of the National Academy of Sciences* **97**, 6896-6901.

Soulages, J. L., Kim, K., Arrese, E. L., Walters, C. and Cushman, J. C. (2003). Conformation of a group 2 late embryogenesis abundant protein from soybean. Evidence of poly (L-proline)-type II structure. *Plant physiology* **131**, 963-975.

Storey, R. and Walker, R. (1998). Citrus and salinity. *Scientia Horticulturae* **78**, 39-81.

Taiz, L. (2013). Agriculture, plant physiology, and human population growth: past, present, and future. *Theoretical and Experimental Plant Physiology* **25**, 167-181.

Teakle, N. L. and Tyerman, S. D. (2010). Mechanisms of Cl^- transport contributing to salt tolerance. *Plant, Cell & Environment* **33**, 566-589.

Tester, M. and Langridge, P. (2010). Breeding technologies to increase crop production in a changing world. *Science* **327**, 818-822.

Tsai, S. N. (2003). Cloning and Characterization of Ion Transporters Genes from a Salt-tolerant Soybean Variety, vol. M.Phil.: The Chinese University of Hong Kong.

USDA-ARS. (2008). Research Databases. Bibliography on Salt Tolerance. *George E. Brown, Jr. Salinity Lab. US Dep. Agric., Agric. Res. Serv. Riverside, CA.* http://www.ars.usda.gov/Services/docs.htm?docid=8908

Wan, C., Shao, G., Chen, Y. and Yan, S. (2002). Relationship between salt tolerance and chemical quality of soybean under salt stress. *Chinese Journal of Oil Crop Sciences* **24**, 67-72.

Wege, S., Gilliham, M. and Henderson, S. W. (2017). Chloride: not simply a "cheap osmoticum", but a beneficial plant macronutrient. *Journal of Experimental Botany*. **68**: 3057-3069.

Xu, G. H., Magen, H., Tarchitzky, J. and Kafkafi, U. (2000). Advances in chloride nutrition of plants, vol. 68, pp. 97-150. San Diego: Academic Press Inc.

Yokoi, S., Quintero, F. J., Cubero, B., Ruiz, M. T., Bressan, R. A., Hasegawa, P. M. and Pardo, J. M. (2002). Differential expression and function of *Arabidopsis thaliana* NHX Na^+/H^+ antiporters in the salt stress response. *The Plant Journal* **30**, 529-539.

Yu, B. and Liu, Y. (2002). Effects of salt stress on the metabolism of active oxygen in seedlings of annual halophyte *Glycine soja*. *Acta Botanica Boreali-Occidentalia Sinica* **23**, 18-22.

Zhang, G., Chen, M., Li, L., Xu, Z., Chen, X., Guo, J., & Ma, Y. (2009). Overexpression of the soybean *GmERF3* gene, an AP2/ERF type transcription factor for increased tolerances to salt, drought, and diseases in transgenic tobacco. *Journal of Experimental Botany*, **60** (13), 3781-3796.

Zhou, G. A., Chang, R. Z., & Qiu, L. J. (2010). Overexpression of soybean ubiquitin-conjugating enzyme gene *GmUBC2* confers enhanced drought and salt tolerance through modulating abiotic stress-responsive gene expression in Arabidopsis. *Plant Molecular Biology*, *72* (4-5), 357-367.

Zhou, L., Wang, C., Liu, R., Han, Q., Vandeleur, R. K., Du, J., Tyerman, S. and Shou, H. (2014). Constitutive overexpression of soybean plasma membrane intrinsic protein GmPIP1; 6 confers salt tolerance. *BMC Plant Biology* **14**, 181.

Chapter 2 Salinity tolerance in soybean is modulated by natural variation in GmSALT3

Brief introduction

This project was initiated through a collaboration with CAAS (Chinese Academy of Agricultural Science). Our collaborators were building on a previous salt-tolerance gene mapping study in soybean (Zhang, 2005) and identified a dominant gene associated with the greater salt-tolerance of Tiefeng 8 (salt-tolerant parent) compared to the salt-sensitive parent 85-140. The dominant gene was mapped to a 209-kb region on soybean chromosome 3 (Guan *et al.*, 2014a). Then, *GmSALT3* (*Glycine max* salt tolerance-associated gene on chromosome 3) was fine-mapped to be the dominant gene associated with limiting the accumulation of sodium ions (Na^+) in shoots and a substantial enhancement in salt tolerance in soybean.

At this point, Prof. Rongxia Guan (the lead researcher from CAAS on this project) contacted us, seeking our assistance to further characterise the role of the gene. They sent us the seeds of soybean cultivars Tiefeng 8 and 85-140 and clones of the gene from the sensitive and tolerant parent.

In 2014, for this initial publication it was decided that I would: perform a phylogenetic analysis according to GmSALT3's amino acids sequence; carry out cellular localisation analysis through *in-situ* PCR; identify GmSALT3 subcellular localisation analysis in the transient expression system of *Arabidopsis* mesophyll protoplasts; and, draft the manuscript. Our collaborators performed qPCR of *GmSALT3* in different tissues; subcellar localisation of GmSALT3 in *Nicotiana benthamiana* protoplasts; Na^+ content measurement and grafting experiments; distribution analysis of *GmSALT3* haplotypes in China. We then worked on the manuscript together and published our work in *The Plant Journal* as the featured and cover article in December 2014 (Guan *et al.*, 2014b).

In addition, we have since published a summary of this work for industry after being contacted by the online newsletter, Information Systems for Biotechnology (ISB) from the US (Qu *et al.*, 2015), included in Appendix I. This research received significant attention from plant scientists (e.g. a feature in the Society of Experimental Biology magazine, v1. 2015) and the

media (Altmetric Score 48); we even received a letter from the Premier of South Australia to congratulate us on the product of our research collaboration. We have been contacted by breeders from the major soybean growing areas of China, US, Argentina/Brazil and Canada for advice on how to use the primers to screen for the presence of the gene.

Statement of Authorship

Title of Paper	Salinity tolerance in soybean is modulated by natural variation in GmSALT3
Publication Status	☑ Published ☐ Accepted for Publication ☐ Submitted for Publication ☐ Unpublished and Unsubmitted w ork w ritten in manuscript style
Publication Details	The Plant Journal (2014) 80, 937–950

Principal Author

Name of Principal Author (Candidate)	Yue Qu		
Contribution to the Paper	YQ performed the in situ expression and subcellular localisation, and phylogeny analysis of the *GmSALT3*, I also played the major role in writing the paper.		
Overall percentage (%)	50%		
Certification:	This paper reports on original research I conducted during the period of my Higher Degree by Research candidature and is not subject to any obligations or contractual agreements with a third party that would constrain its inclusion in this thesis. I am the primary author of this paper.		
Signature		Date	12.08.17

Co-Author Contributions

By signing the Statement of Authorship, each author certifies that:

i. the candidate's stated contribution to the publication is accurate (as detailed above);

ii. permission is granted for the candidate in include the publication in the thesis; and

iii. the sum of all co-author contributions is equal to 100% less the candidate's stated contribution.

Name of Co-Author	Rongxia Guan		
Contribution to the Paper	RG performed the map-based cloning of GmSALT3, and analysed the data, also contributed to writing the paper.		
Signature		Date	08.08.2017

Name of Co-Author	Yong Guo		
Contribution to the Paper	YG performed the genomic variation screen of GmSALT3 in Tiefeng 8 and 85–140		
Signature		Date	11.08.2017

Name of Co-Author	Lili Yu		
Contribution to the Paper	LY performed gene expression, variation of promoter region analysis and statistical analysis		
Signature		Date	11.08.2017

Name of Co-Author	Ying Liu		
Contribution to the Paper	YL, JJ and JC performed recombinant identification and NIL testing		
Signature		Date	11.08.2017

Name of Co-Author	Jinghan Jiang		
Contribution to the Paper	YL, JJ and JC performed recombinant identification and NIL testing		
Signature		Date	10.08.2017

Name of Co-Author	Jiangang Chen		
Contribution to the Paper	YL, JJ and JC performed recombinant identification and NIL testing		
Signature		Date	11.08.2017

Name of Co-Author	Yulong Ren		
Contribution to the Paper	YR performed subcellular localization of GmSALT3		
Signature		Date	11.08.2017

Name of Co-Author	Guangyu Liu		
Contribution to the Paper	GL performed evaluation of the salt tolerance of germplasm		
Signature		Date	11. 08. 2017

Name of Co-Author	Lei Tian		
Contribution to the Paper	LT made the cross of Tiefeng 8 and 85–140		
Signature		Date	09. 08. 2017

Name of Co-Author	Longguo Jin		
Contribution to the Paper	LJ helped construct vectors		
Signature		Date	11. 08. 2017

Name of Co-Author	Zhangxiong Liu		
Contribution to the Paper	ZL and HH performed the field experiment on populations		
Signature		Date	11.08.2017

Name of Co-Author	Huilong Hong		
Contribution to the Paper	ZL and HH performed the field experiment on populations		
Signature		Date	11.08.2017

Name of Co-Author	Ruzhen Chang		
Contribution to the Paper	RC contributed to the experimental design and material selection		
Signature		Date	11.08.2017

Name of Co-Author	Matthew Gilliham		
Contribution to the Paper	LQ and MG designed most of the experiments and directed the project, also contributed to writing the paper.		
Signature		Date	7/9/2017

Name of Co-Author	Lijuan Qiu		
Contribution to the Paper	LQ and MG designed most of the experiments and directed the project, also contributed to writing the paper.		
Signature		Date	8.8.2017

the plant journal

VOLUME 80 | NUMBER 6 | DECEMBER 2014
http://www.theplantjournal.com | ISSN 0960–7412
WILEY Blackwell

the plant journal

SEB Society for Experimental Biology

The Plant Journal (2014) **80**, 937–950 doi: 10.1111/tpj.12695

Salinity tolerance in soybean is modulated by natural variation in *GmSALT3*

Rongxia Guan[1,†], Yue Qu[2,†], Yong Guo[1,†], Lili Yu[1,†], Ying Liu[1], Jinghan Jiang[1], Jiangang Chen[1], Yulong Ren[1], Guangyu Liu[1], Lei Tian[1], Longguo Jin[1], Zhangxiong Liu[1], Huilong Hong[1], Ruzhen Chang[1], Matthew Gilliham[2,*] and Lijuan Qiu[1,*]

[1]The National Key Facility for Crop Gene Resources and Genetic Improvement (NFCRI), Institute of Crop Science, Chinese Academy of Agricultural Sciences, No. 12 Zhongguancun South Street, Haidian District, 100081 Beijing, China, and

[2]ARC Centre of Excellence in Plant Energy Biology, School of Agriculture, Food and Wine and Waite Research Institute, University of Adelaide, Glen Osmond, SA 5064, Australia

Received 18 July 2014; revised 25 September 2014; accepted 30 September 2014; published online 10 August 2014.
*For correspondence (e-mails qiulijuan@caas.cn; matthew.gilliham@adelaide.edu.au).
†These authors have contributed equally to this work.

SUMMARY

The identification of genes that improve the salt tolerance of crops is essential for the effective utilization of saline soils for agriculture. Here, we use fine mapping in a soybean (*Glycine max* (L.) Merr.) population derived from the commercial cultivars Tiefeng 8 and 85–140 to identify *GmSALT3* (salt tolerance-associated gene on chromosome 3), a dominant gene associated with limiting the accumulation of sodium ions (Na^+) in shoots and a substantial enhancement in salt tolerance in soybean. *GmSALT3* encodes a protein from the cation/H^+ exchanger family that we localized to the endoplasmic reticulum and which is preferentially expressed in the salt-tolerant parent Tiefeng 8 within root cells associated with phloem and xylem. We identified in the salt-sensitive parent, 85–140, a 3.78-kb copia retrotransposon insertion in exon 3 of *Gmsalt3* that truncates the transcript. By sequencing 31 soybean landraces and 22 wild soybean (*Glycine soja*) a total of nine haplotypes including two salt-tolerant haplotypes and seven salt-sensitive haplotypes were identified. By analysing the distribution of haplotypes among 172 Chinese soybean landraces and 57 wild soybean we found that haplotype 1 (H1, found in Tiefeng 8) was strongly associated with salt tolerance and is likely to be the ancestral allele. Alleles H2–H6, H8 and H9, which do not confer salinity tolerance, were acquired more recently. H1, unlike other alleles, has a wide geographical range including saline areas, which indicates it is maintained when required but its potent stress tolerance can be lost during natural selection and domestication. *GmSALT3* is a gene associated with salt tolerance with great potential for soybean improvement.

Keywords: *Glycine max* (L.) Merr., *Glycine soja* Sieb. et Zucc, salt tolerance, natural variation, salt exclusion, haplotype, geographical distribution, CHX20, CHX.

INTRODUCTION

Excessive dissolved salts in soils can limit crop yield (Munns and Tester, 2008). Salt-affected soils currently account for 8% of the world's total land area (FAO, 2000), and the area of salt-affected agricultural land is predicted to double by 2050 for irrigated agriculture and some semi-arid areas (Pitman and Läuchli, 2002; Rengasamy, 2006). The area of salt-affected irrigated land, which produces 40% of the world's food, already stands at 20% (Pimentel *et al.*, 2004). In light of the predicted 70–110% increase in food production that will be needed by 2050 to feed the rapid growth in global population over the same period (Tilman *et al.*, 2011), and with no current option for expanding the area of agricultural land, an increase in the salt tolerance of conventional crops will be required to assist in improving crop productivity and food security (Yamaguchi and Blumwald, 2005).

Soybean (*Glycine max*) is a major agricultural crop that is used widely for providing human and animal food because of its high oil and protein content (18 and 38%, respectively) (Singh, 2010). Soybean is classified as a moderately salt-sensitive crop (Munns and Tester, 2008). In one study soybean production was reduced by 40% with increasing salinity stress (from 2 to 7 dS m^{-1}; 1 dS m^{-1} = 700 mg L^{-1}) (Papiernik *et al.*, 2005). However, soybean germplasm has been shown to display a

spectrum of salt-tolerance phenotypes (Phang *et al.*, 2008), with salt-sensitive cultivars encountering a 37% lower yield than tolerant cultivars under saline field conditions (Parker *et al.*, 1983). This natural variation in salt tolerance indicates there is potential for identifying genes that increase soybean production under saline conditions. However, there is limited detailed information on the mechanisms that impart this variation in salt tolerance in soybean. The primary lead is a major quantitative trait locus (QTL) related to salt tolerance that has been repeatedly mapped within a region of soybean linkage group N (chromosome 3) (Lee *et al.*, 2004; Hamwieh and Xu, 2008; Hamwieh *et al.*, 2011; Ha *et al.*, 2013). We have previously mapped a dominant gene associated with improved salt tolerance to the same region using three F_2 populations derived from the following crosses between salt-tolerant and salt-sensitive varieties: Wenfeng 7 × Union, Jindou 33 × Hark, and Tiefeng 8 × Zaoshu 6 (Zhang, 2005). Recently, by using a $F_{2:3}$ population derived from the salt-tolerant variety Tiefeng 8 and the salt-sensitive variety 85–140, we mapped the dominant salt-tolerance gene from Tiefeng 8 to a 209-kb region on soybean chromosome 3 (Guan *et al.*, 2014).

In this study, we use map-based cloning to identify the causal gene underlying this salt-tolerance locus. We found that the dominant gene associated with salt tolerance (*GmSALT3*, *Glycine max* salt tolerance-associated gene on chromosome 3) was expressed predominantly in roots within vascular-associated cells and encoded a protein from the cation/H^+ exchanger family that we localized to the endoplasmic reticulum (ER). Expression of *GmSALT3* was associated with lower sodium accumulation in shoots and a significantly greater salt tolerance. We genotyped and phenotyped a combined total of over 200 soybean landraces and wild soybean originating from across China to identify nine haplotypes for this gene. The tolerant haplotypes were found to have a wider geographical range but were most commonly found close to salinized areas, whereas the salt-sensitive haplotypes predominantly originated from areas that are not known for high salt concentrations in soils. This coupled with the low genetic diversity of the salt-tolerant alleles suggests that *GmSALT3* is under strong selection pressure when required but can be lost when this pressure is removed resulting in a decrease in the salt tolerance of the plant. The identification of *GmSALT3*, which encodes a cation/proton exchanger family member, is likely to have significance for soybean and other crop breeding programmes.

RESULTS

Map-based cloning of the salt-tolerance associated gene in soybean variety Tiefeng 8

We constructed a population of 367 recombinant inbred lines (RILs) derived from the F_2 population of a cross between the salt-tolerant variety Tiefeng 8 and the salt-sensitive variety 85–140 (Figure 1a). The dominant gene associated with the salt-tolerance phenotype was mapped between indel markers QS1101 and QS100011 on chromosome 3 (Figure 1b), and was named *GmSALT3*. To fine map the *GmSALT3* locus, we self-pollinated the F_5 plants heterozygous between indel markers QS1101 and QS100011, and planted the $F_{5:6}$ population (5769 individuals) in the winter of 2010 on Hainan Island, China. Seventy-four recombinants between QS1101 and QS100011 were identified, and we determined their salt tolerance phenotypes in 2011 and 2012 by progeny testing. We obtained five plants containing recombinants between two markers QS100001 and QS1119. Two recombinants exhibited salt sensitivity and two exhibited salt tolerance, while line 3751 was segregating for the phenotype. The progeny testing of the recombinant plants allowed the locus *GmSALT3* to be mapped to a 17.5-kb region between indel marker QS100001 and cleaved amplified polymorphic sequence marker QS1119 (Figure 1c, Table S1 in Supporting Information). There was only one gene predicted to be present within this 17.5-kb region according to the soybean reference genome that has been obtained from the variety Williams 82. This gene, *Glyma03g32900.1*, was regarded as the candidate causal gene underlying *GmSALT3*. To explore whether variation in the salt-tolerance phenotype was due to a difference in the coding sequence of *Glyma03g32900.1*, RNA sequencing (RNA-seq) of two RNA pools consisting of either 20 salt-sensitive or 20 salt-tolerant F_6 plants derived from the cross between 85–140 and Tiefeng 8 was performed. The results indicated that the *GmSALT3* cDNA obtained from Tiefeng 8 was 2640 bp in length, consisting of an open reading frame (ORF) of 2436 bp with 5′ and 3′ untranslated regions (UTR) of 50 and 204 bp, respectively, whilst the ORF from 85 to 140 was 1131 bp (Figure S1a). After comparing the genomic sequence in the two parents it was apparent that there was a 3.78-kb fragment inserted in exon 3 of *Gmsalt3* in 85–140, comprising of long terminal repeats (LTRs) of length 643 and 647 bp that had 99.1% similarity to each other. The element was flanked with a 5-bp target-site duplication sequence (CATGG) and reverted 2-bp repeat (TG ... CA) (Figure 1d). This resulted in a truncated *Gmsalt3* transcript in 85–140 yielding only 376 amino acids (Figure S1b).

Identity and expression of *GmSALT3*

Basic local alignment search tool (BLASTX, NCBI, http://blast.ncbi.nlm.nih.gov) (translated) analysis of the GmSALT3 cDNA sequence showed that GmSALT3 shared 73% identity with an uncharacterized protein annotated as a K^+/H^+ antiporter (MTR_7g099820) from *Medicago truncatula* and 59% identity with the characterized *Arabidopsis thaliana* AtCHX20 (Figure 2a). Accordingly, GmSALT3 had a confidently predicted 'sodium/proton exchanger' (NHE) domain (Pfam00999, *e*-value of 2.9e-69), a diagnostic of cation/proton exchangers in plants (Chanroj *et al.*, 2011),

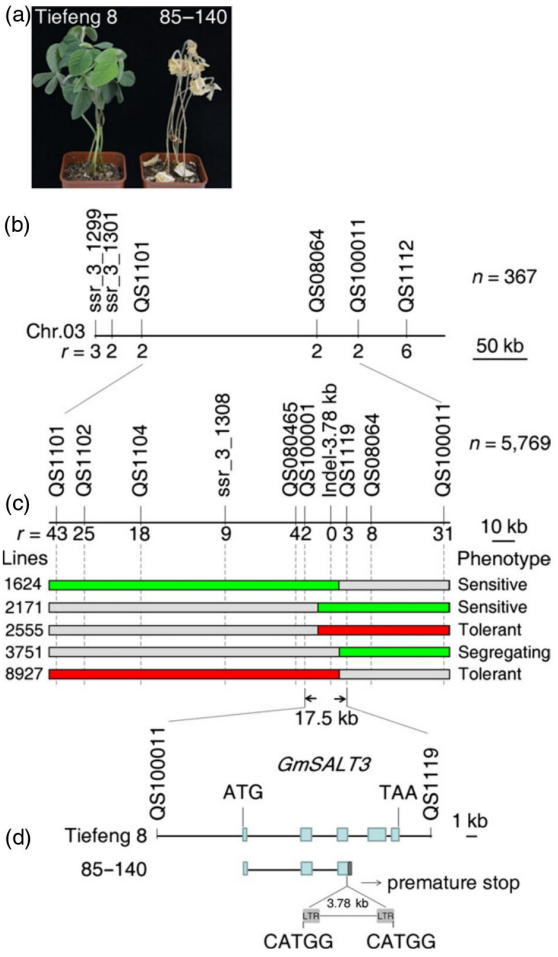

Figure 1. Positional cloning of *GmSALT3* in soybean.
(a) The phenotype of Tiefeng 8 (left) and 85–140 (right) treated with 200 mM NaCl for 18 days.
(b) *GmSALT3* was first mapped on chromosome 3 between indel markers QS1101 and QS100011 using 367 F_6 recombinant inbred lines. R is the number of recombinants containing the marker.
(c) Chromosomal constitutions of five recombinants (lines 1624, 2171, 2555, 3571 and 8927) are shown with their salt tolerance. Positional cloning narrowed the *GmSALT3* locus to a 17.5-kb region between QS100001 and QS1119, and only one gene is predicted to be located in this region. Red and green represent homozygous Tiefeng 8 and 85–140, respectively, grey represents heterozygous.
(d) Sequencing revealed a 3.78-kb copia retrotransposon insertion in the coding region of the respective gene in 85–140; this insertion resulted in a truncated transcript in 85–140 that we called *Gmsalt3*.

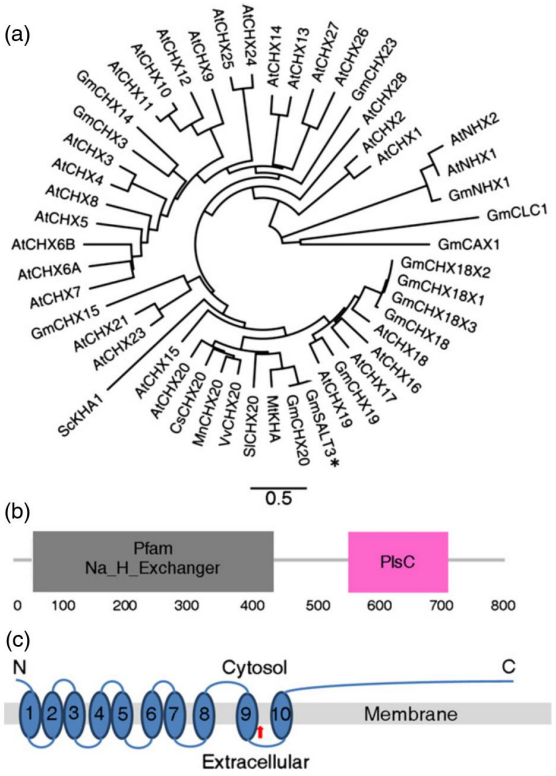

Figure 2. Sequence analysis of *GmSALT3*.
(a) Phylogenetic tree based on multiprotein sequence alignment of *GmSALT3* to Arabidopsis CHX proteins and other related proteins. Multiprotein sequence alignment (Geneious Alignment) was achieved using Geneious Pro version 5 (Drummond *et al.*, 2011). All the protein sequences were obtained from the NCBI database (http://www.ncbi.nlm.nih.gov/protein/). At, *Arabidopsis thaliana*; Sc, *Saccharomyces cerevisiae*; Vv, *Vitis vinifera*; Cs, *Cucumis sativus*; Gm, *Glycine max*; Sl, *Solanum lycopersicum*; Mn, *Morus notabilis*; Mt, *Medicago truncatula*. GmCHX20* indicates CHX20 from the sequenced soybean cultivar Williams 82. The scale bar denotes the scale of amino acid substitutions.
(b) Structural schematics of soybean GmSALT3 according to SMART analysis (Schultz *et al.*, 2000); two predicted domains are observed in the GmSALT3 protein sequence. PlsC is an outlier homologue defined as a phosphate acyltransferase.
(c) Predicted topology of GmSALT3 in the membrane using TMHMM version 2.0 (Möller *et al.*, 2001). Putative transmembrane domains are numbered (N-best algorithm). The arrow indicates the beginning of truncation of GmSALT3. N, N-terminus; C, C-terminus.

that started near the N-terminus between amino acids 30 and 428 as well as 10 predicted transmembrane domains (TMDs) (Figures 2b,c and S1b). The truncation of GmSALT3 (at amino acid 370) lies between TMD 9 and TMD 10, which would result in the loss of the TMD 10 domain and the C-terminus.

We investigated the expression pattern of *GmSALT3* by quantifying the relative abundance of the mRNA in different organs of Tiefeng 8 and 85–140. The expression was much higher in roots than shoots of Tiefeng 8, while the transcripts were not detectable in tissues of 85–140 (Figure 3a). After 6 h of 200 mM salt treatment the transcript abundance of *GmSALT3* decreased in Tiefeng 8; however, after 3 days it recovered to higher levels (Figure 3a). Using *in situ* PCR, as shown in Figure 3, we detected the expression of *GmSALT3* predominantly within endodermal cells and cells associated with phloem and xylem of salt-tolerant Tiefeng 8 soybean root (Figure 3b,c) and within proto-phloem cells in young secondary root

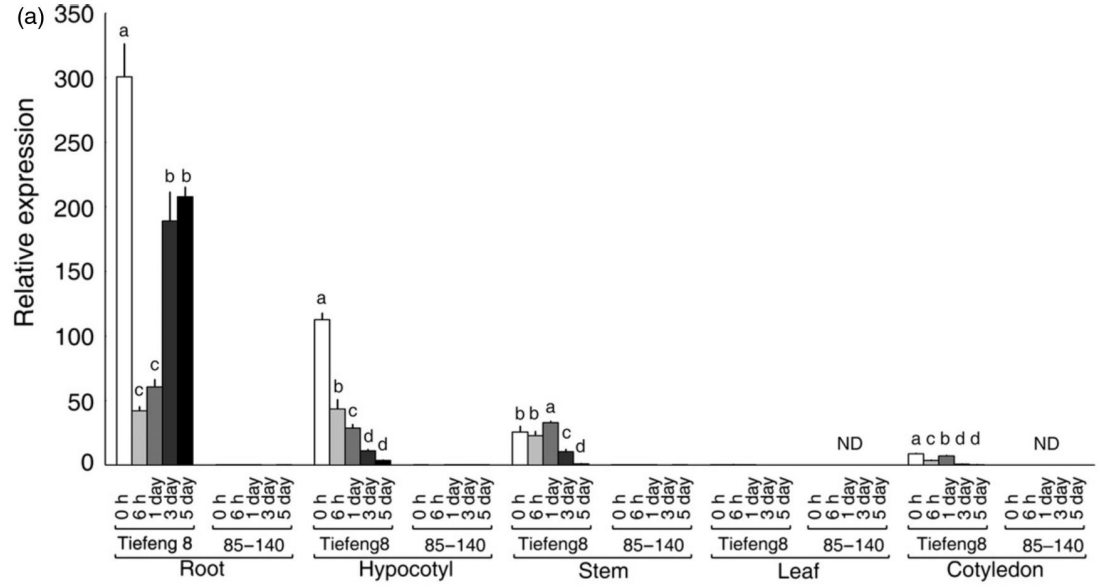

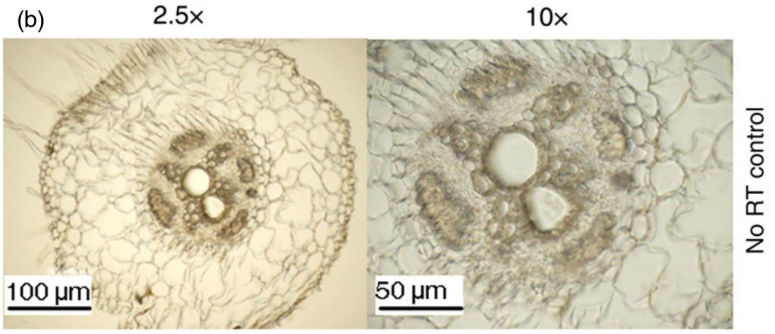

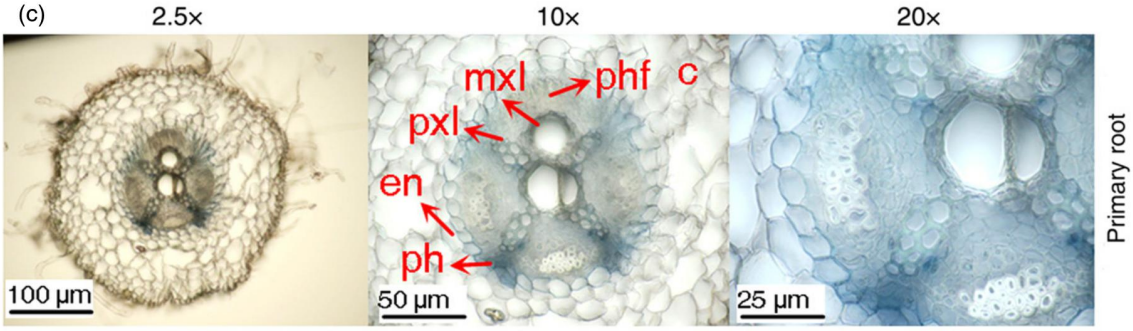

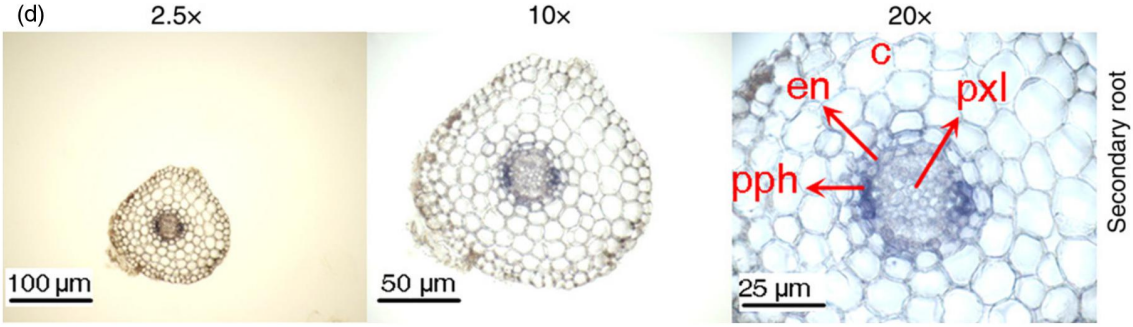

Figure 3. *GmSALT3* expression and tissue localization.
(a) Expression of *GmSALT3* analysed using quantitative real-time PCR (qRT-PCR) in root, hypocotyl, stem, leaf and cotyledon tissue of Tiefeng 8 and 85–140. The numbers (0, 6 h; 1, 3, 5 days) indicate time points after growing plants under control or salt stress (200 mM NaCl). Transcription levels was calculated as a percentage of the *GmUKN1* transcript. Error bars indicate standard deviations ($n = 3$). Different letters indicate significant differences between treatments for a given organ according to Dunan's multiple range test at $P < 0.05$.
(b) *In situ* PCR in sections (60 μm) of roots of a 4-week-old Tiefeng 8 soybean plant grown in 50/50 perlite/vermiculite with no salt treatment. Blue-stained cells are where transcripts are present. Negative controls (b) without RT (reverse transcription) were included to show lack of genomic DNA contamination.
GmSALT3 is localized in phloem- and xylem-associated primary root cells (c) and in protophloem of secondary root tissues (d). c, cortex; ph, phloem; mxl, metaxylem; phf, phloem fibre; en, endodermis; pxl, protoxylem; pph, protophloem.

(Figure 3d); the localization was unchanged under salinity treatment (Figure S2). In stems and leaves, *GmSALT3* shared a similar expression pattern as in the root (Figure S3). In order to corroborate cell localization we cloned the putative promoter of *GmSALT3* and expressed *GmSALT3-pro::β-glucuronidase* in *A. thaliana*; GUS was detected mainly in vascular tissues of root, hypocotyls and leaves (Figure S4).

It is noteworthy that the expression pattern of *GmSALT3* was different from that of *AtCHX20*, the closest functionally characterized homolog of *GmSALT3*, expressed in stomatal guard cells (Padmanaban *et al.*, 2007). However, as was found for AtCHX20 (Chanroj *et al.*, 2011), we observed an endomembrane (ER) localization for the GmSALT3 protein. This was initially determined by transiently expressing *P35S:GmSALT3-GFP* (green fluorescent protein) in *Nicotiana benthamiana* leaves with more than 90% of the protoplasts expressing the construct displaying clear tubular and sheet-like structures (Figure 4a). This contrasts with the expression of free GFP where more than 90% of the protoplasts displayed cytosolic and nuclear fluorescence (Figure 4d). To further assess the localization, *GmSALT3-GFP* was co-expressed with mCherry with an ER retention sequence (Figure 4g). As shown in Figure 4(i), GFP signals overlapped with the mCherry signals, consistent with GmSALT3-GFP being localized to the ER, whereas cytosolic GFP did not overlap with ER-localized mCherry (Figure 4f). Furthermore, N- and C-terminal *YFP* (yellow fluorescent protein) fusions of *GmSALT3* were transiently expressed in Arabidopsis mesophyll protoplasts and were found to co-localize with a fluorescent ER marker not a late endosomal/vacuolar marker (Figure S5).

Collectively, these results indicate that *GmSALT3* is likely to encode an ER-localized protein that is expressed in vasculature-associated cells, predominantly within roots.

GmSALT3 confers sodium exclusion in shoots

Salt tolerance in soybean is associated with limiting Na^+ accumulation in shoots (Liu *et al.*, 2011; Jiang *et al.*, 2013). To investigate the role of *GmSALT3*, the Na^+ accumulation within the two parents was compared. The Na^+ content in roots of the parents was similar, but following NaCl treatment (200 mM), Tiefeng 8 accumulated significantly less Na^+ than 85–140 in both stems (after 5 days) and leaves (after 7 days) (Figure 5a). To compare the function of the two *GmSALT3*/*Gmsalt3* alleles, we developed a pair of near isogenic lines (NILs) NIL-T (*GmSALT3*) and NIL-S (*Gmsalt3*). Both NIL-T and NIL-S were derived from a single F_6 plant of a cross between 85–140 and Tiefeng 8 that was heterozygous for the *GmSALT3* locus. These lines had no polymorphism among 147 simple sequence repeat (SSR) markers distributed throughout the genome except for those located within the *GmSALT3* locus. Under control conditions, the NILs had no significant difference in agronomic traits, such as 100-seed weight, protein and oil content, but had differential salt tolerance (Figure S6). The Na^+ content in stems and leaves of self-grafted NIL-S was much higher than that in NIL-T (Figure 5b). When the NIL-S scion was grafted on the NIL-T rootstock, the Na^+ content in stems and leaves decreased by 48.7 and 70.65%, respectively, compared with the self-grafted NIL-S. In contrast, the Na^+ content in stems and leaves of the NIL-T scion grafted to the NIL-S root increased by 79.0 and 139.1%, respectively, compared with self-grafted NIL-T (Figure 5b). These results suggest that *GmSALT3* is likely to function in the root (and hypocotyl) and constrain Na^+ translocation to the lamina; this is consistent with the predominant expression pattern of *GmSALT3* in Tiefeng 8 in roots and hypocotyls (Figure 3a).

Geographical distribution of haplotypes reveals that the salt-tolerant H1 is a likely target of natural and artificial selection

To identify allelic variation, the coding region of the *GmSALT3* locus from 31 soybean landraces was sequenced. Five haplotypes (H) were observed in these accessions including the haplotypes found in Tiefeng 8 (H1) and 85–140 (H2) (Table S2). Of the newly identified haplotypes, when compared with H1, H3 had nine non-synonymous SNPs, H4 had seven non-synonymous SNPs and an 18-bp deletion in exon 3 due to a nucleotide substitution (AG to AT) that was 3′ of the intron 2 splicing site and H5 had a 4-bp deletion in exon 2 that resulted in a premature stop codon (Figure 6a). The promoter region starting 540-bp upstream of the start codon was also sequenced; this which identified eight SNPs and three indels of 1, 4 and either 148 or 150 bp. For the fixed variation between the salt-tolerant and salt-sensitive haplotypes, two insertions of 148 and 4 bp were observed in the promoter

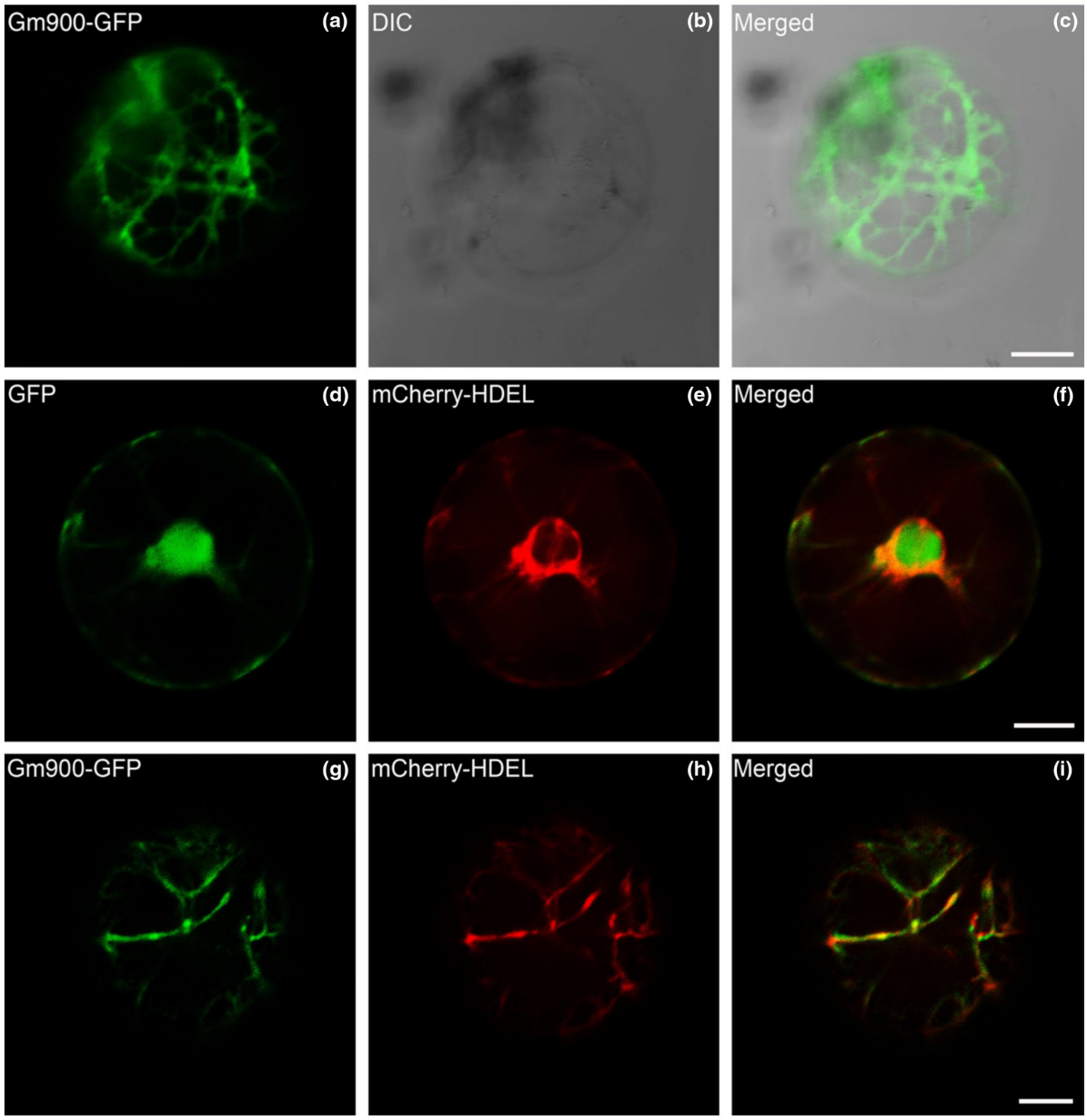

Figure 4. Subcellular localization of GmSALT3.
(a–c) Subcellular localization of GmSALT3 in *Nicotiana benthamiana* protoplasts. Confocal microscopy images of GmSALT3-GFP expression. DIC, differential interference contrast.
(d–f) Co-expression of free GFP and mCherry-HDEL (an endoplasmic reticulum marker).
(g–i) Co-expression of GmSALT3-GFP and mCherry-HDEL. Bars = 10 μm.

region 152 and 103 bp before the start codon, respectively, in H3 and H4, whilst insertions of 150 and 4 bp were identified at those same locations in the promoter region of H5 (Figure 6a).

Using this sequence information we developed a set of haplotype-specific markers to genotype 172 soybean landraces from the Chinese soybean minicore collection (this included the 31 sequenced accessions used above) (Tables S1 and S3). The soybean minicore collection was selected to represent the maximum genetic diversity of Chinese soybean landraces and has been successfully used to study natural variation in the domestication-related gene *GmTfl1* (Tian *et al.*, 2010). The salt sensitivity of these landraces was screened four times from 2009 to 2011

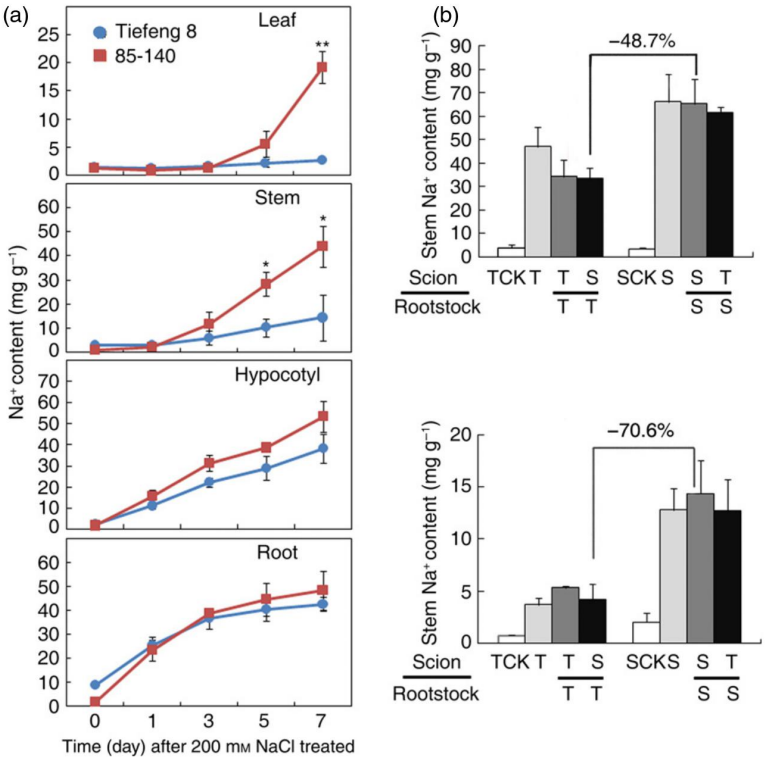

Figure 5. Variation in Na^+ accumulation related to the presence of *GmSALT3* or *Gmsalt3*.
(a) The Na^+ content in Tiefeng 8 (blue) and 85–140 (red) under control or NaCl stress (200 mM NaCl) for 0, 1, 3, 5 or 7 days. Data are means of three replicates ± SE. Asterisks indicates a significant difference between Tiefeng 8 and 85–140 at $*P < 0.05$, $**P < 0.01$.
(b) The Na^+ content in the stem and leaf of non-grafted, self-grafted and reciprocally grafted lines NIL-T (*GmSALT3*) and NIL-S (*Gmsalt3*) under salt stress for 8 days. TCK and SCK: NIL-T and NIL-S, respectively, under control conditions. Data are means of three replicates ± SE.

(Table S2). Of the 172 representative accessions, 73 out of the 76 salt-tolerant accessions shared H1; 14 salt-sensitive and 1 salt-tolerant landraces contained H2; 5 salt-sensitive accessions contained H3; 25 salt-sensitive and 3 salt-tolerant accessions contained H4; and 45 salt-sensitive accessions contained H5. Three heterozygous landraces were excluded from further analyses. We analysed the geographical distribution of the five haplotypes represented in this minicore collection. Haplotype 1 was observed in the three main growing ecoregions (Tian *et al.*, 2010), and was mostly distributed in the northern eco-region (NR) and the Huang-Huai ecoregion (HR); most H2-containing accessions originated from the northern eco-region (NR), H3 was distributed mainly in the southern eco-region (SR); H4 and H5 were observed in the SR and Huang-Huai ecoregion (HR), but were mainly found in SR (Figure 6b,c).

To further examine the relationship between salt tolerance and the *GmSALT3*/*Gmsalt3* alleles, we sequenced 22 wild soybean (*Glycine soja* Sieb. et Zucc.) that differed in their salt tolerance. Four of the haplotypes observed in soybean landraces were found in wild soybean but not H2, and four new haplotypes (H6–H9) were found. Compared with H1, H6 had a 21-bp deletion in exon 5, and H8 and H9 had three different non-synonymous SNPs from that of H3 (Figure 7a). Haplotype-specific markers were used to genotype the 57 wild soybean (including the 22 that we had sequenced). As we observed for the soybean landraces, H1 was mainly in salt-tolerant germplasm (Figure S7a,b). In addition the two wild accessions containing H7 were both salt tolerant, whilst the other haplotypes were predominantly found in salt-sensitive wild accessions (Figure S7a,b, Table S4). In wild soybean, H1 and H7 were mainly distributed in the NR and HR regions, H3 was seen only in the SR, H4 was present in both NR and SR regions and H5 and wild soybean-specific H6, H8 and H9 haplotypes were mainly present in SR. This suggests that the distribution of haplotypes in landraces and wild soybean plants were similar (Figure 7b). As annotated in Figure 7(b), most of the saline soil in China is distributed in four main areas: the eastern coast of China including Jiangsu, Shandong, Hebei and Liaoning provinces; the North China plain, the north-east Songnen plain and the inland region of north-east China. There are also isolated saline fields with a scattered distribution south of the Yangtze River, within Zhejiang, Fujian and Guangdong provinces (Wang, 1993; Tang and Qiao, 2008; Yang, 2008). The coincidence of salt-affected soils and the salt-tolerant H1 and H7 haplotypes indicates that these alleles are likely to be a major selection factor determining the distribution and utilization of soybean especially on saline soils. Consistent with this hypothesis is the significant association observed between those wild soybean accessions that contain H1 and H7 and their proximity to the known saline-affected regions compared with those that

(a)

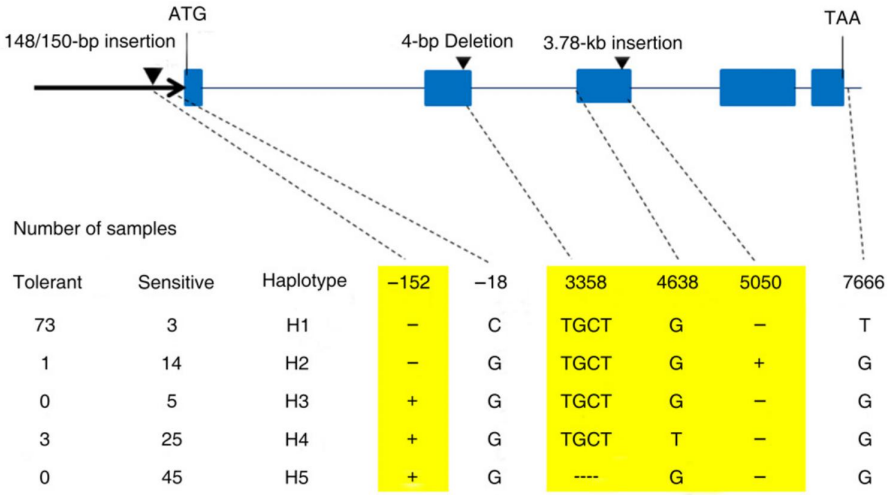

Number of samples

Tolerant	Sensitive	Haplotype	−152	−18	3358	4638	5050	7666
73	3	H1	−	C	TGCT	G	−	T
1	14	H2	−	G	TGCT	G	+	G
0	5	H3	+	G	TGCT	G	−	G
3	25	H4	+	G	TGCT	T	−	G
0	45	H5	+	G	----	G	−	G

(b)

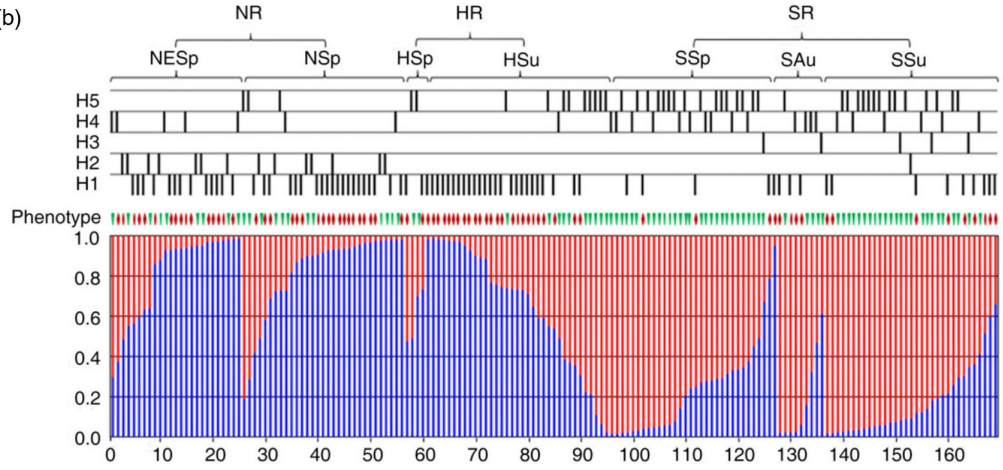

(c)

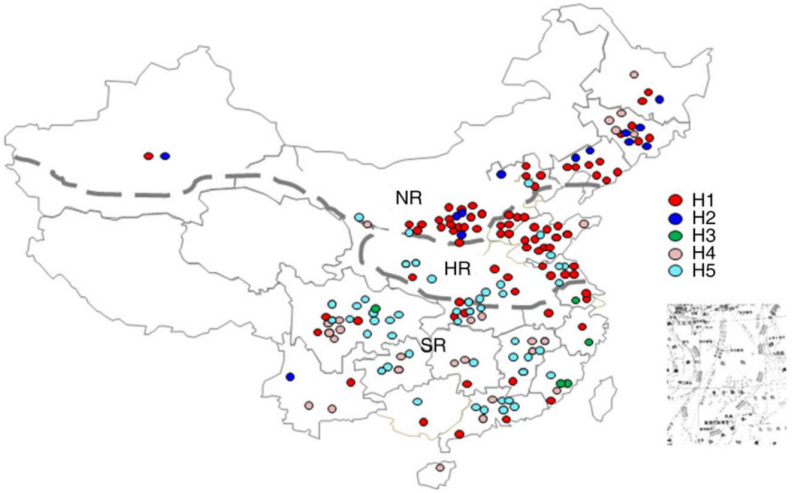

Figure 6. Distribution of five haplotypes of the *GmSALT3* gene in a soybean minicore collection from different ecoregions of China.
(a) Five haplotypes in the 172 minicore collection of Chinese soybean landraces and their relationship with salt tolerance. +/–, with or without the insertion in the promoter or exon region.
(b) Genetic structure of populations based on data from 30 simple sequence repeat markers distributed on 20 soybean chromosomes. The length of each coloured segment indicates the attribution of ancestry of each accession. The distribution of each haplotype in ecoregions and phenotypes is indicated by red diamonds and green down triangles and is shown above the plot of population structure. NR, northern ecoregion, including the north-east spring subregion (NESp) and the north spring subregion (NSp); HR, Huang-Huai region, including the Huang-Huai spring subregion (HSp) and the Huang-Huai summer subregion; SR, southern ecoregion, including the south spring subregion (SSp), south summer subregion (SSu) and south autumn subregion (SAu).
(c) Geographic distribution of five haplotypes (H1–H5) in three soybean growing ecoregions (NR, HR and SR) in China.

contain the other haplotypes (Figure S7c) (Wilcoxon–Mann–Whitney test, *P*-value 0.000001).

To seek further evidence that the H1 haplotype has been under selection we analysed the nucleotide diversity of H1–H5 in the landraces within a non-coding region (1267 bp of intron 2) and found the genetic diversity of this introgenic region in H1 (π = 0.00035) was only 5.5% of that in the sensitive haplotypes H3–H5 (π = 0.00632). Furthermore, we examined the genetic diversity of 18 SNPs within 12 genes on chromosome 3 within 194 kb of the *GmSALT3* gene (Figure S8a). The collective genetic diversity in H1 landraces ranged from 0 to 0.1142, with an average of 0.0341, while the diversity in salt-sensitive haplotypes (H2–H5) ranged from 0.0435 to 0.4999, with an average of 0.3250. In contrast, when we analysed the genetic diversity of randomly selected regions of the genome away from *GmSALT3* we found that diversity was similar across all haplotypes, being 0.2428 in H1 and 0.2689 in H2–H5 (Figure S8b). Taken together, we conclude that the low genetic diversity of salt-tolerant haplotypes is likely to be a result of severe selection pressure.

To examine the relatedness of the nine haplotypes and to determine which haplotype is the likely ancestral allele in soybean we again compared their sequence, their geographical distribution and their salt-tolerance phenotypes. The salt-tolerant H1 is the most frequently found haplotype in both wild soybean and landraces, and it has the widest geographical range. The other salt-tolerant haplotype, H7, which was found only twice and only in wild soybean is identical to H1 except for one non-synonymous SNP, whilst H2 was identical to H7 except for the 3.78-kb copia retrotransposon insertion (Figure 7a). Furthermore, both H2 and H7 were found predominantly in the NR (Figures 6c and 7b). By comparing nucleotide polymorphisms within the 540-bp promoter sequences we observed that H1, H2 and H7 shared similar variation and H2 and H7 shared exactly the same sequence, as did H3, H4 and H8, and H5, H6 and H9 (Figure 7a). Collectively, this suggests that H2 was derived from H7 during or after domestication, and H7 was derived from H1. The other six salt-sensitive haplotypes were separated from H1 and H7 by a series of mutation events but shared a fixed variation of a 148/150-bp and 4-bp insertion at the promoter region, indicating that these variations come from a common haplotype that was not detected in the 57 wild soybean used in this study (Figure 7c,d). To explore how these fixed variations in the promoter region affect gene expression we examined *GmSALT3* transcript abundance in the soybean cultivars Mayibao (containing H3) and Jinshanchamoshidou (containing H4) and found that the expression of *GmSALT3* in the roots of these two soybean cultivars was significantly lower than that of Tiefeng 8 under both control and salt-stressed conditions (Figure S8c,d).

To examine if the relationship between salt tolerance and the salt-tolerant alleles held in germplasm introduced from the United States we examined the genotype and phenotype of 12 further soybean accessions including the sequenced Williams 82 (Schmutz *et al.*, 2010). Several formerly reported salt-tolerant accessions, including Lee 68, Forrest and Hartwig, had the H1 haplotype, whilst the sensitive accessions Clark and Williams 82 contained the H2 haplotype (Table S2) (Lee *et al.*, 2008; Valencia *et al.*, 2008).

DISCUSSION

Map-based cloning has been widely used for identifying genes that modulate the salt tolerance of rice, wheat and Arabidopsis, for example *SOS1–3* and *HKT1* (Deinlein *et al.*, 2014). We can now add *SALT3* from soybean to this list. In total, nine haplotypes for this gene were uncovered here, five from landraces and eight from wild soybean. The well-described bottlenecks that occurred during soybean domestication are the likely cause of the fewer haplotypes in landraces compared with wild relatives (Hyten *et al.*, 2006). Similarly, cultivated rice, which like soybean is another species to undergo self-fertilization, contained only 27–32% of the haplotype diversity of wild rice (Londo *et al.*, 2006). Furthermore, our study identified minimal genetic variation between the two salt-tolerant alleles (H1/H7) compared with the more extensive variation in the seven salt-sensitive alleles (H2–H6, H8, H9), with H6–H9 only being found in wild soybean. The observation that H1 is strongly associated with salt tolerance in both landraces and wild soybean indicated that the *GmSALT3* gene is a major salt-tolerance locus in the two species of the *Glycine* genus. This is consistent with both species sharing the major salt-tolerance QTL (Lee *et al.*, 2004; Hamwieh and Xu, 2008; Hamwieh *et al.*, 2011; Ha *et al.*, 2013). Whilst we cannot rule out additional haplotypes, because we surveyed the larger collections of 172 landraces and 57 wild soybean

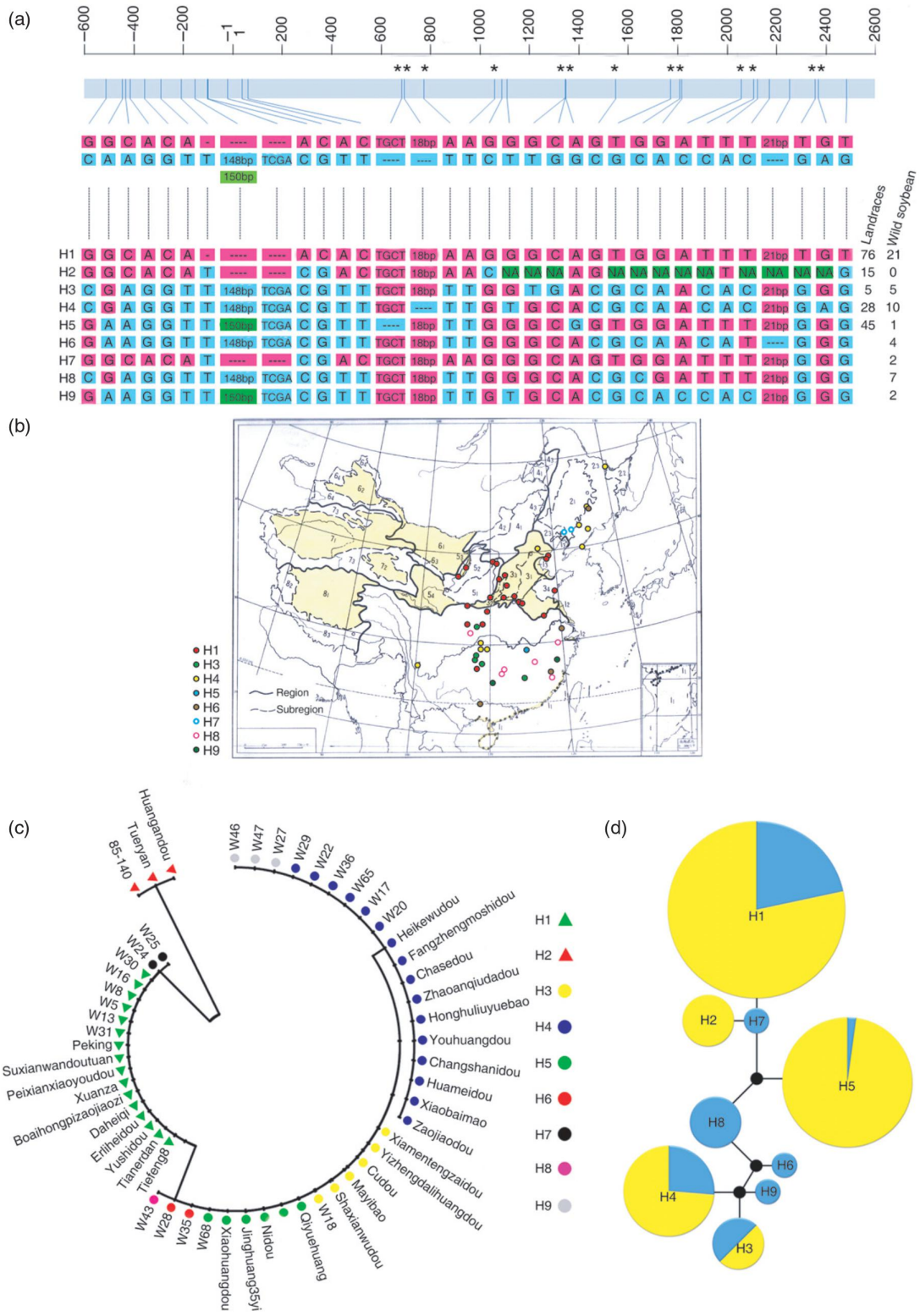

Figure 7. Variation analysis of *GmSALT3* in landraces and wild soybean and haplotype distribution.
(a) Distribution of DNA polymorphisms in the 540-bp promoter region and coding region among 31 landraces and 22 wild soybean. Blue and green indicate the nucleotide difference with Tiefeng 8. The asterisk indicates amino acid change. NA, not detected.
(b) Geographical distribution of eight haplotypes in wild soybean. The regions of saline-affected soil were obtained from Wang (1993) and are presented in yellow on the map.
(c) Phylogenetic tree of 31 landraces and 22 wild soybean based on the polymorphic sites of the *GmSALT3* coding region. Three major groups were identified, one is mainly for the tolerance alleles H1 and H7, the second is for H2, another is mainly for the sensitive alleles H3–H5, H8 and H9.
(d) Haplotype network of the *GmSALT3* coding region in landraces and wild soybean. Circle size is proportional to the number of samples within a given haplotype, and black spots represent unobserved, inferred haplotypes. Lines between haplotypes represent mutational steps between alleles. Yellow, landraces; blue, wild soybean.

with haplotype-specific primers we see no reason why the trend of greater variation in the salt-sensitive alleles should not continue. Several of the accessions of both the landraces and wild soybean were discovered to be heterozygous for *GmSALT3*/*Gmsalt3*. This may have been caused by the bulk analysis of plants with the same morphological traits (Wang *et al.*, 2014). By analysing individuals we could clarify the frequency of each allele, and this information could serve as a further valuable resource for tracing the evolutionary course of the *GmSALT3* gene.

By integrating genotype and phenotype information we have found a clear relationship between H1 and salt tolerance (Figure 6, Tables S2 and S3). The high frequency of H1, its co-occurrence with salt-affected soils, the low genetic diversity of salt-tolerant alleles and the high genetic diversity in the salt-sensitive alleles (Figures 6 and 7a, Tables S2 and S3) are all hallmarks that the H1 allele has been strongly favoured during natural and/or artificial selection. Equivalent attributes of an allele under selection (for pod shattering) have recently been reported in soybean (Dong *et al.*, 2014). Similarly, metal-tolerance genes were found to be responsible for the adaptation of *Arabidopsis lyrata* to serpentine soils (Turner *et al.*, 2010). Furthermore, the observation of a higher frequency of H1 in landraces and wild soybean and the low genetic diversity around this locus indicated that H1 in landraces is a beneficial haplotype; a similar observation was made for the *Accord* insertion associated with DDT resistance in *Drosophila melanogaster* (Schlenke and Begun, 2004). In contrast, the fixed alleles in modern varieties at *tb1* and *SHAT1-5* occurred from new mutations rather than standing ones (Studer *et al.*, 2011; Dong *et al.*, 2014).

We hypothesize that once the selection pressure was released (i.e. when the plants encountered low concentrations of salt in the soil) *GmSALT3* was no longer sensitive to acquiring genetic change, including insertions and deletions, as it resulted in no detrimental effect on the plant phenotype in the low-salt environment. However, the resulting mutations have led to a loss, or reduced function, of the gene product, resulting in a loss of salt tolerance (Figure 5). This greater mutation rate in the salt-sensitive alleles may indicate that the loss of function of *GmSALT3* confers a growth advantage for these plants on non-saline soils. However, we cannot yet confirm this is the case as we detected no growth or yield advantage in the NIL-S lines compared with the NIL-T line when grown under control conditions for the agronomic traits we tested (Figure S5a,b).

Interestingly, there is a small subset of soybean cultivars that contain H1 but are salt sensitive, such as Peking and Baipihuangdou (Figure 6, Table S2). They are likely to contain recent mutations in key salt-tolerance genes such as *SOS1* or *HKT1* (Shi *et al.*, 2000; Xue *et al.*, 2011) or yet to be determined elements that may be a useful source for discovering novel genes involved in salt tolerance in soybean. Furthermore, the four landraces containing H2 or H4, which had a degree of salt tolerance, will arguably be even more valuable as a source for novel determinants of salt tolerance as these accessions are likely to contain gain-of-function mutations in genes other than *GmSALT3*.

GmSALT3 is expressed in root stelar cells, cell types that are already known to have a role in limiting salt transport to the shoot. For instance, HKT1;5-like proteins expressed in these cells retrieve Na^+ from the xylem, and in plants expressing functional alleles this is associated with reduced Na^+ content in shoots and superior salt tolerance in rice, wheat and Arabidopsis (Ren *et al.*, 2005; Møller *et al.*, 2009; Xue *et al.*, 2011; Munns *et al.*, 2012; Byrt *et al.*, 2014). A similar lower Na^+ content in the shoots of salt stressed H1-containing plants, compared with H2, suggests that this gene may also affect transport of Na^+ from root to shoot, and the grafting of NIL-T and NIL-S lines showed that the root and hypocotyls were sufficient to limit the accumulation of Na^+ in the shoot. However, the *GmSALT3* transcript level was first downregulated and then gradually recovered in roots; this is different from the pattern of other salt-tolerance genes (Liu *et al.*, 2000; Shi *et al.*, 2000; Ren *et al.*, 2005), indicating a distinct salt response in soybean or a different role for this gene. Consistent with this is the ER localization we observed for GmSALT3 compared with the plasma membrane localization of HKT or SOS1 proteins. Therefore, *GmSALT3* is unlikely to play a direct role in the retrieval of salt from the xylem but instead may have a role in sensing or responding to salt. CHX proteins have been associated with pH regulation and osmoregulation of cells and are predicted to have a role in vesicle trafficking (Padmanaban *et al.*, 2007). Whether this is the case for *GmSALT3*, and how this confers salt tolerance via the stelar cells of soybean, is a future research priority. Regardless of this, the identification of the gene underlying

this important soybean salt-tolerance allele has provided a clear insight into the molecular basis of both natural and human selection of salt tolerance in soybean, and should facilitate the rapid development of new elite salt-tolerant soybean germplasm by marker-assistant selection.

EXPERIMENTAL PROCEDURES

Plant materials and growth conditions

The minicore collection of Chinese soybean landraces (Table S2) and wild soybean (Table S3) was obtained from Chinese Academy of Agricultural Sciences (CAAS). The parent Tiefeng 8 is a highly salt-tolerant soybean cultivar released in 1970 in Liaoning province. The other parent 85–140 is a salt-sensitive cultivar from Beijing. Soybean was grown in a greenhouse at the Institute of Crop Sciences, Chinese Academy of Agricultural Sciences, Beijing. *Arabidopsis thaliana* ecotype Col-0 and transgenic plants, and *Nicotiana benthamiana* were grown at 22°C in a growth chamber with a 16-h light cycle.

Evaluation of salt tolerance

Evaluation of the salt tolerance of the soybean accessions was carried out in July 2009, 2010 and 2011 using hydroponics (Liu *et al.*, 2011), performed with three replications each time. In 2011, these materials and wild soybean were screened for salt tolerance using vermiculite as the growth medium (Jiang *et al.*, 2013). After being treated for 2 weeks, five to eight plants of each accession in each replication were scored for salt tolerance. A salt-tolerance rating for each of the accession was assigned by the respective level of leaf chlorosis. The salt-tolerance ratings ranged on a scale from 1 (normal green leaves) to 5 (complete death). Accessions showing a leaf scorch score of 1 and 2 were defined as salt tolerant, and those from 3 to 5 were salt sensitive (Tables S2 and S3).

Mapping and cloning of *GmSALT3*

We derived F_1 plants from a cross between 85–140 and Tiefeng 8 and then genotyped the F_1 plants using polymorphic SSR markers between the two parents. A segregating F_2 population ($n = 392$) was developed from the cross between 85–140 × Tiefeng 8. An F_6 RIL mapping population ($n = 367$) developed by single-seed descent was employed in salt-tolerance gene mapping. For fine mapping, 35 F_5 plants heterozygous between marker QS1101 and QS100011 were selected and after selfing we selected recombinants between QS1101 and QS100011 in the 5769 F_6 progeny. Seventy-four recombinants were selected and selfed to produce F_7 seed. We developed markers from the sequence between QS1101 and QS100011 in the Tiefeng 8 and 85–140 genomic DNA for genotyping (Table S1). *GmSALT3* was mapped to within a 17.5-kb region. To obtain candidate gene variations, roots of 20 salt-sensitive and 20 salt-tolerant F_6 families were pooled for RNA-seq. We examined the variation within the mapped region by using the Integrative Genomics Viewer (IGV) to visually assess the transcripts (Robinson *et al.*, 2011). All primers for gene mapping and genotyping are listed in Table S1.

DNA isolation and genotyping of soybean landraces and wild soybean

Genomic DNA was isolated from soybean leaves by using a DNA Purification Kit (Thermo Fisher Scientific, http://www.thermofisher.com/). The insertion/deletion in the promoter and coding regions were screened by using specific primers for the indels (Table S1). The genotyping of SNPs related to the haplotypes and used for genetic diversity testing was done using a Mass ARRAY system following the guidelines of iPLEX Gold Application from Sequenom. Primers of the SNPs are listed in Tables S3 and S5.

Phylogenetic analysis

Coding sequences of *GmSALT3* in 31 landraces and 22 wild soybean were used for phylogenetic analysis. A haplotype network was constructed based on polymorphic sites of the whole coding sequences of *GmSALT3* using the Median-Joining method in the NETWORK version 4.6.1.2 software (Fluxus Technology Ltd, Sudbury, Suffolk, UK) with data preparation using DNASP version 5 (Librado and Rozas, 2009).

Grafting and measurement of Na^+ content

We grew lines NIL-T and NIL-S in a growth chamber with a 16-h light (28°C)/8-h dark (25°C) cycle at 60% humidity. Six days after planting, uniformly healthy plants were selected for grafting (Sheng and Harper, 1997). Fifteen days after grafting, plants were treated with 200 mM NaCl. The Na^+ content in different tissues was measured after 8 days under salt stress as described previously (Jiang *et al.*, 2013).

Quantitative real-time PCR (qRT-PCR) and RNA-seq

Total RNA was extracted from various soybean tissues using TRIZOL reagent (Ambion, http://www.ambion.com). To remove the residual DNA, the extracted RNA was treated with RNase-free DNase I (New England Biolabs, https://www.neb.com) for 30 min at 37°C. Library construction was performed according to the Illumina instructions (http://www.illumina.com) and sequenced using a HiSeq 2000. For gene expression, first-strand cDNA synthesis was done with a PrimeScript RT Reagent Kit (TaKaRa, Japan, http://www.takara.co.jp/english). Real-time PCR was performed using SYBR Premix Ex Taq II (TliRNaseH Plus) (TaKaRa). We normalized the level of *GmSALT3* transcript using the control gene *GmUKN1* (Hu *et al.*, 2009).

Construction and transgenic analysis

We amplified a 1749-bp *GmSALT3* promoter region upstream of the ATG start codon by PCR from Tiefeng 8 genomic DNA. The primer (Promoter) sequences are listed in Table S1. We subcloned the promoter to the binary vector pBI121 to obtain the *GmSALT3* promoter-GUS fusion construct. The construct was introduced into the *Agrobacterium* tumefaciens GV3101 strain. Arabidopsis plants were stably transformed by means of floral dipping (Clough and Bent, 1998). Kanamycin-resistant T_3 transgenic plants were used for GUS staining (Hirakawa *et al.*, 2010). *GmSALT3* (*Xba*I–*Bam*HI) was amplified from Tiefeng 8 and inserted into the pCAMBIA1305-GFP. Constructs were introduced into the *Agrobacterum* strain EHA105 and then used to infiltrate *N. benthamiana* leaves, followed by protoplast isolation as described elsewhere (Ren *et al.*, 2014). *GmSALT3* coding sequences were also cloned into the entry vector PCR8 and subcloned into 35S pBS YFP-*attR* and *attR*-YFP vector using Gateway® LR Clonase® II following the manufacturer's instructions (Invitrogen, http://www.invitrogen.com/). Arabidopsis mesophyll protoplasts were transformed with the *GmSALT3* containing pBS vectors on its own or co-transformed with two Wave line markers (Wave6C and Wave7C) and an ER marker pBIN20-ERcfp as described previously (Nelson *et al.*, 2007; Munns *et al.*, 2012). Fluorescent signals were acquired for GFP (green; excitation 488 nm, emission 514 nm, bandpass 10 nm), YFP

(yellow; excitation 514 nm, emission 540 nm, bandpass 10 nm) and cyan fluorescent protein (blue; excitation 420 nm, emission 458 nm bandpass 20 nm), captured from transformed protoplasts using a confocal laser scanning microscope (Leica TCS SP5, http://www.leica.com/).

In situ PCR

In situ PCR followed Athman *et al.* (2014) with the following modifications. Sections were 50 μm for roots and 70 μm for leaves. Cycling parameters were: initial denaturation at 98°C for 30 sec, then 32 cycles of 98°C for 10 sec, 62°C for 30 sec, 72°C for 12 sec and a final extension at 72°C for 10 min.

Association analysis of distance to saline-affected region and haplotypes

The geographic location of each wild soybean accession was obtained from the Chinese National Crop Germplasm Conservation Center database. The distance to the saline-affected region was calculate by using the latitude and longitude of the saline-affected region (Wang, 1993). The distance from each wild accession to the nearest saline-affected region was measured using Google Earth and is shown in Table S3. The accession W43 is an introduction and lacks a location of origin so was excluded from the analysis. To test for the association between the genotype of wild soybean accessions and the distance to the nearest saline-affected region we performed a Wilcoxon–Mann–Whitney test, a non-parametric test used for Arabidopsis (Baxter *et al.*, 2010), with SAS Version 9.1 (SAS Institute, http://www.sas.com/) to see whether the distance from the collection site to the saline-affected region is smaller in accessions with a salt-tolerant haplotype H1 or H7 than in those with salt-sensitive haplotypes (H3–H6, H8, H9).

ACKNOWLEDGEMENTS

This work was funded by the Natural Science Foundation of China (grants 30971801 and 31271752 to RG) and National Key Technologies R&D Program in the 12th 5-Year Plan (2012AA101106-2 to RG and LQ). MG and YQ are funded by ARC FT130100709 and CE140100008.

AUTHOR CONTRIBUTIONS

LQ and MG designed most of the experiments and directed the project; RX performed the map-based cloning of *GmSALT3*, and analysed the data. YQ performed the *in situ* expression and phylogeny analysis of the *GmSALT3*, YG performed the genomic variation screen of *GmSALT3* in Tiefeng 8 and 85–140; LY performed gene expression, variation of promoter region analysis and statistical analysis; YL, JJ and JC performed recombinant identification and NIL testing; YR and YQ performed subcellular localization of *GmSALT3*; GL performed evaluation of the salt tolerance of germplasm; LT made the cross of Tiefeng 8 and 85–140; LJ helped construct vectors; ZL and HH performed the field experiment on populations; RC contributed to the experimental design and material selection. RG, MG, YQ and LQ wrote the paper.

COMPETING FINANCIAL INTERESTS

The authors declare no competing financial interests.

SUPPORTING INFORMATION

Additional Supporting Information may be found in the online version of this article.

Figure S1. Variation in coding and amino acid sequences of *GmSALT3* in Tiefeng 8 and *Gmsalt3* in 85–140.

Figure S2. Tissue localization of *GmSALT3* in soybean primary roots shown using *in situ* PCR.

Figure S3. Tissue localization of *GmSALT3* in soybean stems and leaves shown using *in situ* PCR.

Figure S4. *GmSALT3* promoter-GUS expression pattern in transgenic Arabidopsis.

Figure S5. Transient expression of GmSALT3 fluorescent protein fusions in Arabidopsis mesophyll cells.

Figure S6. Development and phenotype evaluation of near isogenic lines with different *GmSALT3*/*Gmsalt3* alleles.

Figure S7. Relationship of the haplotypes in wild soybean with the distance from their collection sites to that of the nearest saline region.

Figure S8. Genetic diversity and gene expression comparison between salt-tolerant and salt-sensitive haplotypes.

Table S1. Primers used for mapping and genotype evaluation.

Table S2. Phenotypes and genotypes of a 172 minicore collection and 12 accessions from the United States.

Table S3. Primer properties in a eight single nucleotide polymorphism (SNP) iPlex assay in Sequenome SNP genotyping system.

Table S4. Phenotype and genotype of 57 wild soybean accessions used in this study.

Table S5. Primer properties in two iPlex assays in the Sequenome SNP genotyping system for comparing genetic diversity between salt-tolerant and salt-sensitive haplotypes.

REFERENCES

Athman, A., Tanz, S.K., Conn, V., Jordans, C., Mayo, G.M., Ng, W.W., Burton, R.A., Conn, S.J. and Gilliham, M. (2014) Protocol: a fast and simple *in situ* PCR method for localising gene expression in plant tissue. *Plant Methods*, **10**, 29.

Baxter, I., Brazelton, J.N., Yu, D. *et al.* (2010) A coastal cline in sodium accumulation in *Arabidopsis thaliana* is driven by natural variation of the sodium transporter AtHKT1;1. *PLoS Genet.* **6**, e1001193.

Byrt, C., Xu, B., Krishnan, M. *et al.* (2014) The Na^+ transporter, TaHKT1;5-D, limits shoot Na^+ accumulation in bread wheat. *Plant J.* **80**, 516–526.

Chanroj, S., Lu, Y., Padmanaban, S., Nanatani, K., Uozumi, N., Rao, R. and Sze, H. (2011) Plant-specific cation/H^+ exchanger 17 and its homologs are endomembrane K^+ transporters with roles in protein sorting. *J. Biol. Chem.* **286**, 33931–33941.

Clough, S.J. and Bent, A.F. (1998) Floral dip: a simplified method for *Agrobacterium*-mediated transformation of *Arabidopsis thaliana*. *Plant J.* **16**, 735–743.

Deinlein, U., Stephan, A.B., Horie, T., Luo, W., Xu, G. and Schroeder, J.I. (2014) Plant salt-tolerance mechanisms. *Trends Plant Sci.* **19**, 371–379.

Dong, Y., Yang, X., Liu, J., Wang, B.H., Liu, B.L. and Wang, Y.Z. (2014) Pod shattering resistance associated with domestication is mediated by a NAC gene in soybean. *Nat. Commun.* **5**, 1–11.

Drummond, A.J., Ashton, B., Buxton, S. *et al.* (2011) Geneious v5.5. Available from http://www.geneious.com.

FAO, A. (2000) Extent and causes of salt affected soils in participating countries. Available from http://www.fao.org/ag/agl/agll/spush/topic2.htm.

Guan, R., Chen, J., Jiang, J. and Qiu, L. (2014) Mapping and validation of a dominant salt tolerance gene in the cultivated soybean (*Glycine max*) variety Tiefeng 8. *Crop J.* doi: 10.1016/j.cj.2014.09.001 [Epub ahead of Print].

Ha, B.-K., Vuong, T.D., Velusamy, V., Nguyen, H.T., Shannon, J.G. and Lee, J.-D. (2013) Genetic mapping of quantitative trait loci conditioning salt tolerance in wild soybean (*Glycine soja*) PI 483463. *Euphytica*, **193**, 79–88.

Hamwieh, A. and Xu, D.H. (2008) Conserved salt tolerance quantitative trait locus (QTL) in wild and cultivated soybeans. *Breed. Sci.* **58**, 355–359.
Hamwieh, A., Tuyen, D., Cong, H., Benitez, E., Takahashi, R. and Xu, D. (2011) Identification and validation of a major QTL for salt tolerance in soybean. *Euphytica*, **179**, 451–459.
Hirakawa, Y., Kondo, Y. and Fukuda, H. (2010) TDIF peptide signaling regulates vascular stem cell proliferation via the *WOX4* homeobox gene in Arabidopsis. *Plant Cell*, **22**, 2618–2629.
Hu, R., Fan, C., Li, H., Zhang, Q. and Fu, Y.F. (2009) Evaluation of putative reference genes for gene expression normalization in soybean by quantitative real-time RT-PCR. *BMC Mol. Biol.* **10**, 93.
Hyten, D.L., Song, Q., Zhu, Y. *et al.* (2006) Impacts of genetic bottlenecks on soybean genome diversity. *Proc. Natl Acad. Sci. USA*, **103**, 16666–16671.
Jiang, J., Guan, R., Guo, Y., Chang, R. and Qiu, L. (2013) Simple evaluation method of tolerance and salt at seedling stage in soybean. *Acta Agro. Sinica*, **39**, 1248–1256.
Lee, G.J., Carter, T.E. Jr, Villagarcia, M.R., Li, Z., Zhou, X., Gibbs, M.O. and Boerma, H.R. (2004) A major QTL conditioning salt tolerance in S-100 soybean and descendent cultivars. *Theor. Appl. Genet.* **109**, 1610–1619.
Lee, J.D., Smothers, S.L., Dunn, D., Villagarcia, M., Shumway, C.R., Carter, T.E. and Shannon, J.G. (2008) Evaluation of a simple method to screen soybean genotypes for salt tolerance. *Crop Sci.* **48**, 2194–2200.
Librado, P. and Rozas, J. (2009) DnaSP v5: a software for comprehensive analysis of DNA polymorphism data. *Bioinformatics*, **25**, 1451–1452.
Liu, J.P., Ishitani, M., Halfter, U., Kim, C.S. and Zhu, J.K. (2000) The *Arabidopsis thaliana* SOS2 gene encodes a protein kinase that is required for salt tolerance. *Proc. Natl Acad. Sci. USA*, **97**, 3730–3734.
Liu, G., Guan, R., Chang, R. and Qiu, L. (2011) Correlation between Na^+ contents in different organs of soybean and salt tolerance at the seedling stage. *Acta Agro. Sinica*, **37**, 1266–1273.
Londo, J.P., Chiang, Y.-C., Hung, K.-H., Chiang, T.-Y. and Schaal, B.A. (2006) Phylogeography of Asian wild rice, Oryza rufipogon, reveals multiple independent domestications of cultivated rice, *Oryza sativa*. *Proc. Natl Acad. Sci. USA*, **103**, 9578–9583.
Möller, S., Croning, M.D. and Apweiler, R. (2001) Evaluation of methods for the prediction of membrane spanning regions. *Bioinformatics*, **17**, 646–653.
Møller, I.S., Gilliham, M., Jha, D., Mayo, G.M., Roy, S.J., Coates, J.C., Haseloff, J. and Tester, M. (2009) Shoot Na^+ exclusion and increased salinity tolerance engineered by cell type-specific alteration of Na^+ transport in *Arabidopsis*. *Plant Cell*, **21**, 2163–2178.
Munns, R. and Tester, M. (2008) Mechanisms of salinity tolerance. *Annu. Rev. Plant Biol.* **59**, 651–681.
Munns, R., James, R.A., Xu, B. *et al.* (2012) Wheat grain yield on saline soils is improved by an ancestral Na^+ transporter gene. *Nat. Biotechnol.* **30**, 360–364.
Nelson, B.K., Cai, X. and Nebenführ, A. (2007) A multicolored set of *in vivo* organelle markers for colocalization studies in Arabidopsis and other plants. *Plant J.* **51**, 1126–1136.
Padmanaban, S., Chanroj, S., Kwak, J.M., Li, X., Ward, J.M. and Sze, H. (2007) Participation of endomembrane cation/H^+ exchanger AtCHX20 in osmoregulation of guard cells. *Plant Physiol.* **144**, 82–93.
Papiernik, S.K., Grieve, C.M., Lesch, S.M. and Yates, S.R. (2005) Effects of salinity, imazethapyr, and chlorimuron application on soybean growth and yield. *Commun. Soil Sci. Plant Anal.* **36**, 951–967.
Parker, M.B., Gascho, G. and Gaines, T. (1983) Chloride toxicity of soybeans grown on Atlantic coast flatwoods soils. *Agron. J.* **75**, 439–443.
Phang, T.H., Shao, G. and Lam, H.M. (2008) Salt tolerance in soybean. *J. Integr. Plant Biol.* **50**, 1196–1212.
Pimentel, D., Berger, B., Filiberto, D., Newton, M., Wolfe, B., Karabinakis, E., Clark, S., Poon, E., Abbett, E. and Nandagopal, S. (2004) Water resources: agricultural and environmental issues. *Bioscience*, **54**, 909–918.
Pitman, M.G. and Läuchli, A. (2002) Global Impact of Salinity and Agricultural Ecosystems. In: *Salinity: Environment – Plants – Molecules* (Läuchli, A., Lüttge, U., eds). Dordrecht, the Netherlands: Kluwer, pp. 3–20.
Ren, Z.-H., Gao, J.-P., Li, L.-G., Cai, X.-L., Huang, W., Chao, D.-Y., Zhu, M.-Z., Zong-Yang, W., Luan, S. and Hong-Xuan, L. (2005) A rice quantitative trait locus for salt tolerance encodes a sodium transporter. *Nat. Genet.* **37**, 1141–1146.
Ren, Y., Wang, Y., Liu, F. *et al.* (2014) GLUTELIN PRECURSOR ACCUMULATION3 encodes a regulator of post-Golgi vesicular traffic essential for vacuolar protein sorting in rice endosperm. *Plant Cell*, **26**, 410–425.
Rengasamy, P. (2006) World salinization with emphasis on Australia. *J. Exp. Bot.* **57**, 1017–1023.
Robinson, J.T., Thorvaldsdóttir, H., Winckler, W., Guttman, M., Lander, E.S., Getz, G. and Mesirov, J.P. (2011) Integrative genomics viewer. *Nat. Biotechnol.* **29**, 24–26.
Schlenke, T.A. and Begun, D.J. (2004) Strong selective sweep associated with a transposon insertion in Drosophila simulans. *Proc. Natl Acad. Sci. USA*, **101**, 1626–1631.
Schmutz, J., Cannon, S.B., Schlueter, J. *et al.* (2010) Genome sequence of the palaeopolyploid soybean. *Nature*, **463**, 178–183.
Schultz, J., Copley, R.R., Doerks, T., Ponting, C.P. and Bork, P. (2000) SMART: a web-based tool for the study of genetically mobile domains. *Nucleic Acids Res.* **28**, 231–234.
Sheng, C. and Harper, J.E. (1997) Shoot versus root signal involvement in nodulation and vegetative growth in wild-type and hypernodulating soybean genotypes. *Plant Physiol.* **113**, 825–831.
Shi, H., Ishitani, M., Kim, C. and Zhu, J.-K. (2000) The *Arabidopsis thaliana* salt tolerance gene *SOS1* encodes a putative Na^+/H^+ antiporter. *Proc. Natl Acad. Sci. USA*, **97**, 6896–6901.
Singh, G. (2010) *The Soybean: Botany, Production and Uses*. Oxfordshire, UK: CABI Publishing.
Studer, A., Zhao, Q., Ross-Ibarra, J. and Doebley, J. (2011) Identification of a functional transposon insertion in the maize domestication gene *tb1*. *Nat. Genet.* **43**, 1160–1163.
Tang, Y. and Qiao, H. (2008) Resources of saline-alkali land in China and progress of improvement and utilization. *Anhui. Agric. Sci. Bull.* **14**, 19–22.
Tian, Z., Wang, X., Lee, R., Li, Y., Specht, J.E., Nelson, R.L., McClean, P.E., Qiu, L. and Ma, J. (2010) Artificial selection for determinate growth habit in soybean. *Proc. Natl Acad. Sci. USA*, **107**, 8563–8568.
Tilman, D., Balzer, C., Hill, J. and Befort, B.L. (2011) Global food demand and the sustainable intensification of agriculture. *Proc. Natl Acad. Sci. USA*, **108**, 20260–20264.
Turner, T.L., Bourne, E.C., Von Wettberg, E.J., Hu, T.T. and Nuzhdin, S.V. (2010) Population resequencing reveals local adaptation of *Arabidopsis lyrata* to serpentine soils. *Nat. Genet.* **42**, 260–263.
Valencia, R., Chen, P., Ishibashi, T. and Conatser, M. (2008) A rapid and effective method for screening salt tolerance in soybean. *Crop Sci.* **48**, 1773–1779.
Wang, Z. (1993) *Saline Soil in China*. Beijing: Science Press.
Wang, K.J., Li, X.H. and Yan, M.F. (2014) Microsatellite markers reveal genetic diversity of wild soybean in different habitats and implications for conservation strategies (*Glycine soja*) in China. *Conserv. Genet.* **15**, 605–618.
Xue, S., Yao, X., Luo, W., Jha, D., Tester, M., Horie, T. and Schroeder, J.I. (2011) AtHKT1; 1 mediates nernstian sodium channel transport properties in Arabidopsis root stelar cells. *PLoS One*, **6**, e24725.
Yamaguchi, T. and Blumwald, E. (2005) Developing salt-tolerant crop plants: challenges and opportunities. *Trends Plant Sci.* **10**, 615–620.
Yang, J. (2008) Development and prospect of the research on salt-affected soils in China. *Acta Pedol. Sin.* **45**, 837–845.
Zhang, H. (2005) Mapping the salt tolerant gene and development of salt tolerant gene markers in soybean. MD Thesis. Xinjiang Agricultural University, China.

(a)

```
Tiefeng 8   ATGACGTTCAACGCGAGCACCATCACAACGGCGTCGGAAGGAGCCTGGCAGGGCGATAAT   60
85-140      ATGACGTTCAACGCGAGCACCATCACAACGGCGTCGGAAGGAGCCTGGCAGGGCGATAAT   60

Tiefeng 8   CCCCTGAACCACGCTCTTCCTTTGTTGATCGTTCAAACCATCCTCGTAGTCTTCGTGAGC   120
85-140      CCCCTGAACCACGCTCTTCCTTTGTTGATCGTTCAAACCATCCTCGTAGTCTTCGTGAGC   120

Tiefeng 8   CGCACACTCGCCTTTCTCCTCAAACCCTTTCGTCAACCTAAAGTTGTCGCCGAGATTATT   180
85-140      CGCACACTCGCCTTTCTCCTCAAACCCTTTCGTCAACCTAAAGTTGTCGCCGAGATTATT   180

Tiefeng 8   GGTGGAATTTTGTTGGGGCCTTCTGCTATTGGGCGCAACAAGAAATTCATGCACATAGTG   240
85-140      GGTGGAATTTTGTTGGGGCCTTCTGCTATTGGGCGCAACAAGAAATTCATGCACATAGTG   240

Tiefeng 8   TTCCCAGCATGGAGCACTACCATGCTGGAATCAGTGGCAAGCTTCGGCCTCTTATTCTAT   300
85-140      TTCCCAGCATGGAGCACTACCATGCTGGAATCAGTGGCAAGCTTCGGCCTCTTATTCTAT   300

Tiefeng 8   CTATTTCTGGTGGGCCTAGAGCTCGACTTTCGCACCATTCGCCGGAGCGGCAAGCAAGCC   360
85-140      CTATTTCTGGTGGGCCTAGAGCTCGACTTTCGCACCATTCGCCGGAGCGGCAAGCAAGCC   360

Tiefeng 8   TTCAACATCGCGGTGGCCGGAATAACCCTCCCCTTCATCTGCGCCGTGGGAGTAACGTTC   420
85-140      TTCAACATCGCGGTGGCCGGAATAACCCTCCCCTTCATCTGCGCCGTGGGAGTAACGTTC   420

Tiefeng 8   CTTCTCCAGAGAGCCATCCGCTCTGAAAACCATAACATAGGGTACGTTCAGCACTTCGTG   480
85-140      CTTCTCCAGAGAGCCATCCGCTCTGAAAACCATAACATAGGGTACGTTCAGCACTTCGTG   480

Tiefeng 8   TTCTTAGGGGTATCTCTGTCCATCACGGCTTTCCCTGTGCTCGCGCGCATCTTAGCGGAG   540
85-140      TTCTTAGGGGTATCTCTGTCCATCACGGCTTTCCCTGTGCTCGCGCGCATCTTAGCGGAG   540

Tiefeng 8   CTCAAACTGCTGACCACACGTGTGGGAGAAACCGCCATGGCGGCTGCAGCCTTCAACGAC   600
85-140      CTCAAACTGCTGACCACACGTGTGGGAGAAACCGCCATGGCGGCTGCAGCCTTCAACGAC   600

Tiefeng 8   GTCGCTGCGTGGGTTTTGTTGGCCTTGGCGGTGGCTTTGGCTGGCCAGGGACACAAAAGC   660
85-140      GTCGCTGCGTGGGTTTTGTTGGCCTTGGCGGTGGCTTTGGCTGGCCAGGGACACAAAAGC   660

Tiefeng 8   AGCTTGTTGACATCAATATGGGTGCTCTTCTCAGGGATGGCGTTTGTTGCAGCCATGATG   720
85-140      AGCTTGTTGACATCAATATGGGTGCTCTTCTCAGGGATGGCGTTTGTTGCAGCCATGATG   720

Tiefeng 8   ATCCTGGTTCGACCGGTGATGAACCGTGTTGCTCGCAAGTGTTCTCACGAACAAGACGTG   780
85-140      ATCCTGGTTCGACCGGTGATGAACCGTGTTGCTCGCAAGTGTTCTCACGAACAAGACGTG   780

Tiefeng 8   TTACCCGAAATCTACATATGTTTAACTCTAGCGGGAGTAATGTTATCGGGGTTAGTGACA   840
85-140      TTACCCGAAATCTACATATGTTTAACTCTAGCGGGAGTAATGTTATCGGGGTTAGTGACA   840

Tiefeng 8   GACATGATAGGGTTACATTCAATTTTCGGGGGATTTGTTTTCGGGCTAACGATACCGAAA   900
85-140      GACATGATAGGGTTACATTCAATTTTCGGGGGATTTGTTTTCGGGCTAACGATACCGAAA   900

Tiefeng 8   GGTGGCGAATTTGCAAATAGAATGACGAGGAGGATTGAGGACTTCGTGTCCACGTTGTTC   960
85-140      GGTGGCGAATTTGCAAATAGAATGACGAGGAGGATTGAGGACTTCGTGTCCACGTTGTTC   960

Tiefeng 8   CTTCCCTTGTACTTTGCTGCCAGTGGTTTGAAAACTGACGTGACTAAGTTACGAAGCGTG   1020
85-140      CTTCCCTTGTACTTTGCTGCCAGTGGTTTGAAAACTGACGTGACTAAGTTACGAAGCGTG   1020

Tiefeng 8   GTGGATTGGGGGCTTCTTTTGCTGGTTACGTCCACCGCGAGCGTGGGGAAGATTTTGGGA   1080
85-140      GTGGATTGGGGGCTTCTTTTGCTGGTTACGTCCACCGCGAGCGTGGGGAAGATTTTGGGA   1080

Tiefeng 8   ACGTTTGCGGTGGCGATGATGTGCATGGTGCCGGTGAGAGAATCCTTGACGCTTGGAGTG   1140
85-140      ACGTTTGCCGTGGCGATGATGTGCATGGTGTTGG. AAAATAAAATAAAATGA. . . . . .   1131

Tiefeng 8   TTAATGAACACCAAAGGGTTGGTGGAGCTAATCGTTCTCAATATTGGCAGAGAGAAGAAG   1200
85-140      . . . . . .   1131

Tiefeng 8   GTGCTTAACGACGAGATGTTTACCATCCTAGTACTCATGGCTCTCTTCACCACCTTCATT   1260
85-140      . . . . . .   1131
```

Tiefeng 8	ACAACTCCAATAGTCTTGGCCATATACAAACCCTCTCGTATAGTAAACTCCGGTTCGCAA	1320
85-140	. . . . .	1131
Tiefeng 8	AAACCGTCGCGGCTAACAGATTTGCAAGAGAAGCTTCGCATTCTTGCGTGCATCCATGGA	1380
85-140	. . . . .	1131
Tiefeng 8	CCTGGCAACATACCCTCACTAATCAACTTCGTTGAATCAATTCGGGCCACCAACATGTCA	1440
85-140	. . . . .	1131
Tiefeng 8	CGACTCAAACTCTACGTGATGCAACTTACCGAACTCACTGATAGCTCTTCCTCCATCTTG	1500
85-140	. . . . .	1131
Tiefeng 8	ATGGTTCAACGCAGTCGAAAGAATGGTTTTCCCTTCATCAACCGAATGAAGAGTGGACCA	1560
85-140	. . . . .	1131
Tiefeng 8	ATGCATGAGCAAATTGCCACAGCATTCCAGGCTTATGGTGAAGTGGGTAAAGTTACTGTG	1620
85-140	. . . . .	1131
Tiefeng 8	CATCATTTAACATCTATCTCTCTATTGTCAACAATGCACGAGGACATATGCCACGTTGCA	1680
85-140	. . . . .	1131
Tiefeng 8	GAAAAGAAAGGTGTGGCAATGATTATATTGCCCTTCCACAAAAGGTGGGGAGGGGAAGAT	1740
85-140	. . . . .	1131
Tiefeng 8	GAAGAGGTGACAGAAGACTTAGGGCAGGGTTTGAGGGAAGTCAATCAAAGGGTGCTTCAA	1800
85-140	. . . . .	1131
Tiefeng 8	AATGCAGCCTGCTCTGTCGCAGTGCTAGTCAATCGTGGGGTTGCCAGAAGGTACGAACAA	1860
85-140	. . . . .	1131
Tiefeng 8	GAACCTGAGACAAGTGTTGCTGCAAGGAAAAGAGTGTGCATAATTTTCATTGGTGGACCA	1920
85-140	. . . . .	1131
Tiefeng 8	CATGATCGCAAGGTTTTGGAGTTAGGTAGCAGAATGGCAGAGCATCCAGCAATTAGGTTG	1980
85-140	. . . . .	1131
Tiefeng 8	CTTTTAGTGAGATTCACTTCATACACAGAAGTTGGGGACGAGGGACCCAAATATAACTCA	2040
85-140	. . . . .	1131
Tiefeng 8	CCAACATCAACCACCAACTGGGAAAAAGAAAAGGAGTTGGATGAGGAAGCAGTAAACGAG	2100
85-140	. . . . .	1131
Tiefeng 8	TTCAAGGTTAAATGGCAGGAGACTGTGGAGTACATTGAAAAGAACGCAACCAACATAACA	2160
85-140	. . . . .	1131
Tiefeng 8	GAGGAGGTGTTATCAATTGGGAAAGCTAAGGATCACGACCTAGTAATTGTGGGGAAGCAA	2220
85-140	. . . . .	1131
Tiefeng 8	CAACTTGAGACAACCATGTTGACAAACATAGATTTTCGTCACGGGAATGAAGAGCTGGGA	2280
85-140	. . . . .	1131
Tiefeng 8	CCCATTGGAGATCTCTTTGTCTCTTCGGGTAACGGCATTACCAGTTCATTGCTCGTTATA	2340
85-140	. . . . .	1131
Tiefeng 8	CAGGACCGATATTTTATAAATTCAAACGAAAGTAATCTCGTTAAGACATCAAGGGCCGAG	2400
85-140	. . . . .	1131
Tiefeng 8	AGTACTGTGATTAAAGATGCTATCGAAGAACTTTAA	2436
85-140	. . . . .	1131

(b)

Figure S1. Variation in coding and amino acid sequence of *GmSALT3* in Tiefeng 8 and *Gmsalt3* in 85-140.

(**a**) Coding sequence variation of Tiefeng 8 and 85-140 at *SALT3* locus. (**b**) ClustalW alignment of *GmSALT3* amino acid sequences from Tiefeng 8 and 85-140. Conserved amino acids are shown in red box.

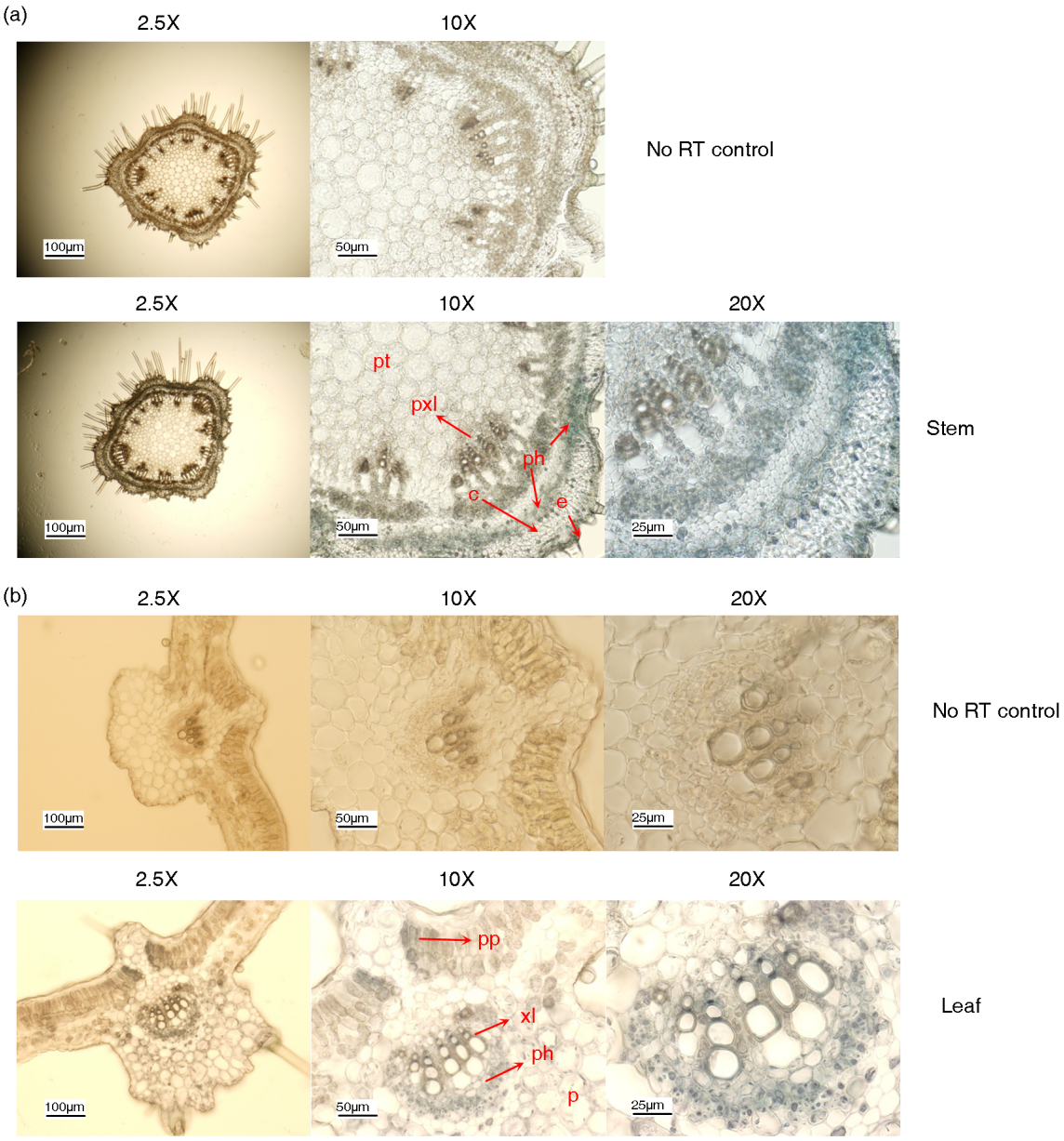

Figure S2. Tissue localization of *GmSALT3* in soybean primary roots shown using *in situ* PCR.

Tissue was 60 µm sections of roots of a 4-week old Tiefeng 8 soybean plant grown in 50/50 perlite/vermiculite with 200mM salt treatment (two days). Blue stained cells are where transcripts present. Negative controls (**a-c**) without RT (reverse transcription) were included to show lack of genomic DNA contamination. *GmSALT3* is localised in extending phloem- and xylem-associated cells of primary root (**d-f**). c, cortex; ph, phloem; mxl, metaxylem; en, endodermis; pxl, protoxylem.

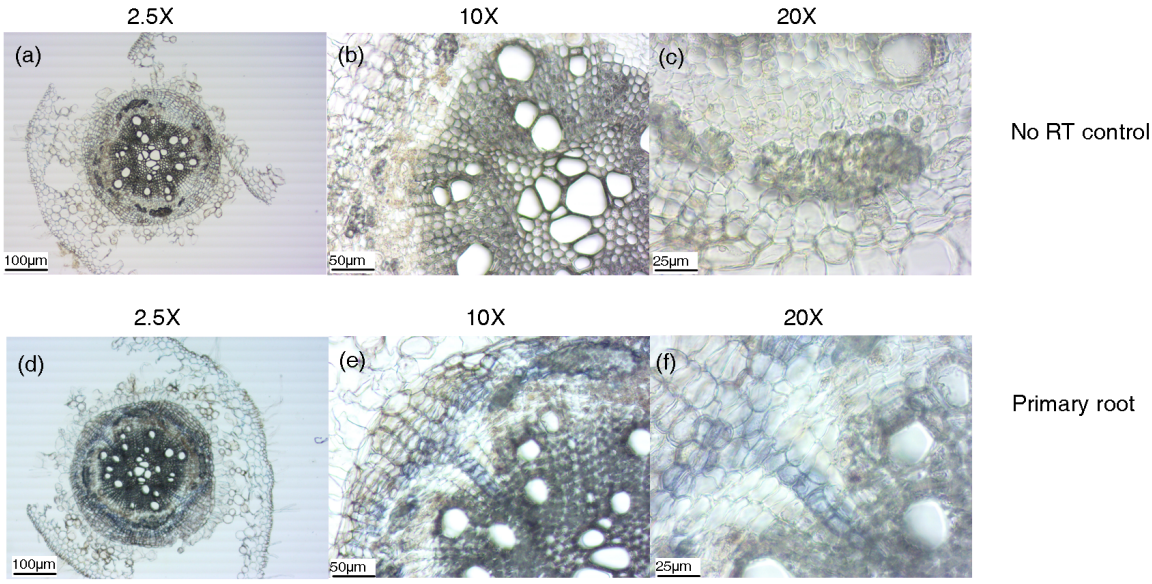

Figure S3. Tissue localisation of *GmSALT3* in soybean stems and leaves shown using *in situ* PCR.

(**a**) Stems and leaves were from a Tiefeng 8 soybean grown in 50/50 perlite and vermiculite, with no salt treatment (the same plant used for root samples). Blue stained cells are where transcripts present. Stem sections were sectioned to 50 μm thickness. (**b**) Negative controls without RT (reverse transcription) were included to show lack of genomic DNA contamination. *GmSALT3* is mainly localized in phloem- and xylem-associated cells of stem and leaf. e, epidermis; pt, pith; c, cortex; ph, phloem; xl, xylem; p, parenchyma; pxl, protoxylem; pp, palisade parenchyma.

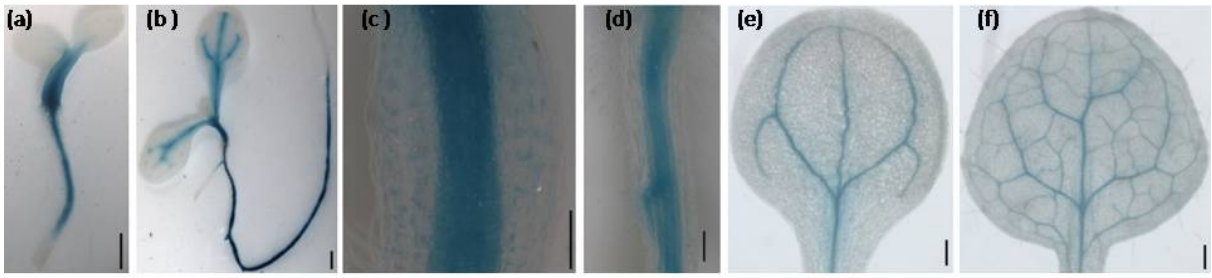

Figure S4. *GmSALT3* promoter-GUS expression pattern in transgenic Arabidopsis.

GUS expression in 2-d-old plant (**a**); 5-d-old plant (**b**); 14-d-old hypocotyl (**c**), root (**d**), cotyledon (**e**) and first leaf (**f**). Scale bars represent 500 μm in a and b; 100 μm in c and d or 200 μm in e and f.

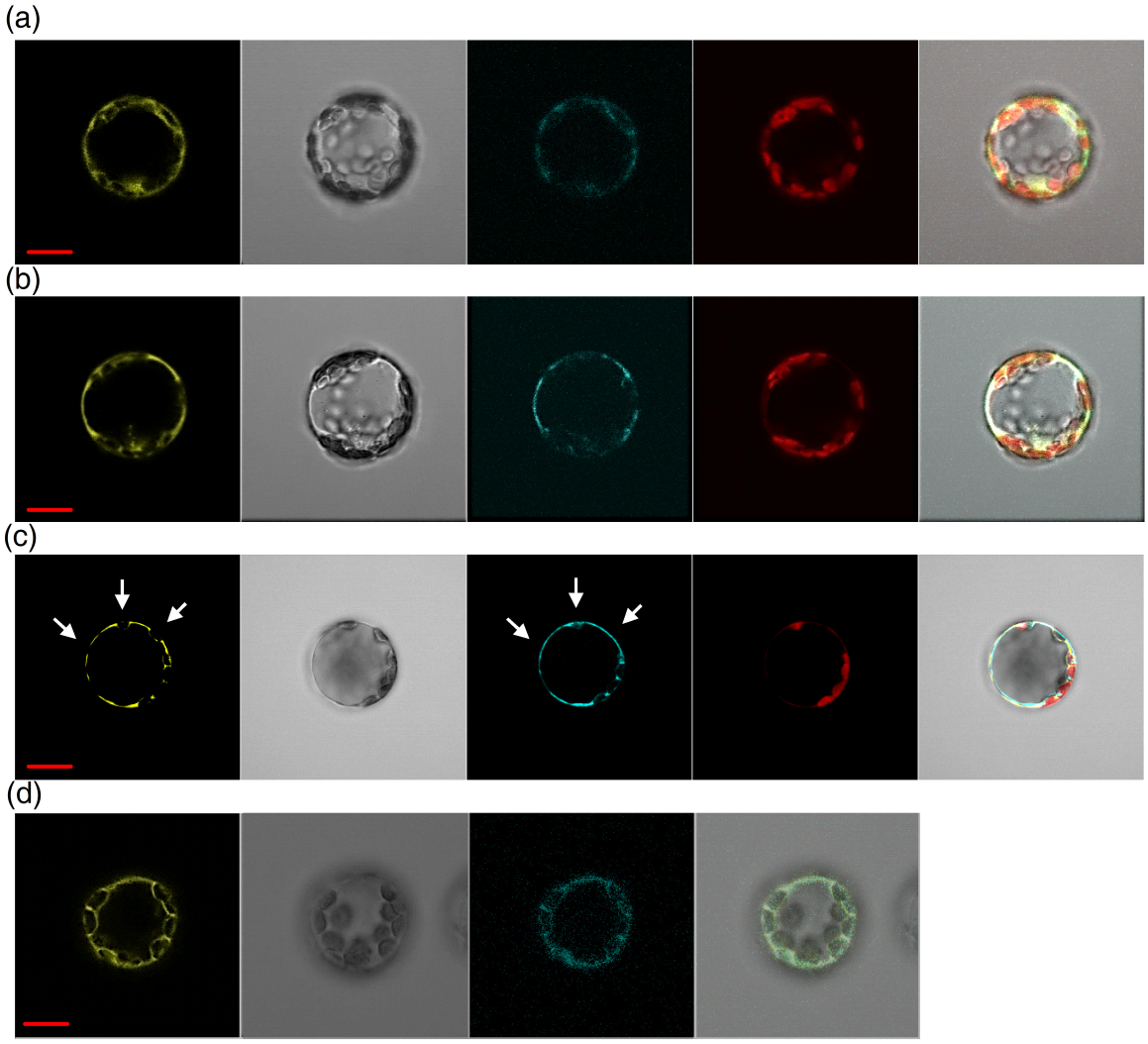

Figure S5. Subcellular localization of GmSALT3 in Arabidopsis mesophyll protoplasts.

(a) Co-expression of *YFP-GmSALT3* and ER marker (CFP). **(b)** Co-expression of *GmSALT3-YFP* and ER marker (CFP). **(c)** Co-expression of *GmSALT3-YFP* and Late endosome/PVC marker (CFP), white arrows indicate non-overlapping positions. **(d)** Co-expression of *GmSALT3-YFP* and ER marker (CFP). **(a-c)** The channels from left to right are YFP, bright field, CFP, chlorophyll, and merged, respectively. **(d)** The channels from left to right are YFP, bright field, CFP, and merged, respectively. Scale bar = 10 μm.

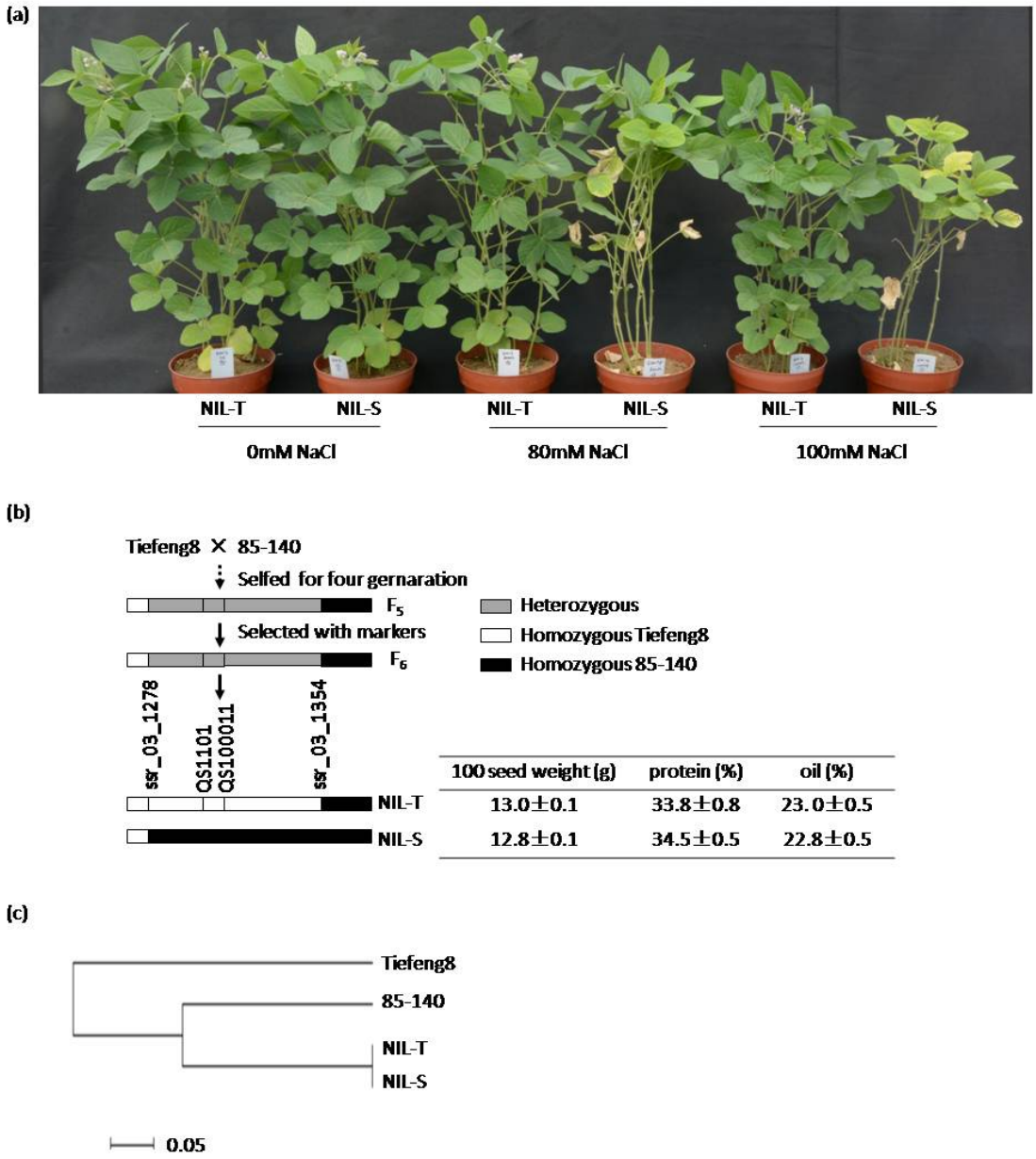

Figure S6. Development and phenotype evaluation of near isogenic lines (NILs) with different *GmSALT3*/*Gmsalt3* alleles.

(**a**) NIL-T and NIL-S growing in control condition or stress condition (watered with 80 or 100 mM NaCl for three time at day 16, 19 and 26 after germination, to every pot 330 mL NaCl solution was added from the bottom of the pot) until 57 d. (**b**) NIL-T and NIL-S were developed from a single F_6 plant, derived from F_5 plant of 85-140×Tiefeng 8 selected with flanked molecular markers which were heterozygous at that locus. Their 100-seed weight, seed protein and oil content are shown. (**c**) Relationship of NIL-T, NIL-S and their parents revealed by using 147 polymorphic SSR markers between parents.

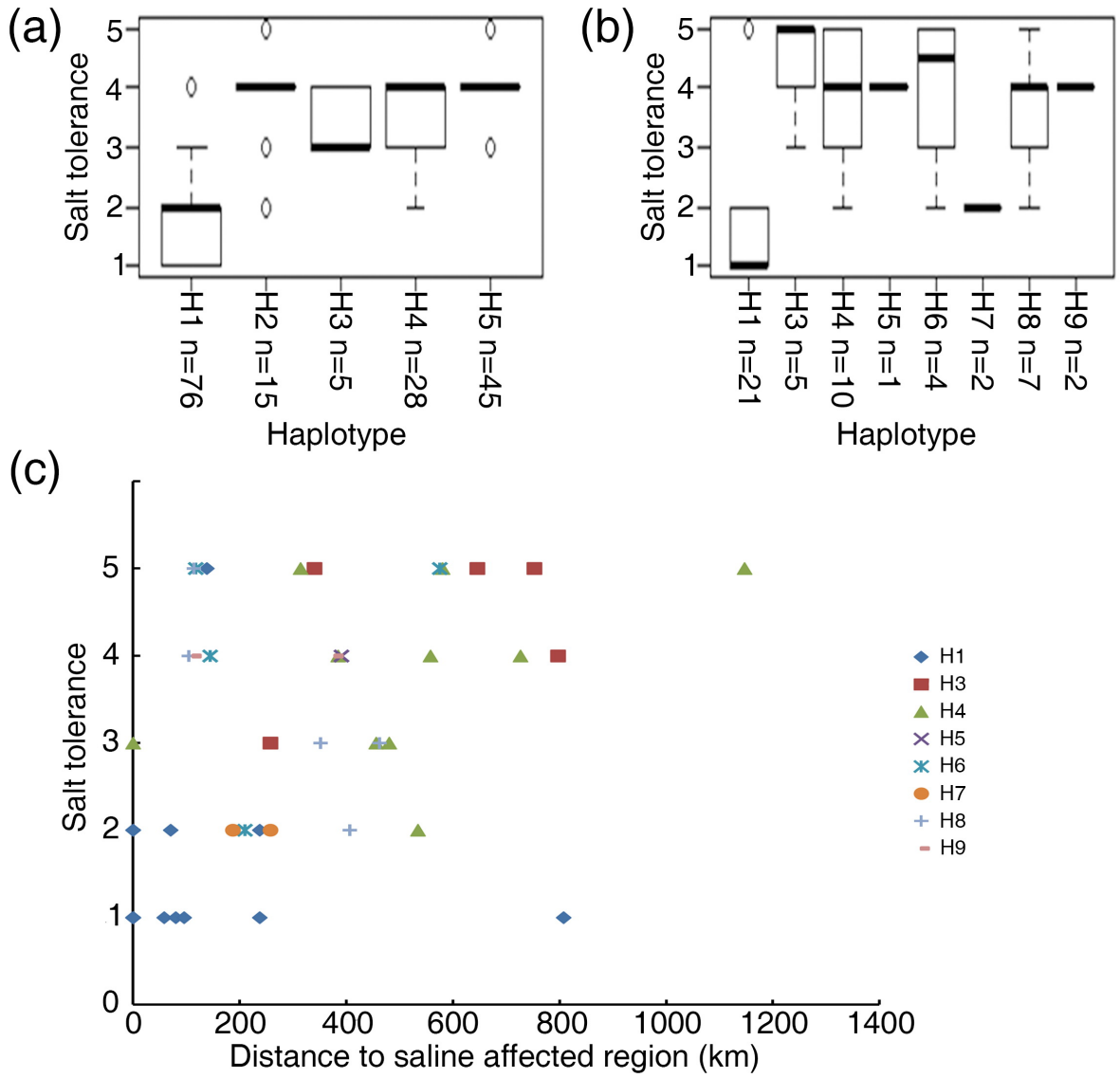

Figure S7. Relationship of the haplotypes in wild soybean with the distance from their collection sites to that of the nearest saline region.

(**a**) Box plot showing differences in salt tolerance level between soybean landraces with different haplotypes. (**b**) Box plot showing differences in salt tolerance level between wild soybean with different haplotypes. For each box plot, top bar and lower bar are maximum and minimum observation, respectively, top of box third quartile, bottom of box is irst quartile, horizontal line is median value and circles are possible outliers. (**c**) The salt tolerance level of 51 wild soybean and its relationship with the distance from where they were collected to the nearest saline affected region. The accessions are shown in different symbols according to their haplotypes at *GmSALT3* locus.

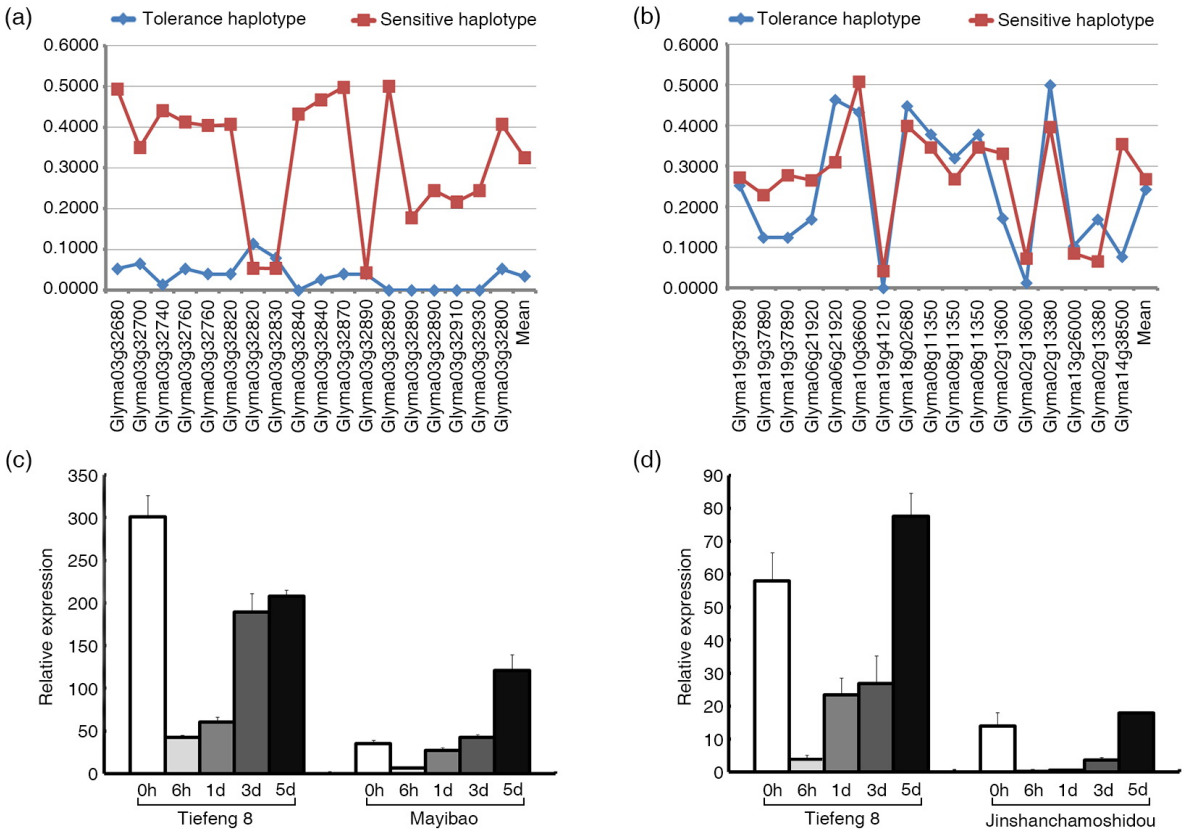

Figure S8. Genetic diversity and gene expression comparison between salt tolerant and sensitive haplotypes.

(**a**) Comparison of genetic diversity between salt tolerant haplotype H1 and salt sensitive haplotypes H2-H5 in landraces at 18 SNP loci around *GmSALT3* gene. (**b**) Comparison of genetic diversity between salt tolerant haplotype H1 and salt sensitive haplotypes H2-H5 in landraces at 17 SNP loci distributed genome wide (Table 5). Genetic diversity of each locus was estimated using Mantel test as implemented in Powermarker. (**c**) Expression of *GmSALT3* analyzed using quantitative real time PCR (qRT-PCR) in root tissue of Tiefeng 8 and Mayibao (H3). (**d**) Expression of *GmSALT3* analyzed using quantitative real time PCR (qRT-PCR) in root tissue of Tiefeng 8 and Jinshanchamoshidou (H4). The number (0, 6h; 1, 3, 5 d) of salt application in vermiculite (c) or hydroponics (d) (150 mM NaCl). Transcription levels was calculated as a percentage of the *GmUKN1* transcript. Error bars indicate standard deviations (n=3).

Table S1. Primers used for mapping and genotype evaluation.

Primer sets	Marker type	Forward primer sequences	Reverse primer sequences	Position*	Purpose
Barcsoyssr_3_1299	SSR	CGAAGGATGATGAGGCTTTT	TTCTTTGCCAGAAAAAGGAAA	40,435,732	Mapping
Barcsoyssr_3_1301	SSR	TGGAATTAATGCAGCAACACA	CACGCAAAATTAATGGAGCA	40,441,396	Mapping
Barcsoyssr_3_1308	SSR	ACCAGCTCGTGTTGTGTTTT	CGCTCTCTCTATGCCTCCAC	40,571,591	Mapping
QS08064	indel	ACGTAAGTGGTTGAAGGCGTT	GCGCCAACTTCAAAATTCACTC	40,650,645	Mapping
QS080465	indel	ACTCAAGAGCAACTCACAAC	GCTAACGACTACCTCAATGC	40,612,426	Mapping
QS1101	indel	CTTACCTTCACGGACGGAGA	CCCATCTCCCAATCCTAACA	40,467,131	Mapping
QS1102	indel	TGCGGGTCCACCTAAAAGTA	ACCTCTTGGGTGGGATGTCT	40,483,946	Mapping
QS1104	indel	TTCTTGTTTCGCTGCCTTTT	CAGCATCTTTCGATGAACCA	40,520,375	Mapping
QS100001	indel	TAGCACATTTGGAAATCCGTTAG	TGAATCACCCAAACGGAAAA	40,618,462	Mapping
QS100011	indel	TTTGATATTGCAGGGATGACA	AACTGACGGACCAATGGAAG	40,690,072	Mapping
QS1112	Indel	TGCACTGCTTTGAGCTTTTT	GGCCTCGAAGCTTTAATGAG	40,765,730	Mapping
QS1119	CAPS	AAGATTCTGGATTGGGTCC	AGTCATCAGGTGGGAAGTTT	40,635,936	Mapping
Indel-3.78kb	indel	P1:GCGGGAGTAATGTTATCGG	P2:GTCGTATCTTGGGAGAGGAG P3:CTATTCTCATAAGAGTCTA	40,627,819	Mapping Genotyping
Indel-152bp	indel	GGGTTGTGCCTAAATAGCA	AAGGAAGAGCGTGGTTCA	40,622,512	Genotyping
Indel-4bp	indel	CTGTCCATCACGGCTTTCC	CTATAGTAGGTCCACCTGAGAA	40,626,237	Genotyping
Splice-18bp	CAPS	AAAGCGCATAAGTTATAACACAAAAT	GAATGTAACCCTATCATGTCTGTCA	40,627,587	Genotyping
Indel-21bp	indel	GGAAGCAACAACTTGAGACA	CGAGCAATGAACTGGTAATG	40,634,330	Genotyping
Promoter		AGATTAGATTAGTCTCCACG	GGCCAAAGACTCAGTGCTTC		Promoter-GUS
GmUKN1		TGGTGCTGCCGCTATTTACTG	GGTGGAAGGAACTGCTAACAATC		q-RT-PCR
q-SALT		TCCTTGACGCTTGGAGTGTT	CGGTTGATGAAGGGAAAAC		q-RT-PCR
Intron2		CTGTCCATCACGGCTTTCC	GAATGTAACCCTATCATGTCTGTCA		Sequencing

Primer sets	Marker type	Forward primer sequences	Reverse primer sequences	Position*	Purpose
GmSALT3		ATGACGTTCAACGCGAGC	R1:AAGTTCTTCGATAGCATCTTTA R2:TTTTATTTTATTTTCCAACAC		Sequencing

Table S2. Phenotypes and genotypes of a 172 minicore collection and 12 accessions from America. Three landraces in mini-core collection, show heterozygous at seven loci tested for haplotypes, are involved in the end of the table. The heterozygous landraces were not used for further analysis.

Cultivar name	Salt tolerance	Province or state	Country	Haplotype
Qingdou	2	Heilongjiang	China	H1
Anqingheidou	1	Heilongjiang	China	H1
Fangzhengmoshidou	2	Heilongjiang	China	H4
Changchunmancangjin	2	Jilin	China	H1
Niumaohuang	2	Jilin	China	H4
Bodigao	2	Jilin	China	H1
Chasedou	3	Jilin	China	H4
Heimoshidou	4	Jilin	China	H2
Jinzhou 4-1	4	Liaoning	China	H2
Tianedan	2	Liaoning	China	H1
Daheiqi	1	Liaoning	China	H1
Huanqi	2	Liaoning	China	H1
Xiaobaiqi	2	Liaoning	China	H1
Xiaohuangdou	1	Liaoning	China	H1
Niumaohuang	4	Liaoning	China	H2
Daliheidou	2	Liaoning	China	H1
Yushidou	1	Liaoning	China	H1
Tueryan	3	Hebei	China	H2
Diliuhuangdou-2	2	Hebei	China	H1
Sijiaoqihuangdou	4	Hebei	China	H1
Tianedan	2	Shanxi	China	H1
Tianedan	2	Shanxi	China	H1
Xiaohuangdou	3	Shanxi	China	H2
Huangandou	4	Shanxi	China	H2
Daheidou	5	Shanxi	China	H2
Huipizhiheidou	3	Shanxi	China	H1

Cultivar name	Salt tolerance	Province or state	Country	Haplotype
Shengli3	2	Shandong	China	H1
Siliyuan	1	Shandong	China	H1
Pingdinghuangdou	4	Shandong	China	H5
Dabaipi	1	Shandong	China	H1
Dahuangdou	2	Shandong	China	H1
Xiaomidou	2	Shandong	China	H1
Qing6	3	Shandong	China	H5
Lvcaodou	2	Shandong	China	H1
Erliheidou	1	Shandong	China	H1
Pingdinghei	2	Shandong	China	H1
Chadou	2	Shandong	China	H1
Miyangxiaozihuang	4	Henan	China	H5
Zhechuanjiwohuang	4	Henan	China	H5
Miyangniumaohuang	4	Henan	China	H5
Zhechengxiaohongdou	2	Henan	China	H1
Boaihongpizaojiaozi	2	Henan	China	H1
Xinyangyangyandou	2	Henan	China	H1
Niumaohuang	2	Shannxi	China	H1
Suiningpingdinghuang	1	Jiangsu	China	H1
Pixiandazihuacao	3	Jiangsu	China	H5
Pixiannianzhuangliuyuexian	3	Jiangsu	China	H5
Pixiansilicao	2	Jiangsu	China	H1
Baqidawandou	2	Hebei	China	H1
Shuyangchunheidoubing	2	Jiangsu	China	H1
Peixianxiaoyoudou	2	Jiangsu	China	H1
Pixianlayanghuang	2	Jiangsu	China	H1
Yizhengdalihuangdou	3	Jiangsu	China	H3
Taixingniumaohuangyi	1	Jiangsu	China	H1
Honghuliuyuebao	3	Hubei	China	H4
Nidou	4	Hubei	China	H5
Jinghuang35yi	4	Hubei	China	H5

Cultivar name	Salt tolerance	Province or state	Country	Haplotype
Daimidou	1	Hubei	China	H1
Cudou	3	Zhejiang	China	H3
Dongshanbaimaidou	2	Fujian	China	H1
Xiamentengzaidou	3	Fujian	China	H3
Tonganzihongdou	3	Fujian	China	H5
Zhaoanqiudadou	2	Fujian	China	H4
Shaxianwudou	4	Fujian	China	H3
Hengfengwudou	5	Jiangxi	China	H5
Shangraobayuebai	4	Jiangxi	China	H4
Yantianqingpidou	4	Jiangxi	China	H5
Shaxindou	4	Jiangxi	China	H4
Ruijinqingpidou	4	Jiangxi	China	H5
Hongzhudou	2	Hunan	China	H1
Longquandadou	2	Heilongjiang	China	H2
Zihua 2	4	Jilin	China	H2
Huaidebaihuadali	4	Jilin	China	H2
Helongyoutai	5	Jilin	China	H2
Tonghuapingdingxiang	3	Jilin	China	H4
Baichengmoshidou	2	Jilin	China	H1
Jinshanchamoshidou	4	Jilin	China	H4
Yanqihuangdou	4	Xinjiang	China	H2
changjihuangdou 1	2	Xinjiang	China	H1
Yangtianxiaohuangdou	4	Hebei	China	H5
Nanguanxiaopiqing	2	Hebei	China	H1
Datunxiaoheidou	1	Hebei	China	H1
Bendidahuangdou	1	Hebei	China	H1
Heidou	2	Hebei	China	H1
Xiaoyuanhuangdou	2	Shanxi	China	H1
Xiaohuangdou	2	Shanxi	China	H1
Huandou<2>	1	Shanxi	China	H1
Xiaohuangdou	4	Shanxi	China	H2

Cultivar name	Salt tolerance	Province or state	Country	Haplotype
Yuxuan13	2	Shanxi	China	H1
Bailudou	5	Shanxi	China	H2
Liushiribaidou	2	Shanxi	China	H1
Xiaobaidou<2>	2	Shanxi	China	H1
Xiaoqingdou	2	Shanxi	China	H1
Xiaoheidou	2	Shanxi	China	H1
Zaoshuhuangdou	4	Shannxi	China	H5
Xiaoheidou	2	Shannxi	China	H1
Laoheidou	2	Shannxi	China	H1
Huichaxiaohuangdou	5	Shannxi	China	H5
Dahuangdou	4	Shannxi	China	H5
Laoshupi	1	Shannxi	China	H1
Youhuangdou	4	Gansu	China	H4
Guanyunhaibaihua	4	Jiangsu	China	H5
Dantuxiaowujia	2	Jiangsu	China	H1
Huasedou	5	Hubei	China	H5
Chihuangdou	4	Hubei	China	H5
Shuguanghuangdou	2	Hubei	China	H1
Shanzibaihuangdou	2	Hubei	China	H1
Huameidou	4	Hubei	China	H4
Xiaobaimao	4	Sichuan	China	H4
Dahuadou	2	Sichuan	China	H1
Shiyuehuang	4	Sichuan	China	H5
Zengjialvhuangdou	4	Sichuan	China	H5
Mayibao	4	Sichuan	China	H3
Bazhongtiankandou	4	Sichuan	China	H5
Pixianxiaohuangdou	4	Sichuan	China	H4
Zizhongliuyuezao	3	Sichuan	China	H5
Jianweiquanshuidou	4	Sichuan	China	H4
Changshoushiyuehuang	1	Sichuan	China	H1
Jiangehualinjiwodou	4	Sichuan	China	H5

Cultivar name	Salt tolerance	Province or state	Country	Haplotype
Qionglaihuangmaozi	5	Sichuan	China	H5
Qionglaiyoujinangheidou	5	Sichuan	China	H5
Huanyuanbalixiaoheidou	4	Sichuan	China	H5
Donghuangdou-1	3	Sichuan	China	H4
Qiyuehuang	4	Sichuan	China	H5
Liuyuebao-2	3	Sichuan	China	H5
Zaohuangdou-4	1	Sichuan	China	H1
Duchangwudou	4	Jiangxi	China	H4
Fengchengzaowudou	4	Jiangxi	China	H5
Yizhangliuyuehuang	5	Hunan	China	H5
Changshanidou	3	Hunan	China	H4
Aishengnidou	4	Hunan	China	H4
Xihuangdou	4	Guizhou	China	H5
Erjizaodou-2	4	Guizhou	China	H5
Dahuangdou-1	4	Guizhou	China	H4
Zaojiaodou	4	Guizhou	China	H4
Zadou-6	4	Guizhou	China	H5
Dabaimaodou	4	Guangdong	China	H5
Longchuanhuangniumao	3	Guangdong	China	H5
Liangjiangpohuangdou	4	Guangdong	China	H1
Yangshanqingdou	3	Guangdong	China	H5
Qingyuandaqingdou	3	Guangdong	China	H4
Yingdehedou	4	Guangdong	China	H5
Heikewudou	3	Guangdong	China	H4
Baizhidou	2	Guangxi	China	H1
Mashanrenfenghuangdou	3	Guangxi	China	H5
Xuanza	2	Yunnan	China	H1
Huangdou	4	Yunnan	China	H2
Yangyandou	4	Yunnan	China	H4
Songzidou	3	Yunnan	China	H4
Huangdali	2	Jilin	China	H1

Cultivar name	Salt tolerance	Province or state	Country	Haplotype
Xiataizimoshid	4	Hebei	China	H4
Maoyandou	2	Hebei	China	H1
Huaheihu	2	Hebei	China	H1
Qingdou	2	Hebei	China	H1
Maoyandou	2	Hebei	China	H1
Lvpihuangdou	1	Shanxi	China	H1
Qisiwa	4	Shandong	China	H4
Zaoshuheidou	1	Shandong	China	H1
Baomuji	4	Shannxi	China	H5
Lvhuangdou	4	Gansu	China	H5
Lvrouheipidou	1	Anhui	China	H1
Xiaokehuangdou	4	Hubei	China	H5
Liuyuehuang	4	Sichuan	China	H5
Pengshanhuangkezi-3	3	Sichuan	China	H4
Zaoshumaopengqing	2	Zhejiang	China	H1
Xinyudaliqing	1	Jiangxi	China	H1
Dahuangdou-2	4	Guangdong	China	H5
Madaiqingdou-2	3	Guangdong	China	H4
Enpingqingdou	1	Guangdong	China	H1
Lee68	1	America	America	H1
Peking	4	America	America	H1
OAC 211	5	America	America	H3
Hartwig	2	America	America	H1
Chestnut	4	America	America	H3
Manchu(Hudson)	1	America	America	H1
Miles	2	America	America	H1
Morse	1	America	America	H1
Virginia	4	America	America	H3
Forrest	2	America	America	H1
Clark	4	America	America	H2
Williams 82	4	America	America	H2

Cultivar name	Salt tolerance	Province or state	Country	Haplotype
Pixianhongmaoyou		Jiangsu	China	H1+H5
Wujiangwuyueniumaohuang		Jiangsu	China	H1+H5
Maodou		Shandong	China	H1+H5

Table S3. Primer properties in a 8-SNP iPlex assay in Sequenome SNP genotyping system.

SNP ID	2nd-PCRP	1st-PCRP	UEPMASS	UEPSEQ	SNP
-20	ACGTTGGATGAACGTCATGGCCAAAGACTC	ACGTTGGATGGCTAGTTTTCATCACCTTCC	5762.8	ttCCAAAGACTCAGTGCTT	G>T
63	ACGTTGGATGAACGCGAGCACCATCACAAC	ACGTTGGATGATCAACAAAGGAAGAGCGTG	4602	GCAGGGCGATAATCC	C>T
774	ACGTTGGATGAGGATCATCATGGCTGCAAC	ACGTTGGATGCTTGAAAGAACTAATCGAGT	5397.5	CTGCAACAAACGCCATCC	A>T
1060	ACGTTGGATGCGGCAAACGTTCCCAAAATC	ACGTTGGATGTTACGAAGCGTGGTGGATTG	4456.9	AAATCTTCCCCACGC	A>T
1349	ACGTTGGATGAAAACCGTCGCGGCTAACAG	ACGTTGGATGTAGTGAGGGTATGTTGCCAG	5836.8	CGGCTAACAGATTTGCAAG	A>G
1548	ACGTTGGATGCAACGCAGTCGAAAGAATGG	ACGTTGGATGATAAGCCTGGAATGCTGTGG	5074.3	CCCTTCATCAACCGAAT	G>C
2124	ACGTTGGATGCCTCTGTTATGTTGGTTGCG	ACGTTGGATGGGATGAGGAAGCAGTAAACG	6297.1	tTTCTTTTCAATGTACTCCAC	T>A
3'UTR	ACGTTGGATGGGTAACGGCATTACCAGTTC	ACGTTGGATGGCCCTTGATGTCTTAACGAG	6420.2	CGTTATACAGGACCGATATTT	T>G

Table S4. Phenotype and genotype of 57 wild soybean accessions used in this study. Five heterozygous accessions observed and were not analyzed further.

Name	Salt tolerance	Province	Ecotype	Haplotype	Long	Lat	Distance (km)
W3	2	Henan	HSu	H1	114.01	34.40	0.0
W4	2	Shannxi	HSu	H1	110.26	35.28	0.0
W5	1	Shannxi	HSu	H1	107.08	34.21	0.0
W6	1	Shannxi	HSu	H1	109.57	33.55	95.1
W7	5	Jiangsu	SSp	H6	120.17	31.40	116.8
W8	2	Sichuan	SSp	H1	106.50	32.21	237.2
W9	3	Sichuan	SSp	H3	108.08	32.05	257.5
W10	1	Anhui	HSu	H1	117.53	33.10	0.0
W11	3	Hubei	SSp	H4	109.28	30.17	455.5
W13	1	Henan	HSu	H1	113.57	35.03	0.0
W15	5	Jiangxi	SSp	H3	115.21	26.20	339.8
W16	1	Guizhou	SSp	H1	108.08	27.03	807.0
W17	5	Heilongjiang	NEs	H4	130.23	48.53	1146.2
W20	5	Jilin	NEs	H4	125.43	44.32	580.3
W21	5	Jilin	NEs	H6	125.50	44.09	574.9
W22	3	Jilin	NEs	H4	125.44	42.17	480.2
W24	2	Liaoning	NEs	H7	122.33	42.24	257.0
W25	2	Liaoning	NEs	H7	121.44	42.03	187.2
W26	5	Liaoning	NEs	H4	124.02	40.27	314.2
W28	2	Guangxi	SSu	H6	109.40	23.57	209.7
W29	3	Hebei	NSp	H4	117.56	40.58	0.0
W30	2	Shanxi	NSp	H1	111.55	37.02	0.0
W31	2	Shandong	HSu	H1	119.25	35.59	70.6
W32	1	Henan	HSu	H1	114.23	34.03	0.0
W33	1	Shannxi	HSu	H1	109.09	32.26	236.8
W35	4	Fujian	SAu	H6	118.19	27.03	143.9
W36	2	Hubei	SSp	H4	110.02	29.53	533.8
W40	4	Hunan	SSu	H4	109.26	29.28	557.2
W41	5	Guizhou	SSu	H3	108.23	28.00	752.3
W42	4	Jiangxi	SSu	H8	116.49	28.12	355.8
W43	4	Introduction		H8			N.D.
W44	5	Fujian	SSu	H8	118.45	26.35	113.3
W45	4	Yunan	SSp	H4	100.51	27.18	726.5
W46	4	Guangxi	SSu	H9	111.04	25.56	378.1
W47	4	Zhejiang	SSu	H9	119.55	28.27	111.8
W48	5	Inner Mongolia	NSp	H1	110.52	39.40	137.7
W51	1	Hebei	NSp	H1	119.09	39.42	0.0
W52	1	Hebei	HSu	H1	119.36	39.56	0.0
W53	1	Ningxia	NSp	H1	105.40	37.29	57.8
W54	1	Ningxia	NSp	H1	106.42	38.48	0.0
W55	1	Shanxi	NSp	H1	111.08	39.23	79.6
W56	1	Shanxi	NSp	H1	112.51	36.50	0.0
W57	1	Shanxi	NSp	H1	112.25	35.29	0.0
W61	1	Shanxi	NSp	H1	112.33	37.47	0.0
W62	3	Sichuan	SSp	H8	107.30	31.13	350.9
W63	4	Sichuan	SSp	H3	108.46	28.50	797.1
W65	4	Liaoning	NEs	H4	124.02	42.33	384.3

Name	Salt tolerance	Province	Ecotype	Haplotype	Long	Lat	Distance (km)
W66	4	Zhejiang	SSu	H8	119.43	30.14	103.9
W68	4	Jiangxi	SSu	H5	115.47	29.28	390.0
W71	5	Hunan	SSu	H3	109.36	27.59	645.5
W72	3	Hunan	SAu	H8	112.48	27.15	462.0
W73	2	Hunan	SAu	H8	112.36	26.54	406.3
*W1		Henan	HSu	H1+H8			
*W2		Henan	HSu	H7+H8			
*W12		Hebei	NSp	H7+H?			
*W38		Guangxi	SAu	H1+H8			
*W50		Beijing	NSp	H1+H9			

Table S5. Primer properties in two iPlex assay in Sequenome SNP genotyping system for comparing genetic diversity between salt tolerance and sensitive haplotypes.

SNP ID	2nd-PCRP	1st-PCRP	UEPMASS	UEPSEQ	Gene
1	ACGTTGGATGTTCCCCTCTACTTCCTTCAC	ACGTTGGATGTCAGAAAAGAGGTTGTGGGC	6278.1	CCAAAATATCCATCTCCAATC	Glyma03g32680
2	ACGTTGGATGACTCGACACCTTAATCACGC	ACGTTGGATGTAGAGTGAGGGAAGGTACAG	5386.5	ATCACGCGTTTGCCCCCT	Glyma03g32700
5	ACGTTGGATGATTGCTGGCATGTACTGCTG	ACGTTGGATGCAGATGATGTCCATGGGATG	7137.7	ggggTGGATTCCAGGAAACATCA	Glyma03g32740
6	ACGTTGGATGAGTATTCCACCAGCAACACC	ACGTTGGATGAGGATGTCCTTGGTTTTCAC	6207.0	ggggtACCGAGCAATGGTCA	Glyma03g32760
7	ACGTTGGATGTGATTCGGACTAACCATCCC	ACGTTGGATGAGGTCGTGATGAGGATCTTG	5787.8	tttgAGCCGCAACGATCAT	Glyma03g32760
10	ACGTTGGATGCTCGTTTCTTTGGATTACCC	ACGTTGGATGACGACACGAACATAAACCAC	5130.4	CCTAGTCAACGACCTTG	Glyma03g32820
11	ACGTTGGATGTTTACCATTGCCAACTGCCC	ACGTTGGATGTTAGTGACTGTGTCGTGTGG	4503.9	GCCCTTCACCGGTTA	Glyma03g32820
12	ACGTTGGATGTAATGTGACTGCAGAGAGCC	ACGTTGGATGCGATAATAAACGTATGCGCC	7602.0	TGTCCCAAATACAATTTAAGACCAA	Glyma03g32830
13	ACGTTGGATGCGAAAACGAAAAGGAAAGGG	ACGTTGGATGAAACTCTCCCTTCGCCTCTC	7646.0	taatGGGATCTTCAATTAGTACCTT	Glyma03g32840
14	ACGTTGGATGAGTTACATGAACGGGCACTC	ACGTTGGATGCTGTGGGATCGAACAAAACC	4839.1	CGTTTCCGTTCAGTGC	Glyma03g32840
20	ACGTTGGATGGAGTGGTGTGGTTACCTTTG	ACGTTGGATGCTAGGAAGCACGACAACAAC	5019.2	GCGGTGGCAGTGGGCG	Glyma03g32870
22	ACGTTGGATGGGGTAATTAATGAGTCTCTC	ACGTTGGATGCGTATTATAATTTCAAATGTCC	6370.2	TTAATGAGTCTCTCAAACTTT	Glyma03g32890
23	ACGTTGGATGGAACAACCATGCATATGGCG	ACGTTGGATGATAGTCCAAAGGGTTGTCGC	5507.6	GGCGTTGAACATAACATC	Glyma03g32890
26	ACGTTGGATGACAGCTTCAGAAGGGACTTG	ACGTTGGATGAGTCTTGGCATGTATCCACG	4649.0	GCGGTGCTGCGAGAT	Glyma03g32890
27	ACGTTGGATGCCAATCCAGCCACCATATTC	ACGTTGGATGAGTAATAGGGAGTAGTGGAG	6744.4	gatgCGACGGAAATCGACCCTT	Glyma03g32890

SNP ID	2nd-PCRP	1st-PCRP	UEPMASS	UEPSEQ	Gene
29	ACGTTGGATGGCACTCCCATAGATATCATC	ACGTTGGATGAGAACCAGCTAAAGGGTCAG	6935.5	cccgTTGGCATTATCCCATCCAG	Glyma03g32910
30	ACGTTGGATGAAGAGAAGCTCTTCCCAACC	ACGTTGGATGGTCAAGTGGAAATTGAGCAG	7921.2	CAACTAGAAATTATCATATAATCTCG	Glyma03g32930
32	ACGTTGGATGTGAAAATAGAGGGCCACCAG	ACGTTGGATGAACAAACGGATACTCCCGTG	7430.8	gggagAGCAGTTTCTGGTTCTCGT	Glyma03g32800
G2	ACGTTGGATGAAGGTTGAGATTGAGGGTGG	ACGTTGGATGAGGAATAAGAAGAGAAGAG	5370.5	GAGGGTGGTGATATGAG	Glyma19g37890
G4	ACGTTGGATGTGTGTTGAAGTGGTCCCTTG	ACGTTGGATGCCATAGGTTTGTGTTTGTCC	5234.4	GTGGAGTAACACACTGT	Glyma19g37890
G5	ACGTTGGATGTAGCTAGCGTCTTCTTGCAG	ACGTTGGATGAATTCGCAGCAGAGAACGAC	4784.1	CTTGCAGCCGTTTCCC	Glyma19g37890
G7	ACGTTGGATGACAACGGTGTCCAACTCTTG	ACGTTGGATGATCAAGCACCACAGAATGGG	6516.2	tggTGGAGTTTGGCCAAAATT	Glyma06g21920
G8	ACGTTGGATGATCAACCCCTCTTTCTGTGC	ACGTTGGATGGCCCAAATGTTCACCAAGAG	5355.5	ccTTGGCTACCACATCCC	Glyma06g21920
G11	ACGTTGGATGCCTGGAATATCTTCCTCGTG	ACGTTGGATGGGTGGAAATGTCCTCTGAAG	6445.2	caATCAGAGGCATGTCTTATG	Glyma10g36600
G13	ACGTTGGATGGAAGAACATCCTGCAAACTC	ACGTTGGATGGGACTTTGTGAAACAATGCC	6319.1	ccgGCAAACTCAAACACTCTT	Glyma19g41210
G19	ACGTTGGATGTGAAGACTAAGCTTCCTGAG	ACGTTGGATGAGCTTCCTTGGAAGGGTTTG	7095.6	agcgTCCTGAGGCCTTGAAGTTG	Glyma18g02680
G21	ACGTTGGATGAACAACTTCTCCTCCGTGTC	ACGTTGGATGTTAGAGGAGGAAGTGAGGTC	7450.8	actgCTCCTCCGTGTCCCCCACCGC	Glyma08g11350
G22	ACGTTGGATGGTCCTGGCTCAATAAGAACC	ACGTTGGATGGAGCTGCAAGTCAGACAAAG	7626.0	ggaatAACCAGTTCACCGGTTCCAT	Glyma08g11350
G23	ACGTTGGATGTAGTTCCAACCATCACACGG	ACGTTGGATGTTTTGCTGCAGATTGCCGAG	4496.9	CTCTGCCAACCGAAT	Glyma08g11350
G26	ACGTTGGATGCAACTCCATCAACCAAACCC	ACGTTGGATGAGGTTTTGGGAGAGGTTGAG	6890.5	gaTCTCTCTCTAAATCTCTCTTT	Glyma02g13600
G27	ACGTTGGATGTTCACTAGCGAGTTGCTGTC	ACGTTGGATGTTTCCCGATGAGCTTGTTCC	5731.8	aCCCAACCTTTATGGCTAA	Glyma02g13600
G32	ACGTTGGATGAGTGGTGGTTGCTGTTGATG	ACGTTGGATGCATGCACTGTCCTTTTCAGC	6104.0	ACATGTTGTCCATTGTTGTT	Glyma02g13380
G36	ACGTTGGATGGGAATGCATGTTTAGCCAAC	ACGTTGGATGCGTGACAAGAAAGTTGCTTC	5154.4	CTTGCAACAGCTCTAAG	Glyma13g26000

SNP ID	2nd-PCRP	1st-PCRP	UEPMASS	UEPSEQ	Gene
G43	ACGTTGGATGGAAGTCCTTATGCTTGTCTG	ACGTTGGATGAGAGCACAACAAGAACAAGG	7983.2	CTGCAATTAAGTTATGATAATTTGAC	Glyma02g13380
G64	ACGTTGGATGCGGTATATCGCAACCTTCTC	ACGTTGGATGGAAAATACCTGAAAATATCCC	6685.4	CTCCACTGGATCCTGATTTAAG	Glyma14g38500

Brief conclusion

This preceding publication clearly demonstrates that *GmSALT3* is associated with soybean shoot Na^+ exclusion and improved salt tolerance of soybean during the vegetative growth phase. However, this work also raised a series of questions that remained unanswered. These included:

- whether GmSALT3 is also related to Cl^- exclusion, which was thought to be the toxic ion in soybean plants (Chapter 1)?
- whether GmSALT3 also confers improved salinity tolerance at the germination phase (Chapter 1)?
- why so many salt sensitive alleles exist for *GmSALT3?* Does the presence of the salt-tolerant allele of this gene impose a yield penalty in non-saline conditions?

Therefore, we decided to develop three sets of near isogenic lines (NILs) from a cross between two varieties 85–140 (salt-sensitive, S) and Tiefeng 8 (salt-tolerant, T) by using marker-assisted selection. These NILs were then used to attempt to answer the questions listed above in the following chapter.

Chapter 3 GmSALT3, which confers improved soybean salt tolerance in the field, increases leaf Cl^- exclusion prior to Na^+ exclusion but does not improve early vigor under salinity

Brief introduction

Agronomic traits are commonly measured to evaluate crops' salt tolerance, such as height, leaf area, biomass, number of internodes, branches, and pods, weight per plant, and weight of 100 seeds. Following group discussions during the writing of our initial publication our collaborators developed NILs of *GmSALT3* and sent us the seeds through Quarantine. In our study, yield related traits, including plant height, pod number per plant, seed number per plant, seed weight per plant, and 100-seed weight per plant were measured in saline and non-saline soil conditions in China. Ion concentration analysis (under 200 mM NaCl treatment for 10 days) and time-course of ion concentration (during 10 days of 200 mM NaCl stress) in different tissues were done in both China and Adelaide, measured ions include Na^+, K^+, and Cl^-. Relative emergence rate and early vigor was analysed to see if *GmSALT3* also affected the salt tolerance of soybean at the emergence stage. We wrote the manuscript together and published our work in *Frontiers in Plant Science* (Liu et al., 2016).

Statement of Authorship

Title of Paper	GmSALT3, which confers improved soybean salt tolerance in the field, increases leaf Cl^- exclusion prior to Na^+ exclusion but does not improve early vigor under salinity
Publication Status	☑ Published ☐ Accepted for Publication ☐ Submitted for Publication ☐ Unpublished and Unsubmitted w ork w ritten in manuscript style
Publication Details	Front. Plant Sci. (2016) 7:1485. doi: 10.3389/fpls.2016.01485

Principal Author

Name of Principal Author (Candidate)	Yue Qu		
Contribution to the Paper	YQ performed the Cl^- concentration test and complementary agronomic measurements to independently confirm those published in the manuscript. YQ also contributed to experimental design and analysis, and played a major part in writing the paper		
Overall percentage (%)	50%		
Certification:	This paper reports on original research I conducted during the period of my Higher Degree by Research candidature and is not subject to any obligations or contractual agreements with a third party that would constrain its inclusion in this thesis. I am the primary author of this paper.		
Signature		Date	12.08.17

Co-Author Contributions

By signing the Statement of Authorship, each author certifies that:

i. the candidate's stated contribution to the publication is accurate (as detailed above);

ii. permission is granted for the candidate in include the publication in the thesis; and

iii. the sum of all co-author contributions is equal to 100% less the candidate's stated contribution.

Name of Co-Author	Ying Liu		
Contribution to the Paper	YL performed development of NILs and K^+, Na^+ concentrations analysis and contributed to writing the paper		
Signature		Date	11.08.2017

Name of Co-Author	Lili Yu		
Contribution to the Paper	LY participated filed experiments and data collection		
Signature		Date	11.08.2017

Name of Co-Author	Jingjing Chen		
Contribution to the Paper	JC participated filed experiments and data collection		
Signature		Date	11.08.2017

Name of Co-Author	Xiexiang Liu		
Contribution to the Paper	XL performed the Cl- concentration test		
Signature		Date	11.08.2017

Name of Co-Author	Huilong Hong		
Contribution to the Paper	HH participated filed experiments and data collection		
Signature		Date	11.08.2017

Name of Co-Author	Zhangxiong Liu		
Contribution to the Paper	ZL participated filed experiments and data collection		
Signature		Date	11.08.2017

Name of Co-Author	Ruzhen Chang		
Contribution to the Paper	RC participated filed experiments and data collection		
Signature		Date	11.08.2017

Name of Co-Author	Matthew Gilliham		
Contribution to the Paper	MG designed experiments and contributed to analysis and writing of the paper		
Signature		Date	11/9/2017

Name of Co-Author	Lijuan Qiu		
Contribution to the Paper	LQ designed experiments and contributed to analysis and writing of the paper		
Signature		Date	8.8.2017

Name of Co-Author	Rongxia Guan		
Contribution to the Paper	RG designed experiments and contributed to analysis and writing of the paper		
Signature		Date	08.08.2017

frontiers in Plant Science

ORIGINAL RESEARCH
published: 30 September 2016
doi: 10.3389/fpls.2016.01485

GmSALT3, Which Confers Improved Soybean Salt Tolerance in the Field, Increases Leaf Cl^- Exclusion Prior to Na^+ Exclusion But Does Not Improve Early Vigor under Salinity

Ying Liu[1], Lili Yu[1], Yue Qu[2], Jingjing Chen[1], Xiexiang Liu[1], Huilong Hong[1], Zhangxiong Liu[1], Ruzhen Chang[1], Matthew Gilliham[2], Lijuan Qiu[1] and Rongxia Guan[1]**

[1] The National Key Facility for Crop Gene Resources and Genetic Improvement, Institute of Crop Science, Chinese Academy of Agricultural Sciences, Beijing, China, [2] Australian Research Council Centre of Excellence in Plant Energy Biology, School of Agriculture, Food and Wine and Waite Research Institute, University of Adelaide, Glen Osmond, SA, Australia

OPEN ACCESS

Edited by:
Andy Pereira, University of Arkansas, USA

Reviewed by:
Mostafa Abdelwahed Abdelrahman, Tohoku University, Japan
Rupesh Kailasrao Deshmukh, Laval University, Canada

***Correspondence:**
Lijuan Qiu
qiulijuan@caas.cn
Rongxia Guan
guanrongxia@caas.cn

Specialty section:
This article was submitted to Plant Abiotic Stress, a section of the journal Frontiers in Plant Science

Received: *18 July 2016*
Accepted: *20 September 2016*
Published: *30 September 2016*

Citation:
Liu Y, Yu L, Qu Y, Chen J, Liu X, Hong H, Liu Z, Chang R, Gilliham M, Qiu L and Guan R (2016) GmSALT3, Which Confers Improved Soybean Salt Tolerance in the Field, Increases Leaf Cl^- Exclusion Prior to Na^+ Exclusion But Does Not Improve Early Vigor under Salinity. Front. Plant Sci. 7:1485. doi: 10.3389/fpls.2016.01485

Soil salinity reduces soybean growth and yield. The recently identified *GmSALT3* (*Glycine max* salt Tolerance-associated gene on chromosome 3) has the potential to improve soybean yields in salinized conditions. Here we evaluate the impact of *GmSALT3* on soybean performance under saline or non-saline conditions. Three sets of near isogenic lines (NILs), with genetic similarity of 95.6–99.3% between each pair of NIL-T and NIL-S, were generated from a cross between two varieties 85–140 (salt-sensitive, S) and Tiefeng 8 (salt-tolerant, T) by using marker-assisted selection. Each NIL-T; 782-T, 820-T and 860-T, contained a common ~1000 kb fragment on chromosome 3 where *GmSALT3* was located. We show that *GmSALT3* does not contribute to an improvement in seedling emergence rate or early vigor under salt stress. However, when 12-day-old seedlings were exposed to NaCl stress, the NIL-T lines accumulated significantly less leaf Na^+ compared with their corresponding NIL-S, while no significant difference of K^+ concentration was observed between NIL-T and NIL-S; the magnitude of Na^+ accumulation within each NIL-T set was influenced by the different genetic backgrounds. In addition, NIL-T lines accumulated less Cl^- in the leaf and more in the root prior to any difference in Na^+; in the field they accumulated less pod wall Cl^- than the corresponding NIL-S lines. Under non-saline field conditions, no significant differences were observed for yield related traits within each pair of NIL-T and NIL-S lines, indicating there was no yield penalty for having the *GmSALT3* gene. In contrast, under saline field conditions the NIL-T lines had significantly greater plant seed weight and 100-seed weight than the corresponding NIL-S lines, meaning *GmSALT3* conferred a yield advantage to soybean plants in salinized fields. Our results indicated that *GmSALT3* mediated regulation of both Na^+ and Cl^- accumulation in soybean, and contributes to improved soybean yield through maintaining a higher seed weight under saline stress.

Keywords: soybean, salt tolerance, near isogenic line, sodium, chloride, *GmSALT3*, salt exclusion

INTRODUCTION

Salinity is a major abiotic stress that reduces crop productivity, with the extent of agricultural land salinization increasing due to climate change and poor land management (Takeda and Matsuoka, 2008). Worldwide, more than 40% of irrigated agricultural land has been predicted to be soon affected by salinity (Munns and Gilliham, 2015). To ensure food security into the future, crops with improved tolerance to salt stress will be required. To speed up the process of creating a new generation of stress tolerant elite crop lines, stress related genes should be used in pre-breeding research. The robustness of the stress related genes can then evaluate in the field prior to the release of new varieties to farmers. Several significant gains in abiotic stress tolerance of crops have been made through manipulating their ion transport properties through such approaches (Schroeder et al., 2013). For example, wheat grain yield in saline fields was improved by up to 25% through the introduction of a root localized Na^+ transporter via marker-assisted breeding (Munns et al., 2012).

Crop plants differ greatly in their salinity tolerance as reflected in their different growth responses at different growth stages (Foolad and Lin, 1997; Foolad, 1999; Takeda and Matsuoka, 2008). Studies on the mechanism of salt tolerance in soybean have focused mainly on seedling ion homeostasis, especially on the relative accumulation of Na^+, Cl^- and K^+ (Abel and MacKenzie, 1964; Läuchli and Wieneke, 1979; Pantalone et al., 1997; An et al., 2002). *Glycine max* seedlings under NaCl stress have been reported to have sensitivity to both Cl^- and Na^+, while *Glycine soja*, a wild relative has been demonstrated to have strong Cl^- tolerance (Umezawa et al., 2000; Luo et al., 2005; Chen and Yu, 2007). It was reported about half century ago that the salt tolerance of soybean was controlled by a single dominant allele q*NaCl3 (Ncl)* (Abel, 1969). A major QTL or dominant locus on soybean chromosome 3 was identified and validated by several research groups in both cultivated and wild soybean (Lee et al., 2004; Chen et al., 2008; Hamwieh and Xu, 2008; Hamwieh et al., 2011; Ha et al., 2013; Guan et al., 2014a). A salt candidate gene proposed to underpin this locus was identified from the wild soybean *G. soja*, accession W05, (*Glysoja01g005509)* by using a whole-genome sequencing approach (Qi et al., 2014). This paper named the homologous gene in soybean (*Glyma03g32900.1*), *GmCHX1*, after its putative function as a cation/H^+ exchanger, and proposed that it improved soybean salt tolerance after functional tests in tobacco BY2 cells and soybean hairy root cultures (Qi et al., 2014). Concurrent with this study, through map-based cloning from a salt tolerant Chinese soybean variety Tiefeng 8, we identified the same gene *Glyma03g32900.1*, and named it *GmSALT3* as it is likely to encode the candidate salt tolerance-associated gene on chromosome 3 (Guan et al., 2014b). Recently, Do et al. (2016) identified the equivalent allele from the salt tolerant Brazilian cultivar FT-Abyara, and named it *Ncl*, which is an abbreviation of the QTL (q*NaCl3*) identified by Abel (1969). The tolerant *GmSALT3* allele was found in *G. max* and *G. soja* germplasm that originated all over China but was most frequently associated with regions with saline soil conditions; however, the sensitive *GmSALT3* alleles (*Gmsalt3*) were much more prevalent in non-saline regions than saline regions (Guan et al., 2014b). It was proposed that the expression of the functional salt tolerance gene resulted in an energy burden on plants when salinity was not present (Qi et al., 2014), and this may explain its limited distribution in germplasm derived from non-saline areas (Guan et al., 2014b). Do et al. (2016) recently showed in the field using near-isogenic lines that there appeared to be no yield penalty in non-saline conditions for harboring *GmSALT3*, but a yield improvement under saline conditions. Such a property would make this gene (*CHX1/GmSALT3/Ncl*) an attractive prospect to breeders and farmers (Guan et al., 2014b), so further field testing in other soil types and different genetic background is required to confirm its potential (Do et al., 2016).

The salt tolerance of different soybean varieties has predominantly been evaluated prior to the identification of alleles associated with soybean salt tolerance (Läuchli and Wieneke, 1979; El-Samad and Shaddad, 1997; Umezawa et al., 2000; An et al., 2002; Essa, 2002). Isolation of *CHX1/GmSALT3/Ncl* has allowed the examination of its effects on Na^+, K^+ and Cl^- accumulation during salt stress and its effect on the salt tolerance of soybean seedlings has been conducted by at least three different research groups (Guan et al., 2014b; Qi et al., 2014; Do et al., 2016). Both transformation of the salt tolerant allele into the soybean variety Kariyutaka and its introgression into the salt-sensitive cultivar Jackson, significantly decreased the leaf Na^+, K^+ and Cl^- under 100 mM NaCl stress, and increased the soybean yield by 3.6–5.5 fold when irrigated the 5-week-old seedling with 1/4 concentration seawater (Do et al., 2016). However, the timecourse for the effect of *CHX1/GmSALT3/Ncl* on the accumulation of ions and its effects in different genetic backgrounds at different developmental stages is yet to be evaluated. Here, in order to identify the behavior of *GmSALT3* in differing genetic backgrounds and in different environments, we developed three sets of near isogenic lines (NILs) derived from progenies of 85–140 × Tiefeng 8 using marker-assisted selection for the target allele *GmSALT3* or *Gmsalt3*. These NILs were used to study whether *GmSALT3* had equivalent salinity tolerance in differing genetic backgrounds, to assess the effect of *GmSALT3* on salt tolerance at the emergence stage and the exclusion of Na^+ and Cl^- in both seedling and mature seeds, to determine whether *GmSALT3* positively impacted soybean yield under saline field conditions and to further examine whether *GmSALT3* conferred a yield penalty to soybean yield under non-saline field conditions.

MATERIALS AND METHODS

Development of Near Isogenic Lines by Marker-Assisted Selection

A $F_{2:3}$ population made by crossing a salt-sensitive soybean variety (85–140) and salt-tolerant variety (Tiefeng 8) was used to map the single dominant salt tolerance gene *GmSALT3* (Guan et al., 2014a). A SSR marker ssr_3_1310, tightly linked to the salt tolerance gene was used to screen heterozygous individuals at the F_4 generation. Three heterozygous individuals,

named 782, 820, and 860, were self-pollinated and screened by molecular markers over the F_5 to F_6 generations. A molecular marker *GmSALT3*-InDel, which was developed according to variation in the *GmSALT3* gene, was used to select three sets of different allele-containing NILs including 782-T (*GmSALT3*), 782-S (*Gmsalt3*), 820-T (*GmSALT3*), 820-S (*Gmsalt3*), 820-T (*GmSALT3*), 820-S (*Gmsalt3*), at the F_7 generation in 2011 (**Figure 1**).

Genetic Background Analysis of Three NIL Sets

Eight markers covering a 1098 kb genomic region flanking the *GmSALT3/salt3* locus were used to test for the presence of the common fragment in three NIL sets (**Figure 2A**). Seven of these markers are SSR markers from SoyBase[1]. *GmSALT3*-InDel is a functional marker developed to categorize the polymorphism found between Tiefeng 8 and 85–140 in the coding region of *GmSALT3/salt3*. To evaluate the relationship between the NILs and with their original parents, 147 SSR markers that were polymorphic between Tiefeng 8 and 85–140, were selected from 342 SSR markers distributed across all 20 chromosomes (Supplementary Figure S1).

[1] www.soybase.org

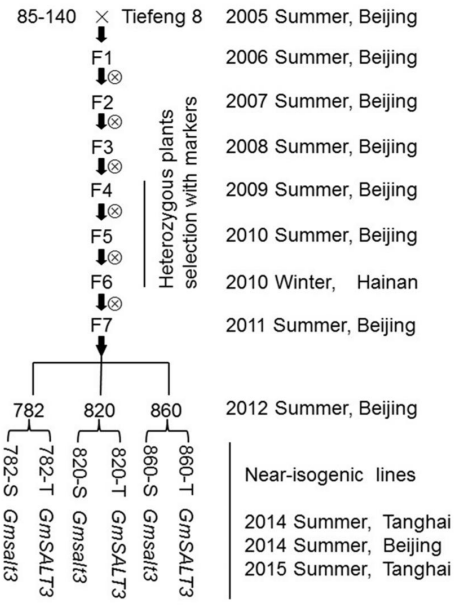

FIGURE 1 | Schematic diagram of the near isogenic lines (NILs) development by marker-assisted selection. Target region selection was employed from generation F_4 to F_6. The NILs (782, 820, and 860) separated at the *GmSALT3* locus were selected by using molecular markers from the progenies of three $F_{6:7}$ families.

Genotyping

For genotyping of the NILs, DNA was extracted from leaves using a Genomic DNA Purification Kit following manufacturers instructions (Thermo scientific, Lithuania). PCR was performed in a 20 μL reaction mixture containing 80 ng genomic DNA, 2 μL 10 × EasyTaq Buffer (with Mg^{2+}), 1.5 μL 2.5 mmol L^{-1} dNTPs, 2 μL each of 2 μmol L^{-1} primer stock, and 1 U EasyTaq DNA Polymerase (TransGen Biotech, Beijing, China) under the following conditions: 95°C for 5 min, and then 35 cycles at 95°C for 30 s, 55°C for 30 s, and 72°C for 50 s, followed by a final extension of 5 min at 72°C. The PCR products were separated on a 1.5% agarose gel or a 6% denaturing polyacrylamide gel.

Treatment and Phenotyping

NaCl Treatment and Ion Measurement

To clarify the effect of *GmSALT3* on salt tolerance at the seedling stage, 12 seeds of a single line were sown at a depth of 2.5 cm in a 6 × 6 × 8-cm pot filled with vermiculite and thinned to five seedlings per pot after 5 days; one pot was considered a replicate (i.e., the mean data from all five plants in the pot per parameter). The experimental design was completely randomized and comprised of two treatments × six genotypes with three replications, giving a total of 36 pots/replicates overall for all treatments and lines. Plants were grown in a growth chamber (RXZ-500D; Ningbo Jiangnan Instrument, China), with a day length of 16 h (with a light-emitting diode light source at 400 μmol m^{-2} s^{-1}) at 28°C, and 8 h dark at 25°C, with 60% relative humidity throughout. Every treatment group (salt or control) consisted of 18 pots (9 NIL-T and 9 NIL-S) placed in a 46 × 32 × 10-cm tray, and 3.6 L of water was added to the tray. The irrigation water available in the growth facility had an electrical conductivity (EC) of 0.4 dS m^{-1} and contained potassium, calcium, sodium and magnesium in the water at a concentration of 0.06, 0.86, 0.43, and 0.46 mmol L^{-1}, respectively, as determined by ICP-AES analysis (Thermo-Jarrell Ash; IRIS Advantage) and 0.46 and 0.02 mmol L^{-1} for fluoride and chloride respectively, as determined by ion chromatography (ICS-1600, Thermo Fisher Scientific). Water and treatment solutions were always added to the tray so plants accessed the solution from the bottom of the pots rather than watering the top of the pots. From the fourth day after sowing (DAS) 1.5 L of this water was added to the tray every 3 days until a salinity treatment was initiated. When the unifoliate leaves of plants were fully expanded at 12 DAS, 1.5 L of NaCl solution at an EC of 17.8 dS m^{-1} (i.e., 200 mmol L^{-1}) was added to one tray, the second dose of 1.5 L of 200 mmol L^{-1} NaCl solution was applied 14 DAS; the same volume of irrigation water was applied to the tray of the control plants. Thereafter, each tray was watered every 3 days with 1.5 L of irrigation water. Twenty-two DAS, the pots were inverted and the plants and vermiculite were carefully extracted so to minimize damage to the root. Then, the roots were quickly washed with deionised water (<15 s) to remove the vermiculite and other soluble components, and blotted dry with paper towel. Root, stem, hypocotyl and unifoliate leaves of five plants in each treatment were harvested separately and placed in labeled paper bags.

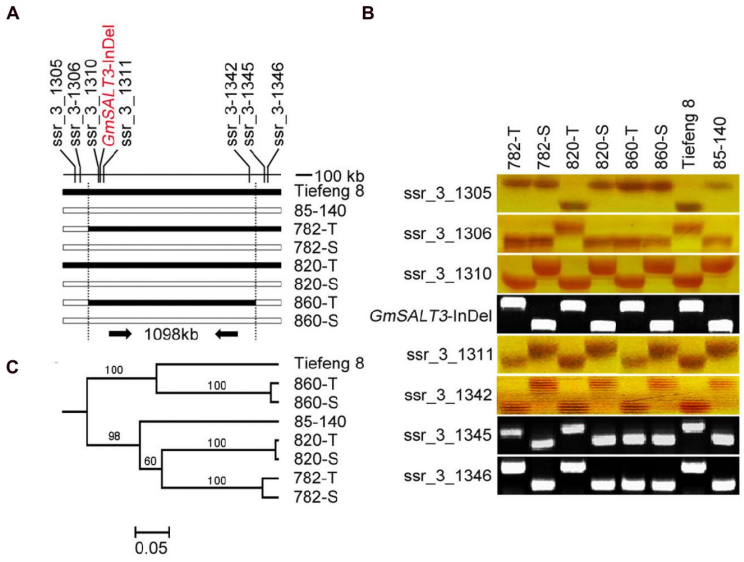

FIGURE 2 | Evaluation of a common region around *GmSALT3* and genetic backgrounds of three sets of NILs. (A) Localization of eight markers used for common region testing of three sets of NILs, black bars indicate the same genotype with Tiefeng 8 and the white bars indicate the same genotype with 85–140. The functional marker *GmSALT3*-InDel was developed from the variation within the coding region of the target gene *GmSALT3*. **(B)** PCR assays of eight markers on chromosome 3 of NILs and their parents. **(C)** Phylogenetic relationship of NILs and their parents based on the data of 147 sets of SSR markers using the UPGMA method, the bootstrap values (%) are indicated above the node.

To evaluate the effect of *GmSALT3* on accumulation of Na^+ and Cl^-, NIL-820 and NIL-860 lines which showed a high similarity of genetic background between each NIL-T and NIL-S were selected. Seeds of NILs were sown in pots as described above. There were three replicate pots of each genotype in each sample collection time point. After the unifoliate leaves of plants were fully expanded, 90 mL of 200 mmol L^{-1} NaCl solution was added 12 and 14 DAS from the bottom of each pot, respectively, after which 90 mL of irrigation water was applied at the bottom of each pot every 3 days. Plants were harvested at 0, 1, 3, 5, 7, and 10 days after beginning the NaCl treatment. The roots were washed gently with deionized water as described above and plants were dissected into roots, hypocotyl, stem and leaves.

Seedling Emergence

To understand whether *GmSALT3* had a positive effect on salt tolerance at the emergence stage, 10 seeds of each NIL were sown 2.5 cm deep in a 6 × 6 × 8-cm pot filled with vermiculite. Each treatment consisting of six soybean lines with three pots per line, giving a total of 18 pots, were placed in a 46 × 32 × 10-cm tray, and 3.6 L of irrigation water or NaCl solution at EC of 10.6 dS m^{-1} (i.e., 100 mmol L^{-1}) or 17.8 dS m^{-1} (i.e., 200 mmol L^{-1}) was applied to the tray. Four days after the first treatment, all plants were watered with 1.5 L irrigation water every 3 days. As mentioned above, the NaCl solution and water were supplied from the bottom of the pots. The experiment was conducted in the growth cabinets with conditions as described above. Emergence was counted 10 DAS. Relative emergence rate was the ratio of emerged seedlings under salt stress compared to the corresponding emerged seedlings under control (non-saline) condition. Fifteen DAS, the pots were inverted and the plants and vermiculite were carefully extracted to minimize damage to the roots. Then, the roots were quickly washed with deionized water to remove vermiculite and other soluble components, and blotted dry with paper towel. Fresh mass and shoot length of the seedlings were obtained through their measurement on weighing scales and manually using a ruler.

Yield of NILs under Saline and Non-saline Field Conditions

Beijing 2014

For the comparison of agronomic traits for each pair of NILs under non-saline conditions the three sets of NILs were planted in a non-saline field in Shunyi Experimental Station, Shunyi, Beijing, China (latitude 40°13′ N, longitude 116°65′ E). Soybean seeds were sown at a depth of 3 cm on 19 June 2014. The rainfall during the June to October at Shunyi in 2014 was 394.0 mm (data from China Meteorological Data Sharing Service System). The soil was fertilized with 375 kg ha^{-1} $(NH_4)_2HPO_4$ and 150 kg ha^{-1} KCl before sowing. Soybean seeds were planted in 1.5 m long three-row plots with three replications, with row spacing of 50 cm and a spacing of 8 cm between plants. The soybean plants were irrigated once in August during seed filling. At maturity, the plants were cut from the surface of the soil. Fifteen plants of each line were bulked per replication three times for agronomic trait evaluation.

Hebei 2014, 2015

The saline soil trials were conducted in Tanghai county (Hebei Province, China), along the Bohai coast, where 40.3% of the fields had saline soil with an average soluble salt of more than 2 g kg^{-1} (Zhang et al., 2012). The saline field used in this experiment was located in No. 11 farm of Tanghai county (latitude 39°27′ N, longitude 118°45′ E). White crusts of salt were observed on the soil surface. The soluble salt concentration was evaluated by measuring the EC of the aqueous extract of the soil cores down to 25–30 cm before sowing the soybean. After coring, the soil was air-dried and passed through a 2 mm mesh sieve. The EC of the 1: 5 soil: water (w/v) mixture (in terms of g water per g dry soil) was measured by using a digital conductivity meter DDS-11A (Leici Instrument Inc., Shanghai, China). The pH was determined with a pH electrode PHS-3C at a soil : water ratio of 1: 5 (w/v) after 30 min in suspension. For the 2014 field trial, the EC and pH of soil : water (1:5) was 0.6 dS m^{-1} and 8.18, the soybean NILs for the field experiment were planted on the 10th June 2014 and harvested on the 20th October, with approximately 15 seeds per row (1.0 m long). The 2015 field trail was located in the same paddock and about 25 m south of the 2014 trial, the EC and pH of soil: water (1: 5) was 0.7 dS m^{-1} and 7.6, the soybean NILs for the field experiment were planted on the 25th June 2015 and harvested the 14th October, with approximately 25 seeds per row (1.5 m long). A completely random design with three replications was used, with each plot containing three rows of each line and no fertilizer was applied. The rainfall during June and October at Tanghai was 265.4 and 396.0 mm in 2014 and 2015, respectively (data from China Meteorological Data Sharing Service System), and the soybean plants were grown without supplemental irrigation. At maturity, the plants were cut from the surface of the soil. Fifteen plants of each line were bulked per replication three times for agronomic trait evaluation.

Tissue Ion Analysis

All plant samples were dried at 75°C for 3 days in a forced air oven. Seeds and pod walls from 2015 saline field trial were oven-dried for 3 days at 40°C. Samples were ground to a fine powder using metal beads in a SPEX 2000 Geno/Grinder (SPEX CertiPrep, USA) and 0.1 g of subsample was extracted with 10 mL of 100 mmol L^{-1} acetic acid at 90°C for 3 h in a water bath shaker. Sodium and potassium concentration was measured with an atomic absorption spectrophotometer SOLAAR s2 (Thermo Elemental, Waltham, MA, USA), to give the concentrations of the two ions in different tissues. Chloride was measured with Chloride Analyzer (Model 926, Sherwood, UK).

Data Analysis

One-way ANOVA followed by Tukey's HSD *post hoc* test was performed on the analysis of ions concentration and yield related trait comparison using Prism 3.0 software (GraphPad Software, La Jolla, CA, USA), lowercase letters were used to indicate statistically significance differences between groups at $P < 0.05$. Student's *t*-tests were used for other data analysis, single or double asterisks indicated statistical significance corresponding to $P < 0.05$ or $P < 0.01$, respectively. The neighbor-joining tree was constructed by using Power Marker 3.23 with 1000 bootstrap replicates (Liu and Muse, 2005)[2], and MEGA (Tamura et al., 2007) was used to view the dendrogram tree.

RESULTS

Genomic Composition of Three Sets of NILs

To evaluate the impact of *GmSALT3* on soybean growth in differing genetic backgrounds, three sets of NILs were developed from the F_7 progeny of a cross (85–140 × Tiefeng 8) after three generations of marker-assisted self-pollination (**Figure 1**). The common interval, 1098 kb on chromosome 3, of the three NIL-T lines was determined using eight markers including the functional marker in *GmSALT3* (**Figures 2A,B**). The lines (782-T, 820-T, 820-T) carrying the functional Tiefeng 8 type allele *GmSALT3*, were named NIL-T and the other corresponding lines (782-S, 820-S, 820-S) carrying the non-functional allele *Gmsalt3* from 85–140 were named NIL-S.

To estimate the similarity of their wider genetic backgrounds, 147 genome-wide polymorphic SSR markers were used to genotype the three sets of NILs (Supplementary Figure S1). The SSR assay showed that the genetic similarity between 860-S and 860-T was 98.0%, between 782-T and 782-S was 95.6%, and between 820-T and 820-S was 99.3%. Phylogenic analysis showed NIL-860 shared a similarity of 64% with Tiefeng 8; the other two sets of NIL-782 and NIL-820 shared similarity of 65 and 55% with 85–140, respectively (**Figure 2C**).

Na^+ Accumulation in Different NILs Was Affected by Genetic Background

Na^+ and K^+ accumulation was explored in the three sets of NILs after NaCl stress for 10 days. Significantly lower Na^+ concentration was observed in both leaf and stem of NIL-T lines compared with their NIL-S plants, regardless of their genetic backgrounds (**Figure 3A**). Given that the different NIL-T had the same *GmSALT3* allele, but differing genetic backgrounds, we compared the effect of the genetic backgrounds on Na^+ accumulation. We found that 782-T accumulated relatively more Na^+ than 820-T and 860-T in both the stem and leaf samples, indicating genetic loci other than *GmSALT3* might influence Na^+ accumulation. This is also supported by the fact that the corresponding NIL-S (820-S and 860-S) also accumulated less Na^+ in the stem, leaf and root than that of 782-S (**Figure 3A**). No significant differences in leaf K^+ concentration was observed within each pair of NILs (**Figure 3B**). This indicated that the *GmSALT3* had little effect on the regulation of K^+ homeostasis and that the regulation of K^+/Na^+ balance in the shoots was mostly dependent on the accumulation of Na^+ in shoots (**Figure 3C**).

[2]http://statgen.ncsu.edu/powermarker/

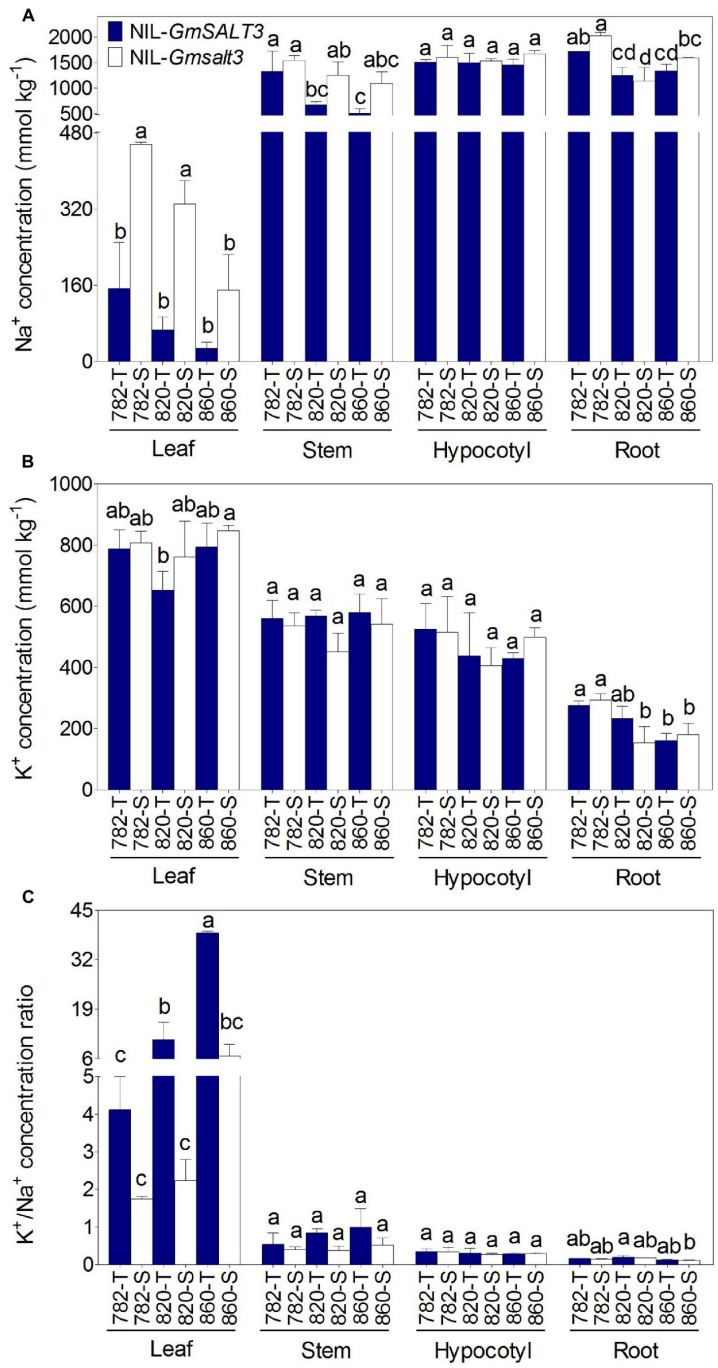

FIGURE 3 | Ion concentration (dry mass) in three sets of NILs after 10 days of NaCl stress (200 mmol L^{-1}; EC = 17.8 dS m^{-1}). (A) Tissue concentration of Na^+ in leaf, stem, hypocotyl and root of three sets of NILs. **(B)** Concentration of K^+ in leaf, stem, hypocotyl and root of three sets of NILs. **(C)** The K^+/Na^+ ratio in leaf, stem, hypocotyl and root of three sets of NILs. Data are means of three replicates consisting of the mean values for five plants grown in the same pot ± SD ($n = 3$). Different letters indicate statistically significant differences between NIL lines for each tissue (one-way ANOVA followed by Tukey's HSD *post hoc* test, $P < 0.05$).

A Detailed Analysis of NIL-820 and NIL-860 Reveals *GmSALT3* Also Affects Cl^- Accumulation

As the effect of *GmSALT3* was similar on shoot Na^+ accumulation between each set of NILs, we undertook a closer examination of Na^+ and Cl^- accumulation in NIL-820 and NIL-860 following a NaCl treatment over 10 days (**Figure 4**). Over the first 3 days of NaCl treatment, Na^+ and Cl^- accumulation in the roots was equal for both tolerant and sensitive genotypes of NIL-820 and NIL-860 (**Figure 4**), whereas the Cl^- concentration in roots of 820-S and 860-S was significantly lower than in the 820-T and 860-T lines after 5 and 7 days respectively (**Figures 4C,D**). In both NIL-T and NIL-S roots the Na^+ and Cl^- concentration plateaued after 5 – 7 days of NaCl treatment, and the accumulation of Na^+ was higher than that of Cl^- (**Figure 4**). In the aerial tissues of NIL-T soybean, Na^+ accumulation occurred later than that of Cl^-. Accumulation of Cl^- was consistently significantly greater in the hypocotyls of both NIL-S compared to their respective NIL-T after 1 day of salt treatment, whereas this was only the case for Na^+ in the first instance after 3 days (**Figure 4**). The soybean leaves accumulated more Cl^- than that of Na^+. The concentration of Na^+ in NIL lines decreased from the root to leaf, but this was not the case for Cl^- concentration in NIL-S lines, which was high across all shoot organs (**Figures 4C,D**). These results indicate that *GmSALT3* influences both Na^+ and Cl^- accumulation in soybean plants under a salt treatment.

GmSALT3 Has Little Effect on Soybean Growth at the Emergence Stage under Saline Stress

We analyzed the relative emergence rate and early vigor of the three NIL sets to see if *GmSALT3* also affected the salt tolerance of soybean at the emergence stage (**Figure 5**, Supplementary Figure S2). We quantified the effect of *GmSALT3* gene on emergence by using relative emergence rate after 10 days. The relative emergence rates were greater for all genotypes when treated with 100 mmol L^{-1} NaCl (EC of 10.6 dS m^{-1}); compared to the NaCl solution of 200 mmol L^{-1} NaCl (EC of 17.8 dS m^{-1}). Whilst NIL-820 showed a higher relative emergence rate than the other two sets of NILs when treated with 200 mmol L^{-1} NaCl (**Figure 5A**), no significant differences in relative emergence rate within each set of NILs was observed when they were treated with 100 and 200 mmol L^{-1} NaCl solution (**Figure 5A**). Early vigor was estimated by measuring shoot length and fresh weight 15 DAS. Early seedling vigor showed no difference within each set of NILs under saline and non-saline conditions except for the 820 NILs, where 820-S had greater shoot length than 820-T treated with 200 mmol L^{-1} NaCl (**Figures 5B,C**).

GmSALT3 Has a Positive Effect on the Yield of NIL-T under Saline Stress

When the three sets of NILs were grown in non-saline field conditions (Shunyi, Beijing), NIL-T lines containing *GmSALT3* had a similar yield to the corresponding NIL-S lines containing *Gmsalt3* for the yield parameters of pod number, seed number, seed weight and 100-seed weight (**Figure 6A**). The yield related components of both NIL-T lines and NIL-S lines were substantially affected by salinity stress when NILs were grown on saline soil (Tanghai, Hebei province) with the respective NIL-S for each set of lines being noticeable smaller at harvest maturity (Supplementary Figure S3). In terms of the plant height, 820-T and 860-T were significantly taller than that of 820-S and 860-S when grown on saline soil whereas 782-T and 782-S were similar in size at Tanghai in 2014; while in 2015 saline field

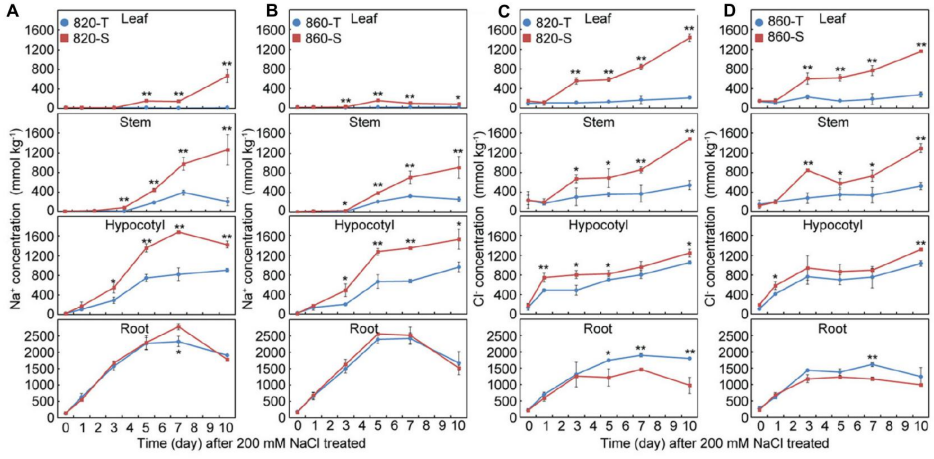

FIGURE 4 | Time-course of ion concentration (dry mass) in different tissues of NIL-820 and NIL-860 during 10 days of NaCl stress (200 mmol L^{-1}; EC = 17.8 dS m^{-1}). Na^+ concentration in leaf, stem, hypocotyl and root of NIL-820 **(A)**, and NIL-860 **(B)**, or Cl^- concentration in leaves, stems, hypocotyls and roots of NIL-820 **(C)**, and NIL-860 **(D)**. Data are means of three replicates consisting of the mean values for five plants grown in the same pot ± SD. Student's *t*-test was used to compare NIL-T and NIL-S at the same time point (*$P < 0.05$, **$P < 0.01$).

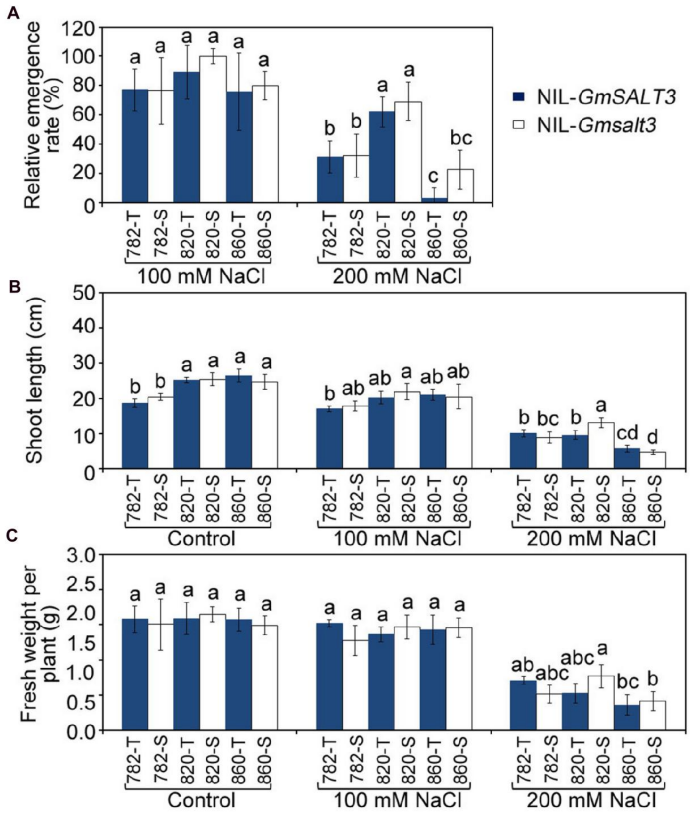

FIGURE 5 | Emergence rate after 10 days and early vigor after 15 days of three sets of NILs under control and NaCl stress conditions. (A) The relative emergence rate of three sets of NILs under NaCl stresses (EC = 10.6 dS m^{-1}, 17.8 dS m^{-1}). **(B)** The seedling length of NIL lines under control and NaCl stress (EC = 10.6 dS m^{-1}, 17.8 dS m^{-1}). **(C)** Average plant weight of three sets of NILs under control and NaCl stress (EC = 10.6 dS m^{-1}, 17.8 dS m^{-1}). Data are means of three replicates ± SD ($n = 3$). Different letters indicate statistically significant differences between NIL lines (one-way ANOVA followed by Tukey's HSD *post hoc* test, $P < 0.05$).

trial plant height was equal between NIL pairs (**Figure 6C**). Under saline conditions no significant difference in pod number and seed number were observed between each pair of NIL-T and NIL-S. However, the NIL-T lines containing *GmSALT3* had significantly greater seed weight and 100-seed weight than related NIL-S lines regardless genetic backgrounds under saline conditions (**Figures 6B,C**). The seed weight of NIL-S lines was 30–57% lower than corresponding NIL-T lines in 2014 saline field trial, and 37–58% lower in 2015 saline field trail. The mean above ground dry mass of the NIL-S lines was lower than the corresponding NIL-T lines, but a significant difference was only observed between 782-T and 782-S (Supplementary Figure S4).

Effects of *GmSALT3* on Na^+, K^+ and Cl^- Concentration in Seeds and Pod Walls under Saline Stress

In the saline field (Tanghai, 2015), the Na^+ concentration in seeds and pod walls of three sets of NILs ranged from 4.1 to 42.9 mmol kg^{-1} and 41.4 to 141.4 mmol kg^{-1} dry mass, respectively. Na^+ concentrations in seeds and pod walls of three NIL-T lines were significantly lower than the corresponding NIL-S lines, except for the Na^+ concentrations between 782-T and 782-S (**Figure 7A**). Pod walls contained higher K^+ concentrations than seeds, but no significant differences were observed for K^+ concentrations in both seeds and pod walls among genotypes grown in saline soil (**Figure 7B**). All three NIL-T lines grown on saline field had low seed Cl^- concentrations ranging from 8.8 to 11.8 mmol kg^{-1} dry mass. The seed Cl^- concentrations in NIL-S lines were greater by 1.5, 3.2, and 1.6 times in 782-S, 820-S, and 860-S compared to their corresponding NIL-T lines, respectively (**Figure 7**), but a significant difference was only observed between 820-T and 820-S. The Cl^- concentrations in pod wall of 782-T, 820-T and 860-T were 48.8, 101.2, and 35.1 mmol kg^{-1} dry mass, respectively. Compared to NIL-T lines, the Cl^- concentrations in pod wall of 782-S, 820-S, and 860-S were greater by 5.3, 3.5, and 6.3 times. As a result the NIL-T lines carrying the functional *GmSALT3*

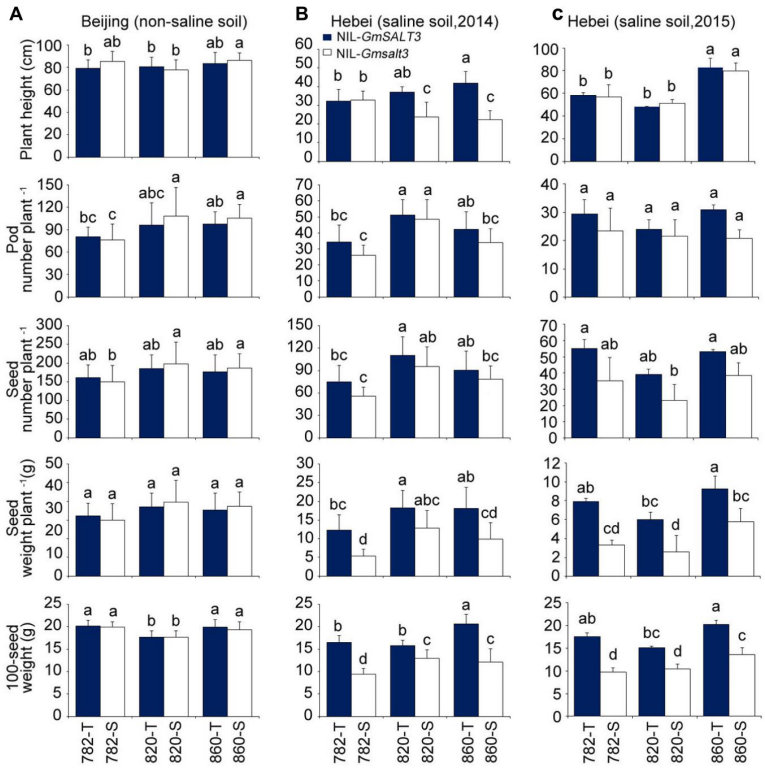

FIGURE 6 | Yield related traits comparison for three sets of NILs grown in saline and non-saline soil conditions. (A) Plant height, pod number per plant, seed number per plant, seed weight per plant and 100-seed weight of three sets of NILs grown in non-saline soil (Shunyi, Beijing). Data are means of three replicates consisting of mean data from 15 plants per replicate ± SD ($n = 3$). **(B)** Plant height, pod number per plant, seed number per plant, seed weight per plant and 100-seed weight of three sets of NILs grown in saline soil (Tanghai, Hebei province, 2014). **(C)** Plant height, pod number per plant, seed number per plant, seed weight per plant and 100-seed weight of three sets of NILs grown in saline soil (Tanghai, Hebei province, 2015). Data are means of three replicates consisting of mean data from 15 plants per replicate ± SD ($n = 3$). Different letters indicate statistically significant differences between NIL lines (one-way ANOVA followed by Tukey's HSD *post hoc* test, $P < 0.05$).

allele accumulated less Cl^- in seeds and pod walls than their corresponding NIL-S lines under saline stress.

DISCUSSION

Previous studies have mostly evaluated the salt tolerance of soybean at the seedling stage. Such studies have repeatedly identified the same major QTL independently (Lee et al., 2004, 2009; Chen et al., 2008; Hamwieh and Xu, 2008; Hamwieh et al., 2011; Ha et al., 2013; Guan et al., 2014a), with only a few studies focusing on QTL mapping at the germination stage (Zhang et al., 2014). Recently, we and other groups have isolated a dominant salt tolerance gene *CHX1/GmSALT3/Ncl* located on chromosome 3 (Guan et al., 2014b; Qi et al., 2014; Do et al., 2016). Here, we successfully created three sets of NILs containing *GmSALT3* and *Gmsalt3*, respectively. The three tolerant NILs had differing genetic backgrounds whilst containing a common ~1000 kb region including the *GmSALT3* gene in NIL-T lines or *Gmsalt3* in NIL-S lines. The NILs differed at the major salt tolerant locus are suitable for assessing the impact of tolerant allele on ions accumulation and yield related traits.

Negative correlations between leaf Na^+ concentration and salt tolerance have been widely observed in soybean and other crop species (Schachtman and Munns, 1992; Kao et al., 2006). Here, significantly higher Na^+ concentrations and a lower K^+/Na^+ ratio were observed in leaves of NIL-S lines compared with the corresponding NIL-T lines when salt treated (**Figure 3A**). Whereas, there was no observable difference in leaf Na^+ concentration and K^+/Na^+ ratio between each pair of NIL-T and NIL-S lines under non-saline conditions (Supplementary Figure S5). This again strengthens the evidence that *GmSALT3* exerts a positive effect on soybean salt tolerance. Furthermore, the significantly lower Na^+ concentration observed in the leaf of 860-S compared to that of 820-S indicated that the degree of Na^+ accumulation exerted by genetic elements in addition to *GmSALT3* deserve further investigation in this set of NILs (**Figures 3A** and **4A,B**). It is suggested that Na^+ inhibits enzyme

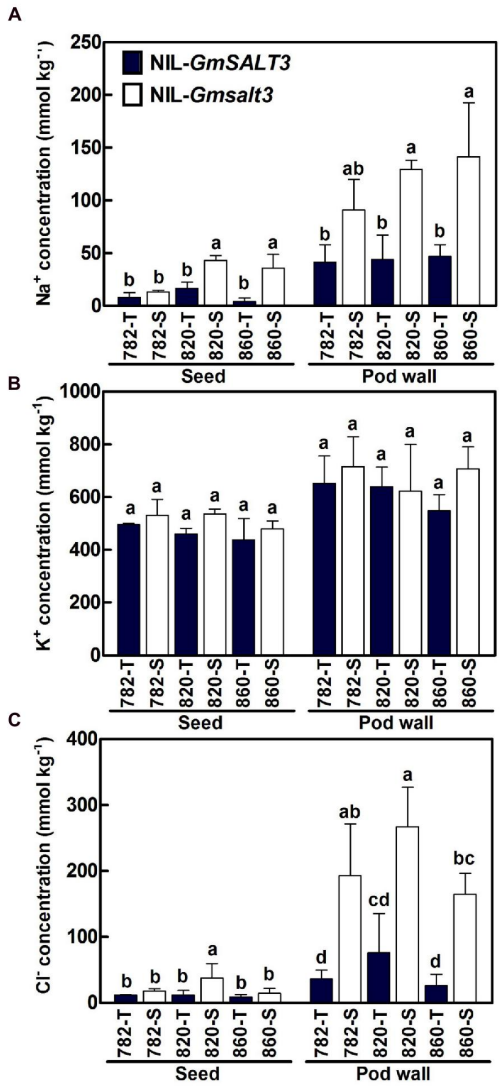

FIGURE 7 | Mean Na^+ (A), K^+ (B), Cl^- (C) concentrations (dry mass) in seeds and pod walls of three sets of NILs grown on saline field (2015, Tanghai). Data are means of three replicates consisting of the mean values for 15 plants for per replicate ± SD ($n = 3$). Different letters indicate statistically significant differences between NIL lines for each tissue (one-way ANOVA followed by Tukey's HSD *post hoc* test, $P < 0.05$).

activity through competing with K^+ for binding sites at high concentration (Tester and Davenport, 2003; Munns and Tester, 2008). The exclusion of Na^+ in plant shoots is controlled by either xylem loading or phloem re-translocation to prevent the toxic accumulation of Na^+ in photosynthetic tissues (Maathuis et al., 2014). Since the export of Na^+ through phloem in soybean is not sufficient to control the accumulation of Na^+ in leaves, the salt tolerance of soybean may depend on its ability of Na^+ delivery into xylem (Durand and Lacan, 1994). The K^+ concentration in each tissue of each NIL was not consistently related to changes in Na^+, which has been also observed in wheat and barley (Genc et al., 2007; Tavakkoli et al., 2011).

Cl^- plays a major role in membrane potential charge balance and in pH control (Teakle and Tyerman, 2010). A limited number of studies have shown that Cl^- concentration was correlated with salt sensitivity in soybean (Abel and MacKenzie, 1964; Läuchli and Wieneke, 1979; Valencia et al., 2008). Luo et al. (2005) documented that in cultivated soybean seedlings, Cl^- was more toxic than Na^+. Although the same osmotic potential (−0.68 MPa) was used for treatment of Na^+, Cl^- and NaCl in the experiments, the altered concentration of other ions (K^+, Ca^{2+} and Mg^{2+}) in the solution may affect the plant response (Luo et al., 2005). In faba bean, Na^+ and Cl^- limits the plant growth simultaneously but through different mechanisms (Tavakkoli et al., 2010). It has been reported that Na^+ and Cl^- had additive effects on the growth of barley (Tavakkoli et al., 2011). Plants containing *GmSALT3* had much less Cl^- accumulating in leaves and more in the roots when salt treated. The significantly lower Na^+ and Cl^- in both 820-T and 860-T compared with 820-S and 860-S strongly suggests that *GmSALT3* has a strong effect on both Na^+ and Cl^- exclusion (**Figures 4A,B**). Interestingly the concentration difference of Cl^- in aerial tissues between NIL-T and NIL-S appeared prior to that of Na^+. Furthermore, it suggests that innate Na^+ exclusion in the NIL-S is greater than that of Cl^- exclusion, but Na^+ exclusion breaks down after several days of salt treatment. The difference of Na^+ and Cl^- accumulations between NIL-T and NIL-S suggests the participation of *GmSALT3* in both Na^+ and Cl^- homeostasis, and that Cl^- accumulation is decoupled from accumulation of Na^+ (and K^+) and occurs via a distinct mechanism. Do et al. (2016) suggested that CHX1/GmSALT3/Ncl controls Na^+, K^+ and Cl^- accumulation simultaneously, and may function as a cation-chloride cotransporter (CCC). Both the CCC in rice and *Arabidopsis* affects the transport of these three ions to the shoot; plants that lack *CCC* expression are salt sensitive (Colmenero-Flores et al., 2007; Kong et al., 2011; Henderson et al., 2015; Chen et al., 2016). Some data has been used to propose a plasma membrane localisation for rice CCC (Kong et al., 2011; Chen et al., 2016) while AtCCC and VviCCC, have both been localized to the Golgi and Trans-Golgi network, and so are unlikely to directly affect Na^+, K^+, and Cl^- transport between the root symplast and xylem apoplast and their accumulation in the shoot (Colmenero-Flores et al., 2007; Henderson et al., 2015). GmSALT3 is also predicted to be an endomembrane protein having been localized to the endoplasmic reticulum (ER) (Guan et al., 2014b); it shares this localisation with several other CHX protein family members from *Arabidopsis* (Sze et al., 2004; Padmanaban et al., 2007; Chanroj et al., 2012). The CHX proteins in *Arabidopsis* mainly function in osmotic adjustment, and K^+ or Na^+ homeostasis (Sze et al., 2004; Hall et al., 2006; Maresova and Sychrova, 2006; Padmanaban et al., 2007; Lu et al., 2011). Therefore, quite how GmSALT3 confers these traits of Na^+ and

Cl^- exclusion is still unknown and is the subject of further research.

The relationship between increased salt accumulations in leaves with decreased soybean yield has been reported (Abel and MacKenzie, 1964; Bustingorri and Lavado, 2013). However, little is known about the concentration of ions in the reproductive structures of soybean. A negative relationship between Cl^- accumulation in seeds with seed yield and weight has been observed in soybeans when KCl was used as fertilizer in a field experiment, indicating the soybeans suffered from chloride toxicity which appeared to come from the KCl fertilizer (Parker et al., 1983). Analysis of the ion concentration in mature seeds and pod walls of NILs grown in a saline field revealed a lower seed Na^+ concentration in NIL-T lines compared with the corresponding NIL-S lines, but the difference was not significant between that of 782-T and 782-S; in pod walls, Na^+ concentrations were 2.6–11.4 fold higher than in the seeds (**Figure 7A**). The difference in seed Cl^- concentrations between each pair of NIL-T and NIL-S were not significant, except for 820-T and 820-S, while all NIL-T lines accumulated significantly lower Cl^- in pod walls than that of NIL-S lines. Whether accumulation of Na^+ and Cl^- in the seed and pod wall interferes directly with seed development or whether the effects are due to accumulation of salt in other parts of the plant and reducing the energy devoted to developing seeds is yet to be tested. In chickpea, a significantly higher concentration of seed sodium and potassium was observed in salt sensitive genotypes compared to tolerant ones (Turner et al., 2013). While a recent study of chickpea genotypes subjected to NaCl stress found that the changes of Na^+ and Cl^- in mature seeds of salt tolerant and sensitive genotypes were not associated with salinity tolerance (Kotula et al., 2015).

The extent to which tolerance factors identified in hydroponic or pot assays under controlled conditions hold up to scrutiny in the field, where the imposition of stress and other environmental factors are more dynamic, is a common problem when translating lab research to the field (Genc et al., 2007). As such, it is important to assess plant tolerance to stress at different growth stages. We have previously identified *GmSALT3* as a dominant gene conferring salt tolerance at the seedling stage. Here, the development of NILs made it possible for us to also evaluate the function of *GmSALT3* at an emergence stage under salt stress. To mimic the natural salinity conditions occurring at our field sites, as salt is likely to be present when the seeds are sown in the field, we sowed the soybean seeds in vermiculite and watered with NaCl solution. Under NaCl stress at EC of 10.6 dS m^{-1} (i.e., 100 mmol L^{-1} NaCl) most of the NILs lines germinated at a relatively high levels, while a higher concentration of NaCl inhibited the emergence of the soybean and limited the plant growth. Under NaCl stress at EC of 17.8 dS m^{-1} (200 mmol L^{-1} NaCl) most of the cotyledons were yellow and unable to maintain turgor (Supplementary Figure S2). Previously, reduction of seed water absorption was observed when the osmotic pressure in germinating solution was increased by NaCl (Rudolfs, 1921). The reduction of emergence rate under higher salinity levels is likely to be a result of an osmotic stress (Bernstein and Hayward, 1958). No significant differences were observed within each set of NIL lines, indicating that the existence of *GmSALT3* did not increase soybean salt tolerance at the emergence stage. This is consistent with previous studies that the salt tolerance at one stage is not always correlated with that of the other growth stages (Abel and MacKenzie, 1964). Furthermore, the sensitivity of soybean seedlings to salinity has previously been proposed to be greater than that of germinating seeds, as is the case for many plant species (Rogers et al., 1995; Hosseini et al., 2002) – our research findings here seem to corroborate this statement. During QTL mapping of salt tolerance of seed germination and vegetative stages of tomato, few common QTL were observed that had significant effects at both stages (Foolad, 1999). With this in mind, when using GmSALT3 in the field it would be wise to use appropriate soil and water management practices to enhance the germination rate (Devkota et al., 2015), or to pyramid the *GmSALT3* gene with the recently identified salt tolerance related candidate genes at the germination stage (Kan et al., 2015). In our study, both NIL-820 lines showed better salt tolerance at the emergence stage compared to the other two sets of NIL lines, so these could potentially be used as a resource for improving salt-tolerance at the emergence stage (**Figure 5A**, Supplementary Figure S2).

The characterization of the different alleles of *GmSALT3* in our previous report suggested that the tolerant allele had been under significant selection pressure; it was frequently lost in non-saline environments (Guan et al., 2014b). Thus, this raises an important question of whether *GmSALT3* incurs a penalty to yield under non-saline conditions. Since most salinity affected soils are not uniformly saline or apply a constant level of salinity during the entire crop growth cycle, genes with no penalty are more appropriate for breeding salt tolerant crops (Munns et al., 2012). In our case, we found that under non-saline field conditions NIL-T lines had similar yield related traits compared to their related NIL-S lines (**Figure 6A**), indicating no yield penalty associated with the presence of *GmSALT3* allele. We therefore find no reason why *GmSALT3* may have been selected against on the basis of yield under modern farming practices. This result corroborates the recent findings of Do et al. (2016) who also found, using different soybean genetic backgrounds, that the functional *GmSALT3* allele does not harbor a yield penalty under non-saline conditions, whilst conferring improved yields under saline conditions.

The effect of GmSALT3 on soybean growth and yield was evaluated by comparing three sets of NIL lines over 2 years in Tanghai, Hebei province. Pod number and seed number per plant decreased for both NIL-T and NIL-S lines, compare with control plants, while the difference between each pair of NIL-T and NIL-S was not significant. The lower yield reduction of a super-nodulating en-b0-1 compared with its normal-nodulating parent Enrei under salinity stress was primarily due to the larger seeds number of en-b0-1 (Yasuta and Kokubun, 2014). Analysis of chloride toxicity of soybeans grown in Flatwoods soils fertilized with KCl identified an average of 25% less 100-seed weight in susceptible cultivars than that for tolerant ones (Parker et al., 1983). Significant differences in 100-seed weight were observed

between each pair of NIL-T and NIL-S, suggesting that NIL-S is compromised in its ability to produce larger seeds and this contributes to the 30–58% loss of seed yield for NIL-S lines (**Figure 6**). Do et al. (2016) also showed that the *Glyma03g32900* gene cold increase soybean yield by 3.6–5.5 fold when treated with diluted seawater in Japan (Do et al., 2016), indicating the wide potential for using this gene to improve the salt tolerance of soybean.

CONCLUSION

In this study, three sets of NILs differing at *GmSALT3* locus were developed through marker-assisted selection, and used to evaluate the possible effect of *GmSALT3* on ion accumulation and yield production. Our results clearly indicate that *GmSALT3* alters both Na^+ and Cl^- accumulation in shoots and mature pod walls of NIL-T lines. The salt tolerance gene *GmSALT3* was found to have no penalty on soybean yield under non-saline condition and contributes to improving soybean yields through increasing seed weight in different genetic backgrounds under salinity stress in the field (**Figures 6B,C**). The salinity tolerance of NIL-T lines was related with the maintenance of seed size under salt stress, with this ability associated, at least partially, with the ability to regulate Na^+ and Cl^- in both vegetative and reproductive tissues. Interestingly we found that GmSALT3 first limits Cl^- accumulation in the leaf and then Na^+, through a yet to be identified mechanism. This study provides useful molecular markers for introducing the *GmSALT3* gene into breeder's varieties; the NIL-T lines used in this experiment have the potential to be used as gene sources to accelerate breeding for improvement of salt tolerance in commercially grown soybean varieties.

AUTHOR CONTRIBUTIONS

LQ, RG, and MG designed experiments. YL performed development of NILs and K^+, Na^+ concentrations analysis. LY, JC, HH, ZL, and RC participated field experiments and data collection. YQ and XL performed the Cl^- concentration test. YL, LQ, RG, YQ, and MG wrote the paper. All authors read and approved the final manuscript.

ACKNOWLEDGMENTS

This work was funded by the National Natural Science Foundation of China (1271752), National High Technology Research and Development Program of China (2012AA101106-2) and the Australian Research Council (CE1400008 and FT130100709).

SUPPLEMENTARY MATERIAL

The Supplementary Material for this article can be found online at: http://journal.frontiersin.org/article/10.3389/fpls.2016.01485

REFERENCES

Abel, G. (1969). Inheritance of the capacity for chloride inclusion and chloride exclusion by soybeans. *Crop Sci.* 9, 697–698. doi: 10.2135/cropsci1969.0011183X000900060006x

Abel, G. H., and MacKenzie, A. J. (1964). Salt tolerance of soybean varieties (*Glycine max* L. Merrill) during germination and later growth. *Crop Sci.* 4, 157–161.

An, P., Inanaga, S., Cohen, Y., Kafkafi, U., and Sugimoto, Y. (2002). Salt tolerance in two soybean cultivars. *J. Plant Nutr.* 25, 407–423. doi: 10.1081/Pln-120003373

Bernstein, L., and Hayward, H. (1958). Physiology of salt tolerance. *Annu. Rev. Plant Physiol.* 9, 25–46. doi: 10.1146/annurev.pp.09.060158.000325

Bustingorri, C., and Lavado, R. (2013). Soybean response and ion accumulation under sprinkler irrigation with sodium-rich saline water. *J. Plant Nutr.* 36, 1743–1753. doi: 10.1080/01904167.2013.810250

Chanroj, S., Wang, G., Venema, K., Zhang, M. W., Delwiche, C. F., and Sze, H. (2012). Conserved and diversified gene families of monovalent cation/H+ antiporters from algae to flowering plants. *Front. Plant Sci.* 3:25. doi: 10.3389/fpls.2012.00025

Chen, H., Cui, S., Fu, S., Gai, J., and Yu, D. (2008). Identification of quantitative trait loci associated with salt tolerance during seedling growth in soybean (*Glycine max* L.). *Aust. J. Agr. Res.* 59, 1086–1091. doi: 10.1071/AR08104

Chen, X., and Yu, B. (2007). Ionic effects of Na+ and Cl-on photosynthesis in *Glycine max* seedlings under isoosmotic salt stress. *J. Plant Physiol. Mol. Biol.* 33, 294–300.

Chen, Z. C., Yamaji, N., Fujii-Kashino, M., and Ma, J. F. (2016). A cation-chloride cotransporter gene is required for cell elongation and osmoregulation in rice. *Plant Physiol.* 171, 494–507. doi: 10.1104/pp.16.00017

Colmenero-Flores, J. M., Martínez, G., Gamba, G., Vázquez, N., Iglesias, D. J., Brumós, J., et al. (2007). Identification and functional characterization of cation–chloride cotransporters in plants. *Plant J.* 50, 278–292. doi: 10.1111/j.1365-313X.2007.03048.x

Devkota, M., Martius, C., Gupta, R. K., Devkota, K. P., McDonald, A. J., and Lamers, J. P. A. (2015). Managing soil salinity with permanent bed planting in irrigated production systems in Central Asia. *Agric. Ecosyst. Environ.* 202, 90–97. doi: 10.1016/j.agee.2014.12.006

Do, T. D., Chen, H., Hien, V. T., Hamwieh, A., Yamada, T., Sato, T., et al. (2016). Ncl synchronously regulates Na+, K+, and Cl- in soybean and greatly increases the grain yield in saline field conditions. *Sci. Rep.* 6:19147. doi: 10.1038/srep19147

Durand, M., and Lacan, D. (1994). Sodium partitioning with the shoot of soybean. *Physiol. Plant.* 91, 65–71. doi: 10.1111/j.1399-3054.1994.tb00660.x

El-Samad, H. A., and Shaddad, M. (1997). Salt tolerance of soybean cultivars. *Biol. Plant.* 39, 263–269. doi: 10.1023/A:1000309407275

Essa, T. (2002). Effect of salinity stress on growth and nutrient composition of three soybean (*Glycine max* L. Merrill) cultivars. *J. Agron. Crop Sci.* 188, 86–93. doi: 10.1046/j.1439-037X.2002.00537.x

Foolad, M. (1999). Comparison of salt tolerance during seed germination and vegetative growth in tomato by QTL mapping. *Genome* 42, 727–734. doi: 10.1139/Gen-42-4-727

Foolad, M., and Lin, G. (1997). Absence of a genetic relationship between salt tolerance during seed germination and vegetative growth in tomato. *Plant Breed.* 116, 363–367. doi: 10.1111/j.1439-0523.1997.tb01013.x

Genc, Y., Mcdonald, G. K., and Tester, M. (2007). Reassessment of tissue Na+ concentration as a criterion for salinity tolerance in bread wheat. *Plant Cell Environ.* 30, 1486–1498. doi: 10.1111/j.1365-3040.2007.01726.x

Guan, R., Chen, J., Jiang, J., Liu, G., Liu, Y., Tian, L., et al. (2014a). Mapping and validation of a dominant salt tolerance gene in the cultivated soybean (*Glycine max*) variety Tiefeng 8. *Crop J.* 2, 358–365. doi: 10.1016/j.cj.2014.09.001

Guan, R., Qu, Y., Guo, Y., Yu, L. L., Liu, Y., Jiang, J. H., et al. (2014b). Salinity tolerance in soybean is modulated by natural variation in GmSALT3. *Plant J.* 80, 937–950. doi: 10.1111/tpj.12695

Ha, B.-K., Vuong, T. D., Velusamy, V., Nguyen, H. T., Shannon, J. G., and Lee, J.-D. (2013). Genetic mapping of quantitative trait loci conditioning salt tolerance in wild soybean (*Glycine soja*) PI 483463. *Euphytica* 193, 79–88. doi: 10.1007/s10681-013-0944-9

Hall, D., Evans, A. R., Newbury, H. J., and Pritchard, J. (2006). Functional analysis of CHX21: a putative sodium transporter in *Arabidopsis*. *J. Exp. Bot.* 57, 1201–1210. doi: 10.1093/jxb/erj092

Hamwieh, A., Tuyen, D., Cong, H., Benitez, E., Takahashi, R., and Xu, D. (2011). Identification and validation of a major QTL for salt tolerance in soybean. *Euphytica* 179, 451–459. doi: 10.1007/s10681-011-0347-8

Hamwieh, A., and Xu, D. (2008). Conserved salt tolerance quantitative trait locus (QTL) in wild and cultivated soybeans. *Breed. Sci.* 58, 355–359. doi: 10.1270/Jsbbs.58.355

Henderson, S., Wege, S., Qiu, J., Blackmore, D., Walker, A., Tyerman, S., et al. (2015). Grapevine and *Arabidopsis* cation-chloride cotransporters localize to the golgi and trans-golgi network and indirectly infuence long-distance ion transport and plant salt tolerance. *Plant Physiol.* 169, 2215–2229. doi: 10.1104/pp.15.00499

Hosseini, M. K., Powell, A. A., and Bingham, I. J. (2002). Comparison of the seed germination and early seedling growth of soybean in saline conditions. *Seed Sci. Res.* 12, 165–172. doi: 10.1079/Ssr2002108

Kan, G., Zhang, W., Yang, W., Ma, D., Zhang, D., Hao, D., et al. (2015). Association mapping of soybean seed germination under salt stress. *Mol. Genet. Genomics* 290, 2147–2162. doi: 10.1007/s00438-015-1066-y

Kao, W. Y., Tsai, T. T., Tsai, H. C., and Shih, C. N. (2006). Response of three *Glycine* species to salt stress. *Environ. Exp. Bot.* 56, 120–125. doi: 10.1016/j.envexpbot.2005.01.009

Kong, X. Q., Gao, X. H., Sun, W., An, J., Zhao, Y. X., and Zhang, H. (2011). Cloning and functional characterization of a cation-chloride cotransporter gene OsCCC1. *Plant Mol. Biol.* 75, 567–578. doi: 10.1007/s11103-011-9744-6

Kotula, L., Khan, H. A., Quealy, J., Turner, N. C., Vadez, V., Siddique, K. H., et al. (2015). Salt sensitivity in chickpea (*Cicer arietinum* L.): ions in reproductive tissues and yield components in contrasting genotypes. *Plant Cell Environ.* 38, 1565–1577. doi: 10.1111/pce.12506

Läuchli, A., and Wieneke, J. (1979). Studies on growth and distribution of Na+, K+ and Cl- in soybean varieties differing in salt tolerance. *Z. Pflanzenernähr. Bodenkd.* 142, 3–13.

Lee, G., Boerma, H., Villagarcia, M., Zhou, X., Carter, T. Jr., Li, Z., et al. (2004). A major QTL conditioning salt tolerance in S-100 soybean and descendent cultivars. *Theor. Appl. Genet.* 109, 1610–1619. doi: 10.1007/s00122-004-1783-9

Lee, J. D., Shannon, J. G., Vuong, T. D., and Nguyen, H. T. (2009). Inheritance of salt tolerance in wild soybean (*Glycine soja* Sieb. and Zucc.) accession PI483463. *J. Hered.* 100, 798–801. doi: 10.1093/jhered/esp027

Liu, K., and Muse, S. V. (2005). PowerMarker: an integrated analysis environment for genetic marker analysis. *Bioinformatics* 21, 2128–2129. doi: 10.1093/bioinformatics/bti282

Lu, Y., Chanroj, S., Zulkifli, L., Johnson, M. A., Uozumi, N., Cheung, A., et al. (2011). Pollen tubes lacking a pair of K+ transporters fail to target ovules in *Arabidopsis*. *Plant Cell* 23, 81–93. doi: 10.1105/tpc.110.080499

Luo, Q., Yu, B., and Liu, Y. (2005). Differential sensitivity to chloride and sodium ions in seedlings of *Glycine max* and *G. soja* under NaCl stress. *J. Plant Physiol.* 162, 1003–1012. doi: 10.1016/j.jplph.2004.11.008

Maathuis, F. J., Ahmad, I., and Patishtan, J. (2014). Regulation of Na+ fluxes in plants. *Front. Plant Sci.* 5:467. doi: 10.3389/fpls.2014.00467

Maresova, L., and Sychrova, H. (2006). *Arabidopsis thaliana* CHX17 gene complements the kha1 deletion phenotypes in *Saccharomyces cerevisiae*. *Yeast* 23, 1167–1171. doi: 10.1002/yea.1424

Munns, R., and Gilliham, M. (2015). Salinity tolerance of crops - what is the cost? *New Phytol.* 208, 668–673. doi: 10.1111/nph.13519

Munns, R., James, R. A., Xu, B., Athman, A., Conn, S. J., Jordans, C., et al. (2012). Wheat grain yield on saline soils is improved by an ancestral Na+ transporter gene. *Nat. Biotechnol.* 30, 360–U173. doi: 10.1038/nbt.2120

Munns, R., and Tester, M. (2008). Mechanisms of salinity tolerance. *Annu. Rev. Plant Biol.* 59, 651–681. doi: 10.1146/annurev.arplant.59.032607.092911

Padmanaban, S., Chanroj, S., Kwak, J. M., Li, X., Ward, J. M., and Sze, H. (2007). Participation of endomembrane cation/H+ exchanger AtCHX20 in osmoregulation of guard cells. *Plant Physiol.* 144, 82–93. doi: 10.1104/pp.106.092155

Pantalone, V., Kenworthy, W., Slaughter, L., and James, B. (1997). Chloride tolerance in soybean and perennial *Glycine* accessions. *Euphytica* 97, 235–239. doi: 10.1023/A:1003068800493

Parker, M. B., Gascho, G., and Gaines, T. (1983). Chloride toxicity of soybeans grown on Atlantic coast flatwoods soils. *Agron. J.* 75, 439–443. doi: 10.2134/agronj1983.00021962007500030005x

Qi, X., Li, M. W., Xie, M., Liu, X., Ni, M., Shao, G., et al. (2014). Identification of a novel salt tolerance gene in wild soybean by whole-genome sequencing. *Nat. Commun.* 5:4340. doi: 10.1038/ncomms5340

Rogers, M., Noble, C., Halloran, G., and Nicolas, M. (1995). The effect of NaCl on the germination and early seedling growth of white clover (*Trifolium repens* L.) populations selected for high and low salinity tolerance. *Seed Sci. Technol.* 23, 277–287.

Rudolfs, W. (1921). Effect of salt solutions having definite osmotic concentration values upon absortion by seeds. *Soil Sci.* 11, 277–294. doi: 10.1097/00010694-192104000-00004

Schachtman, D., and Munns, R. (1992). Sodium accumulation in leaves of *Triticum* species that differ in salt tolerance. *Funct. Plant Biol.* 19, 331–340.

Schroeder, J. I., Delhaize, E., Frommer, W. B., Guerinot, M. L., Harrison, M. J., Herrera-Estrella, L., et al. (2013). Using membrane transporters to improve crops for sustainable food production. *Nature* 497, 60–66. doi: 10.1038/nature11909

Sze, H., Padmanaban, S., Cellier, F., Honys, D., Cheng, N.-H., Bock, K. W., et al. (2004). Expression patterns of a novel AtCHX gene family highlight potential roles in osmotic adjustment and K+ homeostasis in pollen development. *Plant Physiol.* 136, 2532–2547. doi: 10.1104/pp.104.046003

Takeda, S., and Matsuoka, M. (2008). Genetic approaches to crop improvement: responding to environmental and population changes. *Nat. Rev. Genet.* 9, 444–457. doi: 10.1038/nrg2342

Tamura, K., Dudley, J., Nei, M., and Kumar, S. (2007). MEGA4: molecular evolutionary genetics analysis (MEGA) software version 4.0. *Mol. Biol. Evol.* 24, 1596–1599. doi: 10.1093/molbev/msm092

Tavakkoli, E., Fatehi, F., Coventry, S., Rengasamy, P., and McDonald, G. K. (2011). Additive effects of Na+ and Cl– ions on barley growth under salinity stress. *J. Exp. Bot.* 62, 2189–2203. doi: 10.1093/jxb/erq422

Tavakkoli, E., Rengasamy, P., and McDonald, G. K. (2010). High concentrations of Na+ and Cl- ions in soil solution have simultaneous detrimental effects on growth of faba bean under salinity stress. *J. Exp. Bot.* 61, 4449–4459. doi: 10.1093/jxb/erq251

Teakle, N. L., and Tyerman, S. D. (2010). Mechanisms of Cl– transport contributing to salt tolerance. *Plant Cell Environ.* 33, 566–589. doi: 10.1111/j.1365-3040.2009.02060.x

Tester, M., and Davenport, R. (2003). Na+ tlerance and Na+ transport in higher plants. *Ann. Bot.* 91, 503–527. doi: 10.1093/aob/mcg058

Turner, N. C., Colmer, T. D., Quealy, J., Pushpavalli, R., Krishnamurthy, L., Kaur, J., et al. (2013). Salinity tolerance and ion accumulation in chickpea (*Cicer arietinum* L.) subjected to salt stress. *Plant soil* 365, 347–361. doi: 10.1007/s11104-012-1387-0

Umezawa, T., Shimizu, K., Kato, M., and Ueda, T. (2000). Enhancement of salt tolerance in soybean with NaCl pretreatment. *Physiol. Plant.* 110, 59–63. doi: 10.1034/j.1399-3054.2000.110108.x

Valencia, R., Chen, P., Ishibashi, T., and Conatser, M. (2008). A rapid and effective method for screening salt tolerance in soybean. *Crop Sci.* 48, 1773–1779. doi: 10.2135/cropsci2007.12.0666

Yasuta, Y., and Kokubun, M. (2014). Salinity tolerance of super-nodulating soybean genotype En-b0-1. *Plant Prod. Sci.* 17, 32–40. doi: 10.1626/pps.17.32

Zhang, G., Wang, X., Lu, X., and Liu, Y. (2012). Analysis of salinity and pH of topsoil in the coastal areas of east Hebei. *Chin. Agric. Sci. Bull.* 26, 243–246.

Zhang, W., Niu, Y., Bu, S., Li, M., Feng, J., Zhang, J., et al. (2014). Epistatic association mapping for alkaline and salinity tolerance traits in the soybean germination stage. *PloS ONE* 9:e84750. doi: 10.1371/journal.pone.0084750

Conflict of Interest Statement: The authors declare that the research was conducted in the absence of any commercial or financial relationships that could be construed as a potential conflict of interest.

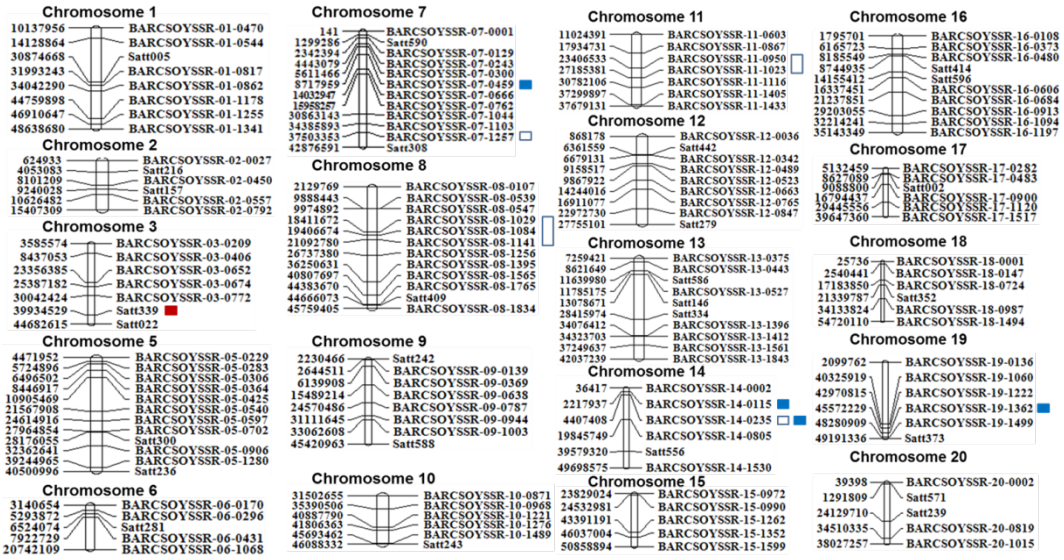

Supplementary FIGURE 1. Distribution of 147 SSR markers which are polymorphic between Tiefeng 8 and 85-140 on 19 chromosomes of soybean. The empty bars, red bars and blue bars indicated polymorphic regions within 782-T and 782-S, 820-T and 820-S, and, 860-T and 860-S.

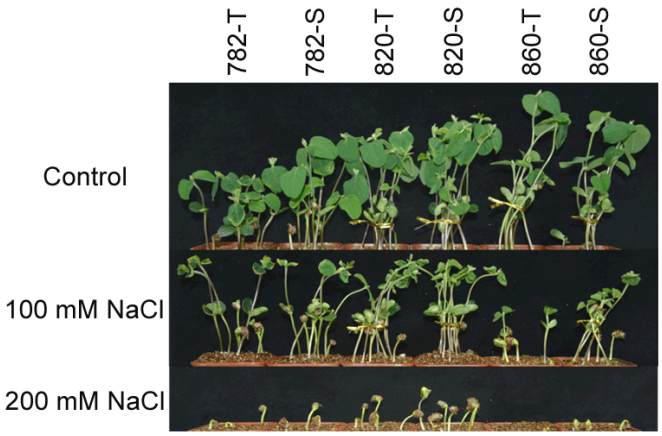

Supplementary FIGURE 2. Phenotype of three sets of NILs under control and 100, 200 mmol L^{-1} NaCl stress (EC = 10.6 dS m^{-1}, 17.8 dS m^{-1}) 15 days after sowing.

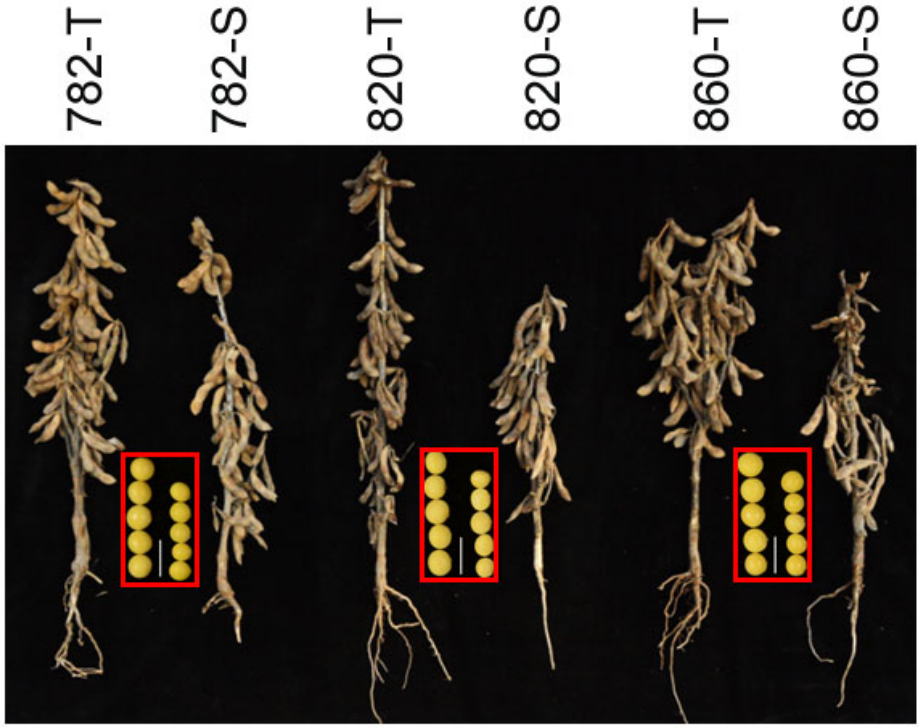

Supplementary FIGURE 3. Plant and seed phenotypes of three sets of NILs grown in saline soil (Tanghai, 2014). Image is showing plants at harvest maturity. Seeds from representative plant of each NIL are shown in red box between each pair of NIL (left for NIL-T, right for NIL-S). Scale bar for seeds, 1 cm.

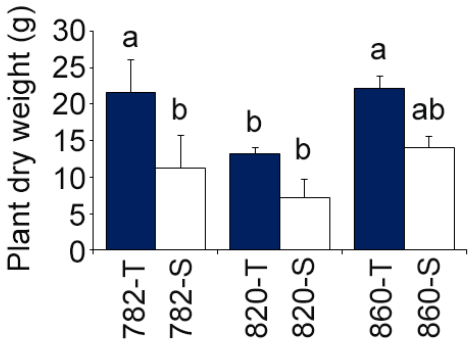

Supplementary FIGURE 4. Above ground dry mass of NIL lines grown on saline field at Tanghai, Hebei during 2015. Data are means of three replicates consisting of 15 bulked plants per replicate ± SD (n=3). Different letters indicate statistically significant differences between NIL lines (one-way ANOVA followed by Tukey's HSD post hoc test, $P < 0.05$).

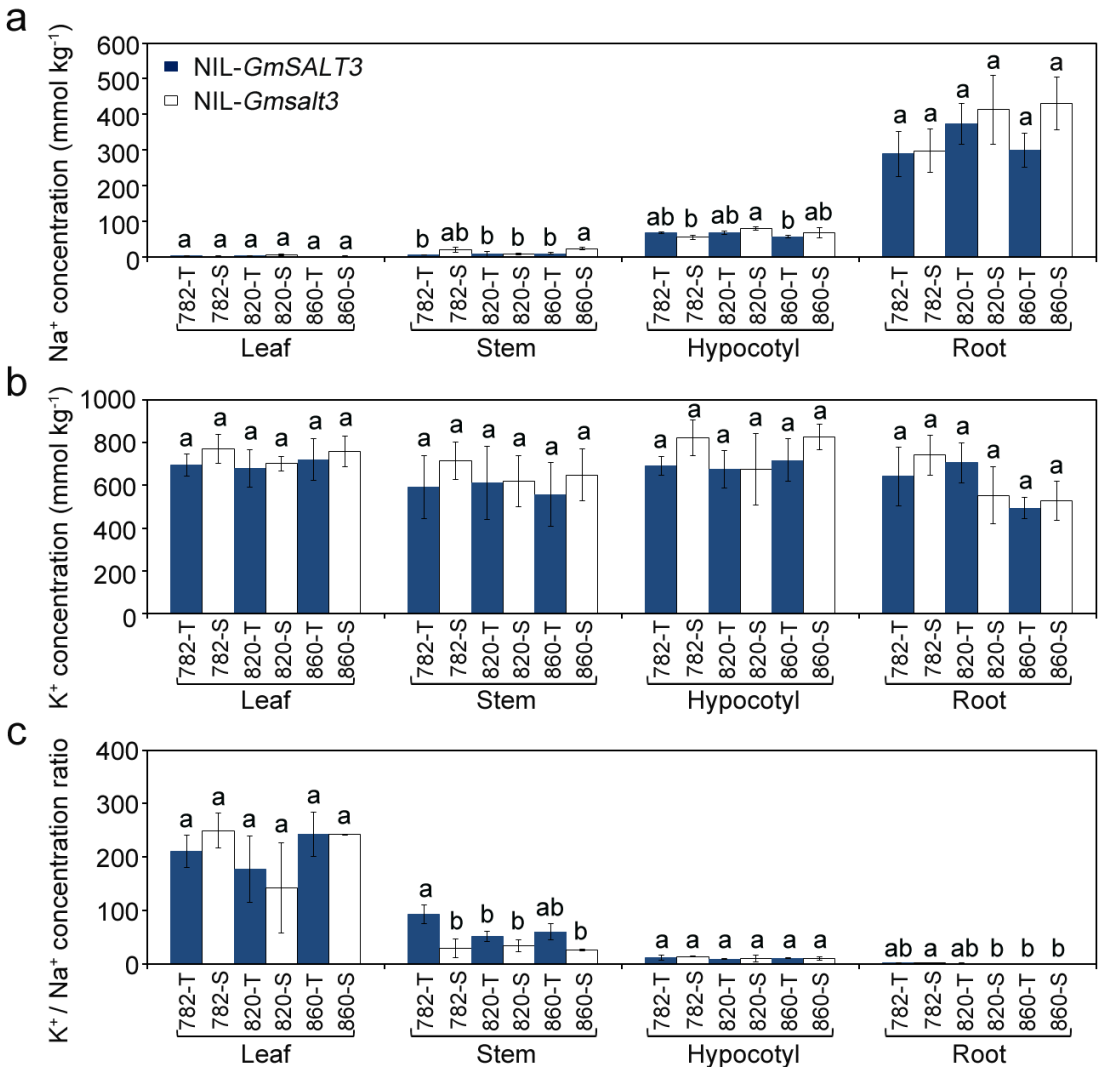

Supplementary FIGURE 5. Ion concentration in three sets of NILs of control treatment. **a** Concentration of Na^+ in leaf, stem, hypocotyl and root of three sets of NILs. **b** Concentration of K^+ in leaf, stem, hypocotyl and root of three sets of NILs. **c** The K^+ / Na^+ ratio in leaf, stem, hypocotyl and root of three sets of NILs. Data are means of three replicates consisting of the mean of 5 plants grown in the same pot ± SD (n=3). Different letters indicate statistically significant differences between NIL lines (one-way ANOVA followed by Tukey's HSD *post hoc* test, $P < 0.05$).

Brief conclusion

We set ourselves three questions on page 73. The key results of Liu *et al.* (2016) can be summarised as:

- *GmSALT3* does not contribute to an improvement in seedling emergence rate or early vigour under salt stress. So only confers improved salt tolerance during the vegetative growth phase through the reproductive phase to yield.
- NIL-T lines accumulated significantly less leaf Na^+ and Cl^- compared with their corresponding NIL-S using 12-day-old seedlings. In addition, NIL-T lines accumulated less Cl^- in the leaf and more in the root prior to any difference in Na^+.
- In the field, *GmSALT3* was found to have no penalty on soybean yield under non-saline condition and contributes to improving soybean yields through increasing seed weight in different genetic backgrounds under salinity stress. This still leaves the question open as to why there are some many non-functional haplotypes of *Gmsalt3* derived from landraces with their origin in non-saline conditions.

Again, several questions remain from this work. For instance, how Na^+ and Cl^- homeostasis is regulated in NIL-T lines still was not identified, in particular, how expression the *GmSALT3* allele confers both Na^+ and Cl^- exclusion in soybean. As it is a predicted transporter, the transport function of GmSALT3 became a priority and is a focus of the next chapter.

Chapter 4 *GmSALT3* confers different mechanisms of Na^+ and Cl^- exclusion in soybean [*Glycine max* (L.) Merr.]

Yue Qu[1], Rongxia Guan[2], Jayakumar Bose[1], Jinghan Jiang[2], Stefanie Wege[1], Lijuan Qiu[2], Matthew Gilliham[1*]

[1]Australian Research Council Centre of Excellence in Plant Energy Biology, School of Agriculture, Food and Wine and Waite Research Institute, University of Adelaide, Glen Osmond, SA, Australia

[2]The National Key Facility for Crop Gene Resources and Genetic Improvement, Institute of Crop Science, Chinese Academy of Agricultural Sciences, Beijing, China

[*]Correspondence should be addressed to Prof. Matthew Gilliham

(matthew.gilliham@adelaide.edu.au)

Tel: +61 8 8313 3044

Fax: +61 8 8313 5725

Key words: Soybean, salt tolerance, functional characterisation, *GmSALT3*

Running title: Functional analysis of a candidate gene for conferring salt tolerance in soybean

Brief introduction

GmSALT3 was shown to improve soybean salinity tolerance at the seedling stage and confers yield advantage under saline conditions (Chapter 2). To investigate how *GmSALT3* contributes to improved salinity tolerance and exclusion of Na^+ and Cl^- from soybean shoots, NILs of *GmSALT3* were used to investigate tissue and vascular sap ion concentration. In addition, the transport activity of GmSALT3 was studied in heterologous systems to see if it could offer potential insights into the improved shoot exclusion of both Na^+ and Cl^- from soybean shoots. It is the intention that this manuscript is eventually formatted for and submitted for publication in *Journal of Experimental Botany*.

Statement of Authorship

Title of Paper	*GmSALT3* inducing different mechanisms of Na^+ and Cl^- exclusion in soybean [*Glycine max (L.) Merr*.]
Publication Status	☐ Published ☐ Accepted for Publication ☐ Submitted for Publication ☑ Unpublished and Unsubmitted work written in manuscript style
Publication Details	Qu, Y., Guan, R., Yu, L., Bose, J., Jiang, J., Wege, S., Qiu, L., Gilliham, M. (2017)

Principal Author

Name of Principal Author (Candidate)	Yue Qu		
Contribution to the Paper	YQ contributed to experimental design. Performed ion accumulation measurement, TEM, IRGA, *E.coli* and oocyte expression. Analysed the data and wrote the manuscript.		
Overall percentage (%)	85%		
Certification:	This paper reports on original research I conducted during the period of my Higher Degree by Research candidature and is not subject to any obligations or contractual agreements with a third party that would constrain its inclusion in this thesis. I am the primary author of this paper.		
Signature		Date	28.08.17

Co-Author Contributions

By signing the Statement of Authorship, each author certifies that:

i. the candidate's stated contribution to the publication is accurate (as detailed above);

ii. permission is granted for the candidate in include the publication in the thesis; and

iii. the sum of all co-author contributions is equal to 100% less the candidate's stated contribution.

Name of Co-Author	Rongxia Guan		
Contribution to the Paper	Contributed to experimental design.		
Signature		Date	28.08.17

Name of Co-Author	Jayakumar Bose		
Contribution to the Paper	Performed MIFE in oocytes.		
Signature		Date	18/09/2017

Please cut and paste additional co-author panels here as required.

Name of Co-Author	Jinghan Jiang		
Contribution to the Paper	Performed net ion flux measurement in soybean roots		
Signature		Date	28.08.17

Name of Co-Author	Stefanie Wege		
Contribution to the Paper	Assisted in experimental design and editing the final version of the manuscript.		
Signature		Date	01.09.2017

Name of Co-Author	Lijuan Qiu		
Contribution to the Paper	Contributed to experimental design.		
Signature		Date	28.08.17

Name of Co-Author	Matthew Gilliham		
Contribution to the Paper	Contributed to experimental design, supervised the research, and assisted in editing the final version of the manuscript.		
Signature		Date	1/9/2017

Abstract

Soybean (*Glycine max*) is one of the major staple crops, providing a key source of protein consumed globally. Soybean plants are moderately-sensitive to salinity; however, soybean yields are severely reduced under saline conditions. *GmSALT3* was previously found to be the dominant gene in a salinity tolerance QTL in soybean and we recently observed that expression of full-length *GmSALT3* in roots leads to both Na^+ and Cl^- exclusion in shoots. However, how *GmSALT3* confers this, and how it functions is poorly understood. Here, we further investigate the function of GmSALT3 in both heterologous systems and in near isogenic lines (either containing the full-length gene, which are salt-tolerant (NIL-T) or contain a truncated transcript and are salt-sensitive (NIL-S)). In addition to confirming that Cl^- exclusion occurs prior to Na^+ exclusion using a time course analysis we also find that stem secretion of Na^+ contributes to its exclusion from leaves. We also find that Cl^-concentration is significantly higher in both the stem xylem and phloem sap of NIL-T. This likely means that whilst more Cl^- is transported from root-to-shoot more Cl^- is recirculated back to roots, and this contributes to a greater accumulation of Cl^- in NIL-T roots. Na^+ is significantly greater in concentration in NIL-S xylem sap but no differences were detected in phloem sap and roots between NILs, which indicates Na^+ is most likely regulated by exclusion at the root xylem, so in a different way in NIL-T compared to Cl^-. Plants with full-length GmSALT3 maintain a significantly higher photosynthetic rate than NIL-S plants before and after salt treatment. In heterologous expression systems, GmSALT3 could restore bacterial growth of *E. coli* strain LB2003 (*trkAΔ, kup1Δ, kdpABCDEΔ*) that is defective in K^+ uptake systems; when expressed in *Xenopus laevis* oocytes, GmSALT3 contributes to higher accumulation of Na^+, K^+, and Cl^- and higher net influx of Na^+, K^+, and Cl^- (measured by MIFE, Microelectrode Ion Flux Estimation) compared to water-injected oocytes. Overall, our findings provide new insights into the transport activity of GmSALT3 and how *GmSALT3* contributes to salinity tolerance in soybean.

Introduction

Food security is being challenged by a booming global population and environmental damage, such as climate change, freshwater shortage, and arable land loss (Alexandratos and Bruinsma, 2012; Gilliham *et al.*, 2017; Godfray *et al.*, 2010; Taiz, 2013; Tester and Langridge, 2010). Suitable land and water resources are essential for the required sustainable agricultural growth to meet the demands of the growing population, but the incidence and severity of stress events are on the increase (Munns and Gilliham, 2015). Soil degradation and salinisation of irrigated land areas are big challenges for protecting global food security targets, as they can reduce crop yield and lead to arable land loss (Godfray *et al.*, 2010). One pathway to maintain or improve crop productivity in saline soils is to increase the salinity tolerance of conventional crops (Roy *et al.*, 2014; Yamaguchi and Blumwald, 2005).

Among conventional crops, soybean production is expected to increase by nearly 80 percent to 390 Mt in 2050 (Alexandratos and Bruinsma, 2012). In addition to large market demand for providing edible oil and food, soybean (*Glycine max*) is also a vital crop in mixed/intercropping and sequential cropping agricultural systems (Singh, 2010). Soybean has many beneficial features in improving soil properties, such as the shed leaf residue being incorporated as green manure, a developed underground system with deep and proliferated tap-root improving aeration and water penetration, and most importantly, increasing soil fertility through efficient Biological Nitrogen Fixation (BNF) in association with *Bradyrhizobium* in root nodules (Singh, 2010). Salinity stress threatens soybean production; saline conditions of 18–20 dS/m (about 180 – 200 mM NaCl) reduces yield by 61.1%, from 2 261.4 ± 438.3 kg/hm^2 under control conditions to 880.8 ± 259.9 kg/hm^2 (Chang *et al.*, 1994). The efficiency of BNF is also reduced by salinity stress, with a decreased number and biomass of root nodules (Delgado *et al.*, 1994; Elsheikh, 1998; Singleton and Bohlool, 1984). Nevertheless, not all soybean cultivars are equally as sensitive to salinity stress, with some soybean germplasm found to be relatively salt-tolerant. In a large-scale evaluation of soybean salinity tolerance, only 2.8% of the 10,128 evaluated soybean germplasm exhibited salt tolerance at both the

germination stage and seedling stage, and 83 soybean cultivars were found to be highly tolerant to salinity at the vegetative stage only (Shao *et al.*, 1993). Agronomic traits were measured to determine soybean salinity tolerance, including height, leaf area, biomass, number of internodes, branches, and pods, weight per plant, and weight of 100 seeds (Abel and MacKenzie, 1964; Chang *et al.*, 1994). Salt-tolerant soybean germplasm has been observed to generally exhibit better agronomic performance than salt-sensitive cultivars (Phang *et al.*, 2008).

In soybean, a major quantitative trait loci (QTL) for salinity tolerance was consistently mapped to chromosome 3 (Abel, 1969; Ha *et al.*, 2013; Hamwieh *et al.*, 2011; Hamwieh and Xu, 2008; Lee *et al.*, 2004). Since 2014, several papers have been published focusing on the same dominant gene identified in this soybean salt tolerance QTL in wild (*GmCHX1*) and cultivated soybeans (*GmNcl*/*GmSALT3*) (Do *et al.*, 2016; Guan *et al.*, 2014; Qi *et al.*, 2014). All the three identified genes share the same sequence with *Glyma03g32900* in William 82, and based on genetic markers information, this gene is the best candidate for being the dominant gene in the major salinity tolerance QTL, and also in the *Ncl* locus reported by Abel (1969). In this, and our previous studies, we call this dominant gene *GmSALT3*.

According to phylogenetic analysis, GmSALT3 is closely related to the characterized *Arabidopsis thaliana* AtCHX20 (Cation/Proton Exchanger), which belongs to the CPA2 (Cation/Proton Antiporter 2) family of transporters (Guan *et al.*, 2014; Padmanaban *et al.*, 2007). AtCHXs have a proposed common role in modulating cation and pH homeostasis of diverse endomembrane systems (Chanroj *et al.*, 2011; Czerny *et al.*, 2016; Padmanaban *et al.*, 2007). AtCHX20 was characterised as a putative endomembrane K^+ transporter in osmoregulation of guard cells (Padmanaban *et al.*, 2007).

Compared with salt-tolerant soybean cultivar Tiefeng 8, *Gmsalt3* genomic DNA contains a 3.78-kb copia retrotransposon insertion in exon 3 that truncates the transcript *GmSALT3* in the salt sensitive cultivar 85-140. Expression of *GmSALT3* in roots has shown to be associated with limiting the Na^+ accumulation in shoots (Qi et al. 2014; Guan et al. 2014). It is localized to the endoplasmic reticulum (ER) and is preferentially expressed in Tiefeng 8

within root cells associated with phloem and xylem. Most importantly, studies have shown that *GmSALT3* significantly increases crop yield in saline conditions (Do *et al.*, 2016; Liu *et al.*, 2016). Here, the *in vivo* function of *GmSALT3* was further characterised in soybean *GmSALT3* near isogenic lines (NIL), and its *in vitro* function in heterologous systems. Results showed that the possible mechanisms of salinity tolerance in NIL-T (NIL carrying *GmSALT3;* Tolerant) are through affecting phloem retranslocation of Cl^- and net xylem loading of Na^+. In heterologous systems, *GmSALT3* complements a K^+ uptake deficient *E. coli* strain and restores NaCl tolerance in a salt sensitive *E. coli* strain; in *Xenopus laevis* oocytes, *GmSALT3* expression results in net influx of Na^+, K^+ and Cl^-. Plant CHX proteins were shown to be modulating K^+ transport. Results with *GmSALT3* indicate complex physiological role influencing not only K^+ flux but also Na^+ and Cl^- fluxes.

Results

GmSALT3 modulates Na^+, K^+, and Cl^- homeostasis in NIL-T

We previously observed that improved shoot Na^+ and Cl^- exclusion is conferred by the presence of full length *GmSALT3*, and that shoot Cl^- exclusion in salt-tolerant near isogenic lines (NIL-T) occurs prior to shoot Na^+ exclusion (Liu et al. 2016). Here we confirm this result (Fig. 1a;1c), and also observe that K^+ content is increased in NIL-*GmSALT3* salt-sensitive (NIL-S) compared to salt-tolerant (NIL-T) soybean plants (Fig. 1b). The accumulation of K^+ shows a similar trend to Na^+ with significantly higher K^+ content detected in NIL-S leaves compared to NIL-T after 3 days' 100 mmol L^{-1} NaCl treatment, but only increasing from 35 mg/g (day 0) to 51 mg/g (day 10), compared to 0.24 mg/g and 45 mg/g for Na^+ in the same period (Fig. 1a; 1b). The ratio of K^+/Na^+ is significantly higher in NIL-T leaves compared to NIL-S from day 3 (Fig. 1d).

To further investigate how *GmSALT3* contributes to shoot Na^+ and Cl^- exclusion in NIL-T, we picked the 4-day time point following 100 mM NaCl treatment to examine the ion concentrations in a range of tissue types, and in the vascular sap, as this coincided with

statistical differences in several of the parameters in the time-courses shown in Figure 1 and Supplementary Figures 1-3. At the day 4 time point in Fig. 2, Na^+ accumulated more in leaves (both first trifoliate, FL, and youngest trifoliate leaf, YL) in NIL-S compared to NIL-T, which was consistent with the result in Fig. 1a; Na^+ content was also significantly more in petioles of the first trifoliate leaf (FLP) and youngest trifoliate leaf (YLP), higher stem (HS), lower stem (LS), and Hypocotyl (Hy) in NIL-S compared to NIL-T, but no significant differences were observed between NILs for Na^+ in roots (primary, PR and secondary, SR). The accumulation of K^+ was only significantly more in NIL-S leaves (Fig. 2b). As for Cl^-, similar trends could be observed to Na^+ accumulation in aerial parts and hypocotyl; in roots (PR and SR), NIL-T accumulated significantly more Cl^- ions than NIL-S (Fig. 2c). Under control conditions (4 day with RO water), Na^+ content was significantly more in SR of NIL-T, and no differences in other tissues; Cl^- content was significantly more in leaves and stem of NIL-S, and no differences in Hy and roots; no significantly differences observed for K^+ (Supplementary Fig. 4).

Salt concentration within soybean stem phloem and xylem exudates were also examined at the same 4-day time point following the NaCl treatment and it was found that Na^+ and K^+ flux were not significantly different in phloem sap between NIL-T and -S plants, but Cl^- flux was significantly higher in NIL-T phloem sap (Fig. 3a). Glutamine contents within the phloem sap was used to normalize these measures, in case differences in sap volumes led to artefactual results, as its concentration within the phloem remains constant throughout the day (Corbesier *et al.*, 2001). The ratios of Na^+ or K^+ to glutamine concentration ratios gave the same results (Fig 3a; 3b), with a significant difference observed for Cl^-, but no significant differences for Na^+ and K^+ (Fig 3b). In xylem sap, the Na^+ flux within NIL-S was significantly greater compared to NIL-T, but the Cl^- flux was lower (Fig. 3c). This means for Na^+ that there would be less Na^+ moving up within NIL-T xylem sap, which is consistent with the lower Na^+ accumulation in the shoot. However, for Cl^-, our results suggest that more Cl^- is present within the NIL-T xylem but it is not accumulating within the NIL-T leaves, so *GmSALT3* somehow facilitates greater phloem recirculation of Cl^- from shoots-to-roots, where it accumulates in

NIL-T. Under control conditions (4 days with RO water), no significantly differences observed between NIL-T and NIL-S in ion accumulation in stem phloem and xylem saps (Supplementary Fig. 4). As NIL-T plants have a phloem-associated phenotype (Fig. 3), and the ER is particularly enriched within phloem cells (Turgeon and Wolf, 2009), the ultrastructure of phloem cells from three-week old NIL-T and NIL-S roots and stems were examined following 100 mM NaCl treatment for four days. However, TEM results could not detect any obvious significant morphological differences between NIL-T and NIL-S in root phloem cells (Supplementary Fig. 5), this could be because of our tissue fixation method was not optimized enough to detect differences.

Differences in photosynthetic rates can translate into differences in plant growth rate; sustaining photosynthetic capacity is essential for maintaining crop yield under saline conditions. Photosynthetic rates and stomata conductance of H_2O were measured to examine how *GmSALT3* contributes to differences in soybean NIL growth during salt treatment. Trifoliate leaves were measured from NIL-T and -S. Photosynthetic rate and stomatal conductance of H_2O of both NILs was significantly reduced after one-day treatment of 100 mmol/L NaCl (Fig. 4a; 4b). However, by day four of the salt treatment all NIL-T leaves examined maintained a significantly higher photosynthetic rate and stomatal conductance H_2O than NIL-S (Fig. 4). Furthermore, salt-tolerant soybean NIL leaves showed a consistently higher photosynthetic rate and stomata conductance of H_2O from day 0 to day 4 (Fig. 4).

GmSALT3 facilitates Na^+, K^+, and Cl^- transport in heterologous systems

The expression of *GmSALT3*, *Gmsalt3* or empty vector in the yeast mutant (KTA40-2, *Δena1-4 Δnhx1 Δnha1 Δkha1*), which is a yeast strain that had been previously used to characterise other CHX-like proteins, led to no consistent significant differences in growth rates (Appendix II). However, when *GmSALT3* was expressed in *E.coli* strain LB2003 (*trkAΔ, kup1Δ, kdpABCDEΔ*), which is defective in K^+ uptake systems (Stumpe and Bakker, 1997), IPTG (Isopropyl β-D-1-thiogalactopyranoside)-induced expression of full length GmSALT3

improved bacterial growth at pH 5.5 and pH 6.5 compared to the truncated *Gmsalt3* (Fig. 5a; 5b). No differences were detected in *E. coli* expressing truncated *Gmsalt3* and empty-vector controls (Fig. 5). When 50 mM NaCl was added to the same *E. coli* strain, GmSALT3 could only restore bacterial growth at pH 6.5 (Fig. 5c; 5d). With additional 10 mM KCl to YTM (medium containing 1% Yeast extract and 2% Tryptone) with IPTG or YTM without IPTG, full length *GmSALT3*-expressed bacterial growth showed no significant differences compared to cells harbouring *Gmsalt3* or empty vector (Supplementary Fig. 5).

To further examine the transport activity of GmSALT3, *GmSALT3*-cRNA was injected and expressed in *X. laevis* oocytes. Plasma membrane fluorescence was detected in *GmSALT3*-YFP expressing oocytes and in the positive control *Nax2*-YFP (Fig. 6a) (Munns et al., 2012), indicating in oocytes GmSALT3 targeted to the plasma membrane – which is not uncommon for endomembrane proteins from plants. Resting membrane potential of *GmSALT3*-injected oocytes was more positive compared to H_2O-injected oocytes when incubated in ND96 (Fig. 5b). MIFE (Microelectrode Ion Flux Estimation) results indicated that after incubation in ND96 for 72 hours, and then recorded in BSM solution, both *GmSALT3*-injected oocytes and H_2O-injected oocytes showed an efflux of Na^+, K^+, and Cl^-, but the net efflux was significantly reduced in *GmSALT3*-injected oocytes compared to H_2O-injected (Fig. 6c). In agreement with the finding that GmSALT3 reduces net ion efflux, 72 hours incubation in ND96 resulted in significantly more K^+, Na^+, and Cl^- in *GmSALT3*-injected oocytes compared to H_2O-injected oocytes (Fig. 6d). ND96-incubated oocytes were transferred into BSM with or without 100 μM amiloride hydrochloride (an Na^+ channel and Na^+/H^+ exchanger inhibitor from animal studies; Darley et al., 2000) for another overnight incubation. In BSM without amiloride, K^+, Na^+, and Cl^- accumulation decreased in all oocytes but *GmSALT3*-injected oocytes still had higher K^+, Na^+, and Cl^- concentrations than H_2O-injected oocytes (Fig. 6d); in BSM with amiloride, there was no differences between gene- and water-injected oocytes (Fig. 6d).

Discussion

Shoot salt exclusion requires the co-ordinated activity of many ion transporters that may: 1) limit the net entry of salt into the roots, 2) compartmentalise salt in the roots; and or 3) retrieve salt from the root xylem or shoots through the phloem. Examples of transporters that have been implicated in salt tolerance in soybean include: the tonoplast localised GmNHX1 (Na^+/H^+ antiporter 1) and GmCLC1 (chloride channel 1) (Li *et al.*, 2006a); and the plasma membrane localised GmSOS1 (salt overly sensitive 1, Na^+/H^+ antiporter) and GmCAX1 (Ca^+/H^+ antiporter 1) (Luo *et al.*, 2005a; Phang *et al.*, 2008). All these transporters are proposed to be involved in net exclusion of salt entry into roots (*GmSOS1*), its compartmentation (*GmNHX1, GmCLC1*) or signalling (*GmCAX1)*. Significantly, the transporters contributing to reduced net transfer of salt to the shoot, the mechanism by which shoot salt accumulation is commonly regulated in other species, are yet to be resolved in soybean (Munns and Tester, 2008). An example of this that has been characterised in wheat, rice and Arabidopsis are the HKT1;5-like (high affinity K^+ transport) proteins that localise to cells that surround the root xylem and facilitate Na^+ retrieval back into the root (Møller *et al.*, 2009; Munns *et al.*, 2012; Ren *et al.*, 2005; Uozumi *et al.*, 2000).

GmSALT3 has been identified as a dominant gene that contributes to salinity (NaCl) tolerance in wild and domesticated soybean (Do *et al.*, 2016; Guan *et al.*, 2014; Qi *et al.*, 2014), its presence confers greater Na^+, K^+, and Cl^- exclusion to soybean shoot and a yield advantage under saline conditions (Do *et al.*, 2016; Liu *et al.*, 2016). However, the underlying mechanisms behind the relationship between *GmSALT3* and salinity tolerance remain largely unknown. Salt tolerance includes tolerance to elevated levels of both, Cl^- and Na^+. In many plant species one of the two ions is more deleterious to the plant, however, the situation for soybean is currently unclear.

Chloride (Cl^-) is an essential nutrient and an important osmoticum to plants, but when accumulated to excessive concentrations it can be toxic, and this can occur under saline conditions (Li *et al.*, 2017; Wege *et al.*, 2017). Cl^- was thought to be more toxic than Na^+ in

cultivated soybean in contrast to most crop species (Läuchli, 1984), as soybean has a capacity to efficiently hold Na^+ in woody roots and stems preventing it from reaching the leaves, leading to a low leaf Na^+/K^+ ratio (Luo *et al.*, 2005b). At the same time, Cl^- continues to pass into aerial plant parts, resulting in a high shoot Cl^- accumulation in soybean, with high concentrations of Cl^- being toxic to plant cellular metabolism (Xu *et al.*, 2000). However, other reports suggest that different soybean species have little correlation between leaf chlorosis and leaf Cl^- content (Phang *et al.*, 2008). Salt-tolerant soybean germplasm also accumulated less Na^+ in leaves than salt-sensitive varieties (Li *et al.*, 2006b). In addition, several recent studies support the proposition that Na^+ is the toxic ion in soybean (Ikeda, 2005; Lenis *et al.*, 2011; Luo *et al.*, 2005b). In our study, time-course ion concentration measurement in *GmSALT3*-NILs under 100 mM NaCl stress indicates that NIL-T shows a much higher ability to resist salinity stress than NIL-S through mediating exclusion of Na^+ and Cl^- from leaves, and Cl^- accumulates earlier than Na^+ in NIL-S plant tissues (Fig.1). This is consistent with previous results performed with 200 mM NaCl treatment (Liu *et al.*, 2016). Another notable feature is that NIL-T leaves can maintain a constant K^+ concentration throughout the ten days' salt treatment, but Na^+ and Cl^- does increase after salt treatment (Fig.1), this demonstrates GmSALT3 can confer improved K^+ homeostasis in NIL-T.

Sodium and chloride ions are transported to shoots via the xylem transpiration stream, plant roots tend to remain relatively steady levels of those two ions, and regulate their concentrations by eliminating into soils or to the shoot (Tester and Davenport, 2003). Under saline conditions, Na^+ is accumulated to greater concentrations in the aerial parts of NIL-S but no difference was observed in the roots compared to NIL-T (Fig. 2a); in stem xylem sap, there was a lower Na^+ flux in NIL-T but no significant difference in stem phloem sap (Fig. 3), which means more Na^+ is transported in the NIL-S xylem stream. Based on GmSALT3's phloem- and xylem- associated cells localisation in roots (Guan *et al.*, 2014), it suggests that Na^+ is excluded from NIL-T leaves possibly through restricting sodium ions entering root xylem and then effluxed back to the soil by other salt tolerance genes such as SOS1 (Phang *et al.*, 2009; Roy *et*

al., 2014). Interestingly, the net ion flux from the soybean root tip was greater in Tiefeng 8 (Salt-tolerant parent) than 85-140 (Salt-sensitive parent); and amiloride hydrochloride (Na^+ channel and Na^+/H^+ exchanger inhibitor) inhibits Na^+ efflux significantly more in Tiefeng 8 compared to 85-140 roots (Supplementary Fig. 6); this indicates that GmSALT3 may affect Na^+ efflux in salt-tolerant soybean roots. No significant difference could be detected for K^+ content and concentration of roots (Fig. 3). As for Cl^-, higher Cl^- accumulation in NIL-S aerial parts and more Cl^- in NIL-T roots (Fig. 3c) and higher Cl^- content in both NIL-T xylem and phloem sap (Fig. 3) indicates that more Cl^- is transported up in NIL-T xylem but does not stay in the leaves. Therefore, *GmSALT3* might impact Cl^- homeostasis by phloem recirculation of Cl^- and with Cl^- being retained in NIL-T roots.

Some plant species have shown a role for phloem retranslocation of NaCl in salt tolerance. For example, in maize approximately 13-36% of the Na^+ and Cl^- imported to leaves through the xylem was exported by the phloem (Lohaus *et al.*, 2000). The Arabidopsis protein AtHKT1 was also shown to be localised within the phloem tissues in all organs, and proposed to function in Na^+ recirculation from shoots to roots by mediating Na^+ loading into the phloem sap in shoots and unloading in roots (Berthomieu *et al.*, 2003). However, this report has been contradicted by others where AtHKT1;1 is shown to be involved in xylem unloading of Na^+ in roots (Kronzucker and Britto, 2011; Mäser *et al.*, 2002; Munns and Tester, 2008; Rus *et al.*, 2006; Uozumi *et al.*, 2000). In addition, a soluble metal binding protein in companion cells of Arabidopsis phloem, called *sodium potassium root defective1* (NaKR1; previously called NPCC6), plays a role within the phloem in recirculating Na^+ to the roots to limit sodium accumulation in leaves (Tian *et al.*, 2010). Previous grafting experiments have shown that when salt-tolerant scion (*GmSALT3*) grafted on salt-sensitive rootstock (*Gmsalt3*), it can reduce leaf Na^+ content by 14% compared to self-grafted salt-sensitive plants, but when salt-tolerant plant was used as rootstock, it reduces Na^+ content by 70% (Guan *et al.*, 2014). In contrast to the grafting experiments of *GmSALT3* in soybeans, grafting experiments with *AtNaKR1* in Arabidopsis showed that shoot sodium accumulation was due mainly to loss of NaKR1 function

in the leaves (Tian *et al.*, 2010). Phloem transport of Na^+ has also been shown to occur in soybean, but was not sufficient to prevent leaf Na^+ accumulation (Durand and Lacan, 1994). Until now, no reports have shown phloem recirculation as an important salt tolerance mechanism for Cl^- recirculation; *GmSALT3* presents as a very promising candidate for regulating Cl^- long-distance retranslocation.

Most plant cells are interconnected by plasmodesmata to facilitate intercellular symplastic transport of solutes (Taiz and Zeiger, 2010). In phloem regions, plasmodesmata connect the functional cells (Supplementary Fig. 5) (Turgeon and Wolf, 2009), and Endoplasmic Reticulum (ER) plays a critical role in the phloem transport system (Taiz and Zeiger, 2010). No ion transporter has been characterised in plant root phloem ER, but an Arabidopsis Amino acid Permease (AAP) has been localised to root phloem-specific internal membranes along the trafficking pathway, including the plasma membrane, the nuclear membrane, ER, Golgi bodies, and endosomal vesicles, functions as an amino acid proton co-transporter (Okumoto *et al.*, 2004). ER-localised GmSALT3 could facilitate vesicle trafficking in phloem sieve element (SE) and contribute to salinity tolerance in soybean roots. Unfortunately, immunolabelling using GmSALT3 specific antibody was not successful in NIL-T root sections, but new monoclonal antibodies are under investigation (Appendix III).

A close homolog of *GmSALT3*, *AtCHX20* in *Arabidopsis thaliana*, is preferentially expressed in stomatal guard cells (Padmanaban *et al.*, 2007). AtCHX20 enhanced *E.coli* LB2003 (K^+ uptake deficient strain) growth at pH 5.8 – 6.2, and results suggest that it mediates H^+-coupled K^+ transport (Chanroj *et al.*, 2011). GmSALT3 could also complement *E. coli* LB2003 growth at acidic pH. In the presence of 50 mM NaCl, bacterial growth could only be restored at pH 6.5 (Fig. 5d). To determine the significance of this pH dependency the H^+ transport capacity of GmSALT3 needs to be determined in other systems such as with MIFE following expression in *X. laevis*. However, what appears to be clear is that GmSALT3 seems to mediate K^+ transport; probably impacting Na^+ and Cl^- fluxes in *E. coli* cells as evidenced by the NaCl effect on *E. coli* growth. In *X. laevis* oocytes, no plant CPA2 (Cation-Proton

Antiporter 2)/CHX (Cation/H^+ Exchanger) has been characterised. Recently, two animal CPA2 transporters, *Drosophila* NHA1 and NHA2 were described to act as a Na^+/H^+ exchanger and a H^+/Cl^- cotransporter, respectively, in experiments using *Xenopus* oocytes (Chintapalli *et al.*, 2015). GmSALT3 targets to the *Xenopus* oocyte plasma membrane (Fig. 6a) and depolarized the membrane potential of *GmSALT3*-injected oocytes (compared to H2O-injected oocytes) in the ion-rich solution (ND96) is consistent with the ion accumulation (Fig. 6b; 6d). After being transferred from ND96 to a low ionic medium (BSM), *GmSALT3*-injected oocytes show a lower net efflux of K^+, Na^+, and Cl^- compared to H2O-injected oocytes (Fig. 6c). Combined with the ion accumulation test in oocytes (Fig. 6d), it is possible that the lower net efflux of K^+, Na^+, and Cl^- is a direct result of GmSALT3 activity through import of these three ions into the oocytes. Additionally, in BSM with amiloride hydrochloride which inhibits Na^+ channel and Na^+/H^+ exchanger, the effect of GmSALT3 is absent (Fig. 6d), which confirms GmSALT3 could affect transport of K^+, Na^+, and Cl^-.

Members of the Cation-Chloride Cotransporter (CCC) family have been shown to transport Na^+, K^+, and Cl^- and are speculated to be involved in long-distance Cl^- transport (Colmenero-Flores *et al.*, 2007; Henderson *et al.*, 2015). In oocytes, VviCCC localised to the plasma membrane, and has been characterised as a Na^+-K^+-$2Cl^-$ cotransporter (Henderson *et al.*, 2015). In plants, VviCCC and AtCCC are localised to the Golgi and Trans-Golgi network, which suggests that they are unlikely to have a direct role in salt tolerance (Henderson *et al.*, 2015). Similarly, also GmSALT3 is localised to the endomembrane system, this time the ER. Do et al. (2016) hypothesised that GmSALT3 might act as a type of CCC channel; however, the *GmSALT3* sequence has very low similarity to plant *CCC* genes, *AtCCC* tissue localisation shows a different pattern to *GmSALT3*, and despite an endomembrane localisation they reside in different compartments (Colmenero-Flores *et al.*, 2007; Guan *et al.*, 2014), which suggests that GmSALT3 has a distinct role to CCCs, despite potential similarities in transport activity.

To summarize, this work has revealed the potential salinity tolerance mechanisms of GmSALT3 *in planta* and in heterologous systems. We propose that in NIL-T the presence of

full-length *GmSALT3* mediates Na^+ and Cl^- exclusion from shoots through restricting xylem loading of Na^+ and retranslocating Cl^- in the phloem. In heterologous systems, GmSALT3 is involved in K^+ uptake and NaCl tolerance in *E. coli* cells, and its expression in *Xenopus laevis* oocytes mediates net import of Na^+, K^+, and Cl^-. However, as an endomembrane-localised protein, how GmSALT3 contributes to soybean salinity tolerance mechanisms is still not so clear, and how its expression directly impacts salt movement to and from shoots i.e. is it involved directly or indirectly. To help answer this question it still needs to be definitively shown whether GmSALT3 is present on an endomembrane or whether its previous localisation is due to a misexpression artefact. As the heterologous expression of *GmSALT3* led to transport differences in all three ions that are affected in distribution in the plant it is tempting to speculate that GmSALT3 may be actively involved in their distribution in tissues. However, as the effect on Cl^- and Na^+ differ in the xylem and phloem differs according to *GmSALT3* expression the impact of other processes including other transport proteins are likely to be involved in the NIL phenotypes. RNA-sequencing using NIL-T and NIL-S roots may be a good technique to investigate if GmSALT3 confers salinity tolerance in soybean roots via influencing transcription, and what distinctive pathways and genes been significantly changed in NIL-T and NIL-S roots under saline conditions.

Methods

Plant materials and growth conditions

Soybean NIL (salt-tolerant and -sensitive) seeds were received from Prof. Rongxia Guan (Chinese Academy of Agricultural Sciences, Beijing). Soybean plants were grown in a greenhouse (28°C day and 25°C night with 14h light-cycle) at the Plant Research Centre, Waite campus, the University of Adelaide, Australia. Soybean seeds were germinated in pots containing a mixture of perlite and vermiculite (50/50) as described by Obermeyer and Tyerman (2005).

cDNA cloning and plasmid preparation

To synthesize *GmSALT3* and *Gmsalt3* cDNA (2436 and 1131 nucleotides, respectively), total RNA was isolated from roots of 4-week old soybean plants using the TRIzol method (Shi and Bressan, 2006). First-strand cDNA was synthesized using a Thermoscript RT III kit (Invitrogen, USA). Gene specific primers (GmSALT3_gF and GmSALT3_gR, Gmsalt3_gF and Gmsalt3_gR; Supplementary Table S1) were used to amplify the cDNA with Phusion® High-Fidelity DNA Polymerase (New England Biolabs) by 35 cycles (98 °C 30s, 65 °C 30s, and 72 °C 150s). Gel-purified PCR products were A-tailed using Taq polymerase (New England Biolabs) for 30 min at 72 °C, and then recombined into Gateway® entry vector PCR8/GW/TOPO (Invitrogen) for further application. Resulting clones were sequenced using internal primers (GmSALT3_F1, R1, F2, F3, F4, and F5, Gmsalt_F1, F2, and R1; Supplemental Table S1).

Plasmid preparation

GmSALT3 and *Gmsalt3* CDS within entry vector PCR8 were cloned into pGEM-HE and pPAB404 vectors using Gateway ® LR Clonase ® (Invitrogen, USA), for *Xenopus* oocytes expression and E. *coli* expression, respectively.

Growth assay in E. coli (Escherichia coli)

Escherichia coli strain LB2003 (*trkA*Δ, *kup1*Δ, *kdpABCDE*Δ) was donated by Prof. Nobuyuki Uozumi (Tohoku University, Japan). Competent cells preparation and E.*coli* transformation were conducted as described by Chanroj *et al.* (2011). The resulting transformants were grown on YTMK media supplemented with 50 μg/ml ampicillin and incubated at 30 ^{o}C for 2 days, and then colonies were approved positive by colony PCR with gene specific primers. Only fresh transformed cells were used. For liquid E. *coli* culture growth curve experiments, freshly transformed cells were first grown overnight in 5 ml YTMK at pH 7.2. Cell cultures were replenished (A_{600} = 0.5) and grown for 3 h in YTM, and then washed

with YTM for three times. Cells were normalized to A_{600} 0.5 for 96-well plate assay. In each well, 20 µl of normalized cell suspension was added to 180 µl growth solutions. All test media were supplemented with 50µg/ml ampicillin, 0.5 mM IPTG (Isopropyl β-D-1-thiogalactopyranoside) and varied concentration of NaCl, KCl and pH. The 96-well plates were inserted into FLUOstar Omega Fluorescence microplate reader (BMG LABTECH) set to 30 ^{o}C and measured A_{600} every 15 min for 37 h.

Characterization of GmSALT3 in X. laevis oocytes

pGEMHE-DEST containing *GmSALT3* was linearized using SphI-HF (New England BioLabs); cRNA was synthesized using mMESSAGE mMACHINE T7 Kit (Ambion) following manufacturer's instructions. 46 nl/23 ng of cRNA or equal volumes of RNase-free water were injected into oocytes with a Nanoinject II microinjector (Drummond Scientific). Oocytes were incubated for 48 h in Calcium Ringer's solution (96 mM NaCl, 2 mM KCl, 5 mM $MgCl_2$, 5 mM HEPES, 0.6 mM $CaCl_2$). All solution osmolarities were adjusted using mannitol 240–260 mOsmol kg^{-1} (Vapor pressure osmometer, Wescor). Ion profiles in oocytes followed Munns *et al.* (2012) with the following modifications. Six replications of 3 grouped oocytes were used for flame photometry (Sherwood 420), and Cl^- was also measured using chloride analyser (Sherwood 926S).

MIFE (Microelectrode Ion Flux Estimation) in oocytes

The MIFE technique allows noninvasive concurrent quantification of net fluxes of several ions, protocols were followed by Shabala et al. (2013). Oocytes were adopted rather than plant tissues in our experiments, Na^+, K^+, Cl^-, and H^+ fluxes were measured. Oocytes were washed in ND96 (96 mM NaCl, 1 mM KCl, 1 mM $NgCl_2$, 5 mM HEPES, pH 7.5) after incubation (ND96 for 72 hours), and measured in BSM (5 mM NaCl, 0.2 mM KCl, 0.2 mM $CaCl_2$, 5 mM HEPES, pH7.5).

TEM (Transmission Electron Microscopy)

Fresh soybean NIL-T and NIL-S roots were sectioned to 1 mm (length), stems were sectioned to be quartered (1 mm in length and 1 mm in radius). Samples were incubated overnight in 1.5 ml Eppendorf tubes with fixative (2.5% Glutaraldehyde, 4% Formaldehyde, 4% Sucrose, 0.1 M Phosphate buffer). Samples were washed three times in 1X PBS and then washed with osmium for 4 hours. After that, sections were washed three times in 1X PBS and soaked in 1X PBS for 20 mins and then embedded in 1% agarose gel. Agarose gels were cut into blocks (1 cm long) with soybean sections. A series of dehydration steps were done after embedding, using different concentrated ethanol, including 50%, 70%, 90%, 95%, and 100% (each for 30 mins), and dry ethanol for overnight dehydration. Different concentrations of resin (Spurrs) were infiltrated into soybean sections, including 5%, 10%, 15%, 20%, 25%, 30%, 40%, and 50% (each for 1 h), and 50% for overnight infiltration. The following day, samples were further infiltrated with Spurrs resin using 75% (4 h), 100% (4 h), and another overnight infiltration with 100% resins. New resins were substituted in tubes, agarose blocks were put into capsules with resin, and oven incubation at 60^{o}C for 3 days for polymerization. Polymerised samples were cut to 70 nm thickness using Diamond knife and visualized under TEM.

Gas exchange measures

Photosynthesis measurement was conducted with a LCpro-SD (ADC BioScientific Ltd., UK), IRGA (Infrared gas analyzer) following manufacturers' instructions. The leaf chamber environment was set to be 400 ppm CO_2, 26^{o}C, and Q_{leaf} 500.

NaCl treatment and ion accumulation test

Soybean plants were treated with 100 mM NaCl every 2 days, saline solutions were applied into trays that contain pots with soybean plants. Plant tissues were dried in oven overnight at 60 ^{o}C or freeze-dried overnight. Dry weight was recorded. Then dried samples

were digested in 10ml 1% (v/v) nitric acid overnight at 65 ^{o}C or freeze-thawed in Milli-Q water for 3 times. Oven-dried samples were utilized to test Na^+ and K^+ accumulation with flame photometry (Sherwood 420), and Cl^- was also measured using chloride analyzer (Sherwood 926S).

Freeze-dried samples were used to measure NO_3^- accumulation. Measurement method was modified according to Qiu *et al.* (2016). Supernatant (50 µl) of freeze-dried samples in water was added into 200 µl of 5% (W/V) salicylic acid/H_2SO_4, mixed solutions were incubated at room temperature for 20 min. Then 50 µl of the mixture was transferred into 950 µl of 2 M NaOH, and incubated at room temperature for at least 20 min (to cool down to room temperature). From the new mixture, 250 µl was loaded into a flat-bottom transparent 96-well plates (Greiner Bio-One, Austria). Absorbance was measured at 410 nm. Standards were also measured, including 0, 0.5, 1, 2, 2.5, 5, 7.5, and 10 mM KNO_3.

Phloem and xylem sap extraction

Phloem sap was extracted according to the method by Rupassara (2008) and Ren et al. (2005). Soybean plant petioles were cut at the base (approx. 0.5 cm above the main stem) and stems were cut approx. 2 cm above ground (upper part), and immediately dipped in 1.5 ml of 0.1 mM EDTA solution (pH adjusted to 8) in 2 ml Eppendorf tubes for 20 min. The sap extracted in 2 ml tubes were immediately dipped in liquid nitrogen and stored in a -80 ^{o}C freezer until analysis. As described in Ren et al. (2005), technical reasons would result in highly variable collected volume of phloem sap, and glutamine is usually used as an internal standard, since it is abundant and quite constant in the phloem sap (Berthomieu *et al.*, 2003). The glutamine concentration in the EDTA solution was measured using a Glutamine Assay Kit (EGLN-100, EnzyChrom^{TM}, BioAssay Systems). Xylem sap was extracted using a pressure chamber. Lower part of the cut stem with roots were transferred into the pressure chamber. Pressure was increased gradually (0.05 MPa increments) until xylem sap presents. The first two drops emerging were discarded using a micropipette to reduce contamination from damaged

cells or phloem sap (Berthomieu *et al.*, 2003), xylem sap was then collected during the following 5 min, and stored in -20 °C freezer until analysis.

Figures

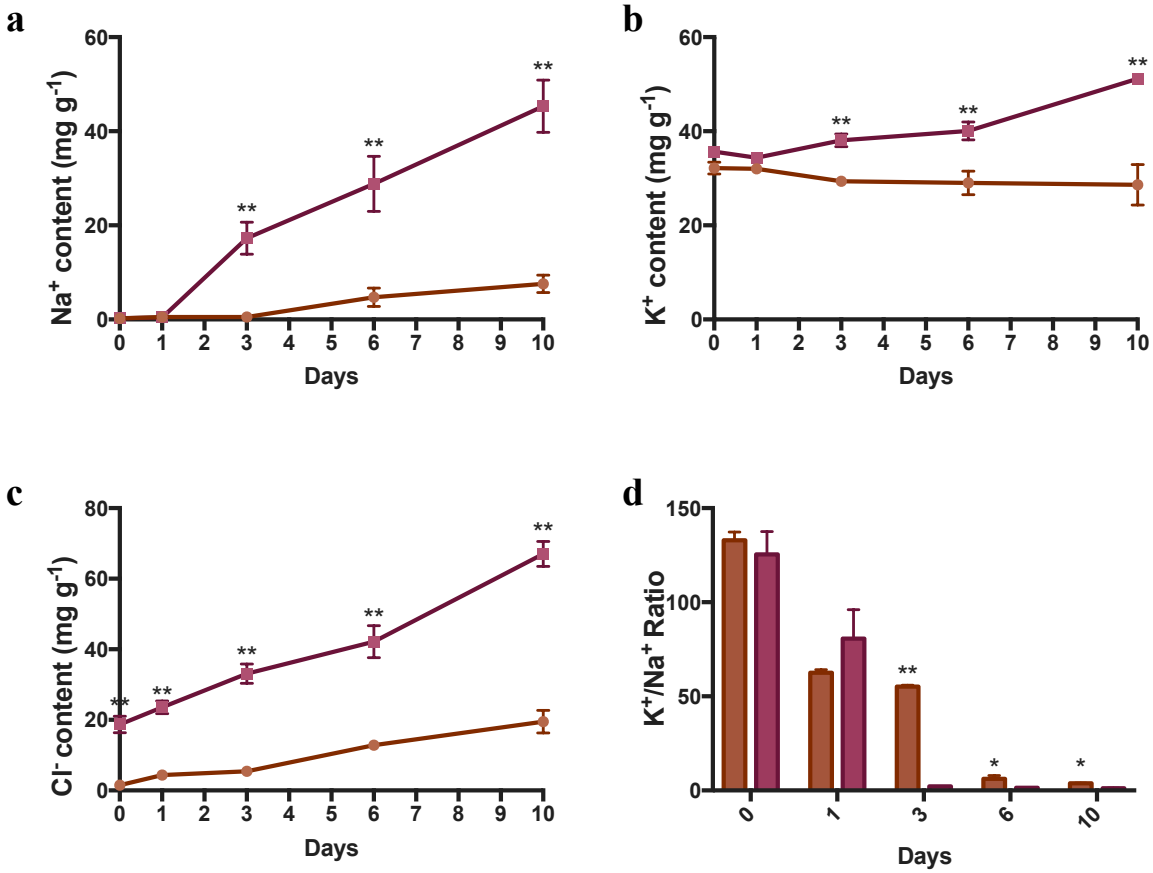

Fig. 1 Time-course ion concentration in NIL-T and NIL-S leaves during 10 days 100 mmol L^{-1} NaCl stress. Na^+ content (**a**), K^+ content (**b**), and Cl^- (**c**) content, and K^+ to Na^+ ratio (**d**) in leaves of NIL-T (brown data) and NIL-S (red data). Observations are means of four replicates ± SEM. Asterisks indicates a significant difference between NIL-T and NIL-S at *P <0.05, **P < 0.01 according to the LSD test.

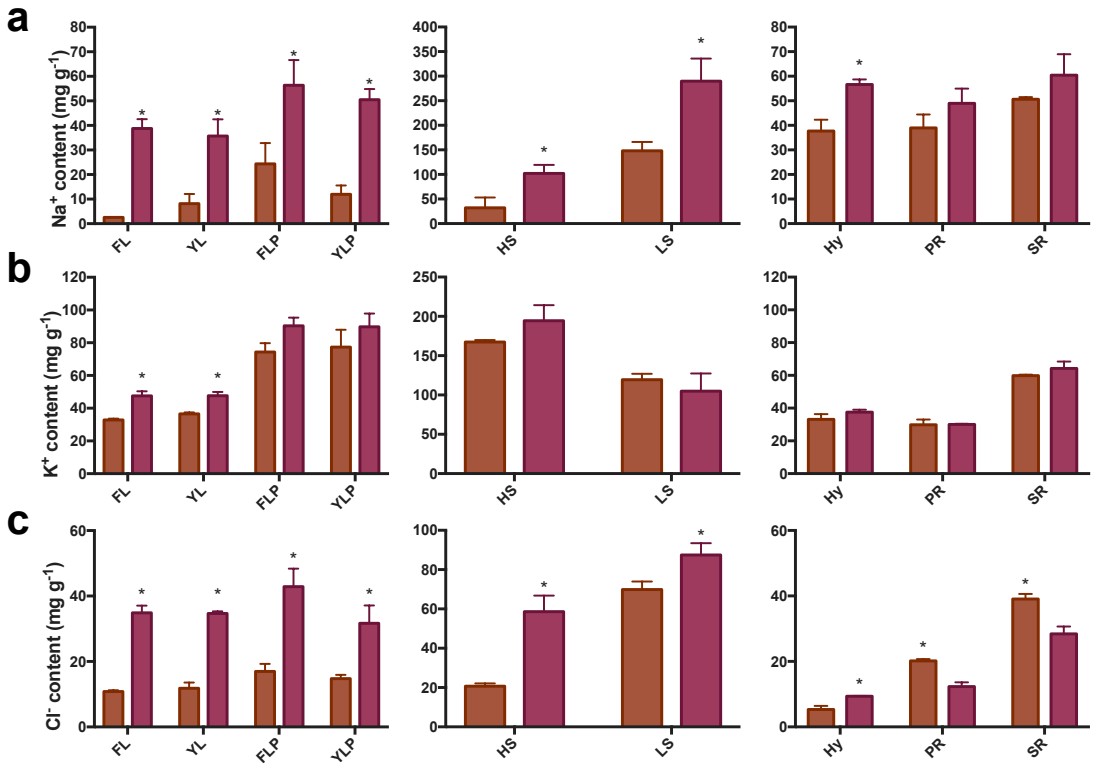

Fig. 2 Ion concentration in different tissues of NIL-T and -S after 4 days of 100 mmol L^{-1} NaCl treatment. a Tissue content of Na^+ in leaf, hypocotyl and root of NILs. **b** K^+ content in leaf, hypocotyl and root of NILs. **c** Cl^- content in leaf, hypocotyl and root of NILs. Ion contents are against tissue dry weight. Data are means of three replicates ± SE. Asterisks indicate a significant difference between NIL-T (brown) and NIL-S (red) at *P <0.05, **P < 0.01 according to the LSD test (ion content data in control plants with water supply can be found in Supplementary Fig. 4). FL, first trifoliate leaves; YL, youngest trifoliate leaves; FLP, first trifoliate leaves petiole; YLP, youngest trifoliate leaves petiole; HS, higher stem; LS, lower stem; PR, primary root; SR, secondary root; Hy, hypocotyl. Data shown here were from one of the two independent experiments with similar results.

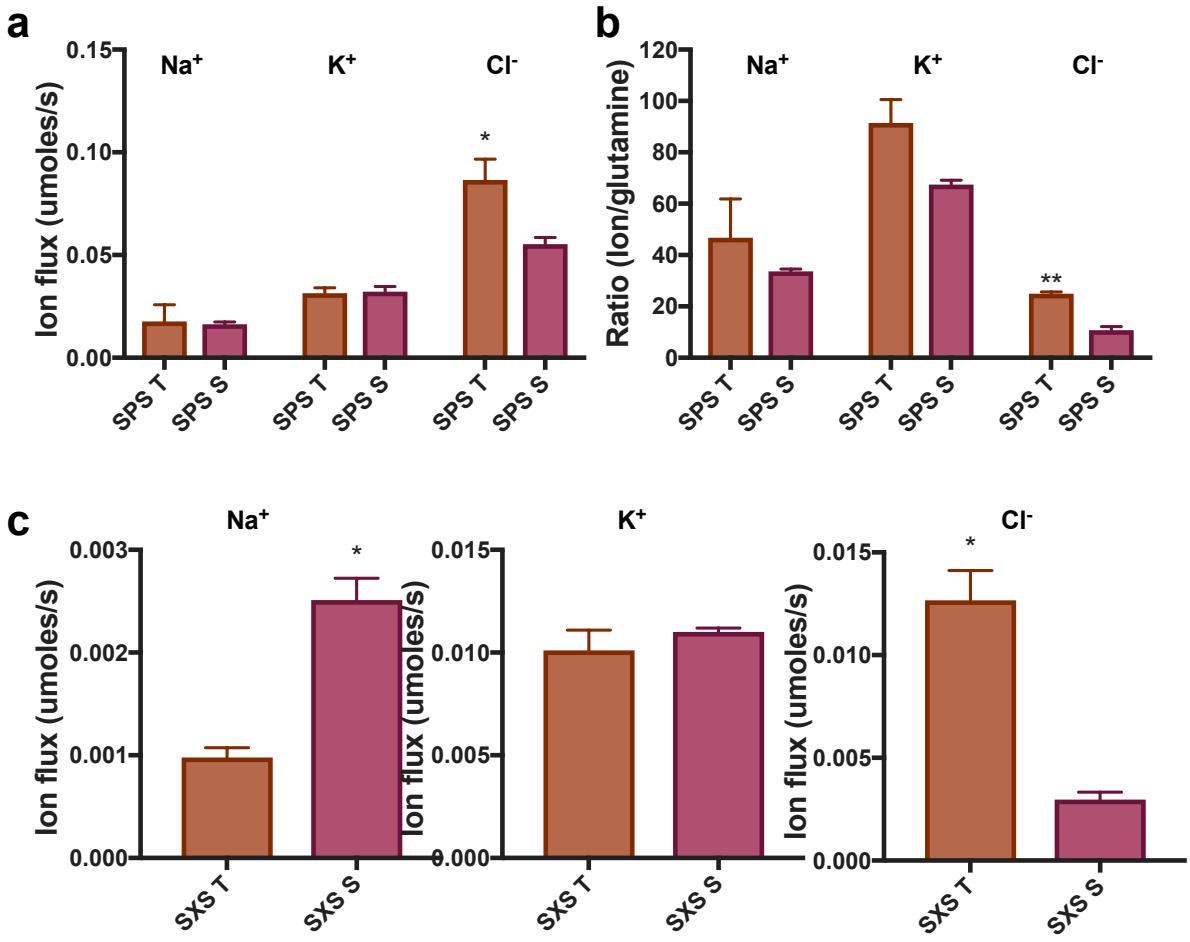

Fig. 3 Ion flux in NIL-T and -S stem phloem and xylem sap after 4 days of 100 mmol L^{-1} NaCl stress. **a** Na^+, K^+, and Cl^- flux (umoles/s) in NIL-T and NIL-S stem phloem sap. **b** Na^+, K^+, or Cl^- content to glutamine ratio in NIL-T and NIL-S stem phloem sap. **c** Na^+, K^+, and Cl^- flux (umoles/s) in NIL-T (brown) and NIL-S (red) stem xylem sap. Data are means of three replicates ± SEM. Asterisks indicate a significant difference between NIL 820-T and 820-S at $*P < 0.05$, $**P < 0.01$ according to the LSD test. SPS, stem phloem sap; SXS, stem xylem sap. Data shown here were from one of the three independent experiments with similar results.

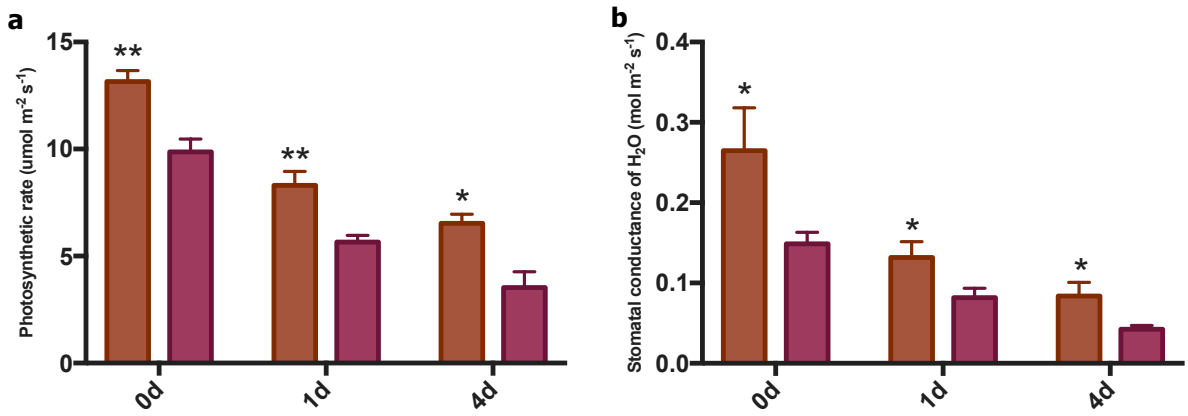

Fig. 4 Photosynthetic rates and stomata conductance of H_2O of NIL-T and -S during 4 days 100 mmol L^{-1} NaCl stress. a Photosynthesis rate comparison. **b** Stomatal conductance of H_2O comparison. Data are means of 6-9 replicates ± SEM. Asterisks indicate a significant difference between NIL-T (brown) and NIL-S (red) at $*P < 0.05$, $**P < 0.01$ according to the LSD test.

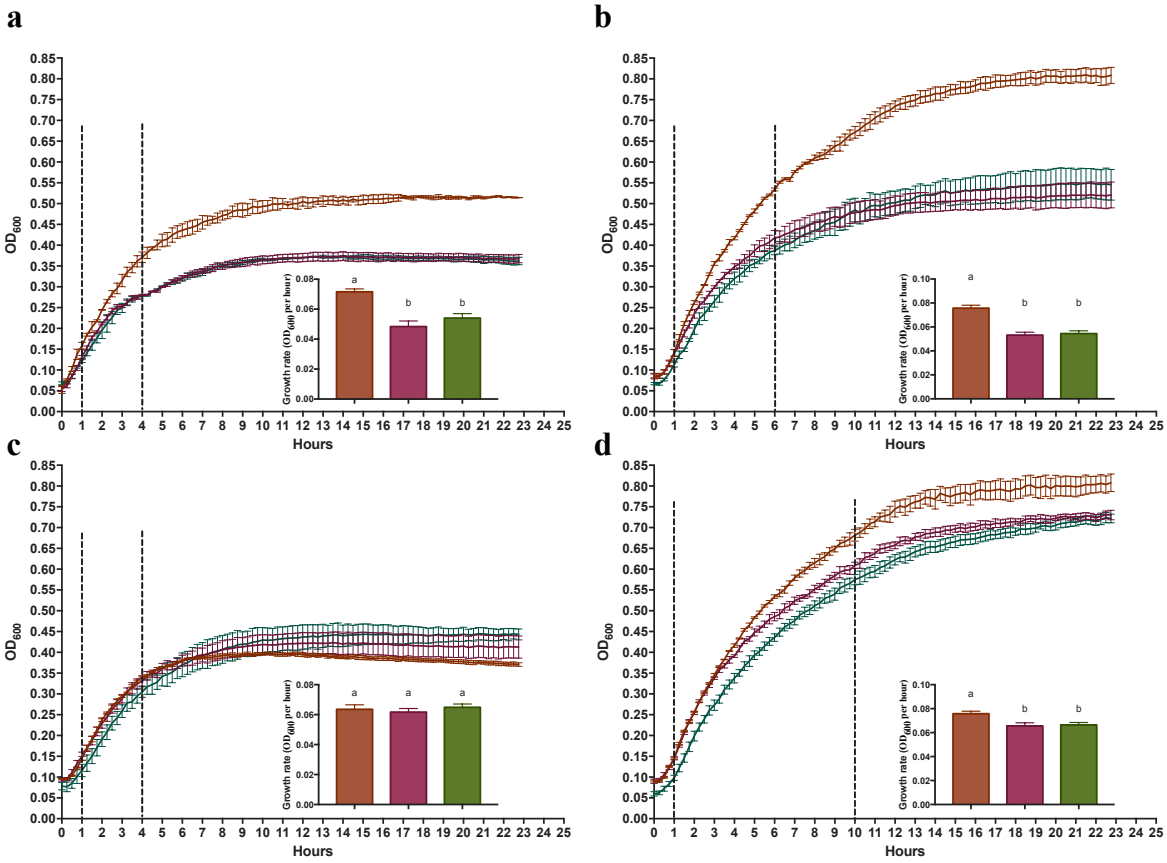

Fig. 5 Functional characterization of *GmSALT3* in *E. coli*. *E. coli* strain LB2003 (*trkAΔ, kup1Δ, kdpABCDEΔ*) harbouring pPAB404 vector only (green), *GmSALT3* (brown), or *Gmsalt3* (red) were grown in different media. YTM medium at pH 5.5 (**a**) and pH 6.5 (**b**). YTM medium with addition of 50 mM NaCl at pH 5.5 (**c**) and pH 6.5 (**d**). All the test media were supplemented with 50μg/ml ampicillin, 0.5 mM IPTG (Isopropyl β-D-1-thiogalactopyranoside). OD_{600} was monitored every 15 min in 96-well microplate reader. Inserted figures show growth rates (OD_{600} per hour) of *E.coli* cells within the log phase indicated by dotted lines; Different letters indicate statistically significant differences between *E.coli* cells harbouring different constructs (one-way ANOVA followed by Fishers's LSD test, $P < 0.05$).

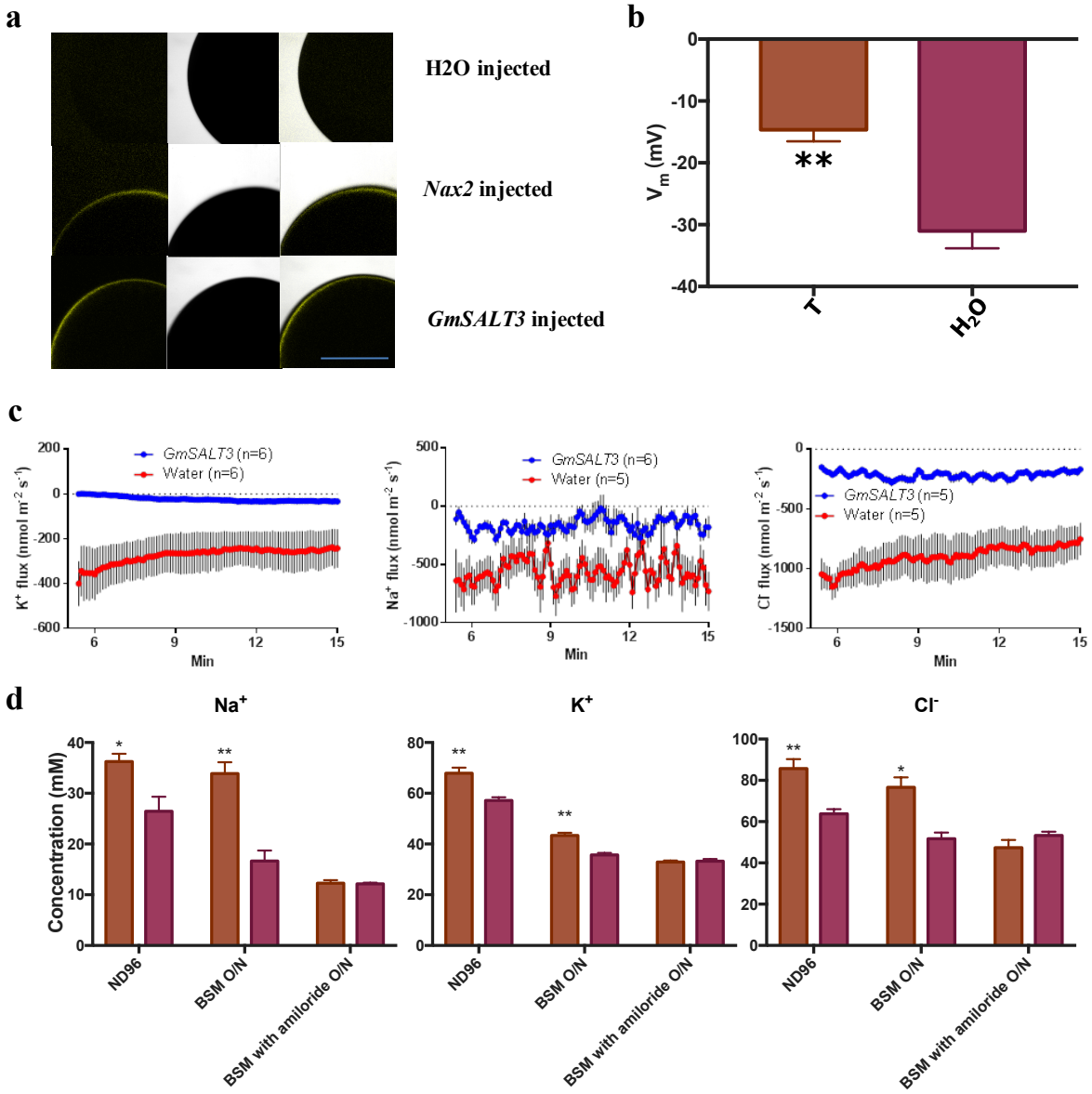

Fig. 6 Functional characterization of *GmSALT3* in *X. laevis* oocytes. a Plasma membrane localisation of expressed *GmSALT3-YFP* in oocytes. H_2O-injected and *Nax2*-YFP (positive control) expressed oocytes are also shown. Scale bar = 0.5 mm. **b** Resting membrane potentials of *GmSALT3*- and H_2O-injected oocytes after incubation in ND96 for 72 hours. Values are means ± SEM (n = 8), Asterisks indicate a significant difference between GmSALT3- and H_2O-injected oocytes at w$^{**}P < 0.01$ according to the LSD test. **c** Net ion fluxes were measured on oocytes plasma membrane using MIFE (Microelectrode Ion Flux Estimation). Oocytes were incubated in ND96 for 72 hours, and washed in ND96 in (96 mM NaCl, 1 mM KCl, 1 mM $NgCl_2$, 5 mM HEPES, pH 7.5). Measurements were done in BSM (5 mM NaCl, 0.2 mM KCl, 0.2 mM $CaCl_2$, 5 mM HEPES, pH7.5). Values are means ± SEM (n = 4 ~ 6). **d** Ions (Na^+, K^+,

and Cl^-) concentration in *GmSALT3* (brown)- and H2O (Red) -injected oocytes after incubation in ND96 (72 hours), BSM (overnight), BSM with amiloride (overnight). Values are means ± SEM (n = 4-7). Asterisks indicate a significant difference between *GmSALT3*-injected and H_2O-injected oocytes at $*P < 0.05$, $**P < 0.01$ according to the LSD test.

Supplementary materials

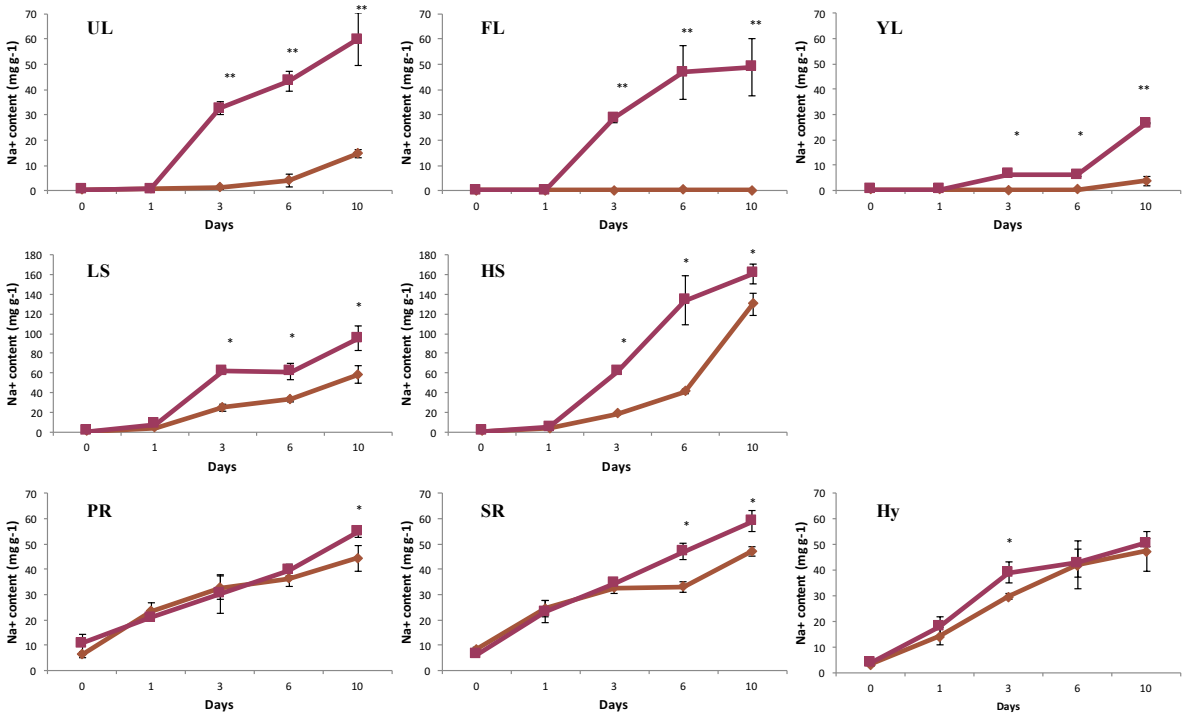

Supplementary Fig. 1 Time-course ion concentration (Na^+) in NIL 820-T and 820-S leaves, stems, hypocotyls, and roots during 10 days NaCl stress (100 mmol L^{-1} NaCl). Data are means of 4 replicates ± SEM. Brown represents NIL-T; red represents NIL-S. Asterisks indicate a significant difference between NIL 820-T and 820-S at **P* <0.05, ***P* < 0.01 according to the LSD test. UL, unifoliate leaves; FL, first trifoliate leaves; YL, youngest trifoliate leaves; LS, lower stem; HS, higher stem; PR, primary root; SR, secondary root; Hy, hypocotyl.

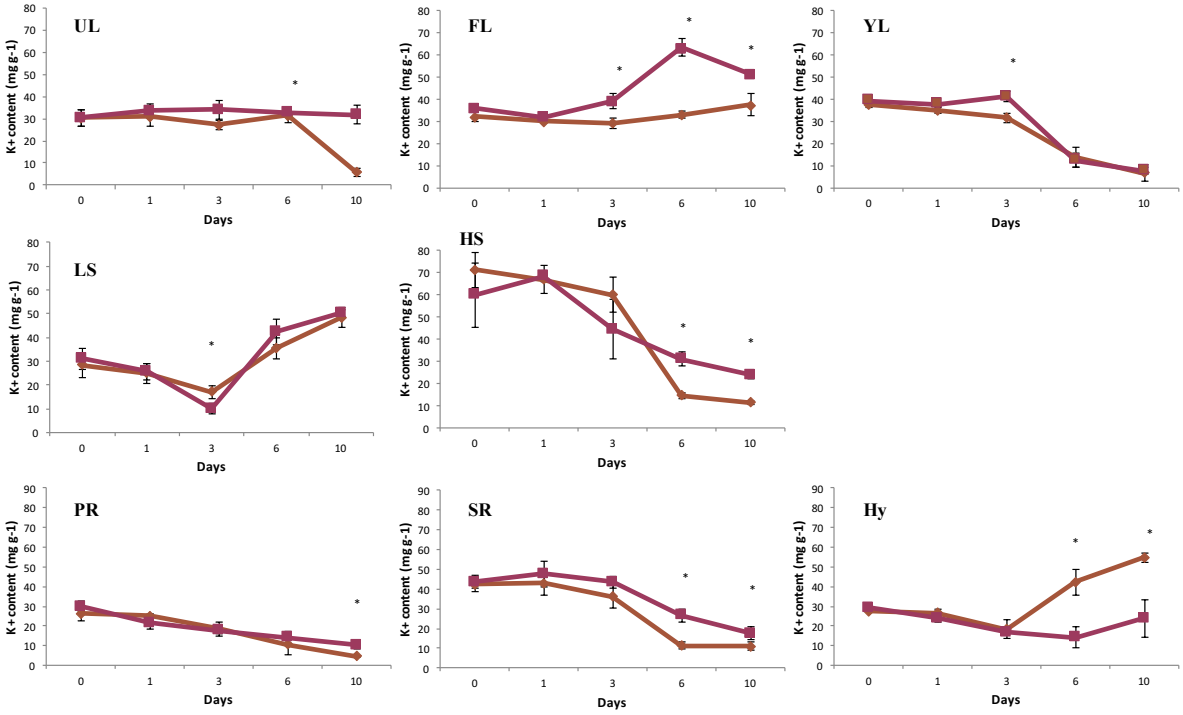

Supplementary Fig. 2 Time-course ion concentration (K^+) in NIL 820-T and 820-S leaves, stems, hypocotyls, and roots during 10 days NaCl stress (100 mmol L^{-1} NaCl). Data are means of 4 replicates ± SEM. Blue represents NIL-T; yellow represents NIL-S. Asterisks indicate a significant difference between NIL 820-T and 820-S at $*P < 0.05$, $**P < 0.01$ according to the LSD test. UL, unifoliate leaves; FL, first trifoliate leaves; YL, youngest trifoliate leaves; LS, lower stem; HS, higher stem; PR, primary root; SR, secondary root; Hy, hypocotyl.

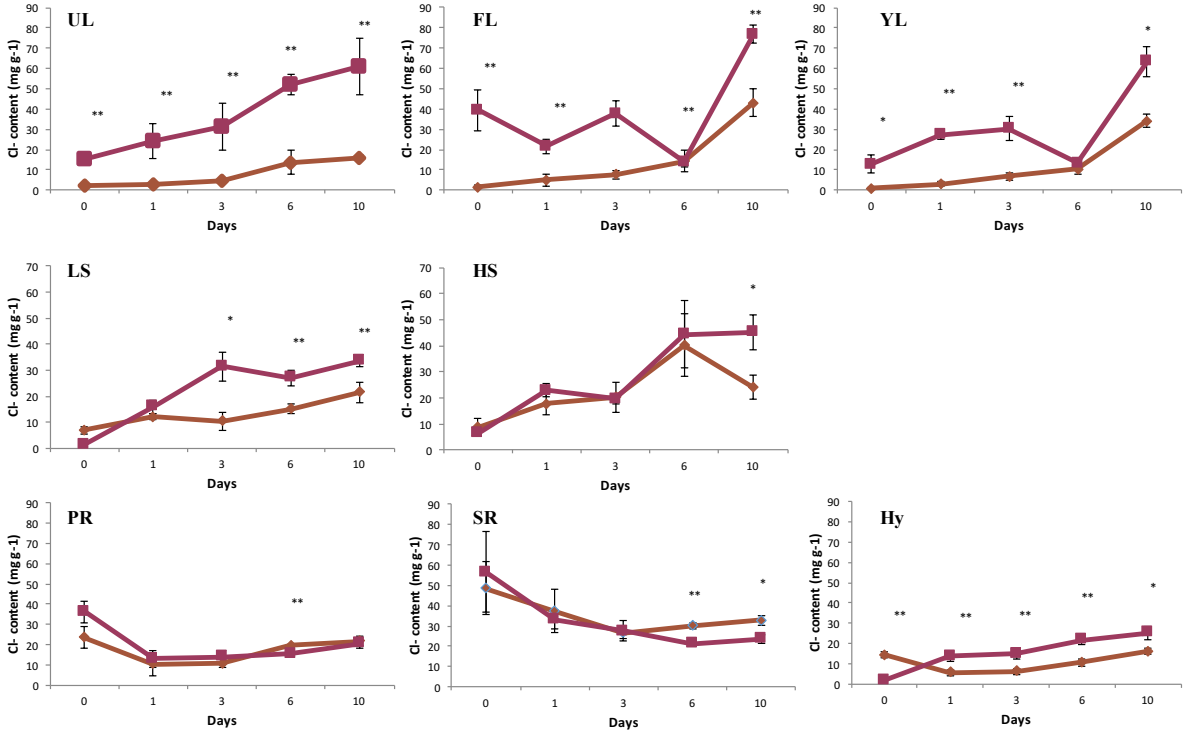

Supplementary Fig. 3 Time-course ion concentration (Cl^-) in NIL 820-T and 820-S leaves, stems, hypocotyls, and roots during 10 days NaCl stress (100 mmol L^{-1} NaCl). Data are means of 4 replicates ± SEM. Blue represents NIL-T; yellow represents NIL-S. Asterisks indicate a significant difference between NIL 820-T and 820-S at $*P < 0.05$, $**P < 0.01$ according to the LSD test. UL, unifoliate leaves; FL, first trifoliate leaves; YL, youngest trifoliate leaves; LS, lower stem; HS, higher stem; PR, primary root; SR, secondary root; Hy, hypocotyl.

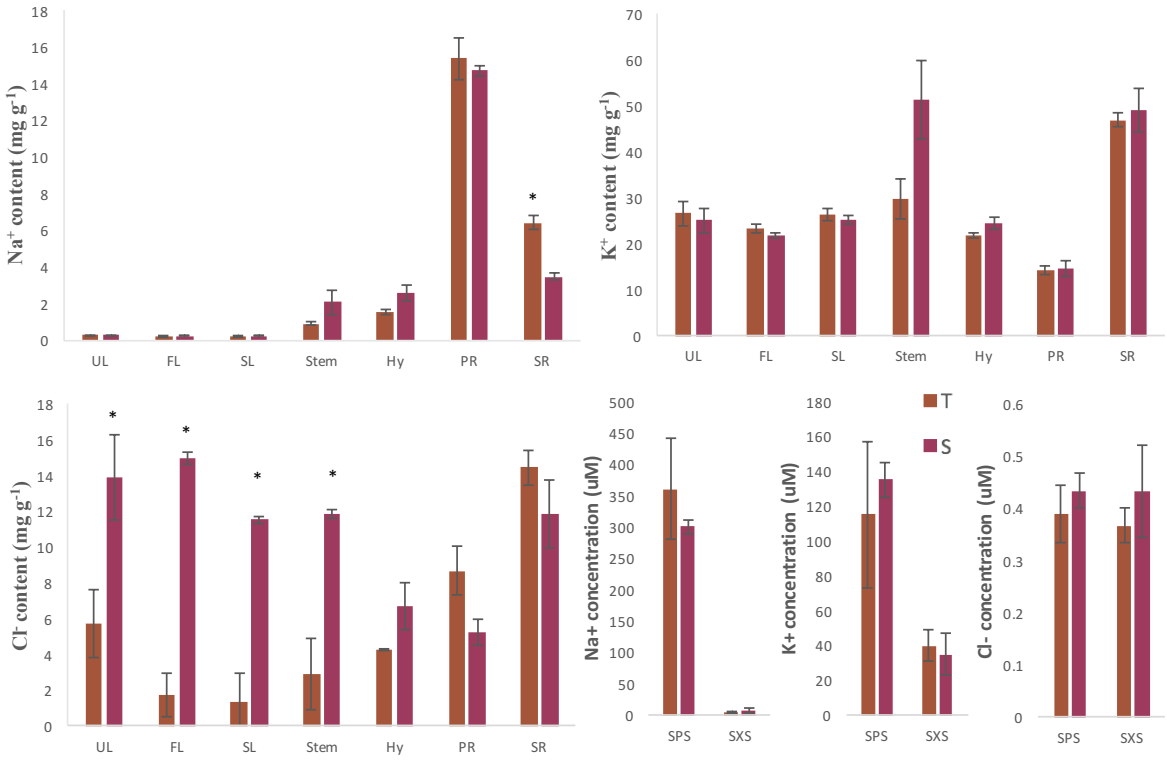

Supplementary Fig. 4 Ion concentration in NIL 820-T and 820-S different tissues after 4 days control condition (RO water). Data are means of 4 replicates ± SEM. Blue represents NIL-T; yellow represents NIL-S. Asterisks indicate a significant difference between NIL 820-T and 820-S at **P* <0.05 according to the LSD test. UL, unifoliate leaves; FL, first trifoliate leaves; YL, youngest trifoliate leaves; PR, primary root; SR, secondary root; Hy, hypocotyl.

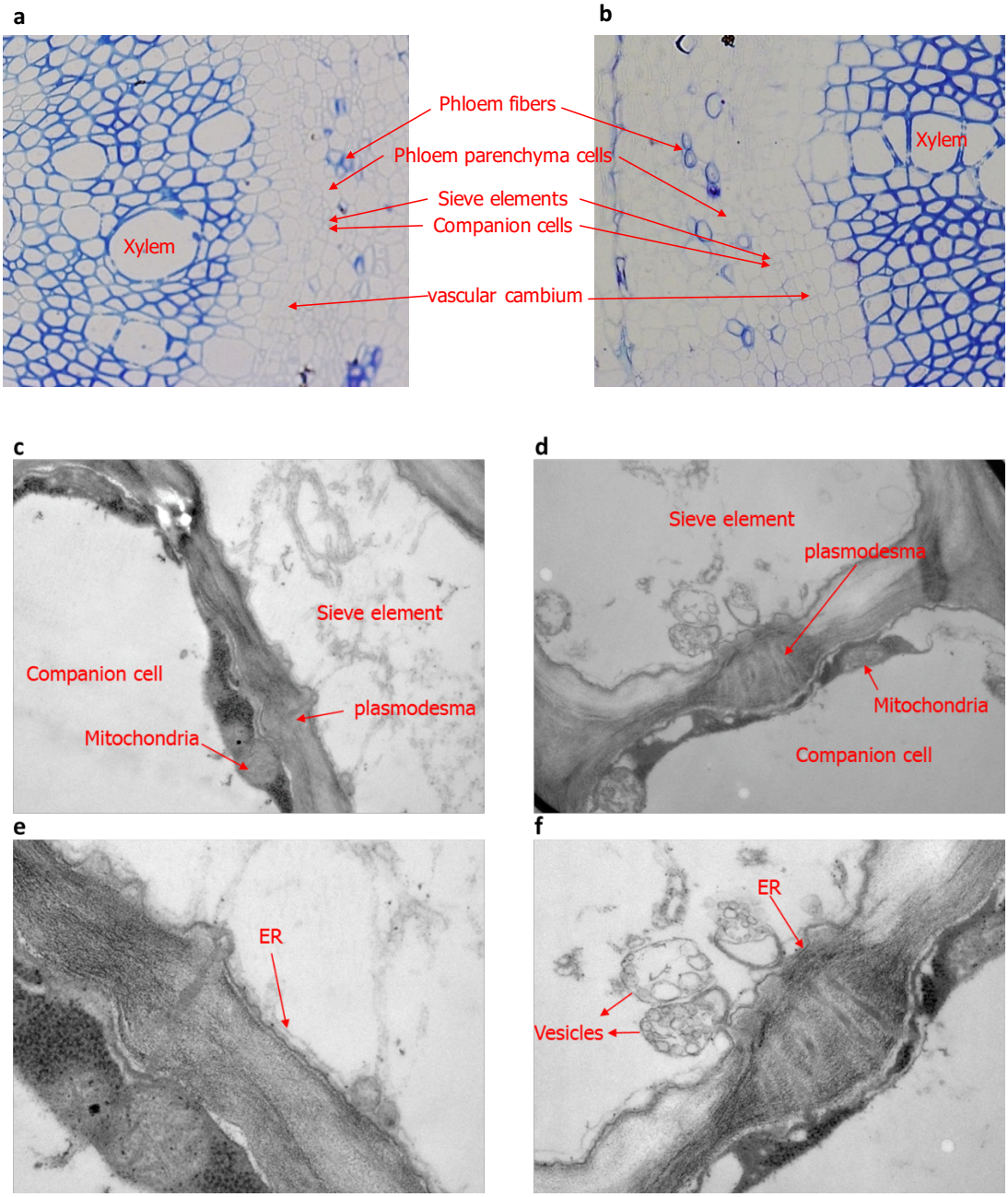

Supplementary Fig. 5 Ultrastructure of NIL-*GmSALT3* and NIL-*Gmsalt3* root cross sections with 4 days NaCl stress (100 mmol L^{-1} NaCl). LDM (LCD Digital Microscope) images of stained NIL-*S* (a) and NIL- *T* (b) root cross sections under 10 X magnification. TEM (Transmission Electron Microscope) images of NIL-*S* (c) and NIL-*T* (d) root phloem plasmadesmata under 19000 X magnification. Higher magnified TEM images of NIL-*S* (e) and NIL-*T* roots (f) under 46000 X and 34000 X magnification, respectively.

Supplementary Fig. 5a and 5b indicates the growth of NIL-T (Supplementary Fig. 5b) and NIL-S (Supplementary Fig. 5a) roots is at the same stage, and four days salt treatment does not change soybean root cell morphology significantly. In phloem bundle cells, companion cells

are distinguished by a dense cytoplasm and numerous mitochondria (Froelich *et al.*, 2011). Sieve elements, the functional units for plant phloem long distance translocation and signal distribution, mainly contain ER, mitochondria, structural phloem specific proteins (P-proteins), and sieve elements plastids (Froelich *et al.*, 2011). Companion cells and sieve elements are connected through plasmodesmata which is shown in Supplementary Fig. 5c-f.

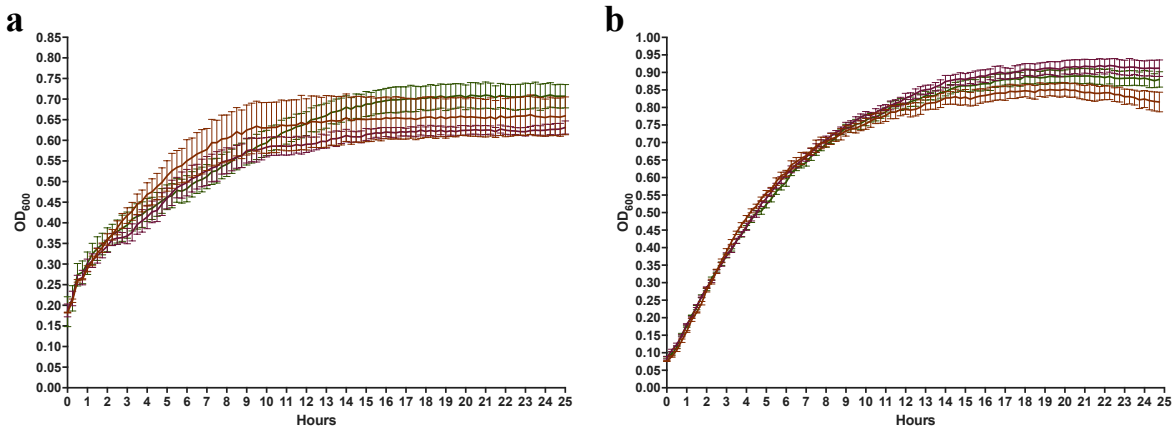

Supplementary Fig. 5 Functional characterization of *GmSALT3* in *E. coli*. *E. coli* strain LB2003 (*trkAΔ, kup1Δ, kdpABCDEΔ*) harbouring pPAB404 vector only (green), *GmSALT3* (brown), or *Gmsalt3* (red) were grown in different medium. **a** YTM without IPTG. **b** YTM with IPTG and 10 mM KCl. All the test media were supplemented with 50µg/ml ampicillin. OD_{600} was monitored every 15 min in 96-well microplate reader.

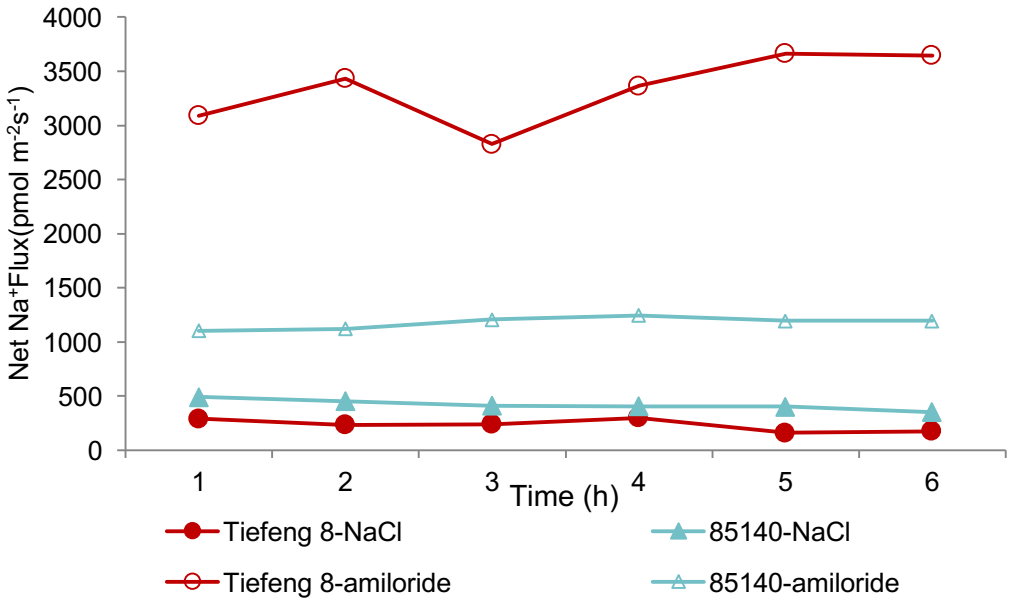

Supplementary Figure 6. Change of Na^+ flux measured in root of Tiefeng 8 and 85-140. Net Na^+ flux was measured after 2d 100 mM NaCl treatment and after 0.5h 100 μM amiloride treatment.

Supplementary Table 1. Primers used in this study. Primers were designed and adjusted using Primer3 (http://bioinfo.ut.ee/primer3-0.4.0/) and Netprimer (http://www.premierbiosoft.com/netprimer/).

Purpose	Primer name	Primer sequence
Sequencing	GmSALT3_F1	5' - CGTTCAAACCATCCTCGTAGT-3'
	GmSALT3_R1	5' - GGCCCACCAGAAATAGATAGA-3'
	GmSALT3_F2	5' - TATGGGTGCTCTTCTCAGGGATG-3'
	GmSALT3_F3	5' - TCATTACAACTCCAATAGTCTTG-3'
	GmSALT3_F4	5' - CAGAAGGTACGAACAAGAACCTG-3'
	GmSALT3_F5	5' - TGTGGAGTACATTGAAAAGAACG-3'
	Gmsalt3_F1	5' - AACTCTAGCGGGAGTAATGTT-3'
	Gmsalt3_R1	5' - AAGTACAAGGGAAGGAACAAC-3'
	Gmsalt3_R2	5' - TGAACGTACCCTATGTTATGG-3'
Gene specific	GmSALT3_gF	5' - ATGACGTTCAACGCGAGC-3'
	GmSALT3_gR	5' - TTAAAGTTCTTCGATAGCATCTTT-3'
	Gmsalt3_gF	5' - ATGACGTTCAACGCGAGC-3'
	Gmsalt3_gR	5' - TCATTTTATTTTATTTTCCAACAC -3'

Literature cited

Abel, G. (1969). Inheritance of the capacity for chloride inclusion and chloride exclusion by soybeans. *Crop Science* **9**, 697-698.

Abel, G. H. and MacKenzie, A. J. (1964). Salt tolerance of soybean varieties (*Glycine max L. Merrill*) during germination and later growth. *Crop Science* **4**, 157-161.

Alexandratos, N. and Bruinsma, J. (2012). World agriculture towards 2030/2050: the 2012 revision: ESA Working paper No.12-03. Rome, FAO.

Berthomieu, P., Conéjéro, G., Nublat, A., Brackenbury, W. J., Lambert, C., Savio, C., Uozumi, N., Oiki, S., Yamada, K. and Cellier, F. (2003). Functional analysis of *AtHKT1* in Arabidopsis shows that Na^+ recirculation by the phloem is crucial for salt tolerance. *The EMBO Journal* **22**, 2004-2014.

Chang, R. Z., Chen, Y. W., Shao, G. H. and Wan, C. W. (1994). Effect of salt stress on agronomic characters and chemical quality of seeds in soybean. *Soybean Science* **13**, 101-105.

Chanroj, S., Lu, Y., Padmanaban, S., Nanatani, K., Uozumi, N., Rao, R. and Sze, H. (2011). Plant-specific cation/H^+ exchanger 17 and its homologs are endomembrane K^+ transporters with roles in protein sorting. *Journal of Biological Chemistry* **286**, 33931-41.

Chintapalli, V. R., Kato, A., Henderson, L., Hirata, T., Woods, D. J., Overend, G., Davies, S. A., Romero, M. F. and Dow, J. A. (2015). Transport proteins NHA1 and NHA2 are essential for survival, but have distinct transport modalities. *Proceedings of the National Academy of Sciences* **112**, 11720-11725.

Colmenero-Flores, J. M., Martínez, G., Gamba, G., Vázquez, N., Iglesias, D. J., Brumós, J. and Talón, M. (2007). Identification and functional characterization of cation–chloride cotransporters in plants. *The Plant Journal* **50**, 278-292.

Corbesier, L., Havelange, A., Lejeune, P., Bernier, G. and Périlleux, C. (2001). N content of phloem and xylem exudates during the transition to flowering in *Sinapis alba* and *Arabidopsis thaliana*. *Plant, Cell & Environment* **24**, 367-375.

Czerny, D. D., Padmanaban, S., Anishkin, A., Venema, K., Riaz, Z. and Sze, H. (2016). Protein architecture and core residues in unwound α-helices provide insights to the function of a plant transporter AtCHX17. *Biochimica et Biophysica Acta (BBA)-Biomembranes*.

Darley, C. P., Van Wuytswinkel, O. C., Van der woude, K. and Mager, W. H. (2000). *Arabidopsis thaliana* and *Saccharomyces cerevisiae NHX1* genes encode amiloride sensitive electroneutral Na^+/H^+ exchangers. *Biochemical Journal* **351**, 241-249.

Delgado, M., Ligero, F. and Lluch, C. (1994). Effects of salt stress on growth and nitrogen fixation by pea, faba-bean, common bean and soybean plants. *Soil Biology and Biochemistry* **26**, 371-376.

Do, T. D., Chen, H., Hien, V. T. T., Hamwieh, A., Yamada, T., Sato, T., Yan, Y., Cong, H., Shono, M. and Suenaga, K. (2016). Ncl synchronously regulates Na^+, K^+, and Cl^- in soybean and greatly increases the grain yield in saline field conditions. *Scientific Reports* **6**: 19147.

Durand, M. and Lacan, D. (1994). Sodium partitioning within the shoot of soybean. *Physiologia Plantarum* **91**, 65-71.

Elsheikh, E. A. (1998). Effects of salt on rhizobia and bradyrhizobia: a review. *Annals of Applied Biology* **132**, 507-524.

Froelich, D. R., Mullendore, D. L., Jensen, K. H., Ross-Elliott, T. J., Anstead, J. A., Thompson, G. A., Pélissier, H. C. and Knoblauch, M. (2011). Phloem ultrastructure and pressure flow: sieve-element-occlusion-related agglomerations do not affect translocation. *The Plant Cell* **23**, 4428-4445.

Gilliham, M., Able, J. A. and Roy, S. J. (2017). Translating knowledge about abiotic stress tolerance to breeding programmes. *The Plant Journal* **90**, 898-917.

Godfray, H. C. J., Beddington, J. R., Crute, I. R., Haddad, L., Lawrence, D., Muir, J. F., Pretty, J., Robinson, S., Thomas, S. M. and Toulmin, C. (2010). Food security: the challenge of feeding 9 billion people. *Science* **327**, 812-818.

Guan, R., Qu, Y., Guo, Y., Yu, L., Liu, Y., Jiang, J., Chen, J., Ren, Y., Liu, G. and Tian, L. (2014). Salinity tolerance in soybean is modulated by natural variation in *GmSALT3*. *The Plant Journal* **80**, 937-950.

Ha, B.-K., Vuong, T. D., Velusamy, V., Nguyen, H. T., Shannon, J. G. and Lee, J.-D. (2013). Genetic mapping of quantitative trait loci conditioning salt tolerance in wild soybean (*Glycine soja*) PI 483463. *Euphytica* **193**, 79-88.

Hamwieh, A., Tuyen, D. D., Cong, H., Benitez, E. R., Takahashi, R. and Xu, D. H. (2011). Identification and validation of a major QTL for salt tolerance in soybean. *Euphytica* **179**, 451-459.

Hamwieh, A. and Xu, D. (2008). Conserved salt tolerance quantitative trait locus (QTL) in wild and cultivated soybeans. *Breeding Science* **58**, 355-359.

Henderson, S. W., Wege, S., Qiu, J., Blackmore, D. H., Walker, A. R., Tyerman, S. D., Walker, R. R. and Gilliham, M. (2015). Grapevine and Arabidopsis cation-chloride cotransporters localize to the golgi and trans-golgi network and indirectly influence long-distance ion transport and plant salt tolerance. *Plant physiology* **169**, 2215-2229.

Ikeda, M. (2005). Distribution of K^+, Na^+ and Cl^- in root and leaf cells of soybean and cucumber plants grown under salinity conditions. *Soil Science and Plant Nutrition* **51**, 1053-1057.

Kronzucker, H. J. and Britto, D. T. (2011). Sodium transport in plants: a critical review. *New Phytologist* **189**, 54-81.

Läuchli, A. (1984). Salt exclusion: An adaptation of legumes for crops and pastures under saline conditions. In *Salinity Tolerance in Plants: Strageiges for Crop Improvement*, eds. R. C. Staples and G. H. Toenniessen), pp. 171-187. New York: Wiley.

Lee, G. J., Carter, J. T. E., Villagarcia, M. R., Li, Z., Zhou, X., Gibbs, M. O. and Boerma, H. R. (2004). A major QTL conditioning salt tolerance in S-100 soybean and descendent cultivars. *Theoretical and applied genetics* **109**, 1610-1619.

Lenis, J., Ellersieck, M., Blevins, D., Sleper, D., Nguyen, H., Dunn, D., Lee, J. and Shannon, J. (2011). Differences in ion accumulation and salt tolerance among *Glycine* accessions. *Journal of Agronomy and Crop Science* **197**, 302-310.

Li, B., Tester, M. and Gilliham, M. (2017). Chloride on the Move. *Trends in Plant Science*.

Li, W. Y., Wong, F. L., Tsai, S. N., Phang, T. H., Shao, G. and Lam, H. M. (2006a). Tonoplast-located *GmCLC1* and *GmNHX1* from soybean enhance NaCl tolerance in transgenic bright yellow (BY)-2 cells. *Plant Cell & Environment* **29**, 1122-37.

Li, X. J., An, P., Inanaga, S., Eneji, A. E. and Tanabe, K. (2006b). Salinity and defoliation effects on soybean growth. *Journal of Plant Nutrition* **29**, 1499-1508.

Liu, Y., Yu, L., Qu, Y., Chen, J., Liu, X., Hong, H., Liu, Z., Chang, R., Gilliham, M., Qiu, L. *et al.* (2016). GmSALT3, which confers improved soybean salt tolerance in the field, increases leaf Cl^- exclusion prior to Na^+ exclusion but does not improve early vigor under salinity. *Frontiers in Plant Science* **7**: 1485.

Lohaus, G., Hussmann, M., Pennewiss, K., Schneider, H., Zhu, J. J. and Sattelmacher, B. (2000). Solute balance of a maize (Zea mays L.) source leaf as affected by salt treatment with special emphasis on phloem retranslocation and ion leaching. *Journal of Experimental Botany* **51**, 1721-1732.

Luo, G. Z., Wang, H. W., Huang, J., Tian, A. G., Wang, Y. J., Zhang, J. S. and Chen, S. Y. (2005a). A putative plasma membrane cation/proton antiporter from soybean confers salt tolerance in Arabidopsis. *Plant Molecular Biology* **59**, 809-20.

Luo, Q., Yu, B. and Liu, Y. (2005b). Differential sensitivity to chloride and sodium ions in seedlings of *Glycine max* and *G. soja* under NaCl stress. *Journal of Plant Physiology* **162**, 1003-1012.

Mäser, P., Eckelman, B., Vaidyanathan, R., Horie, T., Fairbairn, D. J., Kubo, M., Yamagami, M., Yamaguchi, K., Nishimura, M. and Uozumi, N. (2002). Altered shoot/root Na^+ distribution and bifurcating salt sensitivity in Arabidopsis by genetic disruption of the Na^+ transporter AtHKT1. *FEBS letters* **531**, 157-161.

Møller, I. S., Gilliham, M., Jha, D., Mayo, G. M., Roy, S. J., Coates, J. C., Haseloff, J. and Tester, M. (2009). Shoot Na^+ exclusion and increased salinity tolerance engineered by cell type-specific alteration of Na^+ transport in *Arabidopsis*. *The Plant Cell* **21**, 2163-78.

Munns, R. and Gilliham, M. (2015). Salinity tolerance of crops–what is the cost? *New Phytologist* **208**, 668-673.

Munns, R., James, R. A., Xu, B., Athman, A., Conn, S. J., Jordans, C., Byrt, C. S., Hare, R. A., Tyerman, S. D. and Tester, M. (2012). Wheat grain yield on saline soils is improved by an ancestral Na^+ transporter gene. *Nature Biotechnology* **30**, 360-364.

Munns, R. and Tester, M. (2008). Mechanisms of salinity tolerance. *Annual Review of Plant Biology*. **59**, 651-81.

Obermeyer, G. and Tyerman, S. D. (2005). NH_4^+ currents across the peribacteroid membrane of soybean. Macroscopic and microscopic properties, inhibition by Mg^{2+}, and temperature dependence indicate a SubpicoSiemens channel finely regulated by divalent cations. *Plant Physiology* **139**, 1015-1029.

Okumoto, S., Koch, W., Tegeder, M., Fischer, W. N., Biehl, A., Leister, D., Stierhof, Y. D. and Frommer, W. B. (2004). Root phloem-specific expression of the plasma membrane amino acid proton co-transporter AAP3. *Journal of Experimental Botany* **55**, 2155-2168.

Padmanaban, S., Chanroj, S., Kwak, J. M., Li, X., Ward, J. M. and Sze, H. (2007). Participation of endomembrane cation/H^+ exchanger *AtCHX20* in osmoregulation of guard cells. *Plant Physiology* **144**, 82-93.

Phang, T. H., Shao, G. and Lam, H. M. (2008). Salt tolerance in soybean. *the Journal of Integrative Plant Biology* **50**, 1196-212.

Phang, T. H., Shao, G., Liao, H., Yan, X. and Lam, H. M. (2009). High external phosphate (Pi) increases sodium ion uptake and reduces salt tolerance of 'Pi-tolerant'soybean. *Physiologia Plantarum* **135**, 412-425.

Qi, X., Li, M. W., Xie, M., Liu, X., Ni, M., Shao, G., Song, C., Kay-Yuen Yim, A., Tao, Y., Wong, F. L. *et al.* (2014). Identification of a novel salt tolerance gene in wild soybean by whole-genome sequencing. *Nature Communication* **5**, 4340.

Qiu, J., Henderson, S. W., Tester, M., Roy, S. J. and Gilliham, M. (2016). SLAH1, a homologue of the slow type anion channel SLAC1, modulates shoot Cl^- accumulation and salt tolerance in *Arabidopsis thaliana*. *Journal of Experimental Botany* **67**, 4495-4505.

Ren, Z.-H., Gao, J.-P., Li, L.-G., Cai, X.-L., Huang, W., Chao, D.-Y., Zhu, M.-Z., Wang, Z.-Y., Luan, S. and Lin, H.-X. (2005). A rice quantitative trait locus for salt tolerance encodes a sodium transporter. *Nature Genetics* **37**, 1141-1146.

Roy, S. J., Negrão, S. and Tester, M. (2014). Salt resistant crop plants. *Current Opinion in Biotechnology* **26**, 115-124.

Rupassara, S. I. (2008). Metabolite profiling of leaves and vascular exudates in soybean grown under free-air concentration enrichment: ProQuest Dissertations Publishing, 2008. 3337902.

Rus, A., Baxter, I., Muthukumar, B., Gustin, J., Lahner, B., Yakubova, E. and Salt, D. E. (2006). Natural variants of AtHKT1 enhance Na^+ accumulation in two wild populations of Arabidopsis. *PLoS genetics* **2**, e210.

Shabala, S., Shabala, L., Bose, J., Cuin, T. and Newman, I. (2013). Ion flux measurements using the MIFE technique. *Plant Mineral Nutrients: Methods and Protocols*, 171-183.

Shao, G. H., Wan, C. W., Chang, R. Z. and Chen, Y. W. (1993). Preliminary study on the damage of plasma membrane caused by salt stress. *Crops* **1**, 39-40.

Shi, H. and Bressan, R. (2006). RNA extraction. *Methods in Molecular Biology* **323**, 345.

Singh, G. (2010). The soybean: botany, production and uses. Oxfordshire, UK: CABI Publishing.

Singleton, P. W. and Bohlool, B. B. (1984). Effect of salinity on nodule formation by soybean. *Plant Physiology* **74**, 72-76.

Stumpe, S. and Bakker, E. P. (1997). Requirement of a large K^+-uptake capacity and of extracytoplasmic protease activity for protamine resistance of *Escherichia coli*. *Archives of Microbiology* **167**, 126-136.

Taiz, L. (2013). Agriculture, plant physiology, and human population growth: past, present, and future. *Theoretical and Experimental Plant Physiology* **25**, 167-181.

Taiz, L. and Zeiger, E. (2010). Plant Physiology. Sunderland, UK: Mass. : Sinauer Associates.

Tester, M. and Davenport, R. (2003). Na^+ tolerance and Na^+ transport in higher plants. *Annals of Botany* **91**, 503-527.

Tester, M. and Langridge, P. (2010). Breeding technologies to increase crop production in a changing world. *Science* **327**, 818-822.

Tian, H., Baxter, I. R., Lahner, B., Reinders, A., Salt, D. E. and Ward, J. M. (2010). Arabidopsis NPCC6/NaKR1 is a phloem mobile metal binding protein necessary for phloem function and root meristem maintenance. *The Plant Cell* **22**, 3963-3979.

Turgeon, R. and Wolf, S. (2009). Phloem Transport: Cellular Pathways and Molecular Trafficking. In *Annual Review of Plant Biology*, vol. 60, pp. 207-221.

Uozumi, N., Kim, E. J., Rubio, F., Yamaguchi, T., Muto, S., Tsuboi, A., Bakker, E. P., Nakamura, T. and Schroeder, J. I. (2000). The Arabidopsis *HKT1* gene homolog mediates inward Na^+ currents in *Xenopus laevis* oocytes and Na^+ uptake in *Saccharomyces cerevisiae*. *Plant Physiology* **122**, 1249-1260.

Wege, S., Gilliham, M. and Henderson, S. W. (2017). Chloride: not simply a "cheap osmoticum", but a beneficial plant macronutrient. *Journal of Experimental Botany*. **68**: 3057-3069

Xu, G. H., Magen, H., Tarchiftzky, J. and Kafkafi, U. (2000). Advances in chloride nutrition of plants, vol. 68, pp. 97-150. San Diego: Academic Press Inc.

Yamaguchi, T. and Blumwald, E. (2005). Developing salt-tolerant crop plants: challenges and opportunities. *Trends in Plant Science* **10**, 615-620.

Brief conclusion

In chapter 4, *GmSALT3* was shown to have a function related to mediating Na^+, K^+, and Cl^- exclusion in NIL-T; it also facilitates K^+ transport in GmSALT3-expressed *E. coli* cells and Na^+, K^+, and Cl^- transport in *Xenopus laevis* oocytes. However, if it is an endomembrane-localised protein, *GmSALT3* would more likely have an indirect role in affecting soybean's salt exclusion from the shoot which could relate to a homeostatic function in the roots. For instance, this may be through impacting other transport proteins via affecting vesicle trafficking or pH balance in the root. RNA-sequencing is a useful tool to reveal how *GmSALT3* contributes to NIL-T salinity tolerance in the roots.

Chapter 5 *GmSALT3* expression improves ROS detoxification in salt-stressed soybean roots

Yue Qu[2], Lili Yu[1], Rongxia Guan[1], Oliver Berkowitz[3], Rakesh David[2], James Whelan[3], Stefanie Wege[2], Lijuan Qiu[1,*], Matthew Gilliham[2,*]

[1] The National Key Facility for Crop Gene Resources and Genetic Improvement, Institute of Crop Science, Chinese Academy of Agricultural Sciences, Beijing, China

[2] ARC PEB, School of Agriculture, Food and Wine, University of Adelaide, Glen Osmond, SA, Australia

[3]ARC PEB, La Trobe University, Bundoora VIC 3083, Australia

[*]Correspondence should be addressed to:

Prof. Lijuan Qiu

qiulijuan@caas.cn

Prof. Matthew Gilliham (matthew.gilliham@adelaide.edu.au)

Tel: +61 8 8313 3044

Fax: +61 8 8313 5725

Keywords: ROS; salinity tolerance; endomembrane; cation-proton exchanger; *GmSALT3*; *GmCHX1; GmNcl*

Running title: *GmSALT3* contributes to ROS detoxification in salt-tolerant soybeans

Brief introduction

Grafting experiments have indicated that GmSALT3 mainly fulfills its impact on salt tolerance through functioning in soybean roots, where salt enters the plants from soils. The ER-localised GmSALT3 appears to manipulate differences in ion homeostasis (Na^+, K^+, and Cl^-) in NIL-T (Figure 1 and 2, Chapter 4) and its transcript level was first down-regulated and then gradually recovered under salt-stress (Figure 3, Chapter 2). Taken together, *GmSALT3* is unlikely to play a direct role in contributing to salinity tolerance, but instead may act on sensing or responding to salt in roots. Therefore, transcriptomic analysis of NIL-T and NIL-S roots was designed to investigate how *GmSALT3* affects salt responses in those two soybean roots. The intention is to eventually submit this manuscript to *Journal of Experimental Botany*.

Statement of Authorship

Title of Paper	*GmSALT3* expression improves ROS detoxification in salt-stressed soybean roots
Publication Status	☐ Published ☐ Accepted for Publication ☐ Submitted for Publication ☑ Unpublished and Unsubmitted work written in manuscript style
Publication Details	Qu, Y., Guan, R., Berkowitz, O., Yu, L., David, R., Whelan, J., Wege, S., Gilliham, M. (2017)

Principal Author

Name of Principal Author (Candidate)	Yue Qu		
Contribution to the Paper	YQ contributed to experimental design. Analysed the data and wrote the manuscript.		
Overall percentage (%)	85%		
Certification:	This paper reports on original research I conducted during the period of my Higher Degree by Research candidature and is not subject to any obligations or contractual agreements with a third party that would constrain its inclusion in this thesis. I am the primary author of this paper.		
Signature		Date	28.08.17

Co-Author Contributions

By signing the Statement of Authorship, each author certifies that:

i. the candidate's stated contribution to the publication is accurate (as detailed above);

ii. permission is granted for the candidate in include the publication in the thesis; and

iii. the sum of all co-author contributions is equal to 100% less the candidate's stated contribution.

Name of Co-Author	Rongxia Guan		
Contribution to the Paper	RG contributed to experimental design, performed RNA-sequencing, and contributed to analysing the data.		
Signature		Date	28.08.17

Name of Co-Author	Oliver Berkowitz		
Contribution to the Paper	OB performed RNA-sequencing rerun.		
Signature		Date	06/09/2017

Name of Co-Author	Lili Yu		
Contribution to the Paper	LY performed plant samples harvest for RNA-sequencing		
Signature		Date	28.08.17

Name of Co-Author	Rakesh David		
Contribution to the Paper	RD contributed to RNA-sequencing analysis		
Signature		Date	01-09-2017

Name of Co-Author	James Whelan		
Contribution to the Paper	JW performed RNA-sequencing rerun.		
Signature		Date	02/09/2017

Name of Co-Author	Stefanie Wege		
Contribution to the Paper	Contributed to experimental design; assisted in editing the final version of the manuscript.		
Signature		Date	01-08-2017

Name of Co-Author	Lijuan Qiu		
Contribution to the Paper	Contributed to experimental design.		
Signature		Date	28.08.17

Name of Co-Author	Matthew Gilliham		
Contribution to the Paper	Contributed to experimental design, supervised the research, and assisted in editing the final version of the manuscript.		
Signature		Date	1/9/2017

Abstract

Soybean (*Glycine max*) is an important crop globally for food and edible oil production. Soybean plants are sensitive to salinity (NaCl), with their yield moderately impacted under saline conditions (~60% reduction at 18-20 dS/m, ~180-200mM NaCl). *GmSALT3* was recently identified, through fine mapping, as a dominant gene underlying a major QTL for salt tolerance in soybean. *GmSALT3* encodes a transmembrane protein within the CPA2 plant cation/proton exchanger (CHX) family, and is mainly expressed in root phloem and xylem associated cells; the protein was localized to the endoplasmic reticulum. Plants containing a truncated allele (*Gmsalt3*) are more salt-sensitive, but how *GmSALT3* contributes to soybean salinity tolerance still remains unknown. Here, in an attempt to reveal new insights to the potential underlying mechanisms we used RNA-seq analysis of roots from soybean NIL (Near Isogenic Lines); NIL-S (salt-sensitive, *Gmsalt3*) and NIL-T (salt-tolerant, *GmSALT3*). Thirty RNA-seq libraries were constructed and sequenced, including NIL-T and -S roots from three time points of 14 day old plants, 0 hours, 6h, and 3d following salt-treatment (200mM NaCl) and their corresponding non-treatment controls. A total of 804 million clean reads were generated and the average mapping percentage was 81.25%. Under no salt treatment there were 3 consistent up-regulated significantly differentially expressed genes (DEGs) in NIL-S compared to NIL-T at 0h, 6h, and 3d; and no down-regulated DEGs. However, compared to non-salt treated controls after 6h salt treatment there were 1816 and 3045 DEGs for NIL-S and NIL-T, respectively; and at 3d, there were 2844 and 2573 DEGs. Gene ontology (GO) analysis showed that unique DEGs under salt treatment in NIL-T are clustered into GO terms such as response to biotic stimulus, oxidation reduction and oxidoredutase activity, and in NIL-S are more diverse such as cell communication, signalling, and biological regulation. Accordingly, reactive oxygen species (ROS) generation and detoxification was measured and differed in NIL consistent with the RNA-seq data. We propose that GmSALT3 affects the ROS status of roots which improves the ability of NIL-T to cope with stress.

Introduction

Plants use reactive oxygen species (ROS) as signalling molecules at low concentrations to control and regulate various biological processes, such as growth, programmed cell death, hormone signalling, and development (Foreman *et al.*, 2003; Mittler, 2002; Neill *et al.*, 2002; Overmyer *et al.*, 2003; Pei *et al.*, 2000). Under non-stressed conditions ROS molecules are produced and scavenged in an equilibrium (Foyer and Noctor, 2005). However, under biotic and abiotic stresses such as salinity, drought, temperature extremes, flooding, heavy metals, nutrient deprivation, and pathogen attack, intracellular ROS levels can soar dramatically. ROS at high concentrations can damage plant cells through lipid peroxidation, DNA damage, protein denaturation, carbohydrate oxidation, and enzymatic activity impairment leading to significant damage to cellular functions and even cell death (Foyer and Noctor, 2005; Gill and Tuteja, 2010; Mittler *et al.*, 2004; Noctor and Foyer, 1998), and environmental stress induced ROS accumulation reduces global crop production (Mittler, 2002). In plants, stress-induced ROS overproduction is eliminated by enzymatic antioxidant systems including scavengers such as SOD (superoxide dismutase), APX (ascorbate peroxidase), GPX (Glutathione peroxidases), PrxR (proxiredoxin), GST (glutathione-S- transferase), and CAT (Catalase) and non-enzymatic low molecular metabolites, such as ASH (ascorbate), GSH (glutathione), proline, α-tocopherol (vitamin E), carotenoids and flavonoids (Mittler *et al.*, 2004).

Among the above-mentioned stresses, salinity is one of the most prominent factors restricting crop production and agricultural economic growth worldwide, more than US$12 billion is lost annually because of saline-affected agricultural land areas (Bose *et al.*, 2014; Flowers *et al.*, 2010; Gilliham *et al.*, 2017). Soybean (*Glycine max* (L.) Merrill) is an important legume crop that contributes 30% of the globe's edible vegetable oil consumed and 69% of human food and animal feed protein-rich supplements (Lam *et al.*, 2010; Prakash, 2001). The yield of soybean can be significantly reduced by salinity stress, especially during the early vegetative growth stage (Pi *et al.*, 2016).

In soybean, *GmSALT3*/*GmCHX1*/*GmNcl* has been identified as a dominant gene that confers improved salinity tolerance (Do *et al.*, 2016; Guan *et al.*, 2014; Qi *et al.*, 2014). It mainly functions in root phloem- and xylem-associated cells and has been localized to the ER (endoplasmic reticulum) (Guan *et al.*, 2014). NILs (near isogeneic lines) have been developed and show that *GmSALT3* increases leaf Cl^- exclusion prior to Na^+ exclusion (Liu *et al.*, 2016); it has also been reported that *GmSALT3* is related to K^+ homeostasis (Figure 1, Chapter 4; Do *et al.*, 2016). However, how *GmSALT3* functions to improve salinity stress tolerance in soybean plants is not fully understood.

High-throughput "-omic" technologies including transcriptomic, proteomic, and metabolomics approaches were recently applied to understand the soybean root responses to salinity stress (Aghaei *et al.*, 2009; Ge *et al.*, 2010; Lu *et al.*, 2013; Pi *et al.*, 2016; Qin *et al.*, 2013; Toorchi *et al.*, 2009). These studies provide a basis for examining the general responses of soybean roots to salt stress. For instance, one of the proteomic studies utilised *Glycine max* cultivar (Wenfeng07, with *GmSALT3* salt tolerant allele) and *Glycine soja* (wild soybean) cultivar (Union85-140, with *Gmsalt3* salt sensitive allele), and suggested that Wenfeng07's tolerance to salinity stress was associated with flavonoid accumulation in the tolerant accession, which reduces ROS concentration via key enzymes including chalcone synthase (CHS), chalcone isomerase (CHI) and cytochrome P450 monooxygenase (CPM) (Pi *et al.*, 2016).

RNA-sequencing is increasingly being used for crop salinity tolerance transcriptomic studies, such as in wheat (Goyal *et al.*, 2016), grapevine (Sweetman *et al.*, 2012), maize (Kakumanu *et al.*, 2012), chickpea (Garg *et al.*, 2016), and soybean (Severin *et al.*, 2010). Here, RNA-sequencing of NIL-T (salt-tolerant, *GmSALT3*) and NIL-S (salt-sensitive, *Gmsalt3*) soybean roots were used to investigate the mechanism underlying the improvement in salt tolerance conferred by *GmSALT3*. Bioinformatic analyses were conducted after RNA-seq library construction, including gene ontology (GO) enrichment, KEGG (Kyoto Encyclopedia of Genes and Genomes) pathway analysis and gene clustering analysis; qPCR of several DEGs (differentially expressed genes) was run to validate the RNA-seq outcomes. ROS contents and

scavenging enzyme activity measurement were also performed to investigate whether transcriptional changes led to changes in enzymatic capacity. Our results reveal that the presence of *GmSALT3* is essential for maintaining the capacity to detoxify ROS in the roots when challenged with a salinity stress, therefore leading to improved salinity tolerance.

Results

RNA-sequencing preparation and profiles

Previous results have shown that *GmSALT3* expression mainly occurs in soybean roots (Guan *et al.*, 2014), therefore, total RNA was extracted and sequenced from NIL-T and NIL-S soybean plant roots, and used for transcriptomic analysis to gain an overview of the different responses between NIL-T and NIL-S under saline conditions. To investigate short-term and long-term responses, root samples were harvested from three time points, 0h, 6h, and 3d of a 200 mM salt-treatment with the corresponding non-treatment controls (Fig 1a; 1b). Thirty RNA libraries were generated for paired-end reads using an Illumina HiSeq 2500 sequencer, consisting of 3 biological samples per time point per genotype. In total, 1.6 billion paired 100 bp raw reads were generated and mapped to the latest soybean genome sequence Gmax_275 Wm82.a2.v1 (Glyma 2.0) using TopHat2 (Kim *et al.*, 2013). The average mapping percentage was 81.25%, and after trimming of low quality (Q<30), adapter fragments and barcode sequences, a total of 804 million clean mapped reads. Combined with quality control test by fastQC (Andrews, 2010), the quality of RNA-seq libraries construction and sequence alignment was deemed sufficient for further analysis. A summary of mapped reads and quality of sequencing is shown in Table 1.

Firstly, to confirm the material was as expected we examined the transcript corresponding to *GmSALT3/Gmsalt3* in the NIL-T and NIL-S lines. We found that NIL-T had a full-length of *GmSALT3* according to the mapped-reads in RNA-seq libraries, and NIL-S possessed the truncated version, *Gmsalt3* (Fig. 1c), which was due to the 3780 bp insertion in

the *GmSALT3* genomic sequence (Guan *et al.*, 2014). We then examined the overall profile of all transcriptomes gathered.

Overview of DEGs between NIL-T and NIL-S under control condition

Figure 2 indicates DEGs between NIL-T and NIL-S under control condition at 0h, 6h, and 3d. A PCA plot (for the first two principal components) of ten grouped samples shows a good separation between comparisons, Control 0h T vs Control 0h S (grey), Control 3d T vs Control 3d S (purple), and Control 6h T vs Control 6h S (brown) (Fig. 2a). There are 5 up-regulated DEGs at 0h, 9 up-regulated DEGs at 6h, and 6 up-regulated DEGs at 3d in NIL-S (compared to NIL-T), and Venn diagram demonstrates 3 of these genes are common in three time points. There were 1, 5, and 5 down-regulated DEGs at 0h, 6h, and 3d, respectively, but there were no common down-regulated DEGs (Fig 2b). The three common up-regulated DEGs in NIL-S were *Glyma.07G196800* (Linoleate 13S-lipoxygenase 3-1), *Glyma.10G143600* (uncharacterized protein), and *Glyma.20G105500* (3-hydroxybenzoate 6-hydroxylase 1-like) (Fig. 2c).

Overview of DEGs between control and salt-treated samples of NIL-T and NIL-S

Using a Principal Component Analysis (PCA) plot (for the first two principal components), we could separate the 30 transcriptomes into comparison groups consisting of the biological replicates, indicating that they were closely related (Fig. 2a). There was good separation between sample comparisons e.g. Control 6h T vs NaCl 6h T (brown), Control 6h S vs NaCl 6h S (red), Control 3d T vs NaCl 3d T (green), and Control 3d S vs NaCl 3d S (cyan) (Fig. 2a). Gene expression was compared in FPKMs (Fragments Per Kilobase of transcript per Million) calculated using the Cufflinks functions cuffquant and cuffnorm (Trapnell *et al.*, 2012). The cut-offs for differentially expressed genes (DEGs) were Log_2FC (fold change) ≥ 1, FDR (False Discover Rate) < 0.01. Using these parameters there were 1816 DEGs (1263 up-regulated and 553 down-regulated, 6h T) and 2844 DEGs (1333 up-regulated and 1511 down-

regulated, 3d T) in NIL-T roots after 6 hours and 3 days salt-treatment, respectively, compared to non-salt treated tissue. For NIL-S roots there were 3054 DEGs (1911 up-regulated and 1143 down-regulated, 6h S) and 2573 DEGs (1318 up-regulated and 1255 down-regulated, 3d S) after 6h salt-treatment and 3 days salt-treatment, respectively, compared to non-salt treated NIL-S controls (Fig 2b). Clustering of these DEGs is shown in Figure 2c (6h T), 2d (3d T), 2e (6h S), and 2f (3d S). Venn diagrams indicate 341 and 989 DEGs are uniquely up-regulated in 6h T and 6h S, respectively; 608 and 593 DEGs for 3d T and 3d S, respectively (Fig. 2g). There are 127 and 717 DEGs are uniquely down-regulated in 6h T and 6h S, respectively; 861 and 605 DEGs for 3d T and 3d S, respectively (Fig. 2h). To investigate potential functional differences between NIL-T and NIL-S roots under salt stress, these uniquely-regulated genes were further investigated.

GO analysis of DEGs between control and salt-treated samples of NIL-T and NIL-S

To obtain a functional characterisation of distinctive DEGs, the uniquely up- and down-regulated DEGs in 6h T and 6h S were then subjected to GO (Gene Ontology) enrichment analysis, with the representative GO terms shown in Table 2, detailed GO terms are shown in Supplementary Fig. 1-4. The 6h T up-regulated DEGs enriched GO terms were all related to stress response including “response to biotic stimulus (GO:0009607)”, “defense response (GO:0006952)”, “oxidation reduction (GO:0055114)”, “copper ion binding (GO:0005507)”, “oxidoreductase activity (GO:001691)”, and “endopeptidase inhibitor activity (GO:0004866)” (Table 2a), and down-regulated GO term were mainly “integral to membrane (GO:0016021)” (Table 2c); 6h S up-regulated GO term were mainly “regulation of transcription, DNA-dependent (GO:0006355)” (Table 2b), and down-regulated GO terms included “heme binding (GO:0020037)”, “electron carrier activity (GO:0009055)”, “aspartic-type endopeptidase activity (GO:0004190)”, and “protein disulphide oxidoreductase activity (GO:0015035)” (Table 2d).

After 3 days of salt treatment, GO analysis on uniquely up- and down-regulated DEGs showed that only "oxidation reduction (GO:0055114)" and "oxidoreductase activity (GO:0016491)" were up-regulated in NIL-T (Table 3a); "microtubule-based movement (GO:0007018)", "microtubule motor activity (GO:0003777)", "ADP binding (GO:0043531)", "beta-galactosidase-related (GO:0004565)", "serine hydrolase activity (GO:0017171)" and "beta-galactosidase complex (GO:0009341)" were down-regulated (Table 3c). Up-regulated GO terms in NIL-S were "regulation of transcription, DNA-dependent (GO:0006355)", "protein amino acid phosphorylation (GO:0006468)", "recognition of pollen (GO:0048544)", and "malate transport (GO:0015743)" (Table 3b); transmembrane transporter-related GO terms were down-regulated in NIL-S (Table 3d).

"Oxidation reduction (GO:0055114)" and "oxidoreductase activity (GO:0016491)" were consistently up-regulated in NIL-T at both time points. Table 4 shows all the 53 up-regulated genes in "oxidation reduction" and "oxidoreductase activity" GO terms after 3d treatment in NIL-T roots. A group of Cytochrome P450 enzymes-encoding genes were significantly more highly expressed in NIL-T, especially *Glyma.13G173500*, which had a FPKM of 279 compared to 71 under control conditions (Table 4). Other genes encoding oxidoreductase enzymes were also included such as peroxidases and dehydrogenases (Table 4).

KEGG analysis of DEGs between control and salt-treated samples

To understand what pathways were differently altered in NIL-T and NIL-S under salt stress, KEGG (Kyoto Encyclopedia of Genes and Genomes) analysis was performed. In our analysis, 1816 and 3054 DEGs in NIL-T and NIL-S, respectively, were enriched in 58 pathways (corrected *p*-Value <0.05) after 6 hours salt-treatment (Fig 4a). Most of the 58 pathways in both NIL-T and NIL-S were within the metabolism category; "Phenylpropanoid biosynthesis", "Phenylalanine metabolism", and "Starch and sucrose metabolism" were the top three pathways. In other categories, "Endocytosis", "Phagosome", and "Peroxisome" were enriched in within cellular process category; "Plant hormone signal transduction", "Phosphatidylinositol signaling

system", and "ABC transporters" were enriched in environmental information processing; "Protein processing in endoplasmic reticulum", "Ribosome", and "Spliceosome" were enriched in genetic information processing; "Plant-pathogen interaction" was enriched in organismal systems. Overall, in all significantly changed pathways, NIL-S has more DEGs compared to NIL-T after 6 hours salt-treatment.

With regard to 3 days salt stress, 2844 and 2573 DEGs in NIL-T and NIL-S, respectively, were mapped to 57 pathways (corrected P-Value <0.05) (Fig 3b). The metabolism category was also the most enriched after 3 days with similar pathways involved compared to 6 hours; "Peroxisome", "Regulation of autophagy", and "Endocytosis" were enriched in the cellular process category; "Plant hormone signal transduction", "Phosphatidylinositol signaling system", and "ABC transporters" were enriched in environmental information processing; "Protein processing in endoplasmic reticulum", "Ubiquitin mediated proteolysis", and "Spliceosome" were enriched in genetic information processing; "Plant-pathogen interaction" was enriched in organismal system. After 3 days salt-treatment, most of the significantly changed pathways included more DEGs in NIL-T compared to NIL-S, especially in "Protein processing in endoplasmic reticulum" (16 to 11 DEGs), "Ubiquitin mediated proteolysis" (10 to 3 DEGs), "Phenylpropanoid biosynthesis" (71 to 60 DEGs), "Phenylalanine metabolism" (52 to 42 DEGs), "Starch and sucrose metabolism" (43 to 35 DEGs), and "Plant-pathogen interaction" (33 to 20 DEGs).

In the "Plant-pathogen interaction" pathway, the putative CNGC (Cyclic Nucleotide-Gated ion Channel) 15-like gene, *Glyma.13G141000*, was significantly down-regulated in 3d T (Fig. 4a, b), but another probable CNGC 20 gene, *Glyma.09G168700*, was upregulated in 3d S. Several CaM (Calmodulin) and CML (Calmodulin-like) genes were down-regulated in 3d T. CDPK (Calcium-Dependent Protein Kinase 3, *Glyma.08G019700*) and Rboh (Respiratory Burst Oxidase Homolog protein F-like isoform 1, *Glyma.01G222700*) were up-regulated in 3d S. However, at 6h, another CNGC 20-like gene, *Glyma16G218300*, was significantly up-

regulated in NIL-T which results in higher expression of Rhob and CaM/CML (Supplementary Fig. 6).

Genes clustering analysis

Based on gene expression patterns of all 30 RNA-seq libraries, they could be grouped into 17 sub-clusters (Supplementary Fig. 6). The top four hierarchical sub-culsters are shown in Fig. 6. Cluster 1 (Fig. 6a) includes 406 genes that were up-regulated at 6h and down-regulated at 3d in both salt-treated NIL-T and -S compared to control-treated samples; Fig. 6b indicates 639 genes clustered that were up-regulated at 3d salt-treated samples and further up-regulated in NIL-T compared to NIL-S; Cluster 14 (Fig. 6c) has 954 genes that were up-regulated at 6h and further up-regulated at 3d in both salt-treated NIL-T and -S compared to control-treated samples; Cluster 17 (Fig. 6d) includes 404 genes that were up-regulated at 6h in both salt-treated NIL-T and -S compared to control-treated samples.

RT-qPCR validation for RNA-seq results

In order to confirm the RNA-seq results, 10 DEGs were selected for RT-qPCR validation, based on their RPKM transcript abundance. RT-qPCR, shown in supplementary fig. 5, indicates that relative expression values (relative to housekeeping gene *GmUKN1*) of the selected DEGs are significantly correlated with their FPKM values.

ROS contents and scavenger enzymes activity

Due to the enrichment of the "Oxidation reduction" gene ontology category in NIL-T plants under salt (Table 4) we decided to see if this translated into a difference in ROS generation or detoxification in NIL-T compared to NIL-S. H_2O_2 is one form of ROS (Reactive Oxygen Species), its content was measured in the roots of NIL-T and NIL-S at 3 days with or without salt treatment (Fig. 7a). Fig. 7a shows that there are no significant differences between NIL-T and NIL-S under control or saline conditions at 3d; but H_2O_2 concentration was higher

with salt treatment compared to control. The antioxidant properties the roots of NIL-T and NIL-S at 3 days with salt treatment was analysed using H_2O_2 guaiacol. The scavenging enzyme activity of the superoxide anion was significantly higher in NIL-T compared to NIL-S.

Discussion

Soybean cultivars harbouring *GmSALT3* are better able to regulate Na^+, K^+, and Cl^- homeostasis in whole plants (Do *et al.*, 2016; Guan *et al.*, 2014; Liu *et al.*, 2016; Qi *et al.*, 2014), and they also have a yield advantage under saline conditions (Do *et al.*, 2016; Liu *et al.*, 2016). However, as an ER-localised membrane protein (Guan *et al.*, 2014), how its molecular functions contribute to salinity tolerance remain unknown. In the present research, to further decipher connections between *GmSALT3* and soybean salinity tolerance, and to identify other genes and biological pathways involved in responses to salt stress in *GmSALT3*-NIL plants, we generated *de novo* transcriptomes by RNA-seq from roots of NIL-T and NIL-S seedlings from three time points, 0d, 6h, and 3d of salt-treatment (200 mM NaCl) and corresponding non-treatment controls.

Illumina sequencing results were tested through fastQC in FastQ format (Andrews, 2010), reports showed that all the 30 constructed RNA-seq libraries were qualified for further analysis. On average the RNA-seq libraries had 26.8 million clean mapped reads, and reads were mapped to 53,625 annotated soybean genes with 353 new-discovered. Minimal DEGs could be detected between NIL-T and NIL-S at 0h, 6h, and 3d under control conditions (Fig 2), this indicates that NIL-T and NIL-S roots had similar gene expression patterns under non-stressed conditions. Based on our analysis, there were 1816 DEGs (6h) and 2844 (3d) DEGs responsive to salt stress in NIL-T roots; 3054 DEGs (6h) and 2573 (3d) DEGs responsive to salt stress in NIL-S roots (Fig. 2b). Uniquely DEGs at 6h and 3d were further analysed by GO enrichment.

"Oxidation reduction (GO:0055114)" and "oxidoreductase activity (GO:0016491)" were consistently up-regulated in NIL-T at both time points with a greater amount of genes in

this term up-regulated after 3 days, which indicates that NIL-T plants may have a greater capacity to detoxify ROS (Reactive oxygen species) than NIL-S plants. In all the listed up-regulated genes in NIL-T (Table 4), a group of Cytochrome P450 enzymes-coding genes were significantly more highly expressed in NIL-T in response to salt-treatment, especially *Glyma.13G173500,* which has the highest expression level and a fold change of 3.93. The expression of *Glyma.13G173500* was consistent among control-treated samples. (Supplementary Fig. 6).

Cytochrome P450 (CYP) is a large and essential superfamily in plants, which catalyses monooxygenation/hydroxylation reactions in primary and secondary metabolism pathways (Mizutani and Ohta, 2010). In soybean, there are 322 identified CYPs, but most of them have not been functionally elucidated (Guttikonda *et al.*, 2010). *GmCYP82A3* (*Glyma.13g068800*) (Yan *et al.*, 2016) and *GmCYP51G1* (*Glyma.07g110900*) (Pi *et al.*, 2016) were shown to be involved in plant resistance to biotic and abiotic stresses such as salinity and drought.

Soybean Isoflavone synthase (IFS) *GmIFS1* (*Glyma.07G202300*) and *GmIFS2* (*GmCYP93C1*; *Glyma.13G173500*; an isoform of *GmIFS1*; a DEG in our study) are tandem P450 enzymes that are anchored in the ER, interacting with soluble enzymes in the phenylpropanoid and isoflavonoid pathways, including chalcone synthase (CHS), chalcone reductase (CHR), and chalcone isomerase (CHI) (Dastmalchi *et al.*, 2016). GmCHS, GmCHI and GmCPM (cytochrome P450 monooxygenase) mediates the accumulation patterns of flavonoids, and these flavonoids play roles in reducing the ROS or other functions (Pi *et al.*, 2016). *GmIFS1* expression is induced by salt stress and leads to accumulation isoflovanones and improved salt tolerance (Jia *et al.*, 2017). We found *GmIFS2* (*Glyma.13G173500)* has a fold change of 3.93 in NIL-T in response to salt stress (Table 4); it has been previously proposed to increase phenylpropanoid and isoflavonoid synthesis that plays a role in abiotic and biotic stress responses in soybean; phenylpropanoids and isoflavonoids function as antioxidants for ROS homeostasis (Dastmalchi *et al.*, 2016). “Phenylpropanoid biosynthesis” was indeed the most enriched KEGG pathway in both NIL-T and NIL-S in response to salt stress (Fig. 4). The

ER localisation of GmIFS2 provides a possible connection with GmSALT3, also an ER-localised membrane protein (Guan *et al.*, 2014).

NaCl can induce conformational change of cytochrome P450 in animals (Oyekan *et al.*, 1999; Yun *et al.*, 1996), but this has not been investigated in plants. A group of genes (639 genes) were clustered as more highly expressed in NIL-T and NIL-S after 3 days' salt treatment, and even more highly expressed in NIL-T compared to NIL-S (Fig. 6b). These genes are most enriched in the GO term "heme binding (GO: 0020037)" (Fig. 6b). Plant CYP P450 enzymes contain heme as a cofactor, and have a conserved motif of 10 amino acids for the heme binding site (FGAGRRICPG) (Saxena *et al.*, 2013). This motif could facilitate the binding of heme iron to the CYP P450 monooxygenases (Gribskov *et al.*, 1987). GmIFS2 involves this conserved motif (Supplementary Fig. 9), therefore, the 639 genes enriched in heme binding GO term could be, in part related to the potential greater activity of GmIFS2 requiring more heme to be active.

Ions (Na^+ and Cl^-) begin to accumulate in NIL-S leaves after 3 days NaCl treatment (Liu *et al.*, 2016). In KEGG enrichment analysis, NIL-S roots had a quicker salt-stress response compared to NIL-T, with generally more DEGs found in each enriched pathway at 6h (Fig. 4a); however, at 3d, NIL-T showed more DEGs in each enriched pathway (Fig. 4b). This suggests that *GmSALT3* contributes to NIL-T salinity tolerance from roots in a longer term (3 days), but not instantly from salt was applied.

One possible mechanism in NIL-T salinity tolerance is through restricting the expression of the putative CNGC (Cyclic Nucleotide-Gated ion Channel) in the "Plant-pathogen interaction" pathway (Fig. 4). This channel is predicted to allow Ca^{2+} signal transport across the plasma membrane into cytoplasm (Ma *et al.*, 2009), with the subsequent Ca^{2+} cascades activating CDPK (Calcium-Dependent Protein Kinase 3, *Glyma.08G019700*) and Rboh (Respiratory Burst Oxidase Homolog protein F-like isoform 1, *Glyma.01G222700*), which ultimately results in higher ROS production and hypersensitive response in NIL-S (Fig. 4a, c). Several CaM (Calmodulin) and CML (Calmodulin-like) genes are down-regulated in 3d T which may restrict NO (Nitric Oxide) production, which is a gaseous reactive oxygen species

(ROS) in plants (Ma and Berkowitz, 2011). Interestingly, NO was also shown to be able to induce conformational change of cytochrome P450 in animals (Oyekan *et al.*, 1999). Another noteworthy change was that at 6h, *Glyma16G218300*, another CNGC 20-like gene, was significantly up-regulated in NIL-T which results in higher expression of Rhob and CaM/CML. This could be because ROS work as signalling molecules when plant roots are suddenly exposed to salt, and decrease stomatal conductance to avoid excessive water loss (Abogadallah, 2010). Significantly higher scavenging enzyme activity of the superoxide anion (O_2^-) in NIL-T roots supports that *GmSALT3* is related to ROS detoxification (Fig. 7b). However, ROS concentration (H_2O_2) has no difference between NIL-T and NIL-S under salt treatment (Fig. 7a). But other ROS content, such as superoxide and singlet oxygen, could be different and so need to be measured.

Another RNA-seq was performed using the same NIL-T and NIL-S soybean cultivars but grown in an alternative location (Adelaide, Australia compared to Beijing, China for the first run), and later salt treatment at 14 DAS (compared to 10 DAS for the first run). Soybean root samples were harvested prior to and after 200 mM NaCl treatment for 3 days and equivalent control plants (Supplementary Fig. 10a). There was little overlap between the identity of the DEGs between RNAseq run 1 and 2 (Supplementary Fig. 11a) but GO analysis shows that uniquely up-regulated DEGs in NIL-T were also enriched in oxidation-reduction related and heme binding GO terms (Supplementary Fig. 11b; 11c), which emphasises the likely role of ROS management in the salt tolerance phenotype observed in NIL-T.

Plants have adaptations to salinity stress in many pathways, ROS detoxification has shown to be an important cellular mechanism of salt tolerance in many crops (Dong *et al.*, 2013; Munns and Gilliham, 2015; Munns and Tester, 2008; Roy *et al.*, 2014). In the present study, RNA-seq analysis was used to compare transcriptomic responses between NIL-T and NIL-S under salinity stress. To summarize, it is proposed that GmSALT3 improves the salinity tolerance of NIL-T through various ROS detoxification mechanisms, such as induced phenylpropanoid and isoflavonoid biosynthesis by higher expression of GmIFS2; reduced

expression of the putative CNGC to restrict Ca^{2+} signal transporting across plasma membrane into cytoplasm and ultimately restricting production of ROS and NO.

Materials and methods

Plant growth conditions and stress treatments

NIL-T (Salt-tolerant, *GmSALT3*) and NIL-S (Salt-sensitive, *Gmsalt3*) plants were grown in a growth chamber (RXZ-500D; Ningbo Jiangnan Instrument, China), with a day length of 16 h (with a light-emitting diode light source at 400 μmol m^{-2} s^{-1}) at 28 ˚C, and 8 h dark at 25 ˚C, with 60% relative humidity throughout. Soybean seedlings were treated with 200 mM NaCl (salt treatment) or water (control) at 10 days after sowing (DAS). 200 mM NaCl or water were applied again at 12 DAS.

Total RNA extraction and RNA-seq library construction

Total RNA was extracted from soybean roots using TRIZOL reagent (Ambion, http://www.ambion.com). Root samples were harvested from three time points, 0h, 6h, and 3d of a 200 mM salt-treatment with the corresponding non-treatment controls. To remove the residual DNA, the extracted RNA was treated with RNase-free DNase I (New England Biolabs, https://www.neb.com) for 30 min at 37°C. Thirty RNA libraries were generated for paired-end reads using an Illumina HiSeq 2500 sequencer, consisting of 3 biological samples per time point per genotype.

RNA-seq data analysis and assembly

Raw reads were generated and mapped to the latest soybean genome sequence Gmax_275 Wm82.a2.v1 (Glyma 2.0) using TopHat2 (Kim *et al.*, 2013). Clean mapped reads were obtained by removing low quality (Q<30) sequences, adapter fragments and barcode sequences. Combined with quality control test by fastQC (Andrews, 2010), the quality of RNA-seq libraries construction and sequence alignment was deemed sufficient for further analysis.

Gene expression level and DEG analysis

Gene expression was compared in FPKMs (Fragments Per Kilobase of transcript per Million) calculated using the Cufflinks functions cuffquant and cuffnorm (Trapnell *et al.*, 2012). Differential expression analysis of two conditions/groups was performed using the DESeq R package (1.10.1). The resulting P values were adjusted using the Benjamini and Hochberg's approach for controlling the false discovery rate. The cut-offs for differentially expressed genes (DEGs) were Log_2FC (fold change) ≥ 1, FDR (False Discover Rate) < 0.01.

GO enrichment and KEGG pathway analysis

GO enrichment analysis of DEGs was implemented using AgriGO (Du *et al.*, 2010). GO terms with corrected *p* values < 0.05 were deemed significantly enriched. KEGG (Kanehisa *et al.*, 2007) is a database resource for understanding high-level functions and utilities of the biological system, such as the cell, the organism and the ecosystem, from molecular-level information, especially large-scale molecular datasets generated by genome sequencing and other high-throughput experimental technologies (http://www.genome.jp/kegg/). We used KOBAS (Mao *et al.*, 2005) software to test the statistical enrichment of differential expression genes in KEGG pathways.

ROS contents measurement

ROS contents in soybean root samples were measured using Amplex® UltraRed reagent (Invitrogen, USA). Sodium phosphate buffer (0.5 ml 50 mM pH 7.4) was added to 0.1g soybean powder, after mixing and solubilisation, samples were set on ice for 5 min. Then tubes were centrifuged at 12 x 1000 g for 20 min. 500 µl supernatant was transferred into new tubes. An equal volume of 2:1 (v/v) chloroform : methanol was added and centrifuged at 12 x 1000 g for 5 min. 50 µl aqueous phase was took from each sample and add into each well of 96-well microplate. 50 µl working solution (freshly made) was added into each well. Plate was

incubated at 25 °C for 30 min (protect from light). Reactive fluorescence was measure at 540/590 nm.

Scavenging activity of the superoxide anion (O_2^-) assay

The scavenging activity assay was adapted from Pi *et al.* (2016) with slight modifications. Less root homogenate (0.1 g) was used for measurement. Antioxidant enzymes were extracted with 2 ml of 0.05 M phosphate buffer (pH5.5) from 0.1 g root homogenate. The extract was then centrifuged at 12,000 x g (4 ℃) for 10 min. Supernatant (40 ul) was added into 160 ul reaction buffer, which contains 80 ul phosphate buffer, 40 ul 0.05 M guaiacol (Sigmal, US), 40 ul 2% hydrogen peroxide (H_2O_2). The increased absorbance at 470 nm in 96-well plates due to the enzyme-dependent guaiacol oxidation was recorded every 30s until 4 min of reaction.

Real-time quantitative reverse-transcription polymerase chain reaction (RT-qPCR) validation for RNA-seq results

Total RNA was extracted from soybean root tissues using TRIZOL reagent (Ambion, http://www.ambion.com). To remove the residual DNA, the extracted RNA was treated with RNase-free DNase I (New England Biolabs, https://www.neb.com) for 30 min at 37°C. For gene expression, first-strand cDNA synthesis was done with a PrimeScript RT Reagent Kit (TaKaRa, Japan, http://www.takara.co.jp/english). Real-time PCR was performed using SYBR Premix Ex Taq II (TliRNaseH Plus) (TaKaRa). The level of *GmSALT3* transcript was normalised using the control gene *GmUKN1* (Hu *et al.*, 2009).

Figures

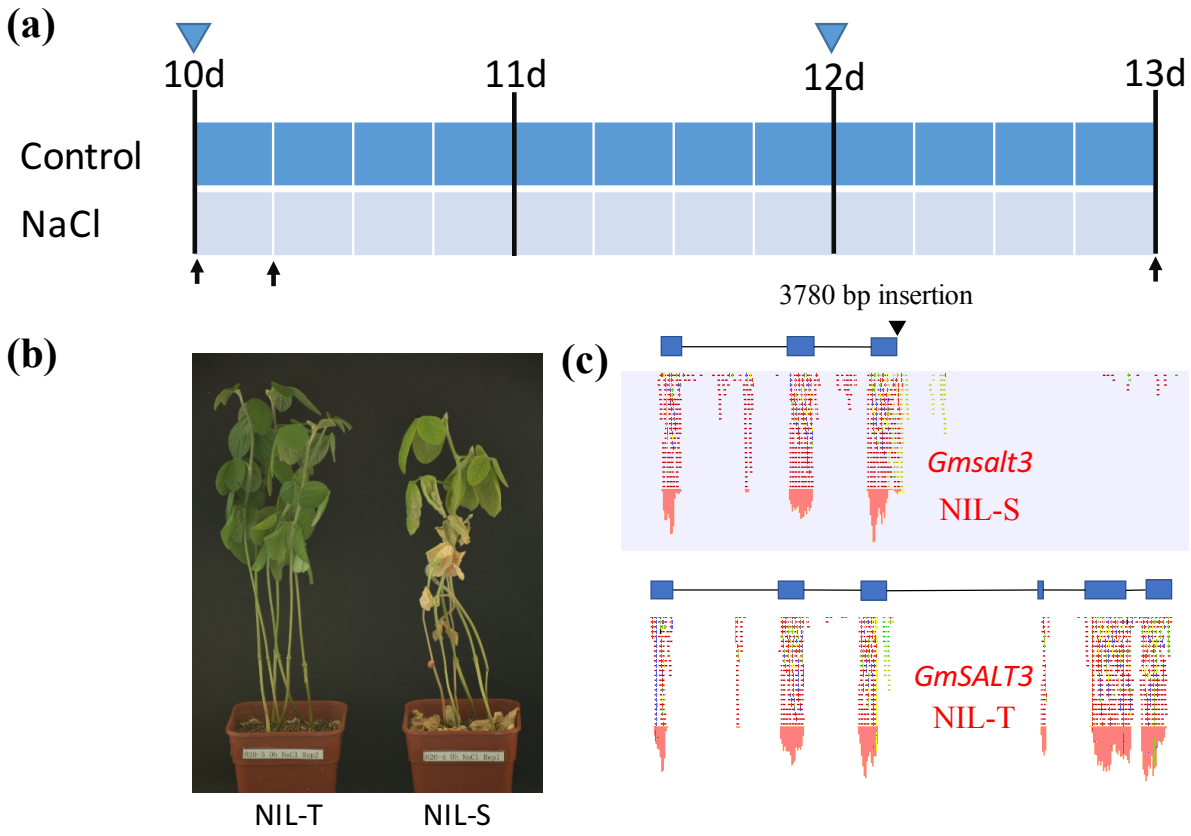

Fig 1. Treatment and sampling strategy. (a) Soybean seedlings were treated with 200 mM NaCl (salt treatment) or water (control) at 10 days after sowing (DAS). Arrows mean the sampling time points (0h, 6h, 3d), triangle indicated the time point when water or NaCl solution was applied. (b) Pictures of soybean that had been treated with NaCl solution for 11 days. (c) Mapped-reads to *GmSALT3* (bottom) and *Gmsalt3* (above). NIL-T, NIL with *GmSALT3* allele; NIL-S, NIL with *Gmsalt3* allele.

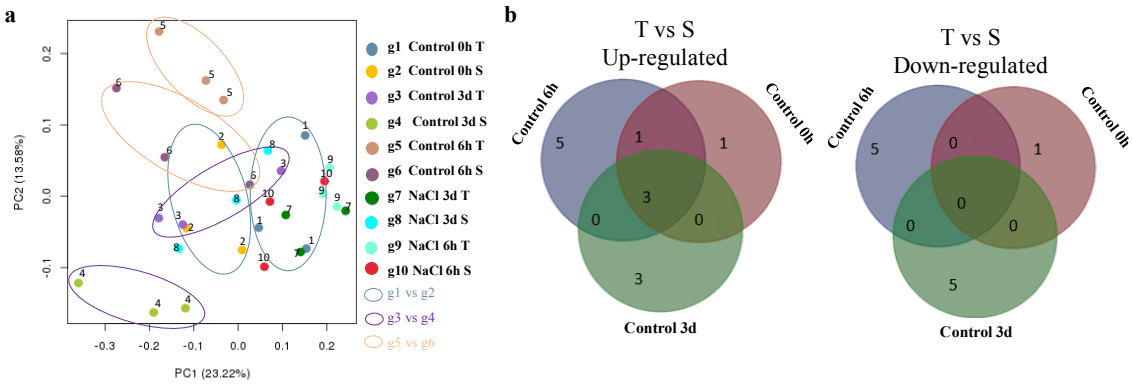

c

Gene ID	Annotation	GO terms	Arabidopsis homolog	Arabidopsis annotation
Glyma.07G196800	BPREDICTED: linoleate 13S-lipoxygenase 3-1, chloroplastic-like [Glycine max]	Biological BProcess: fatty acid biosynthetic process (GO:0006633); Cellular Component: chloroplast (GO:0009507); Molecular Function: oxidoreductase activity, acting on single donors with incorporation of molecular oxygen, incorporation of two atoms of oxygen (GO:0016702);metal ion binding (GO:0046872).	At1g17420	Lipoxygenase 3
Glyma.10G143600	BPREDICTED: uncharacterized protein LOC100780872 [Glycine max]	--	At2g37860	BProtein of unknown function. Mutants have pale leaves, lower cell density
Glyma.20G105500	BPREDICTED: 3-hydroxybenzoate 6-hydroxylase 1-like [Glycine max]	Molecular Function: monooxygenase activity (GO:0004497); oxidoreductase activity (GO:0016491); Biological BProcess: response to stress (GO:0006950); response to abiotic stimulus (GO:0009628) ; cellular metabolic process (GO:0044237); single-organism metabolic process (GO:0044710) ; oxidation-reduction process (GO:0055114). Cellular Component: chloroplast (GO:0009507); response to abiotic stimulus (GO:0009628).	At5g05320	FAD/NAD(BP)-binding oxidoreductase family protein

Fig 2. Overview of DEGs between NIL-T salt-tolerant and NIL-S salt-sensitive soybean samples at the 0h, 6h, and 3d timepoints under non-saline conditions. a PCA plot of ten groups (g1 – g10). Different colored dots represent replicates in each group, different colored circles represent comparisons between groups (g1 vs g2, g3 vs g4, g5 vs g6). **b** Venn diagram of up- and down-regulated DEGs in NIL-S soybeans at 0h, 6h, and 3d under control conditions. **c** Three up-regulated DEGs in NIL-S soybeans at all 0h, 6h, and 3d under control conditions. The cutoffs for DEGs are Log_2FC (fold change) ≥ 1, FDR (False Discover Rate) < 0.01.

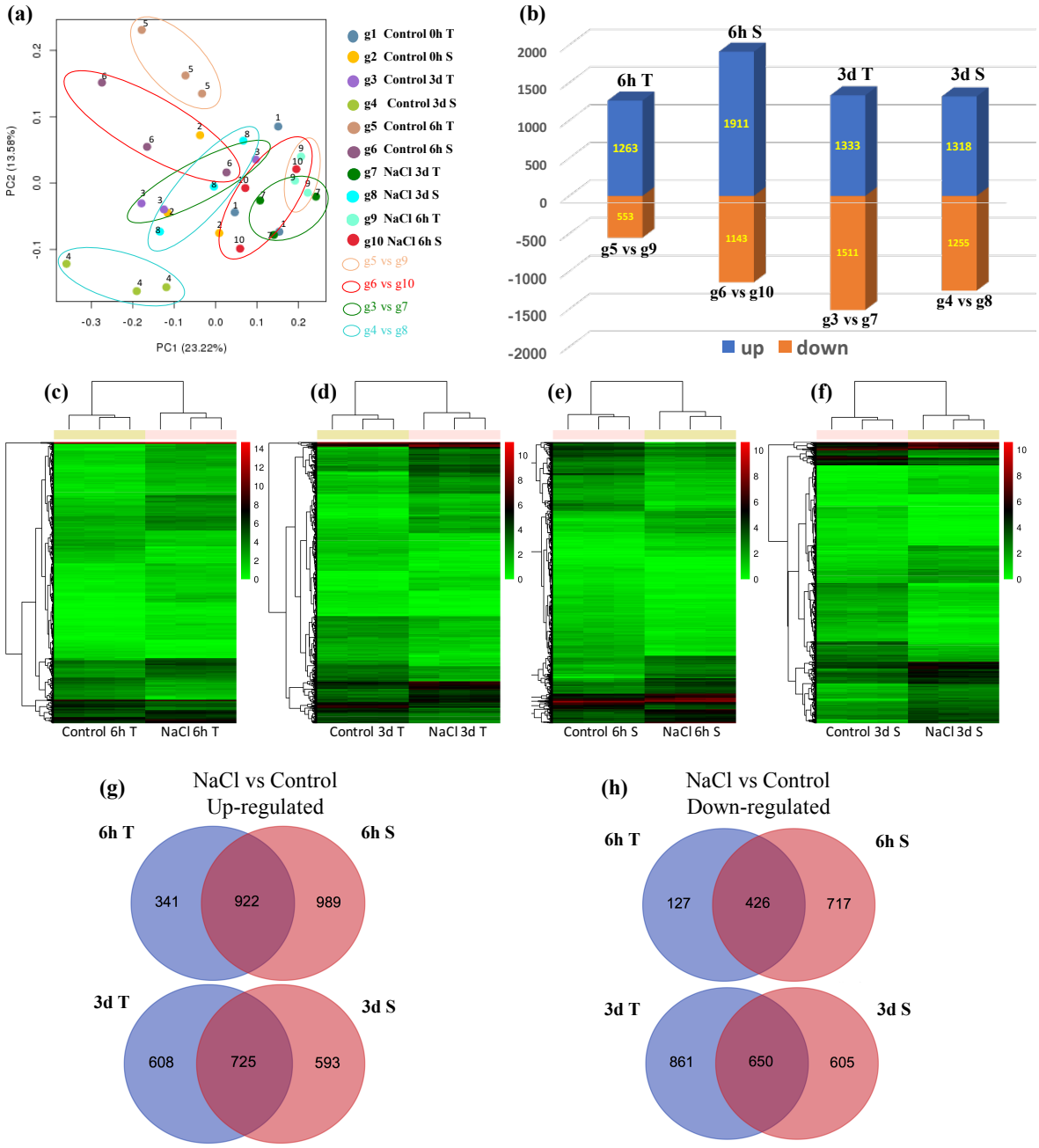

Fig 3. Overview of DEGs (differentially expressed genes) between salt-stressed and control samples in NIL-T and NIL-S soybeans at 6h and 3d. (a) PCA plot of ten groups (g1 – g10). Different colored dots represent replicates in each group, different colored circles represent comparisons between groups (g5 vs g9, g6 vs g10, g3 vs g7, g4 vs g8). (b) Numbers of DEGs (up- and down-regulated) between groups. Clustering of DEGs in FPKMs (Fragments Per Kilobase of transcript per Million) of group 3 to 10 (c-f). The false colour scale from green through to red indicates increasing FPKM. (g) Venn diagram of up-regulated DEGs in NIL-T and NIL-S soybeans at 6h and 3d under NaCl treatment. (h) Venn diagram of down-regulated

DEGs in NIL-T and NIL-S soybeans at 6h and 3d under NaCl treatment. The cut-offs for DEGs are Log_2FC (fold change) ≥ 1, FDR (False Discover Rate) < 0.01.

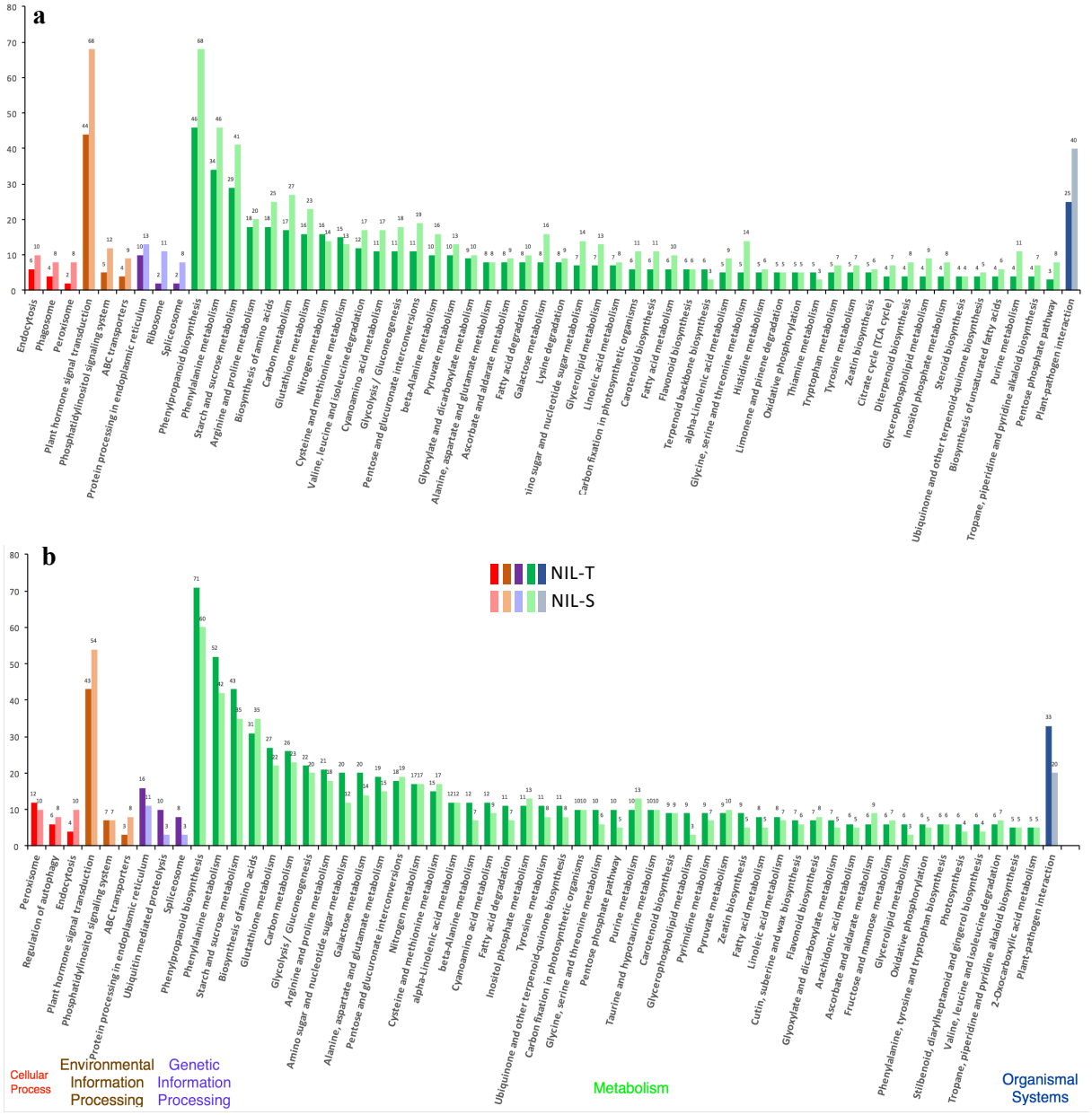

Fig 4. Significantly enriched KEGG (Kyoto Encyclopedia of Genes and Genomes) of all DEGs between salt-stressed and control samples in NIL-T and NIL-S soybeans. a 6h KEGG enrichment. **b** 3d KEGG enrichment. KEGG enrichment P-value cut-off ≤ 0.05.

a

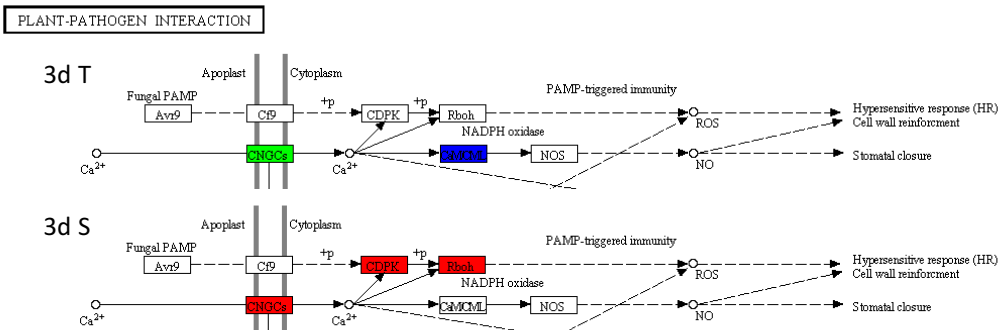

b

CNGCs

ID	log2FC	KEGG_annotation	nr_annotation
Glyma.13G141000	-1.789326976	K05391|0|gmx:100804375|putative cyclic nucleotide-gated ion channel 15-like; K05391 cyclic nucleotide gated channel, other eukaryote (A)	PREDICTED: putative cyclic nucleotide-gated ion channel 15-like [Glycine max]

CaMCML

ID	log2FC	KEGG_annotation	nr_annotation
Glyma.06G034700	2.642449026	K13448|1.35667e-133|gmx:100775336|probable calcium-binding protein CML41-like; K13448 calcium-binding protein CML (A)	PREDICTED: probable calcium-binding protein CML41-like [Glycine max]
Glyma.16G214500	-1.564534966	K02183|0|gmx:100820100|TMV resistance protein N-like; K02183 calmodulin (A)	R 9 protein [Glycine max]
Glyma.02G245700	-1.260414361	K13448|5.94526e-96|gmx:100796491|probable calcium-binding protein CML18-like; K13448 calcium-binding protein CML (A)	PREDICTED: probable calcium-binding protein CML27-like [Glycine max]
Glyma.10G178400	-1.36674556	K13448|3.10298e-102|gmx:547787|SCAM-4; calmodulin (EC:2.7.11.19); K13448 calcium-binding protein CML (A)	calmodulin [Glycine max]
Glyma.13G316100	-1.167992691	K13448|1.40322e-131|gmx:100305637|uncharacterized LOC100305637; K13448 calcium-binding protein CML (A)	uncharacterized protein LOC100305637 [Glycine max]
Glyma.17G128900	-2.909930613	K13448|1.55086e-80|gmx:100816563|putative calcium-binding protein CML19-like; K13448 calcium-binding protein CML (A)	PREDICTED: probable calcium-binding protein CML31-like [Glycine max]

c

CNGCs

ID	log2FC	KEGG_annotation	nr_annotation
Glyma.09G168700	1.296094487	K05391|0|gmx:100795955|probable cyclic nucleotide-gated ion channel 20, chloroplastic-like; K05391 cyclic nucleotide gated channel, other eukaryote (A)	PREDICTED: probable cyclic nucleotide-gated ion channel 20, chloroplastic-like [Glycine max]

CDPK

ID	log2FC		nr_annotation
Glyma.08G019700	1.004584469	K13412|0|zma:100286149|calcium-dependent protein kinase, isoform 2; K13412 calcium-dependent protein kinase [EC:2.7.11.1] (A)	PREDICTED: LOW QUALITY PROTEIN: calcium-dependent protein kinase 3-like [Glycine max]

Rboh

ID	log2FC		nr_annotation
Glyma.01G222700	1.280334686	K13447|0|gmx:100805517|respiratory burst oxidase homolog protein A-like; K13447 respiratory burst oxidase [EC:1.6.3.- 1.11.1.-] (A)	PREDICTED: respiratory burst oxidase homolog protein F-like isoform 1 [Glycine max]

Fig 5. DEGs between control and salt-treated samples of NIL-T and NIL-S in plant-pathogen interaction KEGG pathway at 3d. a Diagram of plant-pathogen pathway. **b** DEGs of NIL-T. **c** DEGs of NIL-S. Green represents down-regulated genes; Red represents Up-regulated genes; Blue represents mixed-regulated genes.

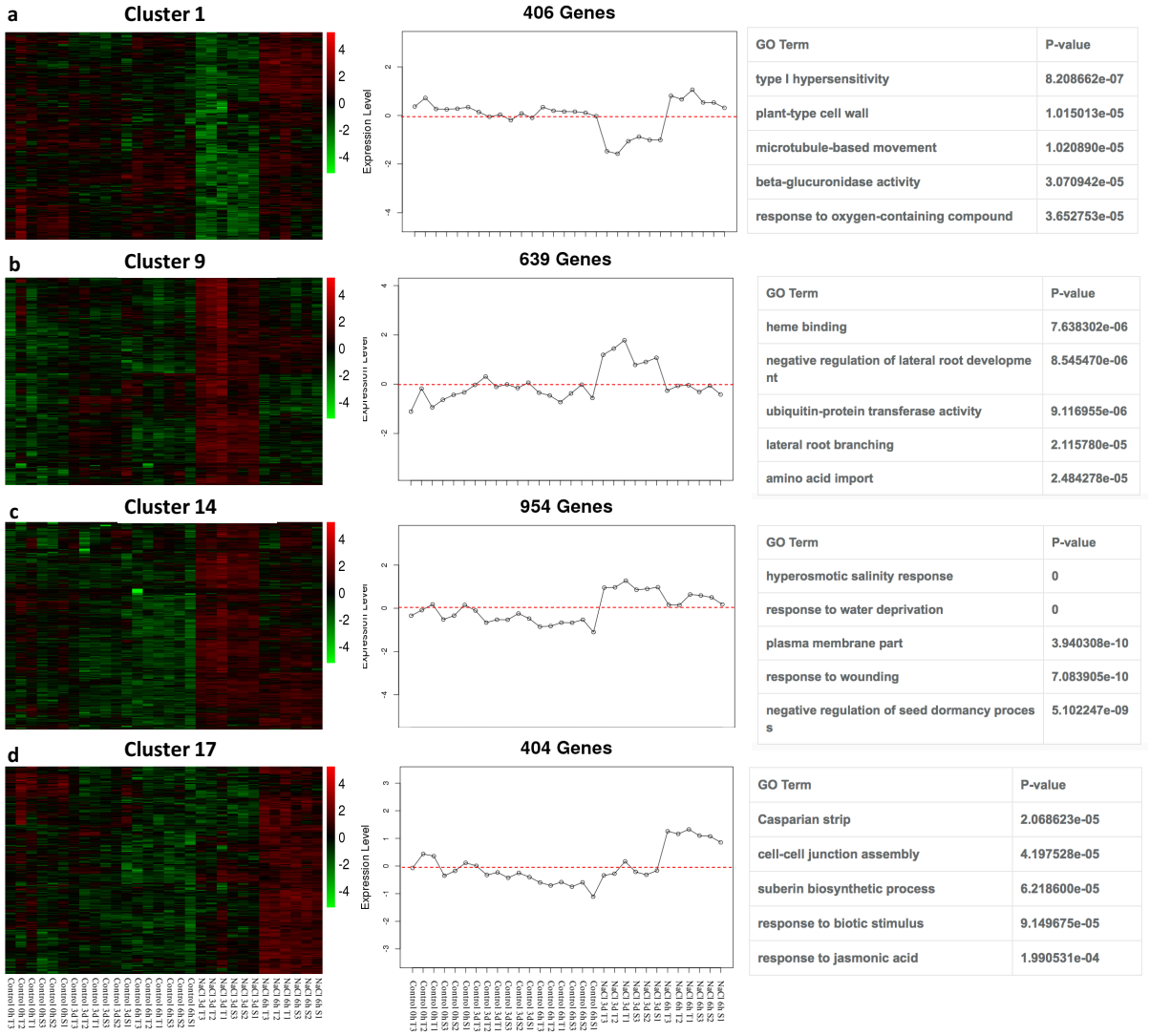

Fig. 6 Clustering of all DEGs in 30 RNA-seq libraries. Top four hierarchical subclusters including cluster 1 (**a**), cluster 9 (**b**), cluster 14 (**c**), and cluster 17 (**d**). Their heatmaps, average gene expression level in each subcluster, and top five enriched GO terms in each subcluster. Different samples are shown on the x-axis and the relative expression level is shown on the y-axis. All subclusters are shown in Supplementary Fig. 8.

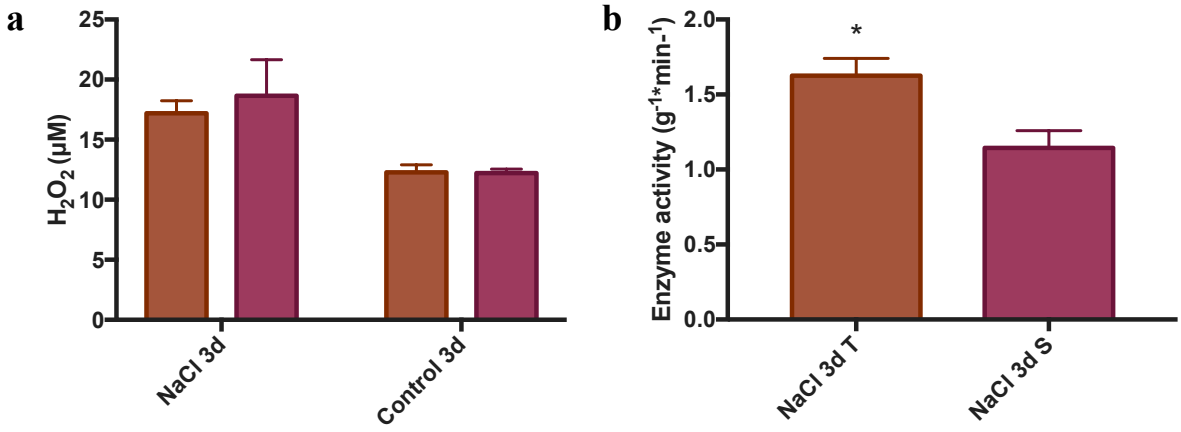

Fig. 7 H_2O_2 concentration and enzyme activity of the superoxide anion (O_2^-) scavenger assay. a H_2O_2 concentration of NIL-T and NIL-S at three days with or without salt treatment. **b** scavenging activity of the superoxide anion (O_2^-) of NIL-T and NIL-S with salt treatment. Asterisk indicates a significant difference between NIL-T (brown) and NIL-S (red) at *P <0.05.

Table 1. Reads mapping and quality of sequencing for 30 *Glycine max* root samples.

Group	Sample	Total Reads	Mapped Reads	Clean reads	Clean bases	GC Content	%≥Q30
g1	Control 0h T1	57,699,406	49,137,608 (85.16%)	28,849,703	7,212,425,750	50.56%	92.05%
	Control 0h T2	59,769,628	51,025,677 (85.37%)	29,884,814	7,471,203,500	52.37%	93.30%
	Control 0h T3	62,070,060	53,862,681 (86.78%)	31,035,030	7,758,757,500	50.01%	93.35%
g2	Control 0h S1	43,642,298	32,134,039 (73.63%)	21,821,149	5,455,287,250	48.70%	88.44%
	Control 0h S2	46,423,344	39,574,288 (85.25%)	23,211,672	5,802,918,000	49.23%	94.08%
	Control 0h S3	56,017,714	43,638,938 (77.90%)	28,008,857	7,002,214,250	50.34%	93.88%
g3	Control 3d T1	48,501,908	42,642,939 (87.92%)	24,250,954	6,062,738,500	48.90%	93.69%
	Control 3d T2	60,432,732	53,220,906 (88.07%)	30,216,366	7,554,091,500	50.86%	94.28%
	Control 3d T3	48,809,732	41,680,164 (85.39%)	24,404,866	6,101,216,500	48.29%	92.51%
g4	Control 3d S1	47,058,528	39,937,443 (84.87%)	23,529,264	5,882,316,000	48.39%	93.58%
	Control 3d S2	48,461,144	40,928,669 (84.46%)	24,230,572	6,057,643,000	47.83%	94.18%
	Control 3d S3	49,796,814	40,986,303 (82.31%)	24,898,407	6,224,601,750	50.35%	94.30%
g5	Control 6h T1	51,648,018	30,700,905 (59.44%)	25,824,009	6,456,002,250	48.37%	84.72%
	Control 6h T2	34,427,522	21,774,315 (63.25%)	17,213,761	4,303,440,250	48.21%	87.04%
	Control 6h T3	84,627,144	55,643,274 (65.75%)	42,313,572	10,578,393,000	48.00%	86.74%
g6	Control 6h S1	62,158,510	50,330,267 (80.97%)	31,079,255	7,769,813,750	48.61%	92.06%
	Control 6h S2	59,768,732	44,180,997 (73.92%)	29,884,366	7,471,091,500	48.12%	89.44%
	Control 6h S3	48,852,622	41,445,404 (84.84%)	24,426,311	6,106,577,750	49.05%	93.76%
g7	NaCl 3d T1	47,478,210	39,318,129 (82.81%)	23,739,105	5,934,776,250	49.12%	93.71%
	NaCl 3d T2	49,524,852	42,007,601 (84.82%)	24,762,426	6,190,606,500	50.44%	94.94%
	NaCl 3d T3	53,918,342	45,880,121 (85.09%)	26,959,171	6,739,792,750	52.93%	93.81%
g8	NaCl 3d S1	55,228,034	45,771,588 (82.88%)	27,614,017	6,903,504,250	47.24%	92.28%
	NaCl 3d S2	57,398,436	46,291,922 (80.65%)	28,699,218	7,174,804,500	48.58%	92.30%
	NaCl 3d S3	58,773,304	47,497,496 (80.81%)	29,386,652	7,346,663,000	48.48%	91.31%
g9	NaCl 6h T1	53,174,654	45,735,099 (86.01%)	26,587,327	6,646,831,750	51.47%	93.56%
	NaCl 6h T2	52,045,484	43,779,481 (84.12%)	26,022,742	6,505,685,500	50.75%	93.30%
	NaCl 6h T3	55,579,826	45,167,976 (81.27%)	27,789,913	6,947,478,250	51.54%	92.62%
g10	NaCl 6h S1	54,197,662	45,095,587 (83.21%)	27,098,831	6,774,707,750	48.34%	92.64%
	NaCl 6h S2	53,274,670	45,180,893 (84.81%)	26,637,335	6,659,333,750	50.44%	92.49%
	NaCl 6h S3	47,601,546	40,826,998 (85.77%)	23,800,773	5,950,193,250	48.16%	94.75%

Table 2. GO term analysis of uniquely up- and down-regulated genes under salt treatment in soybean roots at 6h. (a) Up-regulated genes in NIL-T soybean roots. (b) Up-regulated genes in NIL-S soybean roots. (c) Down-regulated genes in NIL-T soybean roots. (d) Down-regulated genes in NIL-S soybean roots. BP, Biological Process; MF, Molecular Function.

(a)

GO term	Ontology	Description	Number in input list	Number in BG/Ref	p-value	FDR
GO:0009607	BP	response to biotic stimulus	7	64	9.3e-08	2.4e-05
GO:0006952	BP	defense response	7	118	4.4e-06	0.00056
GO:0055114	BP	oxidation reduction	28	2408	6.1e-05	0.0051
GO:0005507	MF	copper ion binding	9	219	3.4e-06	0.00071
GO:0016491	MF	oxidoreductase activity	32	2744	1.5e-05	0.0016
GO:0004866	MF	endopeptidase inhibitor activity	5	92	0.00016	0.0083

(b)

GO term	Ontology	Description	Number in input list	Number in BG/Ref	p-value	FDR
GO:0006355	BP	regulation of transcription, DNA-dependent	69	1874	2e-05	0.0016

(c)

GO term	Ontology	Description	Number in input list	Number in BG/Ref	p-value	FDR
GO:0016021	CC	integral to membrane	11	1419	0.00065	0.0058

(d)

GO term	Ontology	Description	Number in input list	Number in BG/Ref	p-value	FDR
GO:0020037	MF	heme binding	23	728	8e-05	0.012
GO:0009055	MF	electron carrier activity	21	702	0.00033	0.018
GO:0004190	MF	aspartic-type endopeptidase activity	9	169	0.00042	0.018
GO:0015035	MF	protein disulfide oxidoreductase activity	7	96	0.00031	0.018

Table 3. GO term analysis of uniquely up- and down-regulated genes under salt treatment in soybean roots at 3d. (a) Up-regulated genes in NIL-T soybean roots. (b) Up-regulated genes in NIL-S soybean roots. (c) Down-regulated genes in NIL-T soybean roots. (d) Down-regulated genes in NIL-S soybean roots. BP, Biological Process; MF, Molecular Function.

(a)

GO term	Ontology	Description	Number in input list	Number in BG/Ref	p-value	FDR
GO:0055114	BP	oxidation reduction	53	2408	8.9e-06	0.0037
GO:0016491	MF	oxidoreductase activity	57	2744	2e-05	0.0073

(b)

GO term	Ontology	Description	Number in input list	Number in BG/Ref	p-value	FDR
GO:0006355	BP	regulation of transcription, DNA-dependent	51	1874	9.8e-08	3.6e-06
GO:0006468	BP	protein amino acid phosphorylation	45	2356	0.002	0.023
GO:0048544	BP	recognition of pollen	14	135	3.8e-09	3e-07
GO:0015743	BP	malate transport	5	34	0.0001	0.0013

(c)

GO term	Ontology	Description	Number in input list	Number in BG/Ref	p-value	FDR
GO:0007018	BP	microtubule-based movement	17	155	9.8e-09	5.2e-06
GO:0003777	MF	microtubule motor activity	17	155	9.8e-09	2.4e-06
GO:0043531	MF	ADP binding	27	467	2.1e-07	2e-05
GO:0004565	MF	beta-galactosidase activity	6	37	9.5e-05	0.0031
GO:0017171	MF	serine hydrolase activity	17	330	0.00014	0.0041
GO:0009341	CC	beta-galactosidase complex	6	37	9.5e-05	0.009

(d)

GO term	Ontology	Description	Number in input list	Number in BG/Ref	p-value	FDR
GO:0055085	BP	transmembrane transport	29	1167	1.9e-05	0.0075
GO:0022857	MF	transmembrane transporter activity	24	1020	0.00022	0.036

Table 4. Up-regulated genes in oxidation reduction and oxidoreductase activity GO terms of 3 days salt-treated NIL-T roots. Annotations are achieved from https://www.soybase.org/genomeannotation/.

Gmax 2.0 Protein ID	Control 3d T (FPKM)	NaCl 3d T (FPKM)	PFAM_Descriptions	Panther_Descriptions	KOG_Desctiptions
Glyma.13G104100	0.003926	1.178719	Flavin containing amine oxidoreductase	AMINE OXIDASE	Flavin-containing_amine_oxidase
Glyma.01G210400	0.200688	2.578006	alpha/beta C-terminal domain; "lactate/malate dehydrogenase, NAD binding domain"	MALATE AND LACTATE DEHYDROGENASE	Lactate_dehydrogenase
Glyma.11G024100	0.040890	1.424517	Glutathione peroxidase	GLUTATHIONE PEROXIDASE	Glutathione_peroxidase
Glyma.13G173500	71.332430	279.415321	Cytochrome P450	FAMILY NOT NAMED	Cytochrome_P450_CYP2_subfamily
Glyma.02G202500	0.297011	0.974227	Aldehyde dehydrogenase family	ALDEHYDE DEHYDROGENASE-RELATED	Aldehyde_dehydrogenase
Glyma.18G211000	1.800717	5.575660	Peroxidase	NA	NA
Glyma.16G179200	1.461360	2.027147	CobQ/CobB/MinD/ParA nucleotide binding domain	FAMILY NOT NAMED	Predicted_ATPase,_nucleotide-binding
Glyma.06G137000	0.370632	1.164678	2OG-Fe(II) oxygenase superfamily	OXIDOREDUCTASE, 2OG-FE(II) OXYGENASE FAMILY	Iron/ascorbate_family_oxidoreductases
Glyma.14G099000	3.113720	7.206253	Cytokinin dehydrogenase 1, FAD and cytokinin binding; "FAD binding domain "	D-LACTATE DEHYDROGENASE	Proteins_containing_the_FAD_binding_domain
Glyma.16G021200	6.619380	14.499433	Cytochrome P450	FAMILY NOT NAMED	Cytochrome_P450_CYP2_subfamily
Glyma.05G214000	27.504467	64.849500	NAD binding domain of 6-phosphogluconate dehydrogenase	6-PHOSPHOGLUCONATE DEHYDROGENASE	6-phosphogluconate_dehydrogenase
Glyma.11G175900	6.988560	13.550913	Cytochrome P450	FAMILY NOT NAMED	Cytochrome_P450_CYP4/CYP19/CYP26_subfamilies
Glyma.17G225700	1.988862	5.125209	FAD binding domain ; "Cytokinin dehydrogenase 1, FAD and cytokinin binding"	D-LACTATE DEHYDROGENASE	Proteins_containing_the_FAD_binding_domain
Glyma.04G123800	1.602680	3.730430	Alternative oxidase	NA	NA
Glyma.19G123800	0.464332	1.785490	Rubrerythrin	NA	NA
Glyma.08G303800	6.717425	16.957918	Flavin containing amine oxidoreductase	AMINE OXIDASE	Amine_oxidase
Glyma.07G168500	10.873917	21.774467	2OG-Fe(II) oxygenase superfamily	OXIDOREDUCTASE, 2OG-FE(II) OXYGENASE FAMILY	Iron/ascorbate_family_oxidoreductases
Glyma.09G132300	0.903153	1.607179	CobQ/CobB/MinD/ParA nucleotide binding domain	FAMILY NOT NAMED	Predicted_ATPase,_nucleotide-binding
Glyma.01G056100	0.352736	0.825042	2OG-Fe(II) oxygenase superfamily	OXIDOREDUCTASE, 2OG-FE(II) OXYGENASE FAMILY	Iron/ascorbate_family_oxidoreductases
Glyma.18G177000	3.020740	6.342210	Zinc-binding dehydrogenase; "Alcohol dehydrogenase GroES-like domain"	ALCOHOL DEHYDROGENASE RELATED	Alcohol_dehydrogenase,_class_V
Glyma.03G008100	0.296423	0.491798	Cytochrome P450	FAMILY NOT NAMED	Cytochrome_P450_CYP4/CYP19/CYP26_subfamilies
Glyma.05G041200	0.140178	0.587665	Ferric reductase NAD binding domain; "FAD-binding domain"	NADPH OXIDASE	NA
Glyma.03G098600	3.067300	7.794463	Zinc-binding dehydrogenase	ALCOHOL DEHYDROGENASE RELATED	Predicted_NAD-dependent_oxidoreductase
Glyma.17G167200	3.871524	8.781803	FAD dependent oxidoreductase	FAD NAD BINDING OXIDOREDUCTASES	Possible_oxidoreductase
Glyma.17G054500	0.337715	0.774757	FAD binding domain ; "Cytokinin dehydrogenase 1, FAD and cytokinin binding"	GULONOLACTONE OXIDASE	Proteins_containing_the_FAD_binding_domain
Glyma.03G122000	26.622283	34.891684	Cytochrome P450	FAMILY NOT NAMED	Cytochrome_P450_CYP2_subfamily
Glyma.20G169200	30.460700	53.630300	Peroxidase	NA	NA
Glyma.11G185700	6.940457	9.682720	Cytochrome P450	FAMILY NOT NAMED	Cytochrome_P450_CYP4/CYP19/CYP26_subfamilies
Glyma.06G113500	0.626838	1.859539	Pheophorbide a oxygenase; "Rieske [2Fe-2S] domain"	IRON-SULFUR DOMAIN CONTAINING PROTEIN	NA
Glyma.15G071000	14.283107	37.916700	Polyphenol oxidase middle domain; "Common central domain of tyrosinase"	TYROSINASE	NA
Glyma.10G231200	6.984682	16.091238	Fatty acid hydroxylase superfamily	NA	NA
Glyma.10G200800	1.980207	2.714897	Cytochrome P450	FAMILY NOT NAMED	Cytochrome_P450_CYP2_subfamily
Glyma.15G129200	8.068280	20.633733	Peroxidase	NA	NA
Glyma.13G168700	4.586266	11.779662	catalytic domain; "D-isomer specific 2-hydroxyacid dehydrogenase, NAD binding	2-HYDROXYACID DEHYDROGENASE-RELATED	Glyoxylate/hydroxypyruvate_reductase_(D-isomer-
Glyma.10G041800	0.537806	1.160858	Flavin-binding monooxygenase-like	DIMETHYLANILINE MONOOXYGENASE	Flavin-containing_monooxygenase
Glyma.17G015400	4.400850	6.387743	Cytochrome P450	FAMILY NOT NAMED	Cytochrome_P450_CYP2_subfamily
Glyma.19G126000	35.728733	48.534900	Cytochrome P450	FAMILY NOT NAMED	Cytochrome_P450_CYP2_subfamily
Glyma.02G052700	14.152725	29.022591	Peroxidase	NA	NA
Glyma.09G218700	1.588015	2.484951	High-affinity nickel-transport protein	NA	NA
Glyma.06G017900	12.309302	24.021127	Catalase; "Catalase-related immune-responsive"	CATALASE	Catalase
Glyma.12G107000	7.262499	15.171104	Pyridine nucleotide-disulphide oxidoreductase; "Pyridine nucleotide-disulphide	NADH DEHYDROGENASE-RELATED	NADH-dehydrogenase_(ubiquinone)
Glyma.11G149100	0.525827	1.166289	FAD binding domain ; "Cytokinin dehydrogenase 1, FAD and cytokinin binding"	GULONOLACTONE OXIDASE	Proteins_containing_the_FAD_binding_domain
Glyma.20G192200	0.856669	1.672531	lactate/malate dehydrogenase, alpha/beta C-terminal domain; "lactate/malate	MALATE DEHYDROGENASE	Malate_dehydrogenase
Glyma.18G009700	43.848325	60.982450	Glyceraldehyde 3-phosphate dehydrogenase, NAD binding domain	GLYCERALDEHYDE 3-PHOSPHATE	Glyceraldehyde_3-phosphate_dehydrogenase
Glyma.06G302700	12.621392	25.677667	Peroxidase	NA	NA
Glyma.11G122700	29.647954	50.738974	Cytochrome P450	NA	Cytochrome_P450_CYP4/CYP19/CYP26_subfamilies
Glyma.05G207100	36.391806	79.784041	Glutathione peroxidase	GLUTATHIONE PEROXIDASE	Glutathione_peroxidase
Glyma.08G033400	19.221367	37.310567	NAD binding domain of 6-phosphogluconate dehydrogenase	3-HYDROXYISOBUTYRATE DEHYDROGENASE-	Predicted_dehydrogenase
Glyma.20G183100	0.857535	1.409998	FAD dependent oxidoreductase	GLYCEROL-3-PHOSPHATE DEHYDROGENASE	Glycerol-3-phosphate_dehydrogenase
Glyma.02G149900	1.938657	3.676737	2OG-Fe(II) oxygenase superfamily	NA	Uncharacterized_conserved_protein
Glyma.08G226600	1.010831	1.571265	Complex I intermediate-associated protein 30 (CIA30); "NmrA-like family"	NAD DEPENDENT EPIMERASE/DEHYDRATASE	Predicted_dehydrogenase
Glyma.14G205200	91.015528	123.589510	Cytochrome P450	FAMILY NOT NAMED	Cytochrome_P450_CYP2_subfamily
Glyma.15G019300	25.004079	60.218292	Malic enzyme, N-terminal domain; "Malic enzyme, NAD binding domain"	MALIC ENZYME-RELATED	NADP+-dependent_malic_enzyme

References

Abogadallah, G. M. (2010). Insights into the significance of antioxidative defense under salt stress. *Plant Signaling & Behavior* **5**, 369-374.

Aghaei, K., Ehsanpour, A., Shah, A. and Komatsu, S. (2009). Proteome analysis of soybean hypocotyl and root under salt stress. *Amino acids* **36**, 91-98.

Andrews, S. (2010). FastQC: a quality control tool for high throughput sequence data.

Bose, J., Rodrigo-Moreno, A. and Shabala, S. (2014). ROS homeostasis in halophytes in the context of salinity stress tolerance. *Journal of Experimental Botany* **65**, 1241-1257.

Dastmalchi, M., Bernards, M. A. and Dhaubhadel, S. (2016). Twin anchors of the soybean isoflavonoid metabolon: evidence for tethering of the complex to the endoplasmic reticulum by IFS and C4H. *The Plant Journal* **85**, 689-706.

Do, T. D., Chen, H., Hien, V. T. T., Hamwieh, A., Yamada, T., Sato, T., Yan, Y., Cong, H., Shono, M. and Suenaga, K. (2016). Ncl synchronously regulates Na^+, K^+, and Cl^- in soybean and greatly increases the grain yield in saline field conditions. *Scientific Reports* **6**: 19147.

Dong, W., Wang, M., Xu, F., Quan, T., Peng, K., Xiao, L. and Xia, G. (2013). Wheat oxophytodienoate reductase gene TaOPR1 confers salinity tolerance via enhancement of abscisic acid signaling and reactive oxygen species scavenging. *Plant Physiology* **161**, 1217-1228.

Du, Z., Zhou, X., Ling, Y., Zhang, Z. and Su, Z. (2010). agriGO: a GO analysis toolkit for the agricultural community. *Nucleic Acids Research* **38**, W64-W70.

Flowers, T. J., Galal, H. K. and Bromham, L. (2010). Evolution of halophytes: multiple origins of salt tolerance in land plants. *Functional Plant Biology* **37**, 604-612.

Foreman, J., Demidchik, V., Bothwell, J. H., Mylona, P., Miedema, H., Torres, M. A., Linstead, P., Costa, S., Brownlee, C. and Jones, J. D. (2003). Reactive oxygen species produced by NADPH oxidase regulate plant cell growth. *Nature* **422**, 442-446.

Foyer, C. H. and Noctor, G. (2005). Redox homeostasis and antioxidant signaling: a metabolic interface between stress perception and physiological responses. *The Plant Cell* **17**, 1866-1875.

Garg, R., Shankar, R., Thakkar, B., Kudapa, H., Krishnamurthy, L., Mantri, N., Varshney, R. K., Bhatia, S. and Jain, M. (2016). Transcriptome analyses reveal genotype- and developmental stage-specific molecular responses to drought and salinity stresses in chickpea. *Scientific Reports* **6**: 19228.

Ge, Y., Li, Y., Zhu, Y.-M., Bai, X., Lv, D.-K., Guo, D., Ji, W. and Cai, H. (2010). Global transcriptome profiling of wild soybean (*Glycine soja*) roots under $NaHCO_3$ treatment. *BMC Plant Biology* **10**, 153.

Gill, S. S. and Tuteja, N. (2010). Reactive oxygen species and antioxidant machinery in abiotic stress tolerance in crop plants. *Plant Physiology and Biochemistry* **48**, 909-930.

Gilliham, M., Able, J. A. and Roy, S. J. (2017). Translating knowledge about abiotic stress tolerance to breeding programmes. *The Plant Journal* **90**, 898-917.

Goyal, E., Amit, S. K., Singh, R. S., Mahato, A. K., Chand, S. and Kanika, K. (2016). Transcriptome profiling of the salt-stress response in *Triticum aestivum* cv. *Kharchia Local*. *Scientific Reports* **6**.

Gribskov, M., McLachlan, A. D. and Eisenberg, D. (1987). Profile analysis: detection of distantly related proteins. *Proceedings of the National Academy of Sciences* **84**, 4355-4358.

Guan, R., Qu, Y., Guo, Y., Yu, L., Liu, Y., Jiang, J., Chen, J., Ren, Y., Liu, G. and Tian, L. (2014). Salinity tolerance in soybean is modulated by natural variation in *GmSALT3*. *The Plant Journal*. **80**, 937-950.

Guttikonda, S. K., Trupti, J., Bisht, N. C., Chen, H., An, Y.-Q. C., Pandey, S., Xu, D. and Yu, O. (2010). Whole genome co-expression analysis of soybean cytochrome P450 genes identifies nodulation-specific P450 monooxygenases. *BMC Plant Biology* **10**, 243.

Hu, R., Fan, C., Li, H., Zhang, Q. and Fu, Y.-F. (2009). Evaluation of putative reference genes for gene expression normalization in soybean by quantitative real-time RT-PCR. *BMC Molecular Biology* **10**, 93.

Jia, T., An, J., Liu, Z., Yu, B. and Chen, J. (2017). Salt stress induced soybean GmIFS1 expression and isoflavone accumulation and salt tolerance in transgenic soybean cotyledon hairy roots and tobacco. *Plant Cell, Tissue and Organ Culture (PCTOC)* **128**, 469-477.

Kakumanu, A., Ambavaram, M. M., Klumas, C., Krishnan, A., Batlang, U., Myers, E., Grene, R. and Pereira, A. (2012). Effects of drought on gene expression in maize reproductive and leaf meristem tissue revealed by RNA-Seq. *Plant Physiology* **160**, 846-867.

Kanehisa, M., Araki, M., Goto, S., Hattori, M., Hirakawa, M., Itoh, M., Katayama, T., Kawashima, S., Okuda, S. and Tokimatsu, T. (2007). KEGG for linking genomes to life and the environment. *Nucleic Acids Research* **36**, D480-D484.

Kim, D., Pertea, G., Trapnell, C., Pimentel, H., Kelley, R. and Salzberg, S. L. (2013). TopHat2: accurate alignment of transcriptomes in the presence of insertions, deletions and gene fusions. *Genome Biology* **14**, R36.

Lam, H.-M., Xu, X., Liu, X., Chen, W., Yang, G., Wong, F.-L., Li, M.-W., He, W., Qin, N. and Wang, B. (2010). Resequencing of 31 wild and cultivated soybean genomes identifies patterns of genetic diversity and selection. *Nature Genetics* **42**, 1053-1059.

Liu, Y., Yu, L., Qu, Y., Chen, J., Liu, X., Hong, H., Liu, Z., Chang, R., Gilliham, M., Qiu, L. *et al.* (2016). GmSALT3, which confers improved soybean salt tolerance in the field, increases leaf Cl^- exclusion prior to Na^+ exclusion but does not improve early vigor under salinity. *Frontiers in Plant Science* **7**: 1485.

Lu, Y., Lam, H., Pi, E., Zhan, Q., Tsai, S., Wang, C., Kwan, Y. and Ngai, S. (2013). Comparative metabolomics in *Glycine max* and *Glycine soja* under salt stress to reveal the phenotypes of their offspring. *Journal of Agricultural And Food Chemistry* **61**, 8711-8721.

Ma, W. and Berkowitz, G. A. (2011). Ca^{2+} conduction by plant cyclic nucleotide gated channels and associated signaling components in pathogen defense signal transduction cascades. *New Phytologist* **190**, 566-572.

Ma, W., Smigel, A., Verma, R. and Berkowitz, G. A. (2009). Cyclic nucleotide gated channels and related signaling components in plant innate immunity. *Plant Signaling & Behavior* **4**, 277-282.

Mao, X., Cai, T., Olyarchuk, J. G. and Wei, L. (2005). Automated genome annotation and pathway identification using the KEGG Orthology (KO) as a controlled vocabulary. *Bioinformatics* **21**, 3787-3793.

Mittler, R. (2002). Oxidative stress, antioxidants and stress tolerance. *Trends in Plant Science* **7**, 405-410.

Mittler, R., Vanderauwera, S., Gollery, M. and Van Breusegem, F. (2004). Reactive oxygen gene network of plants. *Trends in Plant Science* **9**, 490-498.

Mizutani, M. and Ohta, D. (2010). Diversification of P450 genes during land plant evolution. *Annual Review of Plant Biology* **61**, 291-315.

Munns, R. and Gilliham, M. (2015). Salinity tolerance of crops–what is the cost? *New Phytologist* **208**, 668-673.

Munns, R. and Tester, M. (2008). Mechanisms of salinity tolerance. *Annual Review of Plant Biology* **59**, 651-81.

Neill, S., Desikan, R. and Hancock, J. (2002). Hydrogen peroxide signalling. *Current Opinion in Plant Biology* **5**, 388-395.

Noctor, G. and Foyer, C. H. (1998). Ascorbate and glutathione: keeping active oxygen under control. *Annual Review of Plant Biology* **49**, 249-279.

Overmyer, K., Brosché, M. and Kangasjärvi, J. (2003). Reactive oxygen species and hormonal control of cell death. *Trends in Plant Science* **8**, 335-342.

Oyekan, A., Youseff, T., Fulton, D., Quilley, J. and McGiff, J. (1999). Renal cytochrome P450 ω-hydroxylase and epoxygenase activity are differentially modified by nitric oxide and sodium chloride. *Journal of Clinical Investigation* **104**, 1131.

Pei, Z.-M., Murata, Y., Benning, G., Thomine, S., Klüsener, B., Allen, G. J., Grill, E. and Schroeder, J. I. (2000). Calcium channels activated by hydrogen peroxide mediate abscisic acid signalling in guard cells. *Nature* **406**, 731-734.

Pi, E., Qu, L., Hu, J., Huang, Y., Qiu, L., Lu, H., Jiang, B., Liu, C., Peng, T. and Zhao, Y. (2016). Mechanisms of soybean roots' tolerances to salinity revealed by proteomic and phosphoproteomic comparisons between two cultivars. *Molecular & Cellular Proteomics* **15**, 266-288.

Prakash, A. N., SK Tewari, P. Pushpangadan, Dhan. (2001). Underutilised legumes: potential sources for low-cost protein. *International Journal of Food Sciences and Nutrition* **52**, 337-341.

Qi, X., Li, M. W., Xie, M., Liu, X., Ni, M., Shao, G., Song, C., Kay-Yuen Yim, A., Tao, Y., Wong, F. L. *et al.* (2014). Identification of a novel salt tolerance gene in wild soybean by whole-genome sequencing. *Nature Communications* **5**, 4340.

Qin, J., Gu, F., Liu, D., Yin, C., Zhao, S., Chen, H., Zhang, J., Yang, C., Zhan, X. and Zhang, M. (2013). Proteomic analysis of elite soybean Jidou17 and its parents using iTRAQ-based quantitative approaches. *Proteome Science* **11**, 12.

Roy, S. J., Negrão, S. and Tester, M. (2014). Salt resistant crop plants. *Current Opinion in Biotechnology* **26**, 115-124.

Saxena, A., Singh, P., Yadav, D. K., Sharma, P., Alam, S., Khan, F., Thul, S. T., Shukla, R. K., Gupta, V. and Sangwan, N. S. (2013). Identification of cytochrome P450 heme motif in plants proteome. *Plant Omics* **6**, 1.

Severin, A. J., Woody, J. L., Bolon, Y.-T., Joseph, B., Diers, B. W., Farmer, A. D., Muehlbauer, G. J., Nelson, R. T., Grant, D. and Specht, J. E. (2010). RNA-Seq Atlas of *Glycine max:* a guide to the soybean transcriptome. *BMC Plant Biology* **10**, 160.

Sweetman, C., Wong, D. C., Ford, C. M. and Drew, D. P. (2012). Transcriptome analysis at four developmental stages of grape berry (*Vitis vinifera* cv. Shiraz) provides insights into regulated and coordinated gene expression. *BMC Genomics* **13**, 691.

Toorchi, M., Yukawa, K., Nouri, M.-Z. and Komatsu, S. (2009). Proteomics approach for identifying osmotic-stress-related proteins in soybean roots. *Peptides* **30**, 2108-2117.

Trapnell, C., Roberts, A., Goff, L., Pertea, G., Kim, D., Kelley, D. R., Pimentel, H., Salzberg, S. L., Rinn, J. L. and Pachter, L. (2012). Differential gene and transcript expression analysis of RNA-seq experiments with *TopHat* and *Cufflinks*. *Nature protocols* **7**, 562-578.

Yan, Q., Cui, X., Lin, S., Gan, S., Xing, H. and Dou, D. (2016). GmCYP82A3, a soybean cytochrome P450 family gene involved in the jasmonic acid and ethylene signaling pathway, enhances plant resistance to biotic and abiotic stresses. *PloS one* **11**, e0162253.

Yun, C.-H., Song, M., Ahn, T. and Kim, H. (1996). Conformational change of cytochrome P450 1A2 induced by sodium chloride. *Journal of Biological Chemistry* **271**, 31312-31316.

Supplementary materials

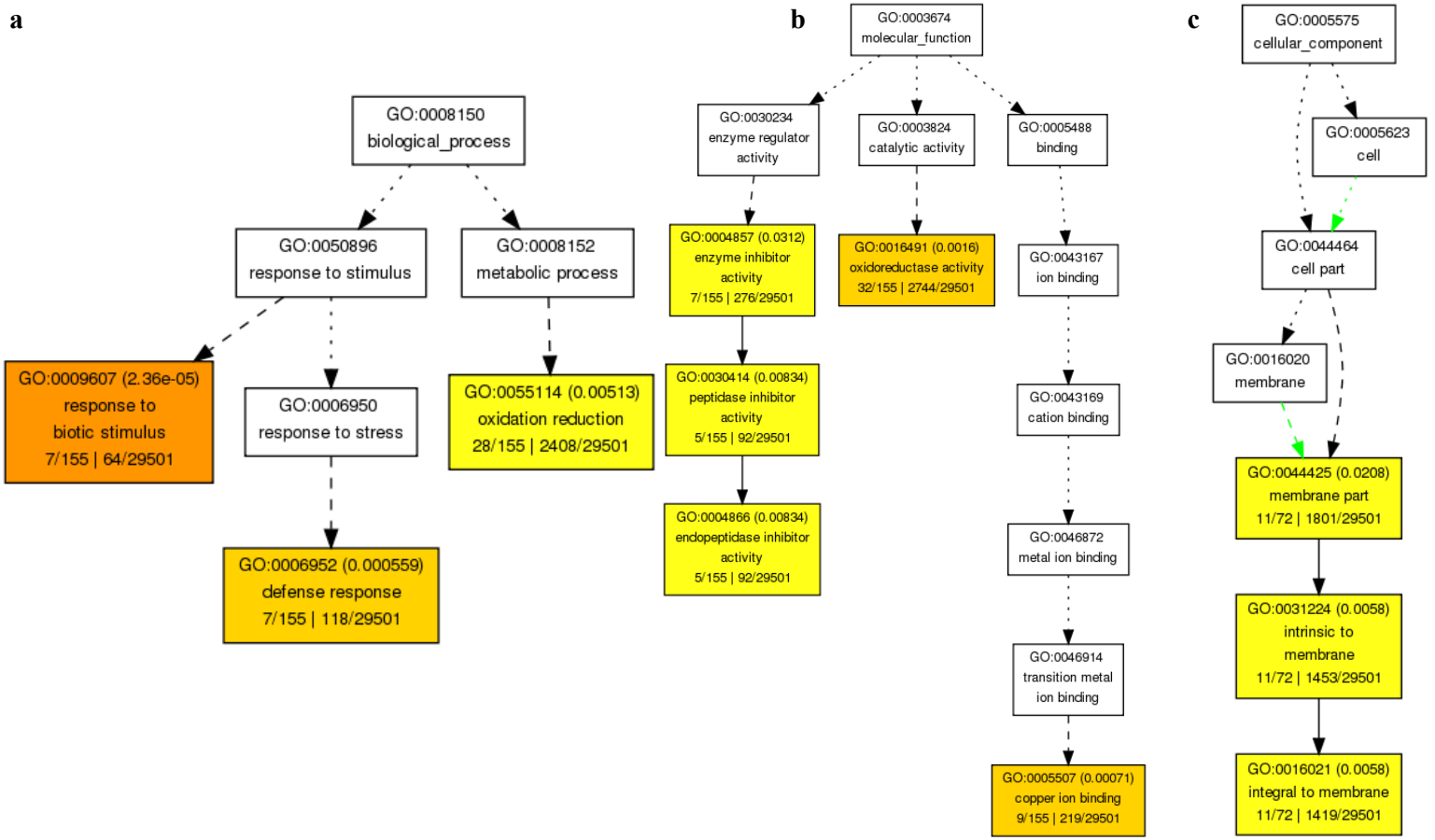

Supplementary Fig. 1 GO term analysis of unique DEGs under salt treatment in NIL-T roots after 6h 200 mM NaCl treatment. **a** Up-regulated GO in biological process. **b** Up-regulated GO in molecular function. **c** Down-regulated GO in cellular component. Darker hues represent higher significance.

a

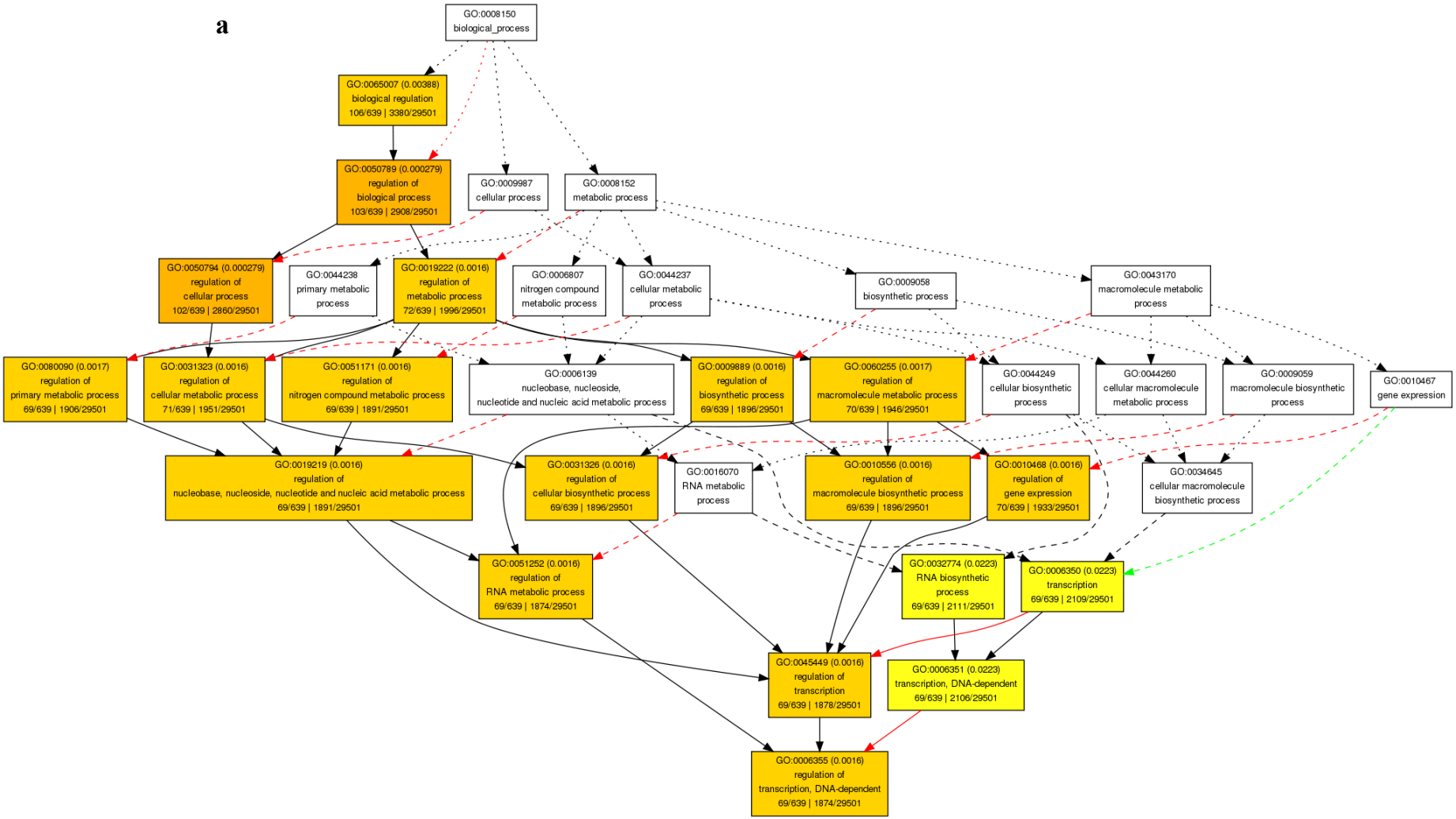
GO:0008150
biological_process
GO:0065007 (0.00388)
biological regulation
106/639 | 3380/29501
GO:0050789 (0.000279)
regulation of
biological process
103/639 | 2908/29501
GO:0009987
cellular process
GO:0008152
metabolic process
GO:0050794 (0.000279)
regulation of
cellular process
102/639 | 2860/29501
GO:0044238
primary metabolic
process
GO:0019222 (0.0016)
regulation of
metabolic process
72/639 | 1996/29501
GO:0006807
nitrogen compound
metabolic process
GO:0044237
cellular metabolic
process
GO:0009058
biosynthetic process
GO:0043170
macromolecule metabolic
process
GO:0080090 (0.0017)
regulation of
primary metabolic process
69/639 | 1906/29501
GO:0031323 (0.0016)
regulation of
cellular metabolic process
71/639 | 1951/29501
GO:0051171 (0.0016)
regulation of
nitrogen compound metabolic process
69/639 | 1891/29501
GO:0006139
nucleobase, nucleoside,
nucleotide and nucleic acid metabolic process
GO:0009889 (0.0016)
regulation of
biosynthetic process
69/639 | 1896/29501
GO:0060255 (0.0017)
regulation of
macromolecule metabolic process
70/639 | 1946/29501
GO:0044249
cellular biosynthetic
process
GO:0044260
cellular macromolecule
metabolic process
GO:0009059
macromolecule biosynthetic
process
GO:0010467
gene expression
GO:0019219 (0.0016)
regulation of
nucleobase, nucleoside, nucleotide and nucleic acid metabolic process
69/639 | 1891/29501
GO:0031326 (0.0016)
regulation of
cellular biosynthetic process
69/639 | 1896/29501
GO:0016070
RNA metabolic
process
GO:0010556 (0.0016)
regulation of
macromolecule biosynthetic process
69/639 | 1896/29501
GO:0010468 (0.0016)
regulation of
gene expression
70/639 | 1933/29501
GO:0034645
cellular macromolecule
biosynthetic process
GO:0051252 (0.0016)
regulation of
RNA metabolic process
69/639 | 1874/29501
GO:0032774 (0.0223)
RNA biosynthetic
process
69/639 | 2111/29501
GO:0006350 (0.0223)
transcription
69/639 | 2109/29501
GO:0045449 (0.0016)
regulation of
transcription
69/639 | 1878/29501
GO:0006351 (0.0223)
transcription, DNA-dependent
69/639 | 2106/29501
GO:0006355 (0.0016)
regulation of
transcription, DNA-dependent
69/639 | 1874/29501

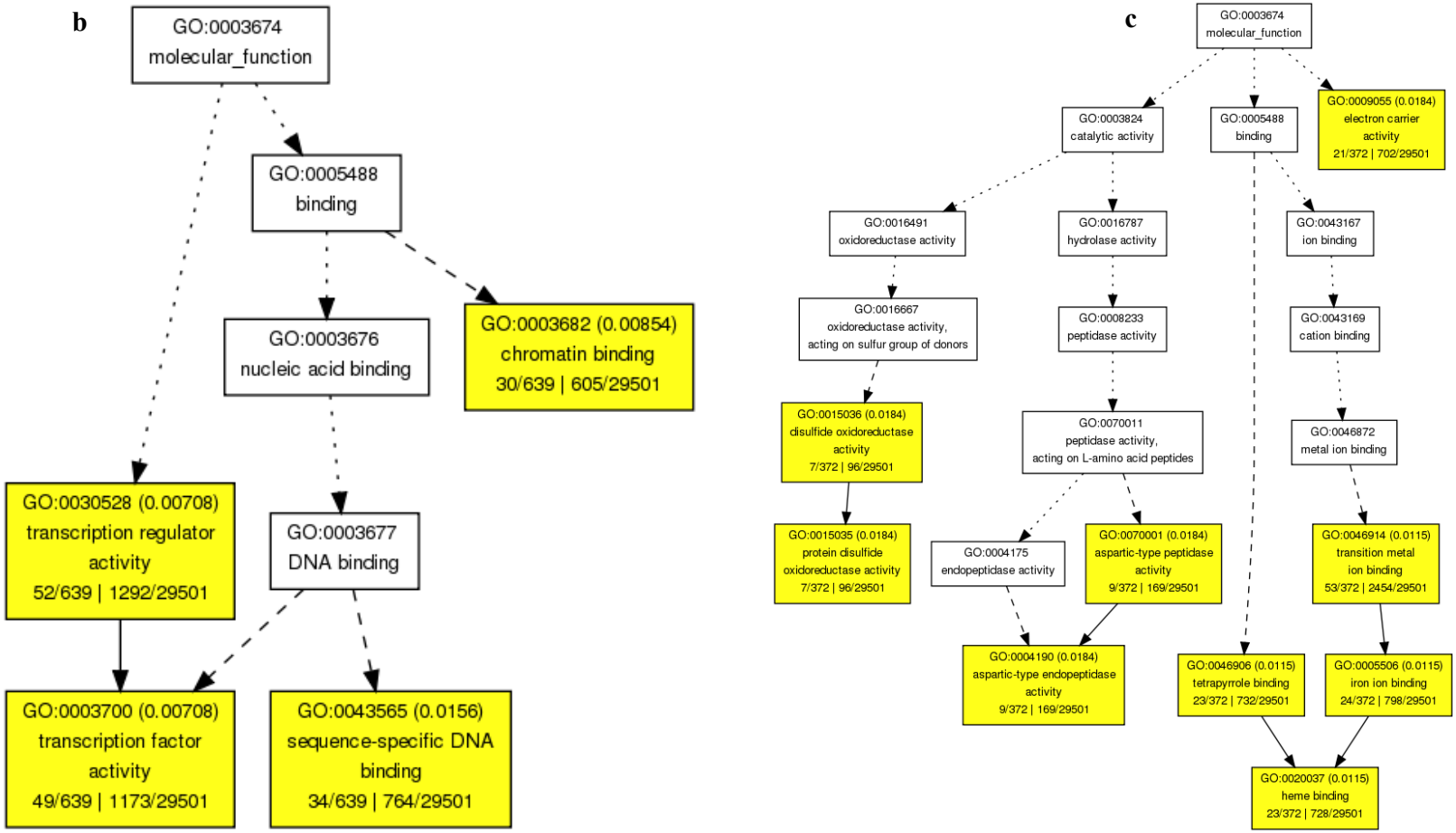

Supplementary Fig. 2 GO term analysis of unique DEGs under salt treatment in NIL-S roots after 6h 200 mM NaCl treatment. (Continued) a Up-regulated GO in biological process. **b** Up-regulated GO in molecular function. **c** Down-regulated GO in molecular function. Darker hues represent higher significance.

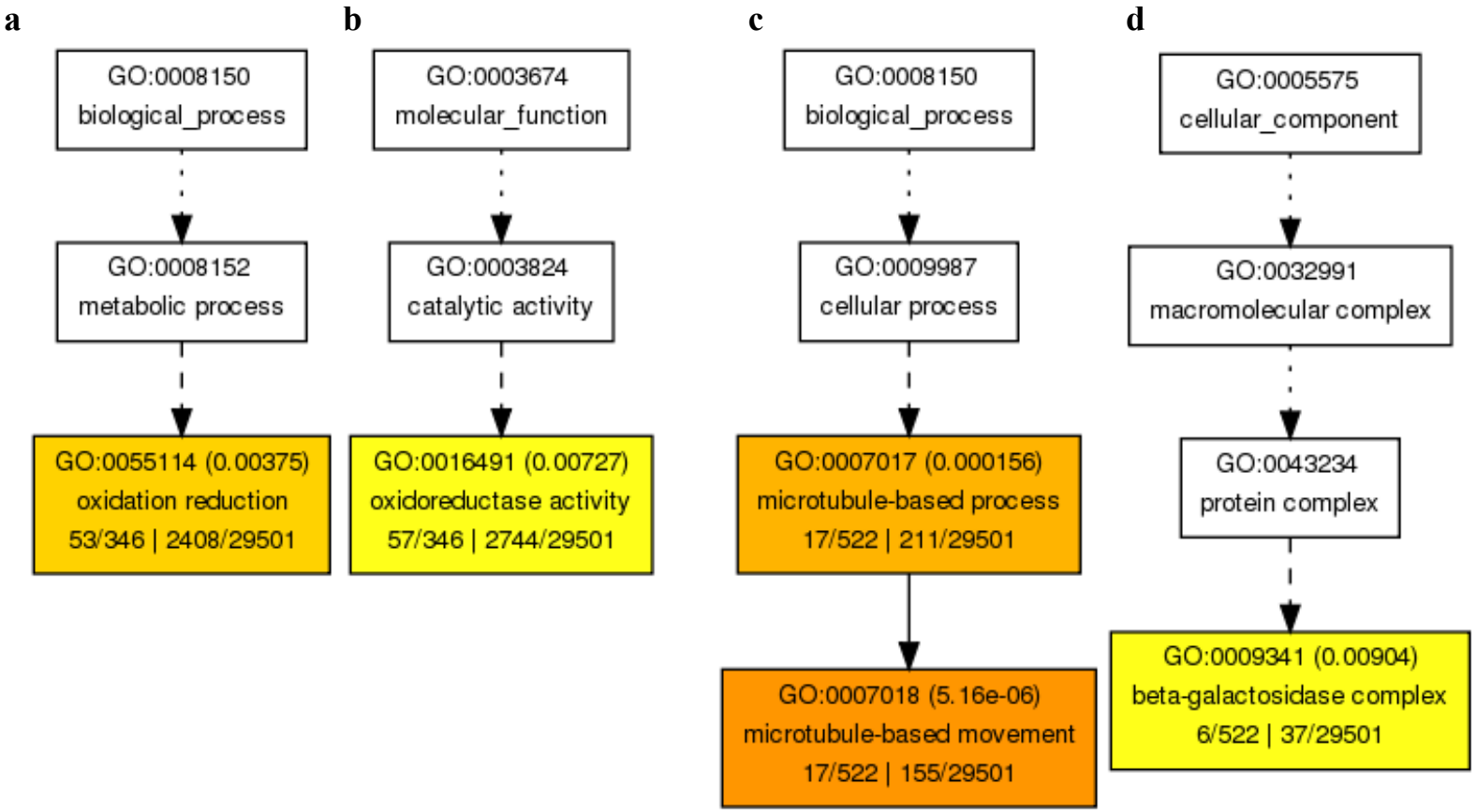
a
GO:0008150
biological_process
GO:0008152
metabolic process
GO:0055114 (0.00375)
oxidation reduction
53/346 | 2408/29501
b
GO:0003674
molecular_function
GO:0003824
catalytic activity
GO:0016491 (0.00727)
oxidoreductase activity
57/346 | 2744/29501
c
GO:0008150
biological_process
GO:0009987
cellular process
GO:0007017 (0.000156)
microtubule-based process
17/522 | 211/29501
GO:0007018 (5.16e-06)
microtubule-based movement
17/522 | 155/29501
d
GO:0005575
cellular_component
GO:0032991
macromolecular complex
GO:0043234
protein complex
GO:0009341 (0.00904)
beta-galactosidase complex
6/522 | 37/29501

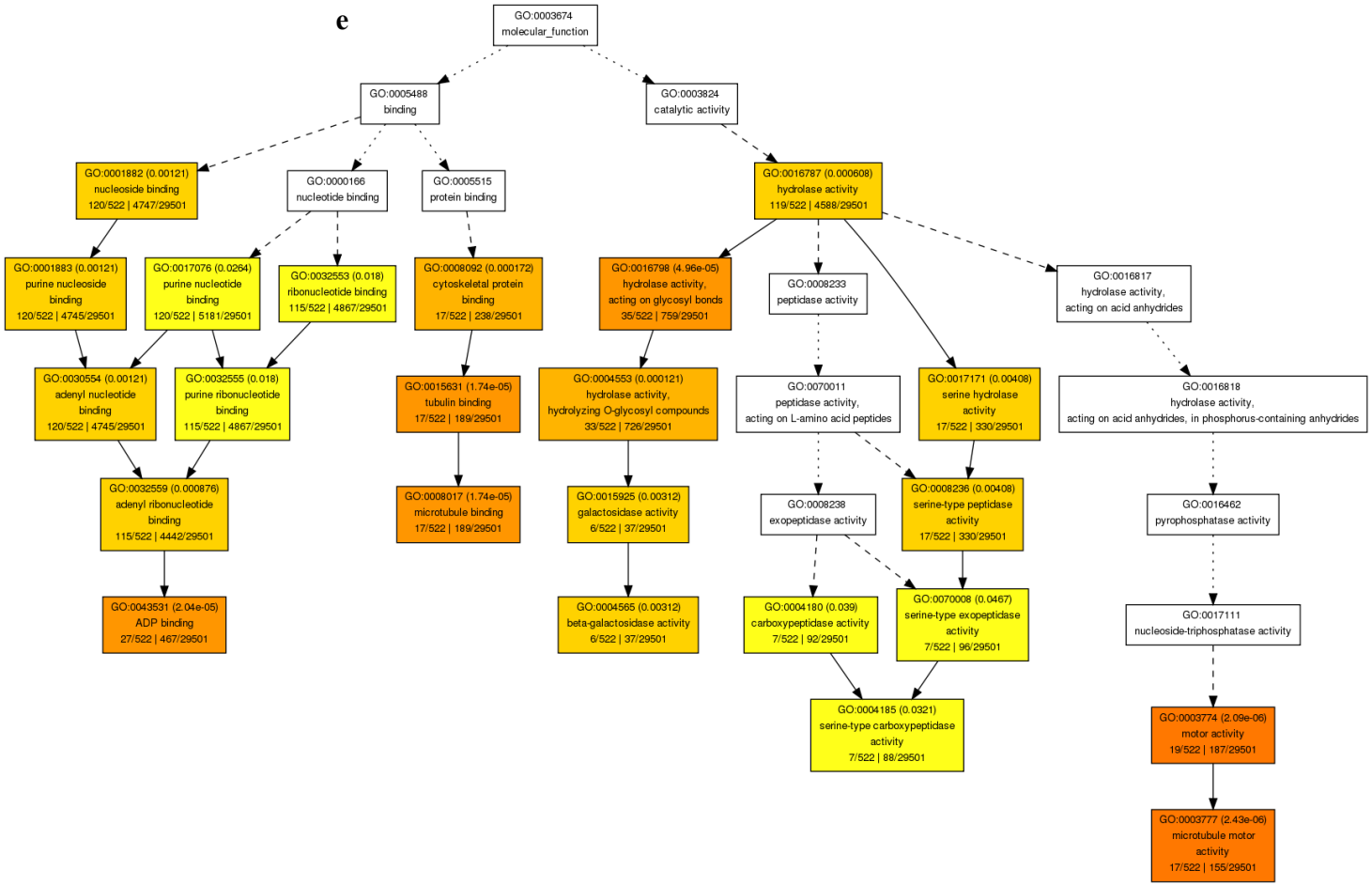

Supplementary Fig. 3 GO term analysis of unique DEGs under salt treatment in NIL-T roots after 3d 200 mM NaCl treatment. (Continued) **a** Up-regulated GO in biological process. **b** Up-regulated GO in molecular function. **c** Down-regulated GO in biological process. **d** Down-regulated GO in cellular component. **e** Down-regulated GO in molecular function. Darker hues represent higher significance.

a

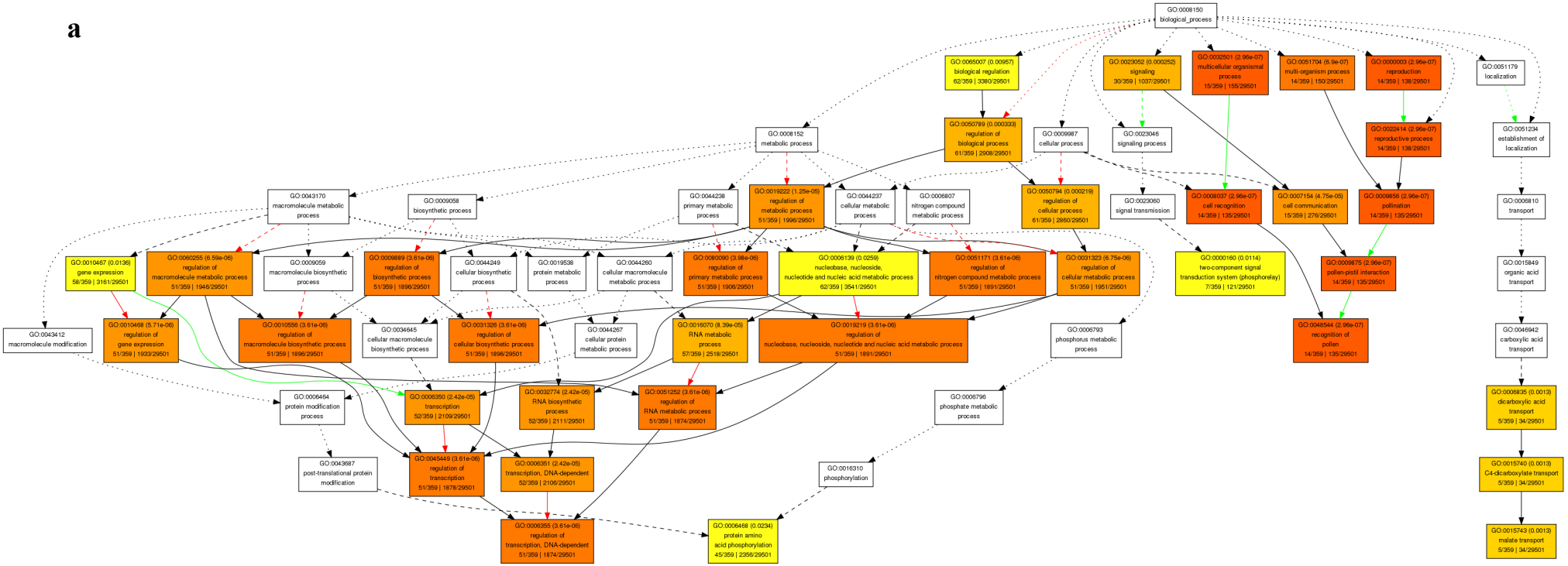
GO:0008150 biological_process
GO:0065007 (0.00957) biological regulation 62/359 | 3380/29501
GO:0023052 (0.000252) signaling 30/359 | 1037/29501
GO:0032501 (2.96e-07) multicellular organismal process 15/359 | 155/29501
GO:0051704 (6.9e-07) multi-organism process 14/359 | 150/29501
GO:0000003 (2.96e-07) reproduction 14/359 | 138/29501
GO:0051179 localization
GO:0050789 (0.000333) regulation of biological process 61/359 | 2908/29501
GO:0008152 metabolic process
GO:0009987 cellular process
GO:0023046 signaling process
GO:0022414 (2.96e-07) reproductive process 14/359 | 138/29501
GO:0051234 establishment of localization
GO:0043170 macromolecule metabolic process
GO:0009058 biosynthetic process
GO:0044238 primary metabolic process
GO:0019222 (1.25e-05) regulation of metabolic process 51/359 | 1996/29501
GO:0044237 cellular metabolic process
GO:0006807 nitrogen compound metabolic process
GO:0050794 (0.000219) regulation of cellular process 61/359 | 2860/29501
GO:0023060 signal transmission
GO:0008037 (2.96e-07) cell recognition 14/359 | 135/29501
GO:0007154 (4.75e-05) cell communication 15/359 | 276/29501
GO:0009856 (2.96e-07) pollination 14/359 | 135/29501
GO:0006810 transport
GO:0010467 (0.0136) gene expression 58/359 | 3161/29501
GO:0062255 (6.59e-06) regulation of macromolecule metabolic process 51/359 | 1946/29501
GO:0009059 macromolecule biosynthetic process
GO:0009889 (3.61e-06) regulation of biosynthetic process 51/359 | 1896/29501
GO:0044249 cellular biosynthetic process
GO:0019538 protein metabolic process
GO:0044260 cellular macromolecule metabolic process
GO:0080090 (3.98e-06) regulation of primary metabolic process 51/359 | 1906/29501
GO:0006139 (0.0259) nucleobase, nucleoside, nucleotide and nucleic acid metabolic process 62/359 | 3541/29501
GO:0051171 (3.61e-06) regulation of nitrogen compound metabolic process 51/359 | 1891/29501
GO:0031323 (6.75e-06) regulation of cellular metabolic process 51/359 | 1951/29501
GO:0000160 (0.0114) two-component signal transduction system (phosphorelay) 7/359 | 121/29501
GO:0009875 (2.96e-07) pollen-pistil interaction 14/359 | 135/29501
GO:0015849 organic acid transport
GO:0043412 macromolecule modification
GO:0010468 (5.71e-06) regulation of gene expression 51/359 | 1933/29501
GO:0010556 (3.61e-06) regulation of macromolecule biosynthetic process 51/359 | 1896/29501
GO:0034645 cellular macromolecule biosynthetic process
GO:0031326 (3.61e-06) regulation of cellular biosynthetic process 51/359 | 1896/29501
GO:0044267 cellular protein metabolic process
GO:0016070 (8.39e-05) RNA metabolic process 57/359 | 2518/29501
GO:0019219 (3.61e-06) regulation of nucleobase, nucleoside, nucleotide and nucleic acid metabolic process 51/359 | 1891/29501
GO:0006793 phosphorus metabolic process
GO:0048544 (2.96e-07) recognition of pollen 14/359 | 135/29501
GO:0046942 carboxylic acid transport
GO:0006464 protein modification process
GO:0006350 (2.42e-05) transcription 52/359 | 2109/29501
GO:0032774 (2.42e-05) RNA biosynthetic process 52/359 | 2111/29501
GO:0051252 (3.61e-06) regulation of RNA metabolic process 51/359 | 1874/29501
GO:0006796 phosphate metabolic process
GO:0006835 (0.0013) dicarboxylic acid transport 5/359 | 34/29501
GO:0043687 post-translational protein modification
GO:0045449 (3.61e-06) regulation of transcription 51/359 | 1878/29501
GO:0006351 (2.42e-05) transcription, DNA-dependent 52/359 | 2109/29501
GO:0016310 phosphorylation
GO:0015740 (0.0013) C4-dicarboxylate transport 5/359 | 34/29501
GO:0006355 (3.61e-06) regulation of transcription, DNA-dependent 51/359 | 1874/29501
GO:0006468 (0.0234) protein amino acid phosphorylation 45/359 | 2356/29501
GO:0015743 (0.0013) malate transport 5/359 | 34/29501

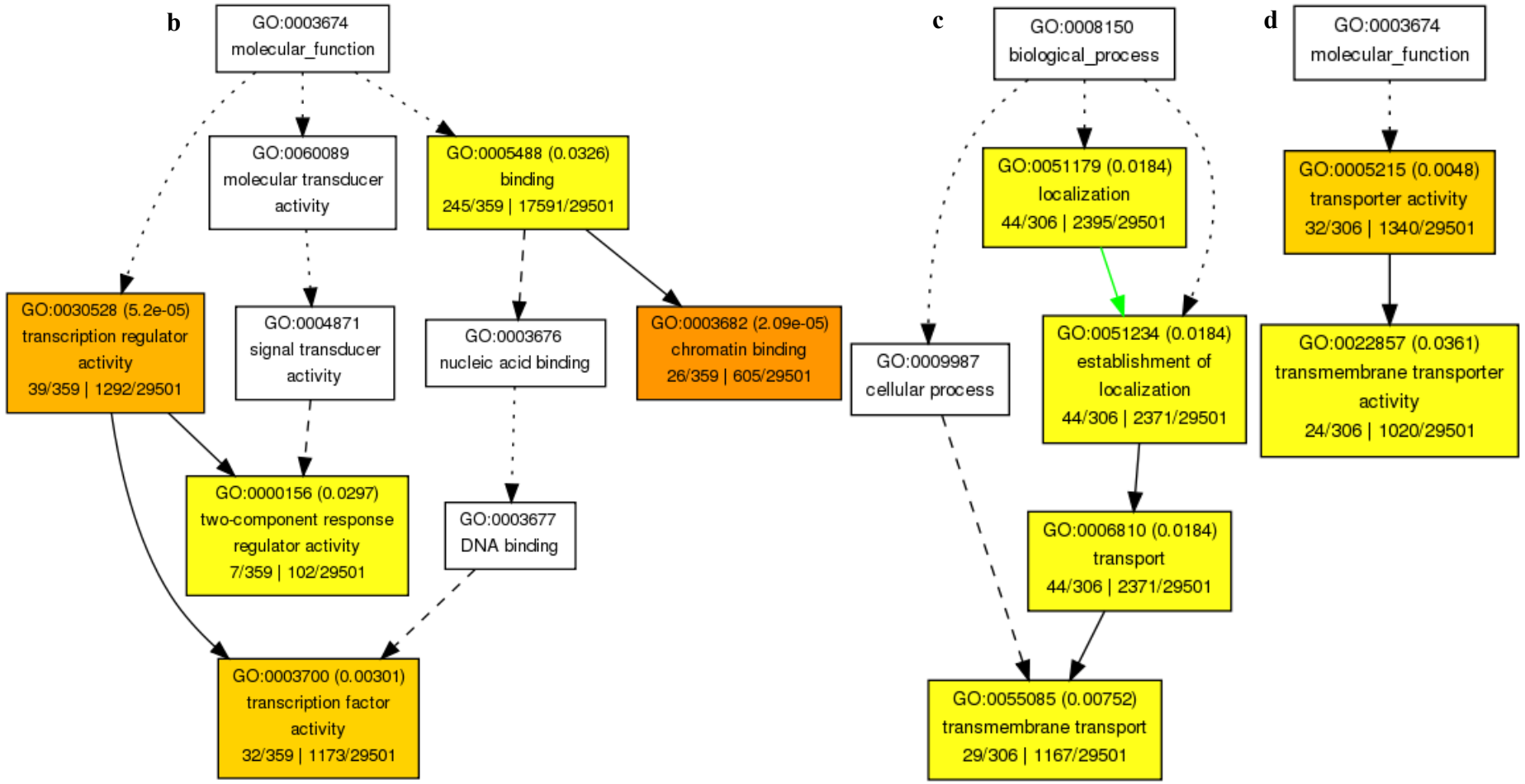

Supplementary Fig. 4 GO term analysis of unique DEGs under salt treatment in NIL-S roots after 3d 200 mM NaCl treatment. (Continued) a Up-regulated GO in biological process. **b** Up-regulated GO in molecular function. **c** Down-regulated GO in biological process. **d** Down-regulated GO in molecular function. Darker hues represent higher significance.

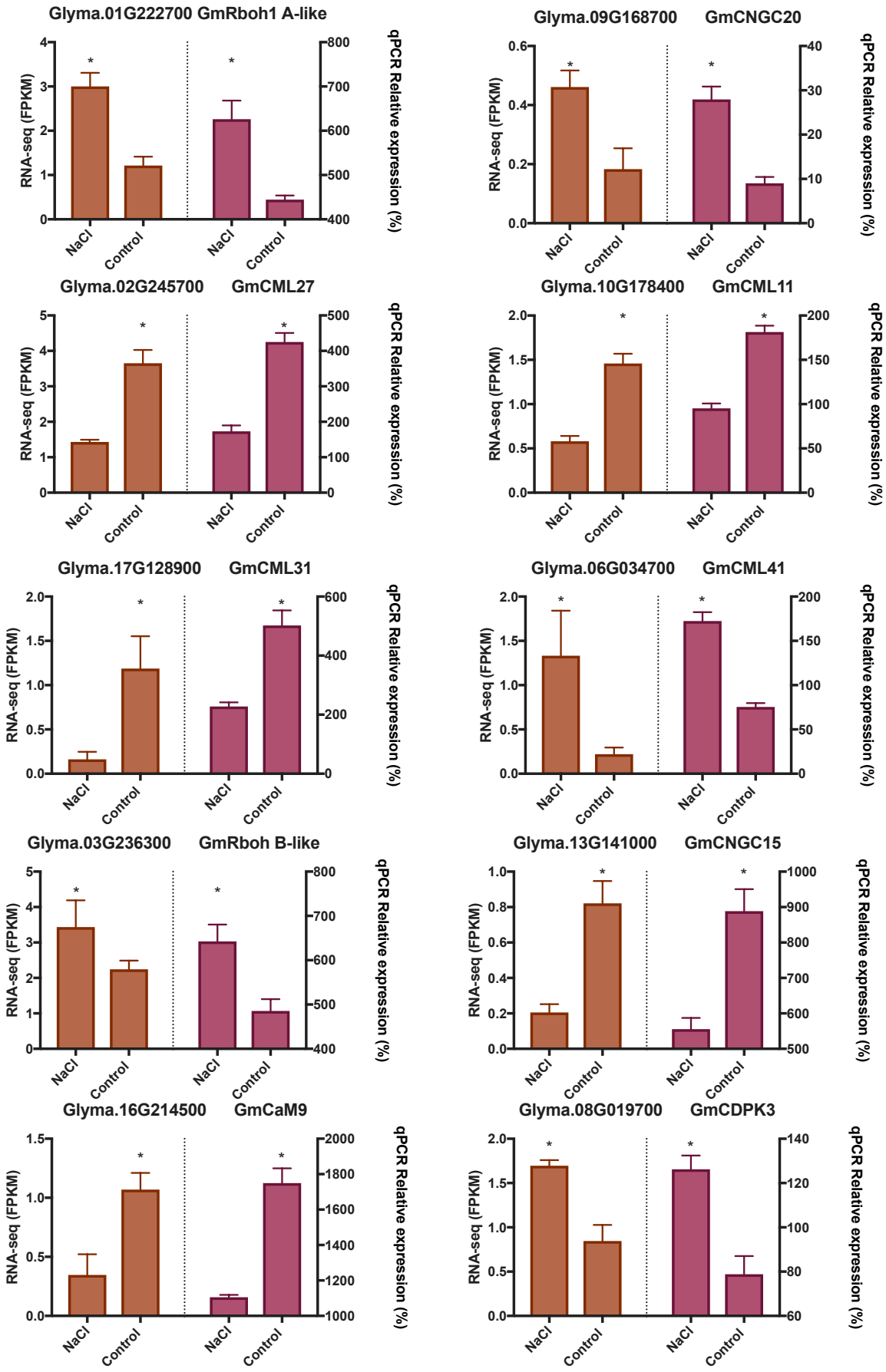

Supplementary Fig. 5 qPCR validation for RNA-seq results of selected genes. Brown bars represent the level of transcripts in FPKM (left *y*-axis); red bars represent the relative expression level to *GmUKN1* in percentage (right *y*-axis). Data are means of 3 replicates ± SEM.

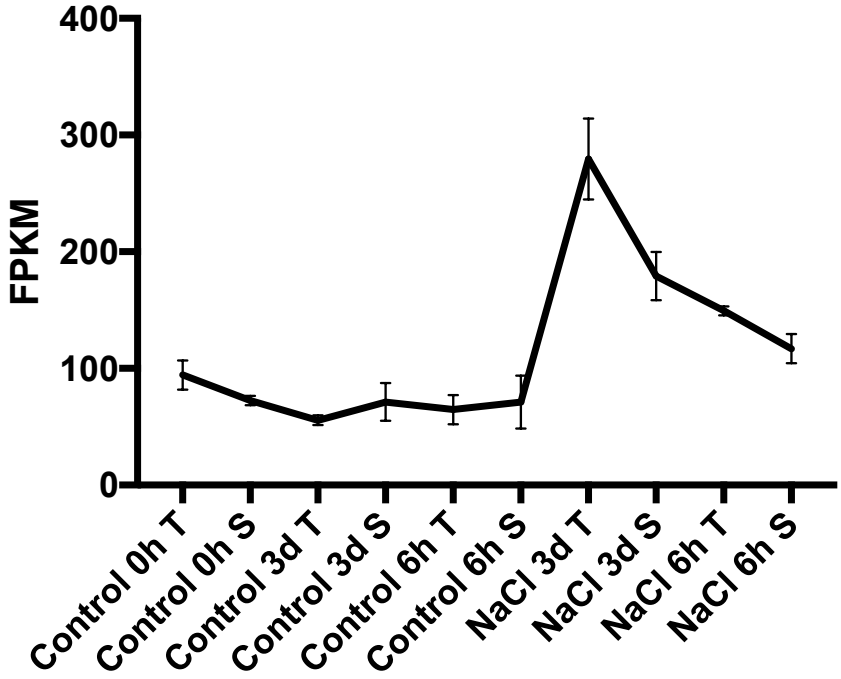

Supplementary Fig.6 *Glyma.13G173500* (*GmIFS2*) gene expression (FPKM) in all samples.

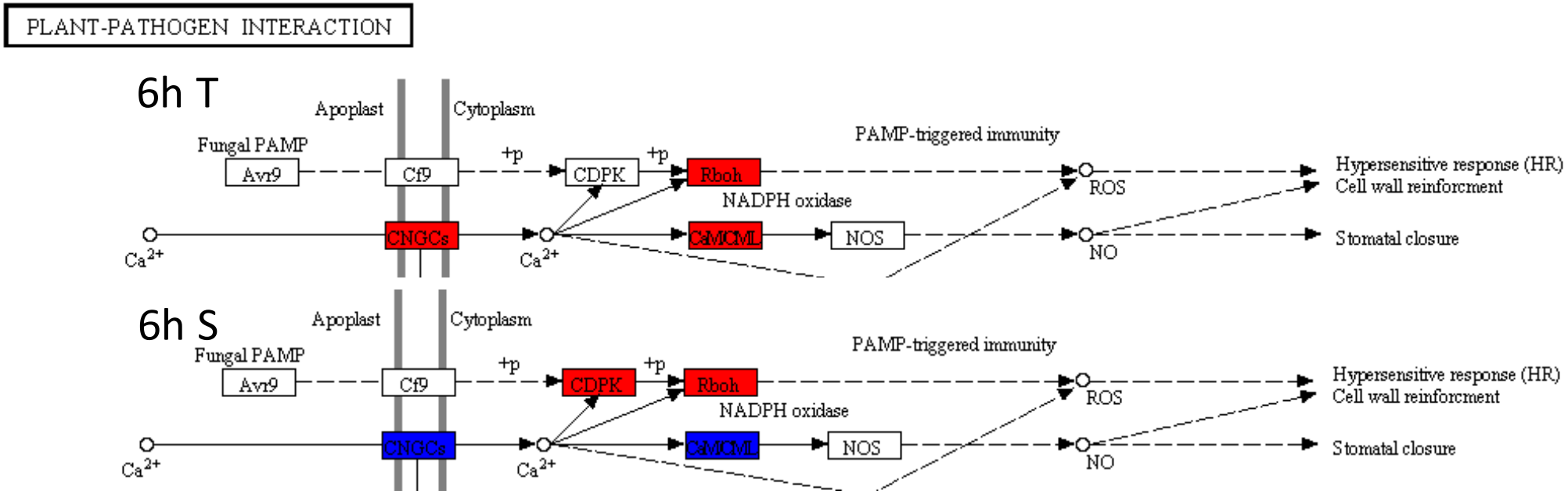

Supplementary Fig. 7 Diagram of DEGs between control and salt-treated samples of NIL-T and NIL-S in plant-pathogen interaction KEGG pathway at 6h. Green represents down-regulated genes; Red represents Up-regulated genes; Blue represents mixed-regulated genes.

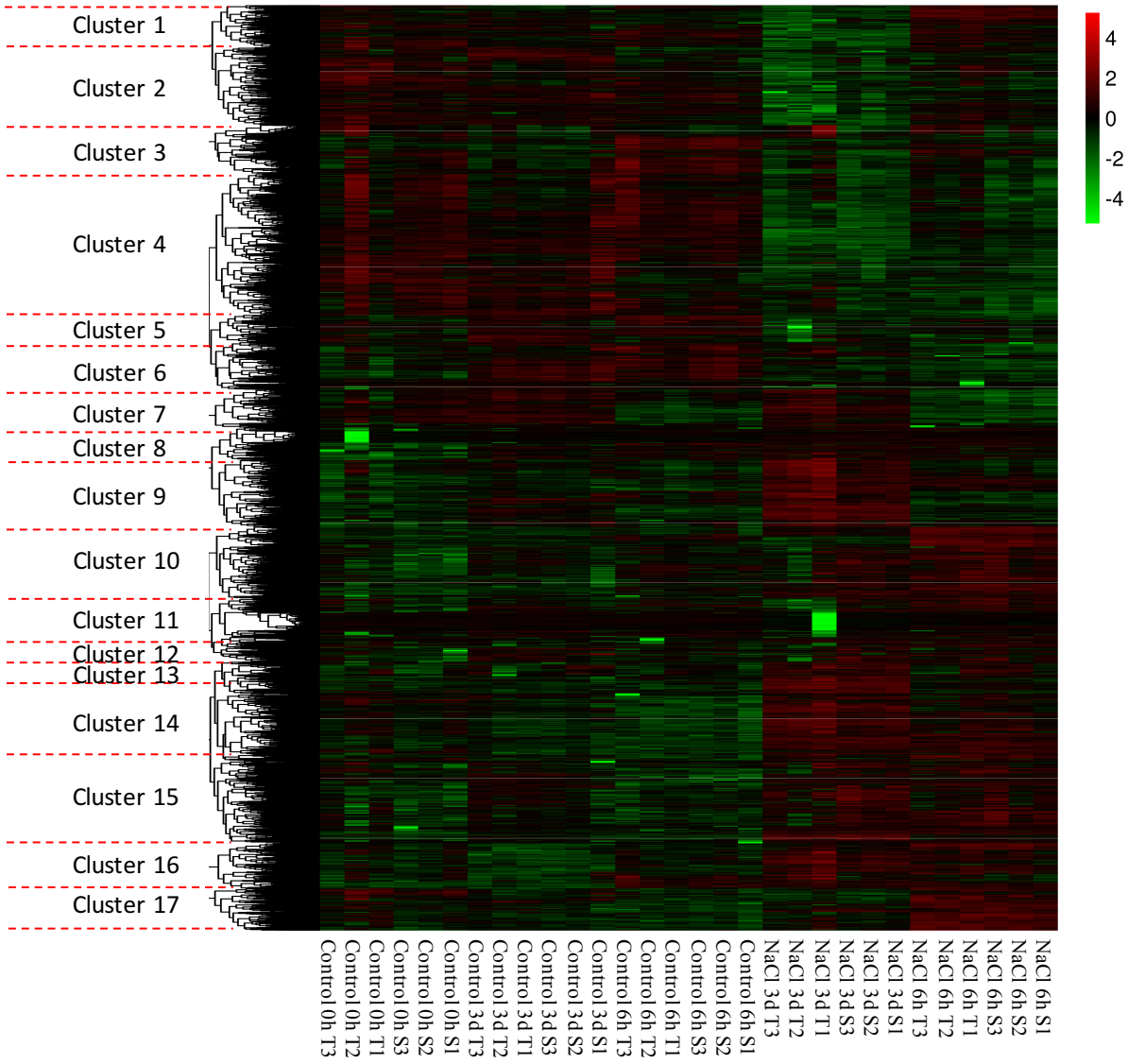

Supplementary Fig. 8 Hierarchical clustering of all DEGs in all individual samples.

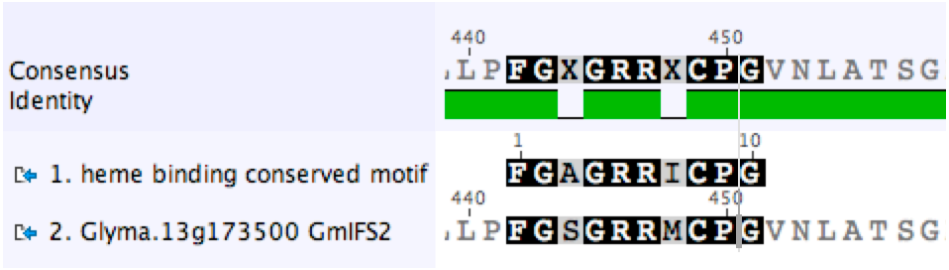

Supplementary Fig. 9 Conserved motif of heme binding alignment with GmIFS2 protein sequence. Protein sequence alignment was done in Geneious.

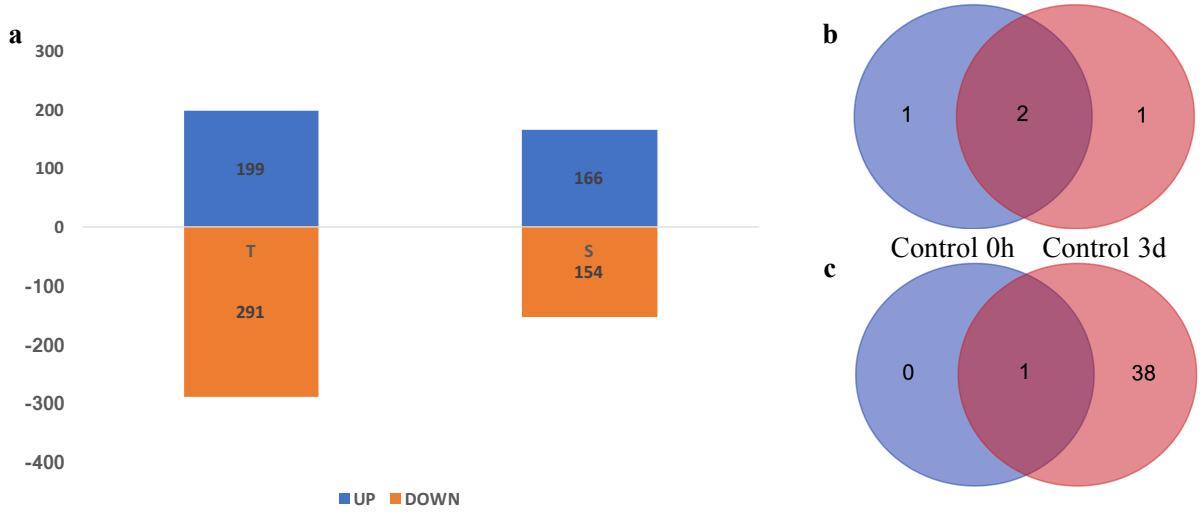

Supplementary Fig. 10 Overview of DEGs (differentially expressed genes) in RNA-seq rerun. a Numbers of DEGs (up- and down-regulated) between salt and control treated NIL-T and NIL-S at 3d. Venn diagram of up- (**b**) and down-regulated (**c**) DEGs in NIL-T against NIL-S soybeans at 0h and 3d under control conditions.

NIL-T and NIL-S plants were grown in a growth chamber located in the Plant Research Centre, Adelaide, with a day length of 16 h (with a light-emitting diode light source at 400 µmol m^{-2} s^{-1}) at 28 ˚C, and 8 h dark at 25 ˚C, with 60% relative humidity throughout. Soybean seedlings were treated with 200 mM NaCl (salt treatment) or water (control) at 14 days after sowing (DAS). 200 mM NaCl or water were applied again at 16 DAS. Total RNA was extracted from soybean roots using TRIZOL reagent (Ambion, http://www.ambion.com). Root samples were harvested from two time points, 0h and 3d of a 200 mM salt-treatment with the corresponding non-treatment controls. Eighteen RNA libraries were generated for single-end reads using an Illumina HiSeq 1500 sequencer, consisting of 3 biological samples per time point per genotype. Raw reads were generated and mapped to the latest soybean genome sequence Gmax_275 Wm82.a2.v1 (Glyma 2.0) using CLC Genomics Workbench (Version 7.0.4); RNA-seq statistics workflow was adopted to generate DEGs list. Again, there were more DEGs in NIL-T than NIL-S after 3 days, despite the numbers of DEGs being lower in the re-run.

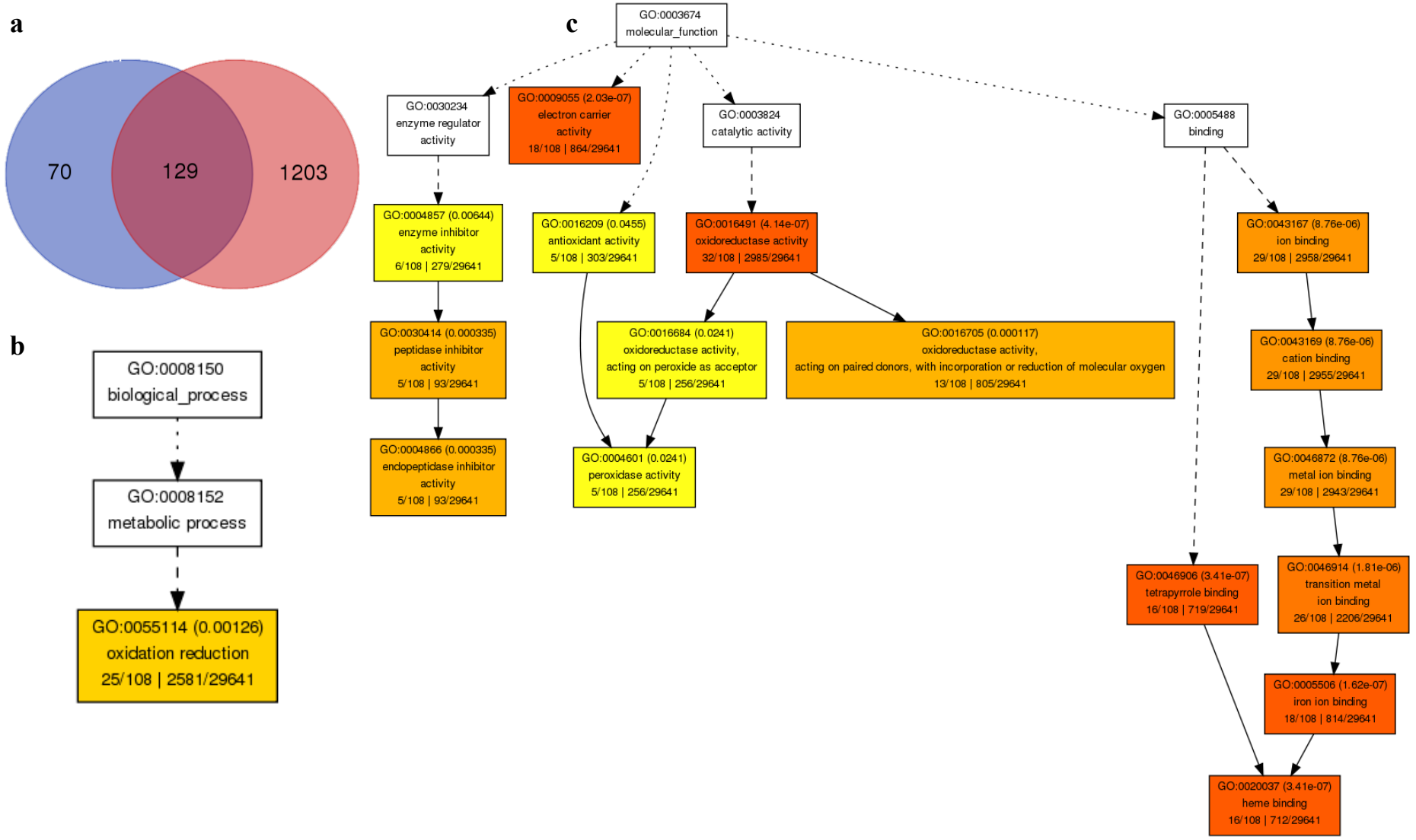

Supplementary Fig. 11 Venn diagram and GO term analysis of unique up-regulated DEGs under salt treatment in NIL-T roots after 3d 200 mM NaCl treatment in second RNA-seq. a Venn diagram of up-regulated DEGs in second RNA-seq against first RNA-seq at 3d under NaCl treatment. **b** Biological process enriched GO terms. **c** Molecular function enriched GO terms. Darker hues represent higher significance.

Brief conclusion

Based on our RNA-seq analysis, ROS detoxification has been proposed to be a major factor of how *GmSALT3* improves salinity tolerance in soybean. All the predicted *GmSALT3*-related ROS detoxification mechanisms are through speculation based on RNA-seq analysis, they need to be verified. How increased ROS detoxification is achieved through *GmSALT3* needs further investigation; two possible mechanisms, among others, are through reducing the conformational change of GmIF2 by mediating NaCl concentration in the ER in soybean roots; or through direct interactions with ROS scavenger enzymes. DEGs in the second RNA-seq are not entirely the same as first RNA-seq, probably because of differences in growth locations/conditions, development state, light conditions/pollution, sample harvest, and RNA purification. But ROS management is consistently shown to be an important mechanism in contributing to salinity tolerance of NIL-T.

Chapter 6 Conclusions and future research directions

GmSALT3 is predicted to encode a cation/H^+ antiporter 20-like protein in soybean (*Glycine max*) (Schmutz *et al.*, 2010). It shares its highest identity to a predicted K^+/H^+ antiporter gene from *Medicago truncatula* (Young *et al.*, 2011) and the closest characterised relative is a cation/H^+ exchanger 20 gene (*AtCHX20*) from *Arabidopsis thaliana* which encodes an endosomal protein that functions in stomatal guard cells to regulate stomatal opening; most likely through regulation of cellular K^+ and pH homeostasis (Padmanaban *et al.*, 2007). In plant cells, ion and pH homeostasis is vital to adapt to a constantly changing environment such as the imposition of salinity, and this homeostasis is regulated in part by solute transporters.

Members of the monovalent cation/proton antiporter (CPA) superfamily are thought to be involved in regulating cation and pH homeostasis by exchanging Na^+, Li^+, or K^+ for H^+ (Christopher *et al.*, 2005). The CPA superfamily contains two major families; CPA1 includes Na^+/H^+ exchanger (NHX) and Na^+/H^+ antiporter (NHAP/SOS1) families, and, CPA2 family includes K^+ efflux antiporter (KEA) and cation/H^+ exchanger (CHX) families (Chanroj *et al.*, 2012). NhaP and NhaA genes from ancestral bacteria are thought to have given rise to eukaryote CPA1 and CPA2 families, respectively (Chanroj *et al.*, 2012). The functions and localizations of characterized *Arabidopsis* CHX proteins are summarized in Table 6.1. The AtCHX proteins so far characterised seem to be implicated in K^+ and pH homeostasis of dynamic endomembranes. However, whether CHX proteins in general exert the same functions or have other roles needs to be further investigated.

Table 6.1 Characterized CHX proteins in *Arabidopsis thaliana*. Abbreviations: PM (plasma membrane); PVC (endosome/prevacuolar compartment); ER (endoplasmic reticulum).

CHX	Tissue localization	Membrane localization	Main functions
AtCHX13 (Zhao *et al.*, 2008)	Pollen	PM in plant	K^+ uptake
AtCHX17 (Cellier *et al.*, 2004)	Pollen (microspore), root epidermis, root cortex, leaf	PVC in plant, PM in plant, endomembrane in yeast	K^+ transport and pH homeostasis
AtCHX20 (Padmanaban *et al.*, 2007)	Guard cells, root tip/cap	Reticulate endomembrane	K^+ transport and pH homeostasis, guard cell movement and osmoregulation
AtCHX23 (Sze *et al.*, 2004)	Pollen grain, pollen tube	Reticulate endomembrane: ER in pollen tube	K^+ transport (*E. coli*)

In this thesis, we examined a gene that encodes a soybean CHX protein, *GmSALT3*, from its identification and physiological benefits under saline conditions, to functional characterisation and transcriptomic analysis. We localized GmSALT3 to the endoplasmic reticulum (ER) and observed it is predominantly expressed in Tiefeng 8 (salt-tolerant parent) within root phloem and xylem -associated cells (Chapter 2). *GmSALT3* contributes to Na^+, K^+, and Cl^- exclusion from leaves (Chapter 3). We proposed that in NIL-T the presence of full-length *GmSALT3* mediates Na^+ and Cl^- exclusion from shoots (Chapter 3), through restricting xylem loading of Na^+ and retranslocating Cl^- in the phloem (Chapter 4). Using a combination of heterologous expression systems (*E. coli* and *Xenopus laevis* oocytes), GmSALT3 was found to be involved in Na^+, K^+, and Cl^- transport (Chapter 4). Further, RNA-seq analysis indicated that ROS detoxification was proposed to be a major factor of how GmSALT3 improves salinity tolerance in soybean (Chapter 5). However, based on questions raised by the findings of this thesis several further investigations into the physiological and molecular functions of GmSALT3 are now warranted.

Firstly, it needs to be established whether *GmSALT3* encodes a co-transporter that transports Na^+, K^+ and Cl^-, a cation/proton exchanger or a Cl^-/proton exchanger that somehow facilitates the transport of the other ions in *Xenopus laevis* oocytes. For instance, GmSALT3 could also be interacting with other intrinsic transporters or channels in oocytes, whether the

protein also transports H^+ would also be important to measure. Electrophysiological experiments have been initiated and preliminary results are shown in Appendix IV. Mutagenesis of the transporters, further pH dependency relations and expression in alternative systems would help determine the transport properties of GmSALT3. Intriguingly, in plants, *GmSALT3* was shown to regulate K^+ accumulation under salt stress (Do et al., 2016), and also in our research, it was able to contribute to K^+ concentration difference between NIL-T and NIL-S leaves (Chapter 4). However, this difference could not be detected in Chapter 3 (Liu *et al.*, 2016). Soybean NIL plants from Chapter 3 were grown in China, and that were grown in Australia in Chapter 4, different growth location and water source could contribute to the differences observed between studies.

Initial analysis using RNA-seq data identified that *GmSALT3* expression is associated with improving ROS detoxification in NIL-T roots (Chapter 5). The link between the clear transport capacity of GmSALT3 and how this leads to a change in ROS status of the plant needs to be further explored. By disturbing the ionic environment of the ER or transport across the ER membrane how does this lead to the generation of ROS in the NIL-S roots? This leads to the question of how *GmSALT3* confers salinity tolerance in the NIL-T? It is our working model that GmSALT3 does not directly confer salt exclusion to the soybean shoot, but rather disturbance in ER function leads to ROS generation, leading to a breakdown in exclusion processes such as those confirmed by HKT or CLC proteins (Munns and Gilliham, 2015). In addition, as there is a phloem phenotype, again the distruption of ER processes in NIL-S could lead to less Cl being recirculated back to the roots. This again needs to be further tested.

Interestingly, when H_2O_2 concentrations were measured in roots they showed no significant differences between NIL-T and NIL-S under saline conditions. As H_2O_2 is only one ROS, more ROS content could be measured, such as superoxide, hydroxyl radical, and singlet oxygen. Nitric Oxide (NO) production was hypothesised to be restricted in NIL-T, its content in NIL-T roots is also of interest. ROS scavenger activity was measured on enzymes scavenging superoxide anion, other antioxidants should also be investigated, such as phenylpropanoid and

isoflavonoid that were predicted to be more highly synthesised in NIL-T roots if it relates to expression.

The ER localisation of *GmSALT3* needs to be validated though immunolabelling; a GmSALT3 specific antibody was designed and appeared to be specific in heterologous systems but was not specific when used in soybean tissue (Appendix III); new monoclonal antibodies are under investigation. If GmSALT3 was confirmed to be on the ER it may be prudent to investigate whether the protein interacts with GmIFS2. GmIFS2 belongs to Cytochrome P450 (CYP) family and is predicted to be vital in synthesising phenylpropanoid and isoflavonoids in soybeans on ER (Dastmalchi *et al.*, 2016). Whether NaCl could induce conformational change of GmIFS2 in soybean roots should be investigated. A considerable hurdle in the functional analysis is that the model organism in which this gene is expressed is soybean. Transgenic soybean plants were attempted during the course of this study to overexpress or knock out *GmSALT3* but no transgenic lines were successfully recovered. Such transgenics would also help with functional analysis. Currently another round of transgenics, with the parents containing the *Gmsalt3* allele transformed with a *GmSALT3*-YFP construct are in preparation. Compared to plants such as Arabidopsis there is a dearth of resources available to study *in vivo* function in soybean. However, if ecotopic expression of *GmSALT3* in Arabidopsis successfully complemented knockouts of *Atchx20* plants, it would indicate that it had a complementary mode of action, which would open many avenues for *in vivo* functional analysis. Examples would include the use of endomembrane pH sensors, or vehicle trafficking mutants that have been used to successfully study NHX proteins (Bassil *et al.*, 2012). Furthermore, if a fluorescently tagged version complemented the function of CHX20 then the localisation of that protein in the ER or other membranes would confirm GmSALT3's likely localisation.

It appears that natural selection and/or domestication in low saline soil selected for multiple and common mutations within *GmSALT3* and its promoter that leads to soybean plants being more salt-susceptible to soil salinity (Chapter 2). This observation leads to the assumption that a functional GmSALT3 leads to a yield penalty under non-saline conditions. However, in

the field, *GmSALT3* was found to have no penalty on soybean yield under non-saline condition (Chapter 3). It is possible that under the conditions examined we could not detect the advantage conferred to the plants that might coincide with loss of a functional GmSALT3. A common pressure in natural and cultivated environments is disease pressure. Testing the NILs under different biotic stresses may give further insights into the possible reasons that loss of *GmSALT3* is so common. Alternatively, the loss of functional GmSALT3 may be a natural consequence of standard mutation rates and the lack of selection pressure when soybean is cultivated in non-saline soil. This may be able to be determined by examining genomic sequences of successive soybean populations for mutation rates and the pedigree information of soybean with the various haplotypes. However, a more extensive field study examining the yield of the NILs in multiple environments would be the more cost-effective and sensible option to determine whether the loss of GmSALT3 does confer an advantage in any environments. Such a study would also determine whether GmSALT3 confers an advantage in environmental conditions other than salinity, where it contributes to improving soybean yields through increasing seed weight.

As well as further field studies, further examination of the NILs under tightly controlled environmental conditions is also warranted. This would allow a closer examination of the effects of GmSALT3 on the salinity tolerance of soybean at the reproductive phases than possible in the field. In addition, we have already gathered preliminary data that suggests that the salt-tolerant NILs of *GmSALT3* also have improved tolerance to other abiotic stresses (e.g. drought), compared to salt-sensitive NILs, greater gas exchange rates and more nitrate in leaves. However, these observations have been difficult to quantify. RNA-seq analysis of NILs under control and salt treatment also show that *GmSALT3* appears to contribute towards reactive oxygen detoxification activity in roots, which indicates the possibility that the protein could increase general stress tolerance to the plant. A phenotyping study has been initiated in *The Plant Accelerator* ® (The Australian Plant Phenomics Facility, Adelaide, Australia), to properly quantify the differential reduction in plant growth between NIL under a physiologically relevant

salt treatment (i.e. one that would be found in the field, 100 mM); to quantify whether there are subtle growth differences in NIL-*GmSALT3* and NIL-*Gmsalt3* under control conditions; and to investigate whether *GmSALT3* can contribute to tolerance to drought. Associating GmSALT3 with such a trait would greatly increase its utility to breeders. In conclusion, this project provides physiological and genetic evidence for a role of *GmSALT3* in contributing to salinity tolerance in soybean plants. Phenotyping and genotyping of twelve Australian commercial soybean cultivars show variations in *GmSALT3* haplotypes and salinity tolerance (Appendix V), expands the significance of this study to the Australian soybean industry building on the American and Chinese varieties that were studied in Chapter 2, which prompted soybean breeders from North and South America to contact us for using molecular markers associated with salinity tolerance in their breeding programs.

References

Bassil, E., Coku, A. and Blumwald, E. (2012). Cellular ion homeostasis: emerging roles of intracellular NHX Na^+/H^+ antiporters in plant growth and development. *Journal of Experimental Botany* **63**, 5727-5740.

Cellier, F., Conejero, G., Ricaud, L., Luu, D. T., Lepetit, M., Gosti, F. and Casse, F. (2004). Characterization of *AtCHX17*, a member of the cation/H^+ exchangers, CHX family, from Arabidopsis thaliana suggests a role in K^+ homeostasis. *Plant journal* **39**, 834-46.

Chanroj, S., Wang, G., Venema, K., Zhang, M. W., Delwiche, C. F. and Sze, H. (2012). Conserved and diversified gene families of monovalent cation/H^+ antiporters from algae to flowering plants. *Plant physiology* **3**, 1-18.

Christopher, L. B., Mark, D. and Rajini, R. (2005). Evolutionary origins of eukaryotic sodium/proton exchangers. *American Journal of Physiology* **288**, 223-239.

Dastmalchi, M., Bernards, M. A. and Dhaubhadel, S. (2016). Twin anchors of the soybean isoflavonoid metabolon: evidence for tethering of the complex to the endoplasmic reticulum by IFS and C4H. *The Plant Journal* **85**, 689-706.

Padmanaban, S., Chanroj, S., Kwak, J. M., Li, X., Ward, J. M. and Sze, H. (2007). Participation of endomembrane cation/H^+ exchanger *AtCHX20* in osmoregulation of guard cells. *Plant Physiology* **144**, 82-93.

Schmutz, J., Cannon, S. B., Schlueter, J., Ma, J., Mitros, T., Nelson, W., Hyten, D. L., Song, Q., Thelen, J. J. and Cheng, J. (2010). Genome sequence of the palaeopolyploid soybean. *Nature* **463**, 178-183.

Sze, H., Padmanaban, S., Cellier, F., Honys, D., Cheng, N. H., Bock, K. W., Conejero, G., Li, X., Twell, D., Ward, J. M. *et al.* (2004). Expression patterns of a novel *AtCHX* gene family highlight potential roles in osmotic adjustment and K^+ homeostasis in pollen development. *Plant Physiology* **136**, 2532-47.

Young, N. D. Schoof, H. Wang, B.-B. Wang, K. Wang, M. Wang, X. Warfsmann, J. Weissenbach, J. White, D. D. White, J. D. *et al.* (2011). The Medicago genome provides insight into the evolution of rhizobial symbioses. *Nature* **480**, 520.

Zhao, J., Cheng, N. H., Motes, C. M., Blancaflor, E. B., Moore, M., Gonzales, N., Padmanaban, S., Sze, H., Ward, J. M. and Hirschi, K. D. (2008). AtCHX13 is a plasma membrane K^+ transporter. *Plant Physiology* **148**, 796-807.

Appendices

Appendix I Improving the Salinity Tolerance of Soybean (ISB News Report)

ISB NEWS REPORT APRIL 2015

Improving the Salinity Tolerance of Soybean

Yue Qu, Rongxia Guan, Lijuan Qiu, Matthew Gilliham

Introduction

Soil salinity reduces crop yield. The extent and severity of salt-affected agricultural land around the globe is predicted to worsen due to the use of poor quality irrigation water, rising water tables, and climate change. The growth and yield of the majority of crop species is adversely affected by soil salinity, but varied adaptations can allow some crop cultivars to continue to grow and produce a harvestable yield under moderate soil salinity. Soybean, which is ranked as the fourth largest crop in terms of global yield, is a major food, fuel and feed crop, and has been classified as sensitive to salinity. Identification of genes that improve soybean salt tolerance would be useful for extending the agricultural range of soybean into soils with moderate salinity and therefore would be of use for meeting the challenging global food security targets set for 2050. Here, we summarize our recent research finding that *GmSALT3* (*Glycine max* Salt Tolerance-associated gene on chromosome 3) is a major gene involved in tolerance of soil salinity by soybean.

GmSALT3, a dominant gene responsible for salt tolerance in soybean

Soybean germplasm displays a spectrum of salt-tolerance phenotypes. We used this natural variation in salt tolerance to identify genes that increase soybean production under saline conditions. In 1969, a major quantitative trait locus (QTL) for salt tolerance was discovered in soybean that was predicted to be conferred by a single gene. Many research groups have since mapped this QTL to the same region on soybean linkage group N (chromosome 3), despite using distinct soybean parents and crosses between cultivated soybeans or crosses between wild and cultivated soybeans. These consistent results for the presence of a salt tolerance QTL indicate that this region on chromosome 3 might play an essential role in salt tolerance of soybean. Furthermore, the same region has been highlighted using different genetic backgrounds, which has led some to hypothesize that a conserved gene or several genes control salt tolerance in diverse soybean germplasm. We used map-based cloning within a soybean population derived from the salt-tolerant variety Tiefeng 8 and the salt-sensitive variety 85-140 to identify the salt-tolerance associated gene *GmSALT3* underlying this major QTL. RNA sequencing (RNA-seq) indicated that the *GmSALT3* coding sequence obtained from Tiefeng 8 was over twice the length of that from 85-140, with the sequence from 85-140 likely to result in a truncated and non-functional protein.

To understand the function of a candidate gene, it is useful to explore where it is expressed in the plant. Expression analysis demonstrated *GmSALT3* was in greater abundance in roots compared to shoots of Tiefeng 8 (the salt tolerant parent), and although the transcript decreased transiently when initially challenged with 200 mM NaCl, it gradually recovered within three days. Using *in situ* PCR, a technique that allows the localization of transcripts within tissue, we detected the expression of *GmSALT3* predominantly within endodermal cells and cells associated with phloem and xylem of salt-tolerant Tiefeng 8 soybean roots; the localization was unchanged under salinity treatment. We used a genetic engineering technique (using the fusion of a fluorescent marker protein with our protein of interest and its expression in cells isolated from tobacco and Arabidopsis) to detect to which membrane the GmSALT3 protein localized. We observed that GmSALT3 localized to an endomembrane, the endoplasmic reticulum (ER), and so shares this localization with the nearest characterized homolog to GmSALT3, CHX20 from the brassica *Arabidopsis thaliana*.

To investigate the role of *GmSALT3*, sodium ion (Na^+) accumulation within the two soybean parents was compared. The Na^+ content in roots of the parents was similar, but following NaCl treatment (200 mM) Tiefeng 8 accumulated significantly less Na^+ than 85-140 in both stems (after 5 days) and leaves (after 7 days). To compare the function of the two *GmSALT3/Gmsalt3* alleles, we developed a pair of near isogenic lines (NILs) NIL-T (*GmSALT3* from Tiefeng 8) and NIL-S (*Gmsalt3* from 85-140). Under control conditions, the NILs had no significant difference in agronomic traits, such as 100-seed weight, and protein and oil content, but had differential salt tolerance. The Na^+ content in stems and leaves of self-grafted NIL-S was much higher than that in NIL-T when the NIL-S scion was grafted on the NIL-T rootstock. The Na^+ content in the NIL-S scion was 49% lower in stems and 71% lower in leaves when grafted to NIL-T roots. In contrast, the Na+ content in stems and leaves of the

NIL-T scion grafted to the NIL-S root increased by 79 and 139%, respectively, compared with self-grafted NIL-T.

Collectively, these results suggest that *GmSALT3* is likely to function in the root (and stem), which is consistent with the predominant expression pattern of *GmSALT3* in Tiefeng 8 in roots and stem, and that this ER-localized protein constrains Na^+ translocation to the leaves.

The salt tolerant haplotype (H1) of *GmSALT3* is likely to be the ancestral allele and a target of natural and artificial selection

By screening 172 landraces and 57 wild soybean, we identified a total of nine haplotypes (i.e., versions of this gene, H1-H9), five from landraces and eight from wild soybean. Two of these alleles were associated with conferring salt tolerance and seven resulted in salt sensitivity. Furthermore, our study identified minimal genetic variation between the two salt-tolerant alleles (H1/H7) compared with the more extensive variation in the seven salt-sensitive alleles (H2–H6, H8, H9), with H6–H9 only found in wild soybean. The salt-tolerant H1 (which is the version of the gene found in Tiefeng 8) is the most frequently found haplotype in both wild soybean and landraces, and it has the widest geographical range. By integrating genotype and phenotype information, we found a clear relationship between H1 and salt tolerance. The high frequency of H1, its co-occurrence with salt-affected soils, the low genetic diversity of salt-tolerant alleles, and the high genetic diversity in the salt-sensitive alleles are all hallmarks that the H1 allele is likely to be the ancestral allele and has been strongly favored during natural and/or artificial selection around salinity affected areas.

Hypothesized model of salt tolerance in soybean related to GmSALT3

Based on the data we have gathered so far, we hypothesize that once the salinity selection pressure was released on soybean (i.e., when the plants encountered low concentrations of salt in the soil) *GmSALT3* was no longer sensitive to acquiring genetic change, including insertions and deletions, as it resulted in no detrimental effect on the plant phenotype in the low-salt environment. However, the resulting mutations have led to a loss, or reduced function, of the gene product, resulting in a loss of salt tolerance. This greater mutation rate in the salt-sensitive alleles may indicate that the loss of function of *GmSALT3* confers a growth advantage for these plants on non-saline soils. However, we find no evidence that this is the case, as we have not detected any growth or yield advantage in the NIL-S lines compared with the NIL-T line when grown under control conditions for the agronomic traits we tested. Interestingly, there is a small subset of soybean cultivars, such as Peking and Baipihuangdou, that contains H1 but is salt sensitive. They are likely to contain recent mutations in other key salt-tolerance genes such as *SOS1* or *HKT1*, or contain genetic elements that are yet to be identified that may be a useful source for discovering novel genes involved in salt tolerance in soybean.

GmSALT3 is expressed in root stelar cells, which are cell types already known to have a role in limiting salt transport to the shoot. For instance, the Na^+ transporters (HKT1;5-like proteins) expressed in these cells directly retrieve Na^+ from the root xylem. In plants expressing the correct *HKT1;5-like* allele, this is associated with reduced Na^+ content in shoots and superior salt tolerance in rice, wheat, and Arabidopsis. A similar lower Na^+ content in the shoots of salt stressed H1-containing plants compared with H2 suggests that this gene may also affect transport of Na^+ from root to shoot, and the grafting of NIL-T and NIL-S lines showed that the root and stems were sufficient to limit the accumulation of Na^+ in the shoot. However, the *GmSALT3* transcript level was first down-regulated and then gradually recovered in roots; this is different from the pattern of other salt-tolerance genes, indicating a distinct salt response in soybean or a different role for this gene. Consistent with this is the ER localization we observed for GmSALT3 compared with the plasma membrane localization of HKT or SOS1 proteins. Therefore, *GmSALT3* is unlikely to play a direct role in the retrieval of salt from the xylem but instead may have a role in sensing or responding to salt.

Conclusions and implications for agri-biotechnology

The identification of the gene underlying this important soybean salt-tolerance allele has provided an insight into the molecular basis of both natural and human selection of salt tolerance in soybean. In light of the predicted 70–110% increase in food production that will be needed by 2050 to feed the global population over the same period, and with no current option for

expanding the area of agricultural land, an increase in the salt tolerance of conventional crops will be required to assist in improving crop productivity and food security. To achieve this goal, both traditional plant breeding programs using marker-assisted selection and genetic engineering (GE) technologies can contribute. We have previously bred durum wheat to contain an ancestral *HKT1;5-like* gene and this led to a 25% increase in grain yield under saline field conditions. We expect *GmSALT3* to confer an even larger increase in yield in soybean—these experiments are underway. Our most recent study in soybean can now provide markers to breeders for targeting the salt resistance traits into new soybean germplasm, which should facilitate the rapid development of new elite salt-tolerant soybean cultivars by marker-assistant selection. Alternatively this gene can also be introduced via GE technology. Whilst the exact mechanism of how GmSALT3 imparts salt tolerance is still unknown, this protein also offers the opportunity for improving salt tolerance in other crop species. To this end, the role of homologs of *GmSALT3* is being currently investigated—as is the exact mechanism by which GmSALT3 impart salt tolerance.

More detailed information about GmSALT3 can be found in the open access publication on the Plant Journal: "Salinity tolerance in soybean is modulated by natural variation in GmSALT3." Markers and additional information are available on request.

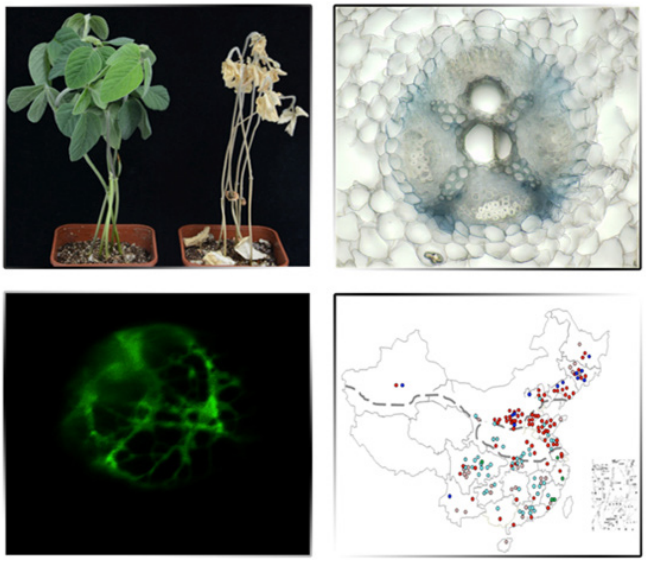

Figure 1. Identification of genes that improve crop salt tolerance is essential for the effective utilization of saline soils by agriculture. Here, we use fine mapping in a soybean [Glycine max (L.) Merr.] population derived from the commercial cultivars Tiefeng 8 and 85-140, to identify GmSALT3 (Glycine max Salt Tolerance-associated gene on chromosome 3), a dominant gene associated with sodium (Na^+) exclusion from the shoot and soybean salt tolerance. The above montage describes the phenotypic variation between Tiefeng 8 and 85-140 treated with 200 mM NaCl for 18 d (top left); the tissue localization of GmSALT3 within root phloem- and xylem-associated cells in the salt-tolerant parent Tiefeng 8, as indicated by blue colour (top right); the subcellular localization of GmSALT3 to the endoplasmic reticulum (ER) in *Nicotiana benthamiana* protoplasts (bottom left); distribution of different haplotypes of GmSALT3 gene in China, indicated by different color dots (bottom right). Source: *Guan et al. 2014*.

References

Abel GH. Inheritance of the capacity for chloride inclusion and chloride exclusion by soybeans. Crop Sci. 1969;9:697.

Athman A, Tanz SK, Conn VM, Jordans C, Mayo GM, Ng WW, et al. Protocol: a fast and simple in situ PCR method for localising gene expression in plant tissue. Plant methods. 2014;10:1-20.

Guan R, Qu Y, Guo Y, Yu L, Liu Y, Jiang J, et al. Salinity tolerance in soybean is modulated by natural variation in GmSALT3. The Plant Journal. 2014;80:937-50.

Munns R, James RA, Xu B, Athman A, Conn SJ, Jordans C, et al. Wheat grain yield on saline soils is improved by an ancestral Na+ transporter gene. Nat Biotechnol. 2012;30:360-4.

Tilman D, Balzer C, Hill J, Befort BL. Global food demand and the sustainable intensification of agriculture. PNAS. 2011;108:20260-64.

Yue Qu[1], Rongxia Guan[2], Lijuan Qiu[2], Matthew Gilliham[1]

[1]ARC Centre of Excellence in Plant Energy Biology, School of Agriculture, Food and Wine and Waite Research Institute, University of Adelaide, Glen Osmond, SA 5064, Australia

[2]The National Key Facility for Crop Gene Resources and Genetic Improvement (NFCRI), Institute of Crop Science, Chinese Academy of Agricultural Sciences, No. 12 Zhongguancun South Street, Haidian District, 100081 Beijing, China
e-mails for correspondence: qiulijuan@caas.cn; matthew.gilliham@adelaide.edu.au.

Appendix II Functional characterisation of *GmSALT3* in a yeast mutant

The characterisation of transport function of *GmSALT3* was attempted in a yeast mutant. The yeast strain used in this experiment was donated by Dr. Heven Sze, University of Maryland, USA, which was KTA40-2 (MATαade2-1 can1-100 his3-11,15 leu2-3,112 trp1-1 ura3-1 mall0 ena1Δ::his3::ena4Δ nha1Δ::lew2 nhx1Δ::trp1 kha1Δ::kanMX) (Maresova and Sychrova, 2005). The yeast was transformed using the LiAc/SS carrier DNA/PEG method (Gietz and Schiestl, 2007). The resulting transformants were selected on SC medium minus Ura (0.67% YNB, 2% Glucose, 2% drop-out mix minus Ura, 2% agar).

For liquid yeast culture experiments, cells were first grown in standard SC minus Ura medium (0.67% YNB, 2% Glucose, 2% drop-out mix minus Ura) overnight, and were adjusted to OD_{600} of 0.04 before adding into 96-well plate with appropriate SC minus Ura medium (0.67% YNB, 2% Glucose or galactose, 2% drop-out mix minus Ura) or with salt (100 mM NaCl) at pH 6.5. MES (20 mM) was added into each solution to stabilize the pH (Maresova and Sychrova, 2005). pH was adjusted using Tris. OD_{600} was measured using FLUOstar Omega Fluorescence microplate reader (BMG LABTECH) every 15 min over 42 h.

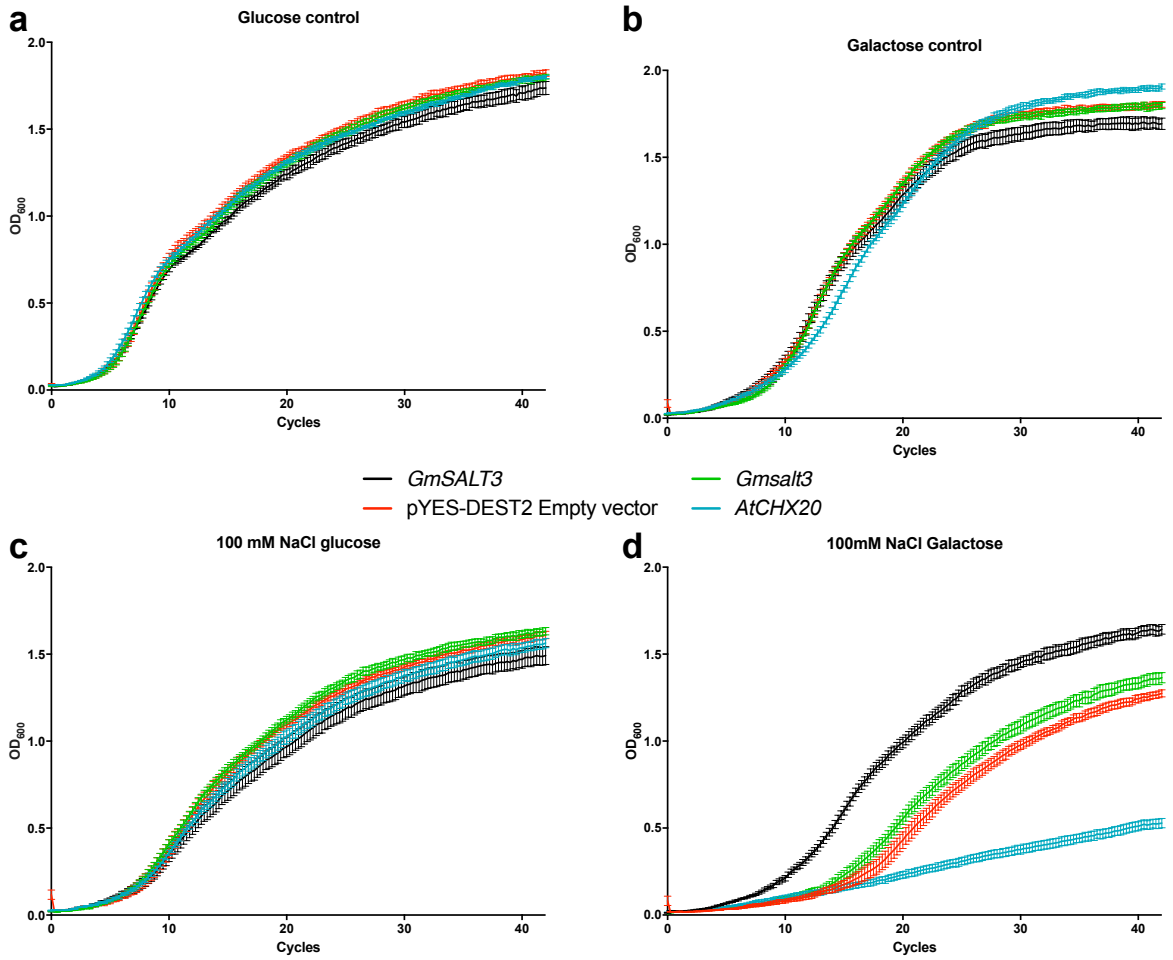

Appendix Fig. 2.1 Functional characterisation of *GmSALT3* in a yeast mutant. a Glucose control. **b** Galactose control. **c** 100 mM NaCl treatment with Glucose. **d** 100 mM NaCl treatment with Galactose. 20 mM MES was added into all samples to stabilize the pH at 6.5. Yeast cells were normalised to 0.04 OD_{600} before adding into 96-well plate. OD_{600} was measure by an interval of 15 mins from 0 h to 42 h at 30°C. Four technical replicates for each transformant were included. Different colours showing different transformant as indicated in graphs. This figure is reproduced from my Master's thesis (Qu, 2013).

Glucose controls were used to make sure yeast cells containing the different vectors show the same growth without gene expression; galactose was used to induce gene expression; 100 mM NaCl treatment with glucose was used to detect the growth condition of yeast containing 4 vectors with salt treatment but without gene expression; 100 mM NaCl treatment with galactose was used to detect the growth condition of yeast containing 4 vectors with salt treatment and gene expression. AtCHX20 had previously been characterised in this system and is used as a

positive control (Padmanaban *et al.*, 2007). In both Appendix Figure 2.1 and 2.2 AtCHX20 reduces the growth rate of the yeast on galactose, especially in the presence of salt, consistent with previous findings (Padmanaban *et al.*, 2007). The improvement in growth seen by *GmSALT3* expressing yeast in Appendix Fig. 2.1d indicated that GmSALT3 may have a role in sodium detoxification to the salt-sensitive yeast mutant. However, while trying to reproduce the phenotypic variation shown in Appendix Fig. 2.1, *GmSALT3* failed to confer consistent salt tolerance to yeast mutant in all subsequent experiments. Appendix Fig. 2.2 is one of those repetitions. Many modifications were performed to improve the consistency, such as changing growth conditions, such as incubation period and temperature; incubation methods, such as grow overnight in Galactose media rather than Glucose media; and pH maintenance, such as adding buffering agent (MES). However, these never produced consistent results; therefore, *GmSALT3* was transformed into other heterologous systems, such as *E.coli* (Chapter 4).

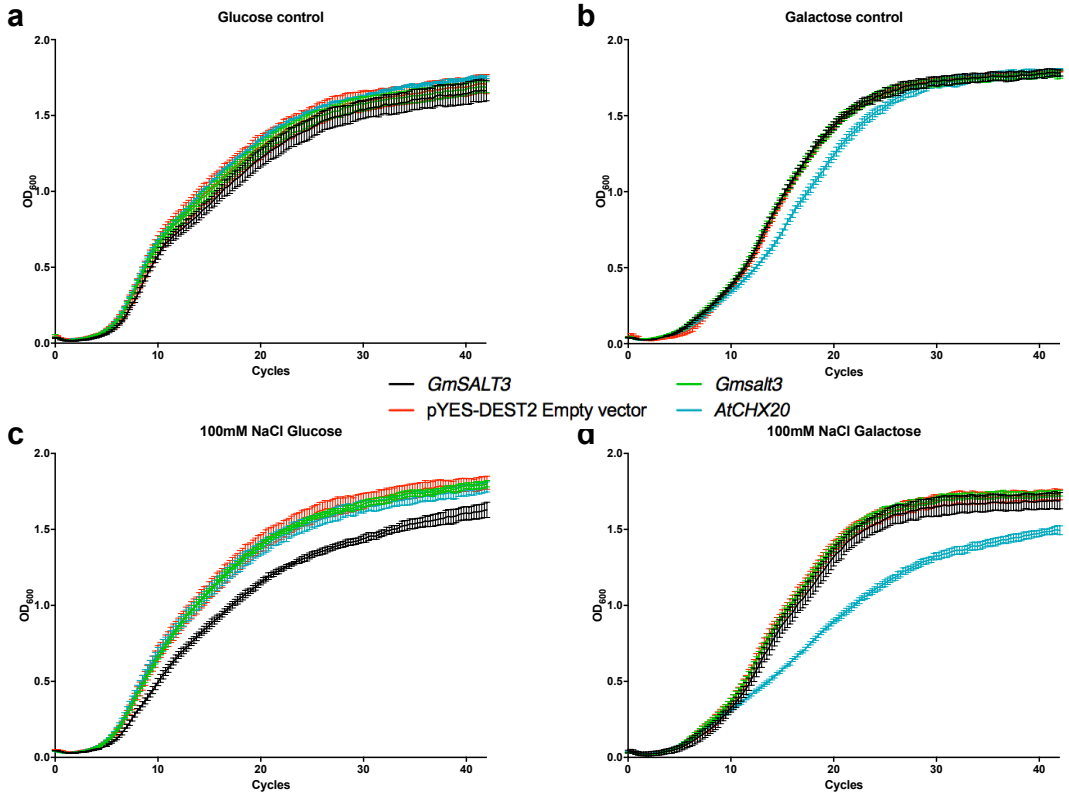

Appendix Fig. 2.2 Functional characterisation of *GmSALT3* in yeast mutant. a Glucose control. **b** Galactose control. **c** 100 mM NaCl treatment with Glucose. **d** 100 mM NaCl treatment with Galactose.

Appendix III - Antibodies and western blot analysis

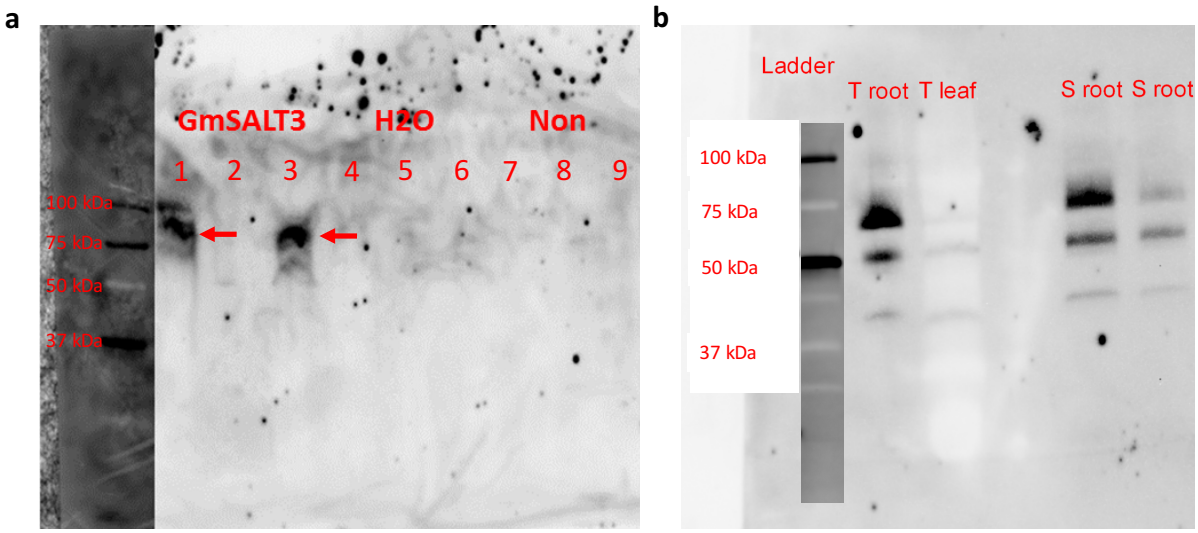

Appendix Fig. 3.1 Antibodies and western blot analysis. Western blot against crude protein extract from *GmSALT3*-expressing oocytes, H_2O-injected and non-injected oocytes (**a**), and soybean NIL-T plant root and leaves (**b**). The arrow indicates the band of interest.

GmSALT3 was localised to ER in *Arabidopsis* mesophyll and Tobacco protoplasts (Chapter 2). To further confirm GmSALT3's ER subcellular localisation, a primary antibody (Rabbit polyclonal antibody) was designed and ordered from the peptide company Mimotopes, Australia, the peptide sequence was H-CSYTEVGDEGPKYNSP-OH. Secondary antibody was Goat anti-Rabbit IgG (H^+L) Secondary Antibody, HRP conjugate (Invitrogen™, USA). The western Blotting protocol was adopted from Bio-Rad V3 Western Workflow (Bio-Rad, USA). Mini-PROTEAN® TGX Stain-Free™ Precast Gels (12% gel percentage, any kD) and used to separate proteins. Separated proteins were transferred to membrane through the Trans-Blot® Turbo™ Transfer System. Membrane was then soaked in 5% skimmed milk for 1 h, followed by fresh 5% skimmed milk with 1:1000 primary antibody incubation with slight shaking for 20 mins at room temperature and 4 °C overnight and 2 h at room temperature. Membrane was washed in 1xPBS for 10 mins and repeated 3 times. The membrane was transferred to fresh 5% skimmed milk with 1:1000 secondary antibody for 1.5 h at room temperature. After washing with 1xPBS again, the membrane was incubated in Clarity™ Western ECL Blotting Substrate

for 5 mins. Chemiluminescent signals on the membrane were visualized by ChemiDoc™ Touch Imaging System. All the 5% skimmed milk solution was made in 1xPBS.

According to GmSALT3's amino acids sequence, its molecular weight is 89.44 kDa. Designed GmSALT3-sepecific was able to target GmSALT3 protein in *Xenopus* Oocytes expression system (Appendix Fig. 3.1a), but failed to specifically target the desired protein in plant tissues (Appendix Fig. 3.1b). New monoclonal antibodies are under investigation.

Appendix IV - Additional electrophysiological characterisation of *GmSALT3* in *Xenopus laevis* oocytes

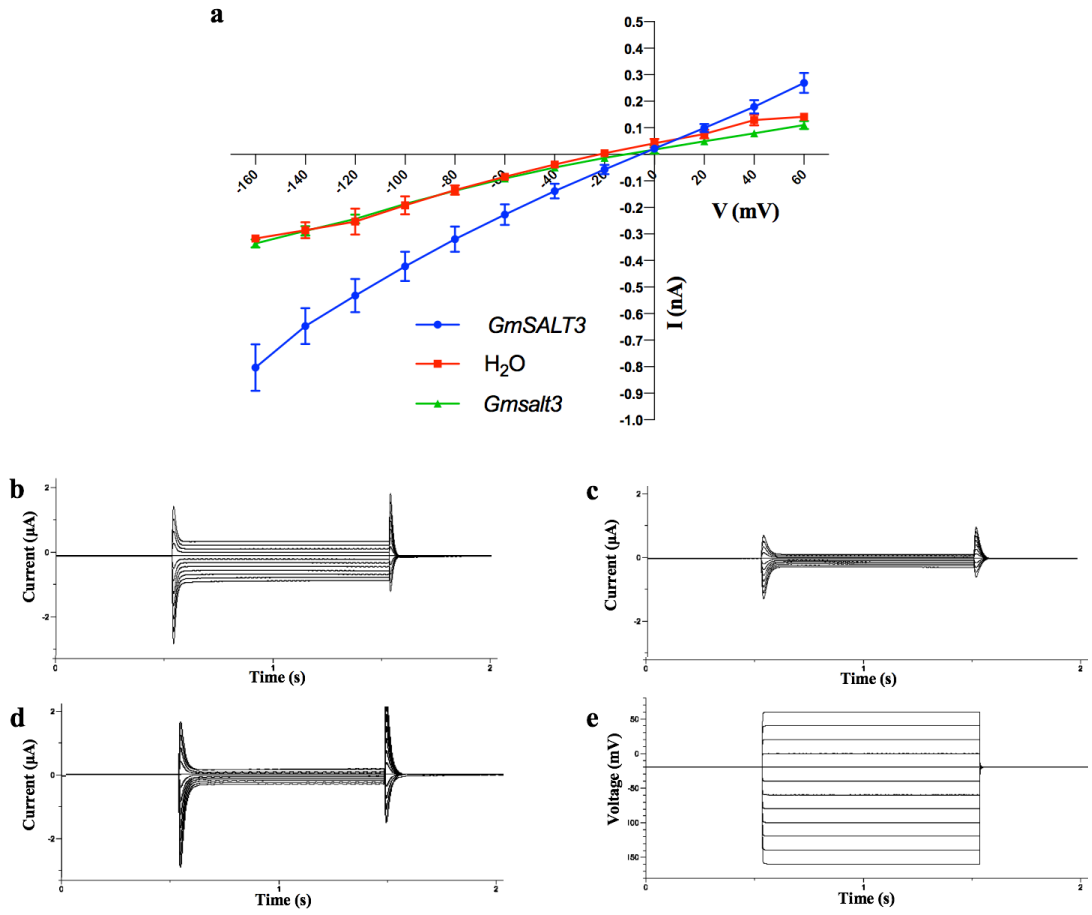

Appendix Fig. 4.1 *GmSALT3* expression in *Xenopus laevis* oocytes with 10 mM KNO_3 and 10 mM NaCl containing solution. a Current-voltage (I - V) curves for *GmSALT3* (blue) and *Gmsalt3* (green) expressing, and H_2O injected oocytes. Data are means ± SEM of currents in n = 4 - 8. Voltage clamp traces of oocytes expressing GmSALT3 (**b**), Gmsalt3 (**c**), and H_2O (**d**). **e** Schematic voltage protocol in millivolts (mV).

GmSALT3 was expressed in *X. laevis* oocytes, and was shown to facilitate Na^+, K^+, and Cl^- transport (Chapter 4). To further investigate GmSALT3's transport properties, *GmSALT3* cRNA, *Gmsalt3* cRNA and water-injected oocytes were incubated for 48 h and two-electrode voltage-clamp electrophysiology done following Roy *et al.* (2008). Membrane currents were recorded in solution containing 10 mM KNO_3, 10 mM NaCl, 5mM HEPES, and 0.6mM $CaCl_2$ at pH 7.5. Appendix Fig. 4.1 indicates that significant inward currents could be detected for *GmSALT3* expressing oocytes in the presence of Na^+, K^+, Cl^-, and NO_3^-.

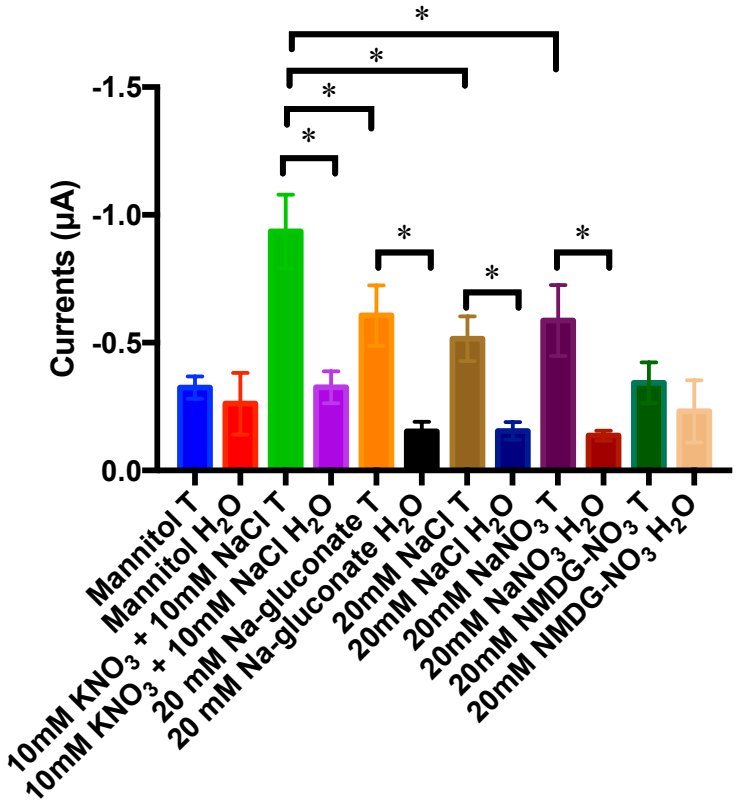

Appendix Fig. 4.1 *GmSALT3* expression in *Xenopus laevis* oocytes with different solutions results in currents variation. Currents of *GmSALT3* (T) or H_2O injected oocytes at -120 mV in different solutions, including mannitol, 10 mM KNO_3 and 10 mM NaCl, 20 mM Na-gluconate, 20 mM NaCl, 20 mM $NaNO_3$, and 20 mM NMDG-NO_3. Values are means ± SEM (n = 4-14). Asterisks indicate a significant difference between *GmSALT3*-injected and H_2O-injected oocytes at $*P < 0.05$.

To determine ion transport selectivity in GmSALT3-expressed oocytes, membrane currents were assayed in different solutions (Appendix Fig. 4.1). There were no currents in mannitol and NMDG-NO_3, which indicates that GmSALT3 is not involved in transporting NO_3^-. Significant inward currents could be detected in solutions containing 10 mM KNO_3 and 10 mM NaCl, 20 mM Na-gluconate, 20 mM NaCl, and 20 mM $NaNO_3$, and currents in 10 mM KNO_3 and 10 mM NaCl were significantly higher compared to other solutions. This indicates that a permeable cation is needed for currents to be shown and that a combination of NO_3^- and Cl^- results in larger currents than when only one of the anions is present. This experiment needs more repetition, with different solutions, to determine its significance and its relation to

GmSALT3 function. It is curious that a predicted electroneutral transporter should facilitate an increase in currents in oocytes; however, this is not the first example of a protein from the NHE family carrying currents (Chintapalli *et al.*, 2015).

Appendix V - Australian commercial soybeans phenotyping and genotyping

Twelve Australian commercial soybean cultivars were kindly provided by Dr. Natalie Moore and Dr. Andrew James, NSW Department of Primary Industries, Australia. Shoot ion contents (Na^+ and K^+) were measured using flame photometry (Sherwood 420), and Cl^- was also measured using chloride analyser (Sherwood 926S). Salt tolerance of these soybean accessions was evaluated based on the level of leaf chlorosis after 2 weeks of growth under saline conditions (100 mM NaCl), the salt-tolerance ratings ranged from 1 (normal green leaves) to 5 (complete death) (Guan *et al.*, 2014). Genomic DNA was isolated from soybean leaves as described by Edwards *et al.* (1991). The insertion/deletion in the promoter (148/150 bp insertion) and coding region (3.78 kb insertion) were screened by using specific primers for the indels. Primer sequences were designed according to Guan *et al.* (2014).

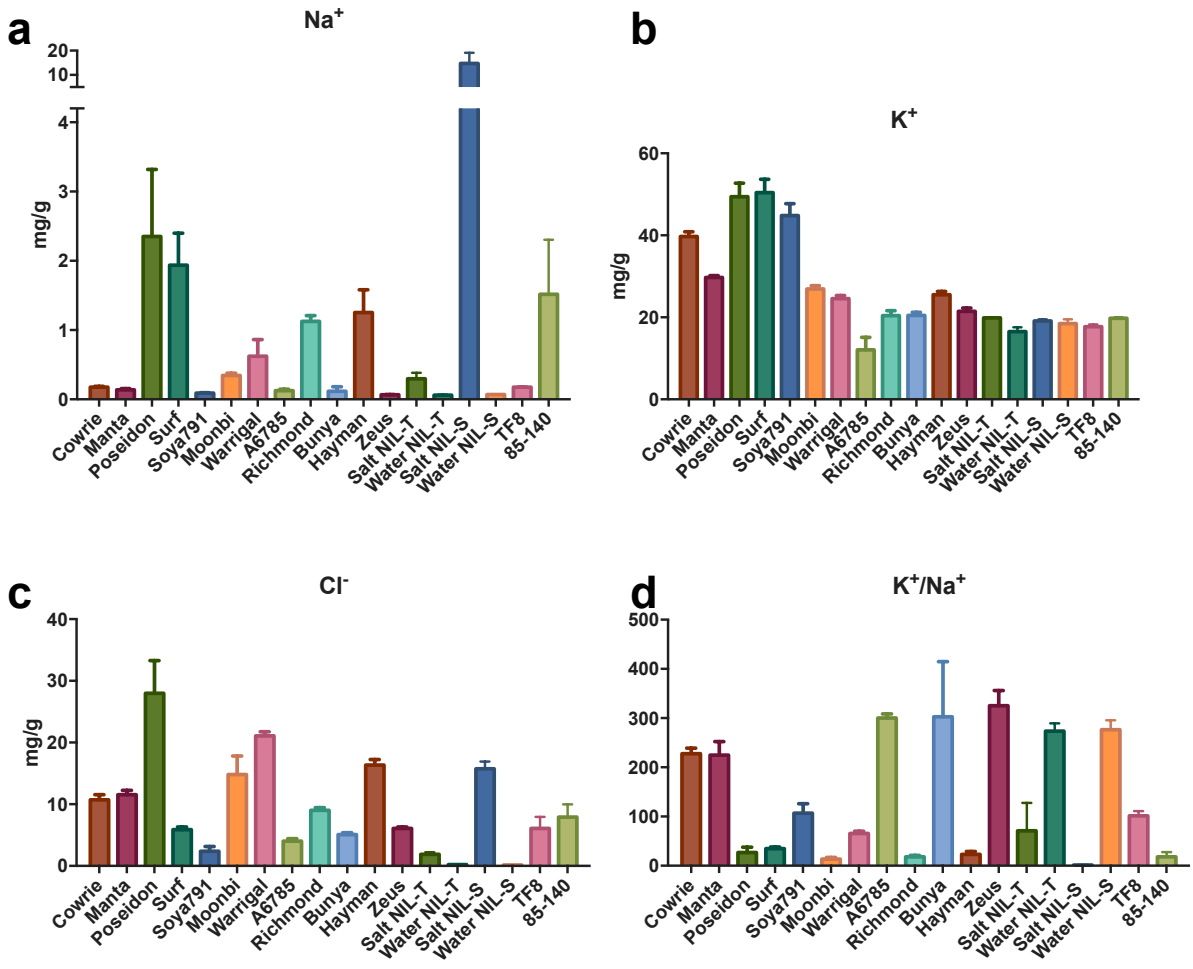

Appendix Fig. 5.1 Ion content in leaves of 12 Australian commercial soybean cultivars,

NIL-T and NIL-S, Tiefeng 8 and 85-140. a Na^+ content. **b** K^+ content. **c** Cl^- content. d K^+ content to Na^+ content ratio. Data are means of 3-4 replicates ± SEM.

Shoot Na^+ and Cl^- contents showed a big variation in the 12 Australian commercial soybean cultivars, using NIL-T and NIL-S, TF8 (Tiefeng 8, salt tolerant parent) and 85-140 (salt sensitive parent) as controls (Appendix Fig. 5.1). Cowrie, Manta, Soya791, Moonbi, Warrigal, A6785, Bunya, and Zeus accumulated significantly less Na^+ compared to Poseidon, Surf, Richmond and Hayman (Appendix Fig. 5.1a); as for Cl^-, Surf, Soya791, Moonbi, A6785, Bunya, and Zeus had lower leaf Cl^- content compared to other varieties (Appendix Fig. 5.1c).

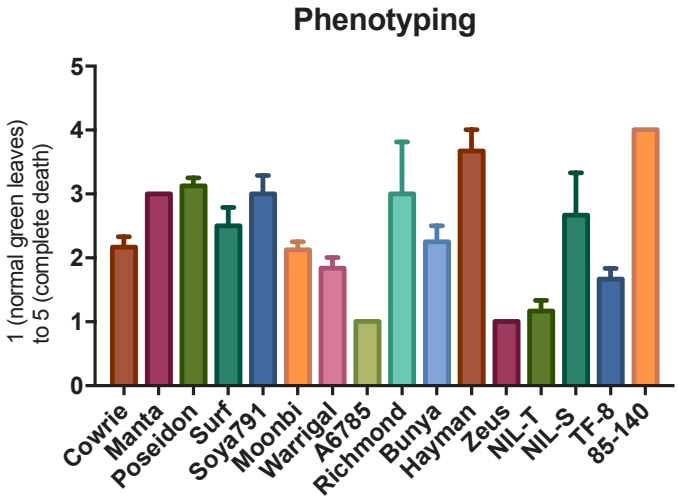

Appendix Fig. 5.2 Phenotyping of 12 Australian commercial soybean cultivars in salinity tolerance. Differences in salt tolerance levels of soybean varieties. The salt-tolerance ratings ranged on a scale from 1 (normal green leaves) to 5 (complete death). Accessions showing a leaf scorch score of 1 and 2 were defined as salt tolerant, and those from 3 to 5 were salt sensitive.

According to Appendix Fig. 5.2, salt-tolerant cultivars are Cowrie, Moonbi, Warrigal, A6785, Bunya, Zeus, NIL-T and TF8.

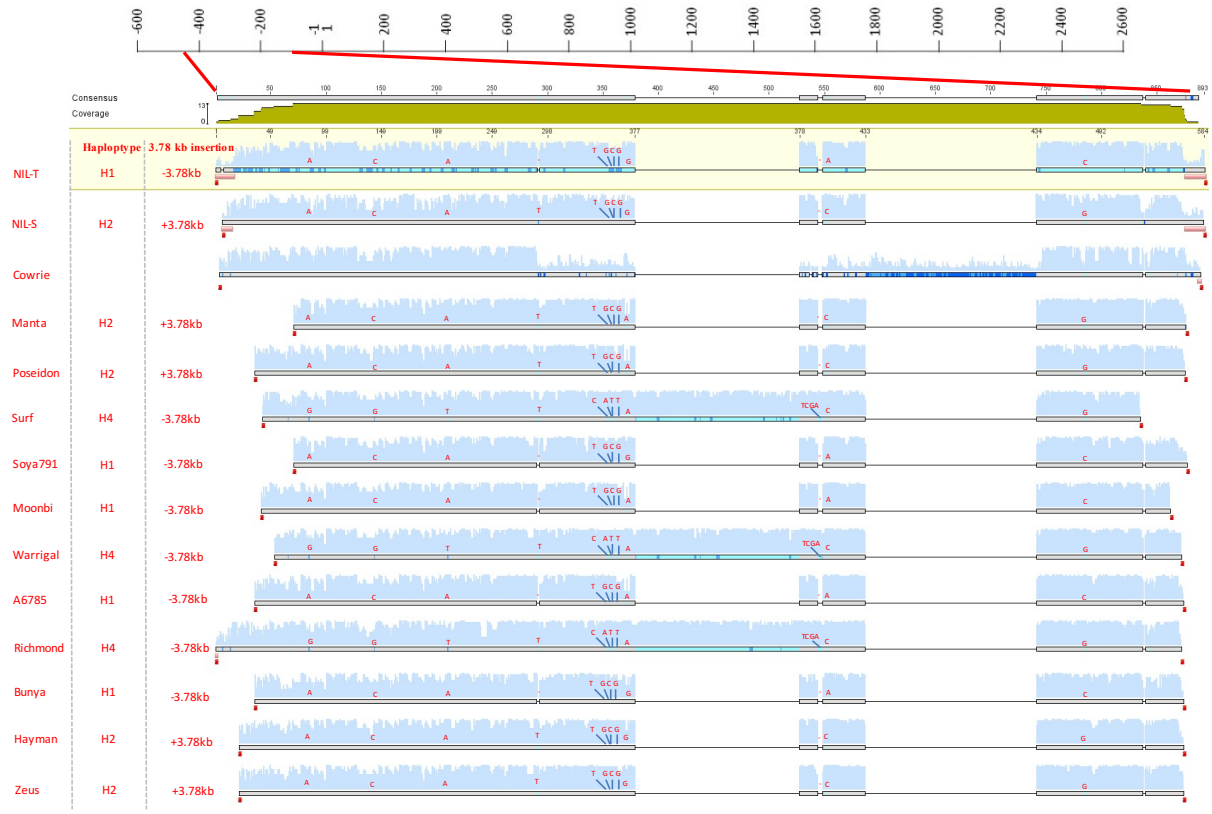

Appendix Fig. 5.3 Genotyping of 12 Australian commercial soybean cultivars. Different haplotypes of *GmSALT3* in soybean varieties based on insertion/deletion/SNPs in promoter and coding regions.

Haplotype analysis indicated that Soya791, Moonbi, A6785, Bunya have *GmSALT3* haplotype 1 (H1); Manta, Poseidon, Hayman, and Zeus have *GmSALT3* haplotype 2 (H2); Surf, Warrigal, and Richmond have *GmSALT3* haplotype 4 (H4) (Appendix Fig. 5.3). In our previous study, a collection of Chinese soybean landraces showed that H1 is mainly salt tolerant (73 out of 76 cultivars; NIL-T has H1); H2 is mainly salt sensitive (14 out of 15 cultivars; NIL-S has H2); H4 is mainly salt sensitive (25 out of 28 cultivars).

A summary of salinity tolerance based on Na^+ content, Cl^- content, and leaf chlorosis is shown in Appendix Table 5.1. To conclude, there are dramatic variations of salinity tolerance ability among current Australian commercial soybean cultivars; and they contain three *GmSALT3* haplotypes (1, 2 and 4). Salt tolerance evaluation based on leaf chlorosis should be repeated with larger sample sizes; cultivar Zeus possess H2 but was extremely salt tolerant in

terms of shoot Na^+ and Cl^- exclusion and should be further investigated, other dominant salt-tolerant genes must be compensating for the loss of full-length *GmSALT3*.

Appendix Table 5.1 Summary of phenotyping and genotyping of 12 Australian commercial soybean cultivars. "+" represents salt tolerant; "-" represents salt sensitive.

Cultivar	Na^+ tolerance (Na^+ content)	Cl^- tolerance (Cl^- content)	Salt tolerance (based on leaf chlorosis)	Haplotype
Cowrie	+	-	+	N/A
Manta	+	-	-	H2
Poseidon	-	-	-	H2
Surf	-	+	-	H4
Soya791	+	+	-	H1
Moonbi	+	+	+	H1
Warrigal	+	-	+	H4
A6785	+	+	+	H1
Richmond	-	-	-	H4
Bunya	+	+	+	H1
Hayman	-	-	-	H2
Zeus	+	+	+	H2
NIL-T	+	+	+	H1
NIL-S	-	-	-	H2

References

Chintapalli, V. R., Kato, A., Henderson, L., Hirata, T., Woods, D. J., Overend, G., Davies, S. A., Romero, M. F. and Dow, J. A. (2015). Transport proteins NHA1 and NHA2 are essential for survival, but have distinct transport modalities. *Proceedings of the National Academy of Sciences* **112**, 11720-11725.

Edwards, K., Johnstone, C. and Thompson, C. (1991). A simple and rapid method for the preparation of plant genomic DNA for PCR analysis. *Nucleic acids research* **19**, 1349.

Gietz, R. D. and Schiestl, R. H. (2007). High-efficiency yeast transformation using the LiAc/SS carrier DNA/PEG method. *Nature protocols* **2**, 35.

Guan, R., Qu, Y., Guo, Y., Yu, L., Liu, Y., Jiang, J., Chen, J., Ren, Y., Liu, G. and Tian, L. (2014). Salinity tolerance in soybean is modulated by natural variation in GmSALT3. *The Plant Journal*. **80**, 937-950.

Maresova, L. and Sychrova, H. (2005). Physiological characterization of Saccharomyces cerevisiae kha1 deletion mutants. *Molecular microbiology* **55**, 588-600.

Padmanaban, S., Chanroj, S., Kwak, J. M., Li, X., Ward, J. M. and Sze, H. (2007). Participation of endomembrane cation/H^+ exchanger *AtCHX20* in osmoregulation of guard cells. *Plant Physiology* **144**, 82-93.

Qu, Y. (2013). Functional analysis of *GmNClT*, a candidate gene for conferring salt tolerance in soybean [*Glycine max* (L.) Merr.]. In *School of Agriculture, Food & Wine*: The University of Adelaide.

Roy, S., Gilliham, M., Berger, B., Essah, P., Cheffings, C., Miller, A., Davenport, R., LIU, L. H., Skynner, M. and Davies, J. (2008). Investigating glutamate receptor-like gene co-expression in *Arabidopsis thaliana*. *Plant, Cell & Environment* **31**, 861-871.